Targeting the CD19/CD21 complex on B cells in the mixed lymphocyte reaction

Broc, S.

https://doi.org/10.34737/vz7zw

Targeting the CD19/CD21 complex on B cells in the mixed lymphocyte reaction

Targeting the CD19/CD21 complex on B cells in the mixed lymphocyte reaction

Sabine Broc

A thesis submitted in partial fulfilment of the requirements of the University of Westminster for the degree of Master of Philosophy

July 2022

AUTHOR'S DECLARATION

I declare that this present work was carried out in accordance with the guidelines and regulations of the University of Westminster. The work is original except where indicated by reference in text.

This submission or part of it is not substantially the same as any I previously or am currently making, whether in published or unpublished form, for a degree, diploma or similar qualification at another university or similar institution.

Until the outcome of the current application to the University of Westminster is known, the work will not be submitted for any such publication at another university or similar institution.

Any views expressed in this work are those of the author and in no way represent those of the University of Westminster.

Signed: Sabine Broc Date: July 2022

ACKNOWLEDGEMENTS

Firstly, I would like to express my gratitude towards the University of Westminster for granting me a PhD Studentship without which such a journey would have been impossible.

I wish to express my deepest gratitude to Dr Stipo Jurcevic for always supporting my research choices, giving me confidence in what I do, and for the long conversions we had which initiated and fuelled my interest for the complement pathway, an aspect I would have never considered otherwise, now the core of my work.

I would like to extend my sincere thanks to Deema, my PhD teammate, whose positive mindset gave me strength.

I owe a massive thank you to the technical staff, particularly Kim and Joe for their patience and incredible support whenever I needed. Also not forgetting Dr Susan Lawson who helped me get through the struggles with deliveries and joined me in the most enjoyable conversations.

Now down to my friends, despite the distance, from Nantes to London, thank you for being by my side. Also, to you Amina, our “routine” was such an essential mental break during this demanding period…감사합니다!

Of course, I cannot thank my parents enough for their undying support and trust in me, they are an incredible driving force, I could not be there without them. And to my brothers, our unity helped me overcome hard times. My last thought goes to you Mélodie, you are amazing!

ABSTRACT

B cells exert antigen presenting functions at the crossroad between immune activation and tolerance induction, a fate notably governed by the B Cell Receptor (BCR) response regulator CD19/CD21 complex. This duality in B cells raises a particular interest in the case of acute graft-versus-host disease (GvHD), a common complication post allogeneic haematopoietic stem cell transplantation (HSCT). In this context, B cells may act either through the disruption of their capacity to present antigens in an attempt to passively hamper GvHD onset, or, conversely, by harnessing their tolerogenic potential to actively protect host tissues from cytotoxic killing by donor T cells. Hence deciphering a way to fine tune B cell functions to fit these purposes is critical. Here, we proposed that the maintenance of B cells in a resting state with the concourse of the anti-CD22 antibody epratuzumab, inducing reduction in surface CD19/CD21 complex, would mitigate their responsiveness to allopeptides and thus, prevent the acquisition of potent antigen presenting functions. Furthermore, the combination with C3d adjunction would direct antigens to CD21-mediated uptake for class II MHC presentation, taking advantage of the incapacity to derive any co-stimulatory activities as part of this process. The subset of B cells hereby generated would therefore have constituted a large repertoire of antigens towards which a tolerogenic state would be established. The plausibility of this strategy was investigated in a newly designed mixed lymphocyte reaction (MLR) model in which we attempted to integrate a critical component of the cytokine network at the backbone of aGvHD pathophysiology, IL-15, stemming as a result of the post-HSCT lymphopenia and initial tissue damage induced by the pre-conditioning regiment. We found a dichotomy in the effect mediated by C3d. It decreased by 1.46-fold granzyme b production when used alone, but failed to sustain such effects when used in conjunction with epratuzumab. The reduction in CD19/CD21 expression induced by epratuzumab could potentially account for this outcome as $CD21^{low}$ B cells are reported to be anergic. C3d usually has a role in breaking tolerance, however an opposite effect was observed here. The targeting of C3d-coated antigens to CD21 independent of BCR engagement appears to be taking place. This study provides an insight on the potential of fine-tuning the CD19/CD21 complex and sets the foundation for future research to better characterise the events taking place. This is crucial for the better optimisation of putative therapeutic strategies targeting the CD19/CD21 complex in the settings of aGvHD.

ABBREVIATIONS

- ADCC: antibody-dependent cellular cytotoxicity
- aGvHD: acute graft-versus-host disease
- Ang: angiopoietin
- APC: antigen presenting cell
- BCR: B cell antigen receptor
- BM: bone-marrow
- Breg: regulatory B cell
- CDC: complement-dependent cytotoxicity
- cGvHD: chronic graft-versus-host disease
- CIA: collagen-induced arthritis
- CLIP: class II-associated invariant chain peptide
- CR2: complement receptor type 2
- DAMP: damage-associated molecular pattern
- DC: dendritic cell
- DLI: donor lymphocyte infusion
- EMC: extracellular matrix
- ER: endoplasmic reticulum
- ESC: embryonic stem cell
- FAK: focal adhesion kinase
- FDCs: follicular dendritic cells
- FHR-3: factor H-related protein-3
- FVS: fixable viability stain
- GC: germinal centres
- GvL: graft-versus-leukaemia
- GvT : graft-versus-tumour
- haplo-HSCT: HLA-haploidentical HSCT
- HLA: human leukocyte antigens
- hu-PBL-SCID: human peripheral blood lymphocytes engrafted in severe-combined immunodeficient mice
- HSC: haematopoietic stem cell
- HSCT : haematopoietic stem cell transplantation

- Ig: immunoglobulin
- iPSC: induced pluripotent stem cell
- iTreg: induced Treg
- ITAM: immunoreceptor tyrosine-based activation motif
- ITIM: immunoreceptor tyrosine-based inhibition motifs
- M: MLR
- M15: MLR+IL-15
- MAC: membrane attack complex
- MBL: mannose-binding lectin
- MBC: memory B cells
- miHA: minor histocompatibility antigen
- MLR: mixed lymphocyte reaction
- MOG: myelin oligodendrocyte glycoprotein
- mTEC: medullary thymic epithelial cell
- NLR: NOD-like receptor
- OS: Overall survival
- PAMP: pathogen-associated molecular pattern
- PGF: poor graft function
- PBMC: peripheral blood mononuclear cell
- PBSC: peripheral blood stem cell
- PC: plasma cells
- PRR: pattern recognition receptor
- PTCy: post-transplantation high-dose cyclophosphamide
- R: Responders
- R15: Responders+IL-15
- RAG: recombination activating gene
- RIC: reduced intensity conditioning
- RM one-way ANOVA: Repeated-measures one-way analysis of variance
- SHP-1: SH2 domain-containing protein tyrosine phosphatase 1
- SLE: systemic lupus erythematosus
- SNP : single nucleotide polymorphism
- SHM: somatic hypermutation
- TAP: transporter associated with antigen processing

- TBI: total body irradiation
- TCD: T-cell depleted
- T_{CM}: central memory T cell
- Tcon: conventional T cell
- TCR: T cell receptor
- TdT: terminal deoxynucleotidyl transferase
- T_{EM}: effector memory T cells
- TLR: Toll-like receptor
- TRA: tissue-restricted peripheral antigen
- Treg: regulatory T cell
- TRM: transplant-related mortality
- UCB: umbilical cord blood
- VLA: very late activation antigen

LIST OF FIGURES

TABLE OF CONTENT

Chapter 1

Introduction

1.1. Allogeneic haematopoietic stem cell transplantation

Allogeneic haematopoietic stem cell transplantation (HSCT) is a potent curative therapy for a variety of haematological malignancies, notably leukaemias, lymphomas and multiple myelomas, and myelodysplastic syndromes, through the restoration of normal haematopoiesis. And yet, it is challenged by the ocurrence of acute graft-versus-host disease (aGvHD), a leading cause of transplant-related mortality clinically diagnosed within 100 days following transplantation. aGvHD primarily results from the massive inflammatory response triggered by donor T cells to host tissues expressing allogeneic antigens, notably class I and II human leukocyte antigens (HLA) encoded by highly polymorphic genes constituting the major histocompatibility complex (MHC), stressing the importance of selecting HLA-matched donor/recipient pairs (Blazar et al., 2012).

Particularly indicated in patients with leukaemia, myeloproliferative neoplasm and bone marrow failure, allogeneic HSCT implementation in clinical practice achieved a sustained expansion, recording a 4.5% annual increased activity with a significant rise in the inclusion of unrelated donors over HLA-identical siblings (Passweg et al., 2016). However, the emergence of aGvHD in the context of HLA-matched unrelated allogeneic HSCT in 45% of patients, associated with a 5-year mortality rate of 40% (Jagasia et al., 2012), highlighted the existence of genetic disparities outside the MHC loci. Predominantly brought about by single nucleotide polymorphism (SNP) involving the alteration of a single amino acid residue in the native peptide, they cause the generation of peptides presented by shared class I or class II MHC molecules, referred to as minor histocompatibility antigens (miHAs), absent from the immunopeptidome of the donor and thus able to elicit an immune response (Warren et al., 2012). The broad frequency of SNP in the human genome implies that the repertoire of potentially immunogenic miHAs generated is substantial, suggesting that achieving complete miHA matching between the donor/recipient pair would be hardly possible. Moreover, it is considered that more than 70% of patients will rely on unrelated donors who, because of the wide genetic diversity, might be unlikely to provide complete HLA-matching, therefore resorting to partially HLA-mismatched grafts which are associated with higher rates of engraftment failure, increased incidence of aGvHD with enhanced progression to severe stage along with a 3-year survival rate dropping by 20% (Kekre and Antin, 2014).

This emphasises the crucial requirement for novel therapies in this area, not only to improve the clinical outcome but also to address the economic challenge it represents which cannot

be overlooked, the management of posttransplant complications in case of aGvHD representing an extra cost of up to $28 000 for each allogeneic HSCT estimated between $100 000 and $200 000, in addition to which the economic burden associated with disease relapse must be accounted for (Khera et al., 2012).

1.1.1. Allogeneic HSCT: genetic considerations, graft sources and conditioning regiments

1.1.1.1. Genetic basis of the HLA system: finding the right donor

Located on chromosome 6p21, the MHC region contains a total of 253 loci among which 45 HLA-like genes encompassing the class I and II subregions are characterised, including the classical class I HLA-A, -B, -C and class II HLA-DP, -DQ, -DR loci, referred as such due to their clinical relevance in transplantation settings (Shiina et al., 2009). HLA molecules are αβ heterodimers involving, for the HLA class I, the association of a non-HLA component β2 microglobulin encoded outside the MHC region on chromosome 15 with a three-domain containing α chain, while HLA class II consist of an α and β chain each comprising two domains, the peptide-binding groove being located on the class I α1/α2 and class II α1/β1 domains (Bertaina and Andreani, 2018). Indeed, they contribute to displaying an extensive repertoire of antigens emerging as a result of the high frequency of substitutions in amino acid residues clustered on the various pockets within the grove, the structure of which defining the affinity for a given peptide categorised as either class I HLA-restricted when endogenously synthesised, or class II HLA-restricted when endocytosed from the extracellular environment. These highly polymorphic regions are located on one chain of the αβ heterodimeric structure of the HLA molecules, thus the selection of matched donors is carried out by screening for allelic variants on the class I HLA α-chain encoded by the HLA-A, -B, and -C loci, and class II HLA β-chain encoded by the HLA-DPB1, -DQB1, -DRB1 loci, for which up to 17191 and 6716 alleles, respectively, were recorded in 2019 (Fleischhauer, 2019). The diversity of the HLA system is further broadened by the co-dominant expression of both alleles inherited from the parents, consequently HLA incompatibilities are also a function of the combination of these alleles within a distinct HLA phenotypic profile (Little et al., 2016). While the impact of the polymorphic nature of the HLA molecule on its immunogenicity is established, the mismatch vector, referring to the direction of the HLA incompatibility where the non-shared HLA allele drives a graft-

versus-host (homozygous donor/heterozygous recipient) or host-versus-graft (heterozygous donor/ homozygous recipient) unidirectional response, otherwise bidirectional when both are homozygous and mismatched at a given HLA locus, and the cell surface expression level of the mismatched HLA antigen are also essential criteria to be considered as they allow to single out high-risk and permissive mismatches and thus, expand the scope of potential donors when HLA-matched sources cannot be identified (Dehn et al., 2019). The complexity of donor selection also resides in the inclusion of non-genetic factors, such as the patient sensitisation status, characterised by the presence of preformed circulating anti-HLA antibodies derived from prior pregnancies or transplantations and revealed by cross-matching the patient's serum with the cells from the potential donor.

With the advances in DNA-based technologies, significant enhancements were achieved in HLA typing in terms of accuracy, robustness and technical implementation, all the more critical for racial and ethnic minority populations for which the serologic methods are limited by the scarcity of available human alloantisera representative of their HLA allotype (Spellman et al., 2008). The terminology associated with HLA matching depends on the level of resolution used to determine the compatibility status of a donor/recipient pair, from reporting results at the antigen level (low resolution) to characterising the set of alleles (high resolution) or unique nucleotide sequence (allelic resolution) encoding a single antigen (Nunes et al., 2011). Hence, although sharing identical HLA antigens, referred to as "antigen-matched", a donor/recipient transplant pair could present disparities at the allele level, referred to as "allele-mismatched", whether which degree of resolution represent a best fit for a given HLA loci is still a matter of research, notably with respect to the class I HLA-A, -B and -C loci for which discrepancies at the allele level would appear to be less detrimental than antigen mismatches on the emergence of graft failure (EW et al., 2001). In order to reach a consensus on HLA typing guidelines, clinical endpoints are scrutinised, including, amongst others, overall survival (OS), GvHD incidence, transplant-related mortality and relapse rates, the outcome of which resulting in the recommendation for the selection of a 10/10 allele-matched donor (HLA-A, -B, -C, -DRB1 and -DQB1), considered a gold standard, with the option to combine matching at the HLA-DPB1 locus, thus reaching a 12/12 matching (Fürst et al., 2019). The inheritance of HLA genes is governed by Mendelian laws, an entire HLA haplotype is passed down from each parent, therefore two siblings have a 25% chance to be an HLA-identical match, a 50% chance to share one HLA haplotype, a status referred to as HLA-haploidentical, and a 25% chance to present different sets of HLA haplotypes (Choo, 2007). Although an HLA-identical sibling is the optimal

choice of donor for HSCT, it is only available for 15-30% of patients, in which case a 10/10 allele-matched unrelated donor, identified for 30-70% of patients, represents a good alternative, eventually resorting to donors exhibiting different degrees of HLA mismatches for which the difficulty lies in the alleviation of bidirectional immune responses (Nowak, 2008).

1.1.1.2. Haploidentical HSCT: crossing the HLA barrier

Indeed, the incidence of graft failure in more than 20% of patients undergoing T-cell depleted (TCD) HLA-haploidentical HSCT (haplo-HSCT), designed to mitigate aGvHD, is due to the predominance of host T cells mediating graft rejection. This is an imbalance that was attempted to be re-adjusted by increasing the donor stem cell dose in the so-called "megadose" $CD34^+$ grafts, without GvHD prophylaxis (Bertaina et al., 2017). However, the 40% incidence of non-relapse mortality called for a refinement of depleting methodologies improving immune recovery by selectively excluding donor alloreactive $CD3^+/CD19^+$ cells, further narrowed by restricting the pool of T cells infused to $\gamma\delta^+$ over $\alpha\beta^+$ subsets, making up 1-20% of peripheral circulating T cells, since they exert no substantial role in the mediation of aGvHD while sustaining anti-pathogen defence mechanisms and anti-tumour responses (Baumeister et al., 2020; Symons and Fuchs, 2008). Conversely, strategies aiming at fostering T cell immunosuppression were developed in the settings of T-cell replete haplo-HSCT where the donor graft is left unmanipulated, introducing an approach referred to as the "GIAC protocol" which combines G-CSF-primed bone-marrow (BM) and peripheral blood stem cells (PBSCs) with GvHD prophylaxis and anti-thymocyte globulin (ATG), thus not only alleviating the extent of donor-mediated alloreactivity but also, as a result of the infusion of a significantly higher number of T cells polarised towards a Th2 phenotype, harnessing protective functions against GvHD (Kanakry et al., 2016). An alternative approach, one of the most popular within this field, although the underlying mechanisms of action have only been recently clarified, is the use of post-transplantation high-dose cyclophosphamide (PTCy) administered at 50mg/kg on day 3 and 4 following T-cell replete haplo-HSCT in patients receiving reduced-intensity conditioning (RIC) and GvHD prophylaxis, referred to as PTCy-haploHSCT, the therapeutic effects being fulfilled through reduction of host-alloreactive donor CD4 T cell proliferation combined with a preferential recovery of donor regulatory T cells (Tregs) exerting immunosuppressive properties contributing substantially to the functional impairment of host-alloreactive donor T cells (Nunes and Kanakry, 2019). The attractiveness of PTCy-haploHSCT lies in that it leaves

haematopoietic stem cells untouched due to their high aldehyde dehydrogenase activity which converts the phosphoramide mustard active metabolite of cyclophosphamide into its inactive carboxycyclophosphamide metabolic form, conferring them a resistance similarly observed in Tregs, recording low incidence of GvHD but similar OS rates as patients undergoing HLA-matched related or unrelated HSCT, indicative of uncompromised immune recovery achieved without resorting to TCD "megadose" grafts (Al-Homsi et al., 2015). What is more, PTCy-haploHSCT could even tolerate less stringent criteria with respect to the degree of HLA-mismatching on the non-shared HLA-haplotype, thus expanding the pool of potential donors (Sugita, 2019).

A similar outcome is reported with umbilical cord blood (UCB) due to its inherent restricted immunological memory and thus, relative paucity of alloreactive T cells, only requiring a minimum of 4/8 high resolution HLA matching at the HLA-A, -B, -C, and -DRB1 loci and yet, presenting with the lowest incidence of GvHD out of the two other sources of haematopoietic stem and progenitor cells (HSPCs), namely BM and peripheral blood (PB) (Gupta and Wagner, 2020). A distinct advantage lies in the existence of established UCB banks allowing a prompt availability of UCB, drastically shortening the selection process from months to weeks, all the more crucial when dealing with rapidly evolving and high-risk malignancies for which delays could compromise the chances of disease recovery (Mayani et al., 2019). Unlike G-CSF-mobilized PB and BM aspirates, UCB collection is a non-invasive and relatively simple procedure where the blood is drawn out by venepuncture of the severed umbilical cord vein, otherwise discarded, however the HSPCs content yielded is the lowest, raising concerns with respect to engraftment delays in adult HSCT recipients, addressed by resorting to double UCB unit grafts (Panch et al., 2017). Nevertheless, prolonged periods of cytopenias surpassing those recorded in PTCy-haploHSCT regardless of the HSPC source still persist, with a neutrophil recovery time extended by at least 7 days for an overall duration of 21.5 days, testifying of a defective immune reconstitution resulting in higher rates of transplant-related mortality (TRM) (Kekre and Antin, 2016). However, conflicting evidence exist suggesting similar endpoints between UCB and haploidentical graft sources used in HSCT, potentially explained by the lack of comparable cases used in retrospective studies, thus no particular consensus was reached as to which source of mismatched donors would be prioritized although in practice there is a pronounced inclination towards haploHSCT (Vanegas et al., 2021).

1.1.2. Mixed chimerism: towards immune tolerance

The most anticipated outcome of the aforementioned non-myeloablative and non-cytoreductive strategies is the establishment of stable mixed chimerism, a state defined as the coexistence of donor and recipient haematopoietic cells, setting the foundation for immune tolerance which characterises a context of unresponsiveness to both host and donor tissues (Sachs et al., 2014). This concept can be divided into two notions, namely central and peripheral tolerance, the former involving intrathymic clonal deletion of reactive clones essential for the establishment of long-term tolerance, and the latter bringing into play anergic/exhaustion, deletional and regulatory mechanisms taking place in secondary lymphoid tissues (Zuber and Sykes, 2017).

T cell anergy and exhaustion are distinct processes yielding antigen-specific hypofunctional T cells, the divergence lying in the very existence of an initial activation conferring exhaustion with a later onset than anergy (Wherry, 2011). Indeed, exhaustion occurs further to chronic persistent antigen exposure in an immunosuppressive environment deprived of adequate support from CD4 helper T cells, rich in IL-10 and TGF-β in addition to providing a high availability of inhibitory receptors, notably PD-1 and CTLA-4 (Yi et al., 2010). Consequently, the acquisition of a quiescent $CD122^{+}$ memory-like phenotype is hampered, thus not only exhibiting poor homeostatic responsiveness to IL-7, which shortens their lifespan, but also exerting poor IL-2 production and proliferation, rendering them susceptible to peripheral deletion (Wherry and Kurachi, 2015). On the other hand, anergy involves an active repression characterised by TCR engagement in the absence of CD28/CD86 co-stimulatory interaction with APCs, here contrary to exhaustion yielding alive but incompetent T cells in terms of proliferative and IL-2 productive capacities (Chappert and Schwartz, 2010). In addition, the lack of initial activation mitigates the induction of CD40L expression which, further to ligating CD40 on the opposing APC, brings an essential feedback loop enforcing even more T cell activation as it upregulates CD86 (Appleman et al., 2001). This state can however be reversed when T cells are exposed to IL-2, hence anergic mechanisms are suggested to represent a barrier against autoreactive T cells mounting an immune response towards cross-specific antigens (Powell, 2006).

The backbone of full chimerism-induced tolerance following HSC engraftment is attributed to the repopulation of the medullary thymic microenvironment by newly-generated donor-derived T cells and DCs which drive the negative selection of donor-reactive T cells (Zuber and Sykes, 2017). However, the part taken by peripheral regulatory mechanisms emerges as

being equally relevant to the generation of tolerising events when the degree of chimerism lessens, here highlighting a reliance inversely correlated with the intensity of the conditioning regiments (Hock et al., 2015). In fact, the induction of mixed chimeras represents a more favourable approach than full chimerism when optimised less stringent conditioning regiments, in addition to avert the risk of toxicity, mitigate GvHD incidence, due to intrathymic recipient APCs building a tissue-specific tolerogenic repertoire, while anti-tumour responses are still fulfilled (Al-Adra and Anderson, 2011). This implies that a subtle balance must be met to allow stable mixed chimeras survival since when overridden by recipient-led haematopoiesis, donor components are at risk of being rejected (Liesveld and Rothberg, 2008). Meanwhile, one of the main challenges of mixed chimerism is to override the increased rates of disease relapse as tolerance established towards the host also includes malignant cells and thus, eliminates the beneficial graft-versus-tumour (GvT) effect, also called graft-versus-leukaemia (GvL) effect (Deeg, 2021).

1.1.3. GvL effect: towards disease eradication

The term GvT effect generalises a concept first described in 1956 in leukaemic mice recipient of isologous BM or spleen cell transplantation showing leukaemia elimination and recovery and thus, rescuing the mortality observed in animals given radiotherapy only (Barnes et al., 1956). The manifestation of GvT effect was evidenced when the outcome of TCD allogeneic HSCT involving a reduced risk of GvHD was paralleled with higher disease relapse rates, this latter being resolved with donor lymphocyte infusion (DLI) after which patients showed durable remission (Negrin, 2015). The relationship between the GvT effect and GvHD is in fact inversely correlated as data indicate that the relapse risk was reduced with the occurrence of aGvHD and cGvHD, thus the strength of the GvT effect is strongly associated with the incidence of GvHD (Barrett, 2008). The implementation of RIC sought to favour this synergistic mechanism, however the high rates of disease recurrence revealed a failure to sustain engraftment and thus, highlighted the requirement for full donor chimerism to be achieved for the GvT effect to be operational (Barrett, 2008; Sweeney and Vyas, 2019). The exact mechanisms at the root of the GvT effect is still a matter of debate, some postulating that the implication of a specific anti-tumour response distinct of a miHA/HLA-disparate-driven process, which is at the core of GvHD, can be at stake, also evoking the sensitivity of leukaemic cells to the cytokine storm characteristic of GvHD settings (Gale and Fuchs, 2016). Among the genetic drivers of the GvL effect are non-shared

miHAs for which the donor is homozygous and recipient is heterozygous, thus triggering a unidirectional response against the host tissues where miHAs restricted to haematopoietic cells would separate the GvT effect from GvHD (Summers et al., 2020). Of note, the concept of permissive mismatches adds another level at which the balance between GvHD and GvT effect can be shifted due to the limited magnitude of the immune response they elicit, only sufficient for the GvT effect to be triggered, notably identifying HLA-DPB1 disparities as clinically relevant in this prospect (Fleischhauer and Shaw, 2017).

1.1.4. Allogeneic HSCT: are there any alternatives?

The therapeutic potential of allogeneic HSCT is thus hindered by histocompatibility barriers which have not yet been overcome since its establishment in the 1960s, representing the only stem cell-based therapy implemented in clinical practice despite the promising outlook of induced pluripotent stem cells (iPSCs) in overriding the requirement for HLA and miHA matching while fulfilling immune reconstitution.

Derived from somatic cells, initially dermal fibroblasts, as part of a reprogramming procedure involving transduction with a lentiviral vector encoding four transcription factors, including *Oct3/4*, *Sox2*, *c-Myc* and *Klf4*, iPSCs were shown to exert similar properties as embryonic stem cells (ESCs) with regards to their unlimited self-renewal abilities while preserving their capacity to give rise to cells of the three germ layers conferred by their pluripotent state (Takahashi et al., 2006). Paving the way for regenerative medicine, the translational application of iPSCs encompasses the fields of cell replacement therapy and gene therapy when autologously generated iPSC, recapitulating patient-specific disease, are genetically corrected and the corresponding differentiated cells are subsequently transplanted, restoring normal cellular functions (Wu and Hochedlinger, 2011). However, their implementation in clinical settings is constrained by inefficient cell-lineage specific differentiation protocols along with unreliable purification of differentiated cell populations ensuring complete removal of any residual iPSCs, presenting a potential hazard of teratoma formation, as well as inadequate reprogramming methods. Indeed, the prospect of deriving complete matched haematopoietic stem cells (HSCs) rose a considerable interest, although the intricate process governing haematopoiesis was hardly reproducible *in vitro*, leading to poorly engraftable cells failing to reconstitute all cell lineages with impaired migratory capacities within the bone marrow, emphasising here that actual differentiation protocols are inaccurate (Slukvin, 2013). Also, the existence of genetic heterogeneity in iPSCs at the

single cell level compared with their embryonic counterparts, evidenced notably by differential responsiveness to robust protocols of cardiomyocyte differentiation, suggests the presence of cells exhibiting a different state of maturity, calling into question the efficacy of the reprogramming procedure (Narsinh et al., 2011). The major outlook of the implementation of self-derived iPSCs in HSCT lies in the generation of immune-tolerated cells, escaping then allorecognition by the newly formed immune system and thus avoiding the emergence of acute GvHD. However, their immunogenicity was brought into light when checking their capacity to form teratomas in syngeneic mice as T cell infiltration was detected with subsequent regression of the teratomas (Zhao et al., 2011), a feature observed in a similar experiment using several iPSCs lines providing T cell infiltration at a varied extent (Araki et al., 2013). This assertion was disputed, arguing that the immunogenicity should be assessed on therapeutically relevant cells, therefore cells representative of the three germ layers obtained from iPSCs-derived embryoid bodies were transplanted into the subcapsular renal space of syngeneic mice, resulting in no rejection (Guha et al., 2013). Despite this pertinent approach, the effects observed are questionable with regards to the site of transplantation chosen as it was demonstrated that the graft microenvironment is determinant for the provision of all components necessary to initiate an immune response, notably mature dendritic cells, absent from the kidney capsule (Todorova et al., 2016). This breach in peripheral tolerance could be explained by the acquisition of somatic mutations throughout the reprogramming process and subsequent expansion of iPSCs, most of them occurring in tumour-related genes (Gore et al., 2011), potentially resulting in the expression of new antigenic determinant in addition to presenting a risk of cancer development.

While major work must be undertaken to refine the reprogramming procedure so as to generate a homogeneous population of mutation-free iPSCs, safety concerns related to the use of a lentiviral vector have been raised. Indeed, it poses a risk of insertional mutagenesis into the host genome, the integration of the vectors occurring randomly, it could potentially reactivate the transcription of oncogenes and lead to disease progression (Wu and Dunbar, 2011). This was particularly observed in a clinical trial for X-linked severe combined immunodeficiency where the integration of the retroviral enhancer upstream of the proto-oncogene LMO2 caused the development of leukaemia 3 years following transplantation of genetically corrected HSCs. This phenomenon was also described in clinical trials for X-linked chronic granulomatous disease, which ended up with the occurrence of myelodysplasia and acute myeloid leukaemia between 2 and 3 years post-transplantation. Thus, the development of integration-free reprogramming systems represented an attractive

approach to iPSC generation, mostly involving the use of replication-defective viruses, episomal plasmids as well as RNA and protein delivery (González et al., 2011). However, these technics were associated with poor reprogramming efficiency, either resulting from impaired transfection efficacy or slow kinetics, also favouring the acquisition of somatic mutations, and tumorigenic risks related to the inclusion of high dose of the proto-oncogene c-*Myc*.

It emerges from these data how complex the challenges surrounding iPSC technology are, hampering their application for HSCT, whether related to the reprogramming itself as it fails to generate a homogenous population of iPSCs. Consequently, this is exerting a mixed response to differentiation protocols, and induces a high rate of genetic alterations compromising the prospect for immune tolerance, or the derivation procedures, failing to reproduce *in vitro* the complex mechanisms behind haematopoiesis resulting in cell-lineage restriction and engraftment failure. Moreover, until the risks of tumour formation are minimised, the implementation of iPSCs-derived HSCs in clinical practice will be hard to achieve, stressing that major progress must be made in the development of integration-free reprogramming vectors restraining as well the inclusion of high dose tumour-related genes. Importantly, besides restoring normal haematopoiesis, allogeneic HSCT mediates its curative potential through the GvT effect which, following the same mechanisms as aGvHD, contributes to the eradication of host residual malignant haematopoietic cells, thus hindering a potential resurgence of the disease (Blazar et al., 2012), a feature not likely to be supported by iPSCs-derived HSCs since immunological ignorance would be acquired.

Taken together, this indicates that allogeneic HSCT will remain the exclusive therapy available, therefore emphasising how crucial the establishment of novel therapies impeding the manifestation of aGvHD is to bypass the inevitable histocompatibility barrier encountered as a result of the increased reliance on incompatible unrelated donors.

1.2. Pathophysiology of aGvHD

A thorough understanding of the pathophysiology of aGvHD has been acquired since the basis of graft-versus-host reactions were first set in the 1960s by Billingham, defining the requirement for immunologically competent cells in the graft and an immunocompromised recipient presenting tissue antigens absent from the graft (Billingham, 1966). Although bringing into play intricate mechanisms, it is conventionally broken down into three distinct

phases. That is the initial breach in tissue integrity triggering the priming of T cells and differentiation into cytotoxic effectors further aggravating the damages incurred by the tissues, the main targets being the liver, the skin and the gut (Kuba and Raida, 2018) (Figure 1).

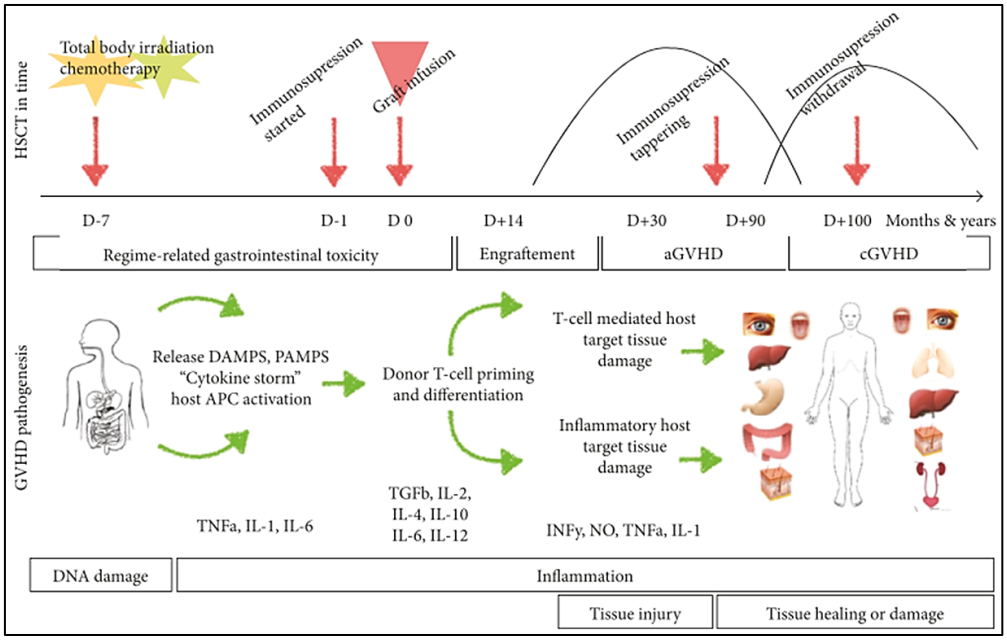

(Kuba and Raida, 2018)

Figure 1. The three phases making up the timeline of GvHD pathophysiology: initiation, priming and effector phases The breach in the gastrointestinal epithelial barrier integrity as a consequence of the toxic nature of the conditioning regiment is a central event at the foundation of GvHD initiation. It results in the release of DAMPs, PAMPs, as well as in the propagation of a cytokine storm (TNF-α, IL-1β and IL-6 being characteristic components), facilitating host APC activation. Subsequently, donor alloreactive T cells are primed and traffic to target organs where they will complete their differentiation program and take part in the effector cytotoxic response.

1.2.1. Initiation phase

The onset of aGvHD is governed not only by the extent of the genetic disparities at the HLA and miHA level, but also by the intensity of the myeloablative and immunosuppressive pre-transplant conditioning regimen. This is central to the eradication of the malignant cells and prevention of graft rejection. However, it sets the breadth of tissue damage, notably associating total body irradiation (TBI), the standard preparative radiotherapy, with an increased risk of progression to grade II-IV aGvHD (Nakasone et al., 2015). The high incidence of mucositis and gastroenteritis, involving endothelium damages in the gastrointestinal tract, consecutive to TBI administration, are among the key drivers.

1.2.1.1. Emerging role of the gastrointestinal tract microbiota

A growing body of evidence shed light on the putative impact of the intestinal microbiota and metabolome in the acceleration of aGvHD subsequent to intestinal epithelium architecture atrophy (Figure 2). The apoptosis of intestinal stem cells located in the crypts is emerging as a key initiator, since their role in the restoration of altered epithelium, Paneth and Goblet cell loss, would not be fulfilled (Teshima et al., 2016). Goblet cells protect from bacterial invasion by maintaining the mucosal barrier integrity through secretion of mucin, which forms a gel-like layer coating the epithelium. Therefore, the consequence of their targeting after allogeneic HSCT results in the permeabilisation of endothelium junctions, allowing the translocation of bacteria, pathogen-associated molecular pattern (PAMP) and damage-associated molecular pattern (DAMP) from the lumen into the mucosa, further recognised by pattern recognition receptors (PRR)-bearing cells and thus, fuelling even more the inflammatory environment.

These "danger signals" are indeed key factors interconnecting the innate and adaptive branch of the immune system. They are categorised as PAMPs for small exogenous conserved motifs of the bacterial cell wall such as LPS, flagellin, peptidoglycans and CpG-DNA, or DAMPs for host-derived fragments released from the intracellular compartment of necrotic cells, such as heat shock proteins, purine metabolites and ATP, or deriving as breakdown products of their extracellular matrix, notably biglycan, heparin sulphate and hyaluronan (Zitzer et al., 2018). They interact with the PRRs-related family Toll-like receptors (TLRs) ubiquitously distributed among haematopoietic cells as well as across non-immune tissues, such as epithelial cells, endothelial cells and fibroblast, and trigger a signalling cascade resulting in the clearance of infected cells and repair mechanisms ultimately shaping an adaptive immune response (El-Zayat et al., 2019). TLRs engage distinct ligands relative to their cellular localisation, cell surface TLRs recognising notably lipoproteins (TLR1, TLR 2 and TLR6), LPS (TLR4) and flagellin (TLR5), while TLRs confined in intracellular vesicles bind double-stranded RNA (TLR3), single-stranded RNA (TLR7 and TLR8) or DNA (TLR9) derived from invading pathogens or uptaken following phagocytosis of infected cells, bearing in mind that a redundancy exists in PAMPs and DAMPs targeting across other PRRs (Kawai and Akira, 2011). Indeed, although not as well described as TLRs, the NOD-like receptor (NLRs)-related NLRP3 inflammasome, a major intracellular sensor of PAMPs and DAMPs highly dependent on the cross-talk with the LPS/TLR4 signalling (Ratajczak et al., 2020), was shown to be critical for the occurrence of aGvHD via an IL-1β-driven

polarisation towards a Th17 effector adaptive response (Jankovic et al., 2013). MyD88 is a central adapter protein operating downstream of all TLRs, except TL3, which converges the signal potentiated towards NF-κB activation resulting in the production of TNF-α, IL-1β, IL-6, IL-12 and IFN-γ. This is ultimately enhancing APCs maturation and alloreactive T cell homing to target organs where their differentiation into Th1/Th2/Th17 effector T cells and Tregs is promoted, thus conferring TLRs with a role at a local level (Tu et al., 2016). However, despite using similar stimuli, diverging outcomes of the signal transduced by TLRs, notably TLR4 and TLR1/TLR2, between leukocytes and non-immune cells are reported, partly explained by the differential functions fulfilled by components of the MAPK pathway and discrepancies in the cellular distribution of TLRs, describing intracellular forms of TLR2 and TLR4 in endothelial cells while these are absent in monocytes, macrophages, neutrophils, DCs and NK cells (Vijay, 2018). Although LPS translocation is an established driver of GvHD lethality, conflicting data arise with respect to the requirement of the LPS/TLR4 signalling for the development of GvHD, revealed notably by the insignificant influence exerted by the introduction of SNPs yielding a dysregulated potentiation of LPS signalling in TLR4, an outcome potentially biased by the routine administration of bacterial control medication to allogeneic HSCT recipients (Penack et al., 2010). A more complex system seems to be at stake since evidence highlights the protective functions of donor TLR4 against aGvHD, its disruption resulting in an increased intestinal infiltration of TNF-α-producing macrophages along with a defective epithelial cells homeostatic response to tissue injury (Imado et al., 2010). On a broader perspective, MyD88 appears to exert diverging functions relative to the cell type considered allowing the distinction between GvHD and GvL effect, however, the direction preferentially sustained needs clarifications. Indeed, while evidence concords to associating donor T cell MyD88 deficiency with a shift from a Th1/Th17 to a Treg/Th2 effector adaptive response ultimately impacting the CD8 T cell-mediated cytotoxicity, it either showed that MyD88 is critical for the preservation of the GvL effect (Lim et al., 2015) or for the sustainment of GvHD (Matsuoka et al., 2020), each mechanism occurring independently of the other, thus holding promising prospects for a targeted approach.

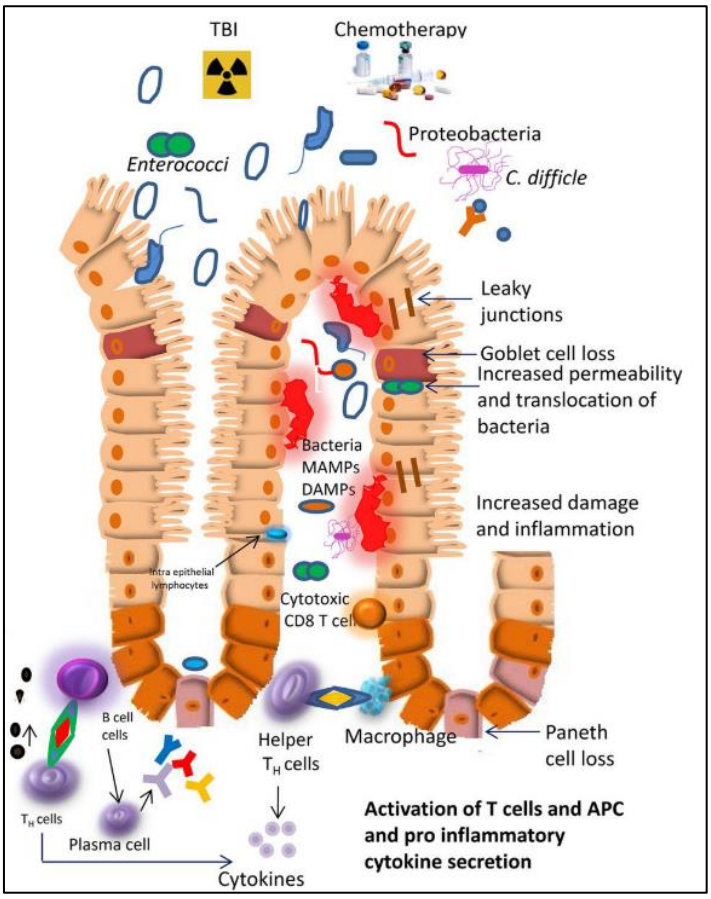

(Kumari et al., 2019)

Figure 2. Atrophy of the intestinal epithelium and dysbiosis, pillar of the onset of aGvHD The integrity of the intestinal epithelium is altered by the conditioning regiment, conducive to the permeabilisation of the endothelial junctions, resulting from Paneth and Goblet cell loss, and further translocation of bacteria, PAMPs and DAMPs from the lumen into the mucosa, recognized by PRR-bearing cells. Moreover, a breach of the microbiota diversity characterised by a progressive replacement of the commensal flora by enteropathogenic species fuels the inflammation with systemic LPS dissemination. These events converge to the exacerbation of the initial cytokine storm and antigen presenting cells **(**APCs) activation propitious to T cells activation and associated target-tissue damage.

The drop in Paneth cell number has been linked to the emergence of intestinal dysbiosis, characterised by a breach in the microbial diversity where the population of commensal bacteria declines, progressively replaced by an enteropathogenic flora exacerbating the inflammation through systemic LPS dissemination (Eriguchi et al., 2012). Indeed, Paneth cells are important regulators of microbiota homeostasis, maintaining its diversity by hampering colonisation and outgrowth of enteric populations through secretion of antimicrobial peptides, notably α-defensins, exerting the strongest bactericidal activity, which levels were shown to be dramatically decreased in aGvHD. In fact, the decline in the antimicrobial peptide-related C-type lectin Reg3α and α-defensins 5 and 6 along with Paneth

cell metaplasia was correlated with the development of grade II-IV aGvHD in the gastrointestinal tract (Weber et al., 2017). While the intestinal microbiota is overwhelmed with the growth of enteropathogens, sustaining a deleterious influence on the escalation of aGvHD pathogenesis, it suffers the loss of Clostridia species, the broad-spectrum antibiotic treatment used to circumvent the neutropenia suggested to be the key mediator, at the expense of their beneficial tissue protective properties through production of short-chain fatty acids, the most often described being butyrate, stressing here how gastrointestinal microbial metabolites can modulate the severity of aGvHD (Staffas et al., 2017). Indeed, as a mean to bypass the observed drastic decrease in butyrate levels, altering epithelium junctional integrity, 17 Clostridial strains were administered via intragastric gavage to mice before allogeneic bone marrow transplantation in an attempt to shift the host intestinal microbiota towards a high butyrate producing microbial flora, resulting in the alleviation of aGvHD severity (Mathewson et al., 2016).

1.2.1.2. Angiogenesis: fuelling or mitigating aGvHD?

Angiogenesis is among the first events ensuing endothelial injury, thus a growing interest in the role of angiogenesis in aGvHD pathogenesis has built up over the years. Indeed, a substantial rise in VEGF levels, a pro-angiogenic factor, and microvessel density, a marker of neovascularization, were correlated with aGvHD pathology, whereas both of these were declining with a disease recovery (Medinger et al., 2013). A more detailed insight on the dynamics of angiogenesis was brought forward, defining an early angiogenic phase driven by endothelial cell metabolic and cytoskeleton alterations, thus independent of the conventional VEGF pathway, occurring ahead of leukocyte infiltration irrespective of conditioning-induced inflammation. Thus, underlining here the intricate relationship between angiogenesis and aGvHD initiation, switching to a more classical pathological process with the establishment of aGvHD and conditioning-associated endothelial cell damage (Riesner et al., 2017). A controversy arose as to what outcome resulted from angiogenesis, whether intensifying the inflammation or supporting tissue healing. It has been suggested that the nature of circulating angiogenic factors at stake could dictate the prognosis of aGvHD, a dysregulation in the balance between promoters of damage/inflammation and repair/regeneration being identified in favour of the former, inferring notably that low levels of EGF, a predominant mediator of tissue healing, resulted from the loss of EGF-producing cells in the gastrointestinal tract, Paneth cells being among

these (Holtan et al., 2015). It was therefore investigated whether counteracting this pattern would mitigate aGvHD, prompting attempts to re adjust angiopoietins (Ang) levels with simvastatin which, by compromising TNF-α-induced release of Ang-2, shifted the angiogenic environment towards a predominant expression of Ang-1, hence propitious to the maintenance of endothelium integrity and hermetic endothelial junctions, resulting in the attenuation of aGvHD-associated organ damages (Zheng et al., 2017).

1.2.2. Priming phase

Altogether, these early events converge to the establishment of an intense inflammatory environment, TNF-α, IL-1β and IL-6 cited as the leading components of the initial wave of cytokine released, facilitating access to target tissues and enhancing host cells antigen presenting functions, through upregulation of class-II MHC antigens and co-stimulatory molecules expression. This is paving the way for potent donor T cell priming and activation, IFN-γ, TNF-α and IL-2 being characteristic of the cytokines secreted at later stage, reinforcing the allogeneic response and tissue injury (Ball and Egeler, 2008) (Figure 3).

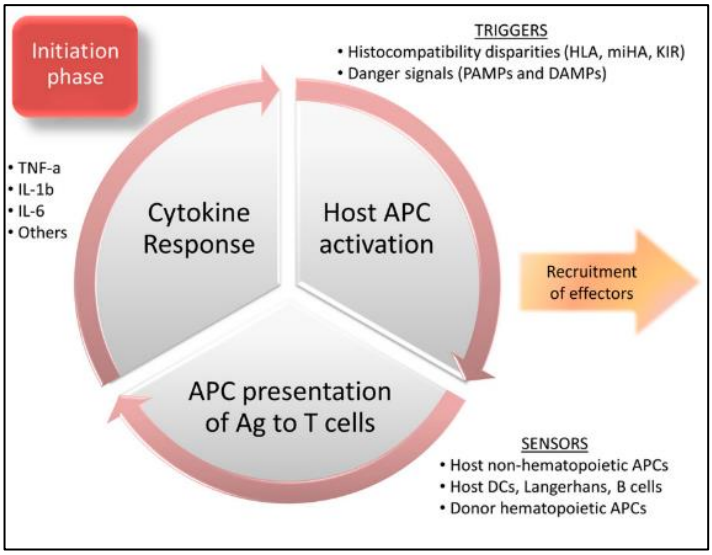

(Holtan et al., 2014)

Figure 3. Key components laying out the foundation for the priming phase of aGvHD
The existence of histocompatibility mismatches and buildup of inflammatory cues (PAMPS/ DAMPS) are critical drivers of APC activation ultimately yielding donor T cell priming. The concurrent propagation of the cytokine storm fuels even more the inflammatory environment, leading to the escalation of the immune response. The source and subsets of APCs involved is manifold, including haematopoietic APCs of host or donor origin and host non-haematopoietic APCs.

A discrepancy in aGvHD outcome arises whether naïve or memory T cells are brought to play. The heterogeneity of the T cell memory compartment reflects diverging temporal contributions to secondary immune responses, describing a fast immediate engagement of T_{EM} ($CD62L^{low}$ /$CCR7l^{ow}$) progressively dominated overtime by T_{CM} ($CD62L^{high}$ /$CCR7^{high}$) (Roberts et al., 2005). In aGvHD settings though, it is commonly accepted that naïve T cells are the main initiators. Their frequency is increased in the PB of GvHD patients (Sairafi et al., 2016). Also, accumulating evidence correlate naïve T cells with GvHD severity, milder or no incidence being recorded with T_{CM} and $T_{EM,}$ respectively (Bleakley et al., 2015; Jiang et al., 2021), rather imparting to them a latter role in perpetuating the inflammation (Holtan et al., 2014). In contrast, a protocol of naïve T cell-deplete PBSC HSCT preserving T_{CM} failed to show any significant protection against aGvHD compared to historical internal clinical data, although a discrepancy in aGvHD prophylaxis and conditioning regimens could explain this outcome (Bleakley et al., 2015). In support of this, lethal GvHD occurred in TCD BMT mice recipients of naïve T cells, gradually resolved as their depletion from bulk T cell grafts increased, however T_{EM} and T_{CM} were unable to exert such effect (Chen et al., 2007).

1.2.2.1. Mechanisms of allorecognition

While only 0.01% of the peripheral T cell repertoire can recognize a specific antigenic determinant presented by a self-MHC molecule, it is in reality up to 1-10% which are reactive against intact mismatched MHC-allopeptide complexes, attributed to a process termed “direct allorecognition” (Koyama and Hill, 2021). Two theories were raised to identify the nature of the interactions at stake. In the peptide-centric model, allogeneic MHC molecules are capable of self-like structural mimicry allowing them to adopt a conformation providing docking sites for self-MHC molecules, the disparities being localised within the peptide-binding groove, hence a diverse antigenic pool encompassing a wide range of specificities can engage a substantial fraction of T cells, fulfilling the “multiple binary hypothesis” (Boardman et al., 2016). Conversely, the MHC-centric model brings into play fundamental discrepancies in polymorphic residues recognised as foreign by self-MHC molecules, irrespective of the peptide presented, a process facilitated by the high ligand content displayed by APCs, here referring to the “high determinant density” hypothesis. While direct allorecognition was long considered the dominant mechanism driving the onset of transplant rejection, it is only a transitory short-lived episode, progressively replaced by

“indirect allorecognition” which becomes the motor of the allogeneic reaction (Benichou and Thomson, 2009). Indeed, driven by the high frequency of the alloreactive T cell repertoire along with a less stringent requirement for co-stimulatory signals, the direct allorecognition yields a strong initial effector cytotoxic response however limited in its extent, the redirection of allopeptides to indirect targeting being favoured (Lin and Gill, 2016). Here, the degradation of allogeneic MHC-peptide complexes by direct alloreactivity generates a pool of antigens available for uptake by donor APCs, further integrated into the indirect presentation process (Sun et al., 2007). Briefly, the proteolysis of internalised antigens in acidic endolysosomal structures, enriched in asparaginyl endopeptidase or cathepsin S, generates peptides capable of loading on class II MHC molecules peptide-binding groove. The newly-formed complex being ultimately exported to the membrane for recognition by CD4 T cells (Roche and Furuta, 2015). Alternatively, DCs possess the unique ability to deliver endocytosed antigens to class I MHC molecules for CD8 T cell priming via a process called “cross-presentation” (Joffre et al., 2012; ten Broeke et al., 2013). The resulting dual licensing is critical considering CD8 T cells requirement for concomitant CD4 helper T cell support to achieve activation and, ultimately, exert cytolytic functions. Two major “tracks” can drive this mechanism, either a vacuolar pathway taking place in endocytic structures akin to the class II MHC machinery, or a proteasome-dependent cytosolic pathway where the degraded peptides translocate to the endoplasmic reticulum (ER) via the transporter associated with antigen processing (TAP) and bind class I MHC molecules (Embgenbroich and Burgdorf, 2018; Segura and Villadangos, 2011). The relevance of cross-presentation was demonstrated in a class I MHC-deficient skin graft model in which CD8 T cells were identified as the sole mediators of the rejection process (He and Heeger, 2004). In contrast, class II MHC molecules can be led to present endogenously synthesised peptides and thus, hijack the class I MHC route. Indeed, while the invariant chain restrains access to the peptide-binding cleft of class II MHC in the ER, an imbalance in the class II MHC to invariant chain ratio is suggested to allow the binding of unfolded proteins (Leung, 2015). In addition, peptide loading on recycling class II MHC molecules could feed into this non-classical form of endogenous presentation, postulated to cause the displacement of the original peptide. Lastly, a “semi-direct allorecognition” in which donor APCs display intact host cell-derived full class I and II MHC-allopeptide complex was reported (Afzali et al., 2008). It sets the foundation for the “three-cell” cluster model of antigen presentation involving a common APC concomitantly indirectly priming CD4 T cells and licencing CD8 T cells directly through acquired host-derived class I MHC-

allopeptide complex (Marino et al., 2016a; Siu et al., 2018). This cross-dressing, stable for 48h, occurs either through a receptor-mediated exchange of membrane material between recipient and host cells termed trogocytosis, or further to interaction with exosomes trafficking to lymphoid organs in which case the transfer of class II MHC molecules are primarily brought into play (Rangaraju et al., 2013). However, despite the characterisation of such events in solid organ and BM transplantation, the functional relevance of semi-direct allorecognition in these settings remains to be elucidated (Marino et al., 2016b).

1.2.2.2. APCs sources and subsets: challenges in defining a targeting strategy

A clear identification of the source and subsets of APCs critical for aGvHD onset still remains a matter of controversy. Indeed, full donor APC chimerism is often precluded by the co-existence of tissue resident radioresistant precursor cells sustaining a pool of reactive host skin macrophages, dermal DCs and epithelial Langerhans cells (Chakraverty and Sykes, 2007). For instance, the kinetic of host tissue resident macrophage replacement, notably Kupffer cells in the liver, alveolar macrophages in the lung and microglia cells in the central nervous system, by BM-derived monocytes appears to be significantly delayed compared to haematopoietic tissue engraftment (Kennedy and Abkowitz, 1997). Host DCs alone were shown to reverse the resistance to CD4-dependent GvHD in a class II MHC-deficient mice and also efficiently directly prime a CD8 T cell-driven GvHD in a class I MHC-disparate mice model of syngeneic BMT, contrasting with the absence of such elicitation by host B cells irrespective of any auxiliary tolerogenic functions (Duffner et al., 2004). A time window of 24h was recorded for the achievement of host DCs-mediated priming of miHA-mismatched CD8 T cells in mice transplanted with grafts depleted from donor $CD8^+CD11c^+$ lymphoid DCs, resulting in lethal GvHD, a temporality explained by the short lifespan of host DCs induced by TBI (Zhang et al., 2002a). In addition, tissue resident macrophages and DCs contribute substantially to the recruitment of CD8 cytotoxic T cells to target organs, notably shown to mediate localised liver and spleen aGvHD (Zhang et al., 2002b). While the role of host resident epidermal Langerhans cells in driving an *in situ* Th2-polarised pathogenicity was demonstrated, fuelled by concomitant skin microbiome dysbiosis, they were found to be sufficient for the initiation of skin GvHD unless they were made redundant by the presence of other APCs, notably tissue-infiltrating macrophages, a trend also described with keratinocytes which would otherwise exert tolerogenic functions in normal

conditions (Santos e Sousa et al., 2018). In fact, the prevailing dogma placing host residual haematopoietic APCs as predominant in the initiation of aGvHD through direct allorecognition is reconsidered as emerging evidence suggests that host non-haematopoietic cells residing in connective tissues, epithelium and endothelium exert such capacity (Koyama and Hill, 2016). Indeed, even refuting any critical involvement of host DCs for the induction of aGvHD in a mice model of class II MHC-restricted peptide BMT, this role is rather attributed to class II MHC-expressing myofibroblast within the gastrointestinal tract (Koyama et al., 2011). On the other hand, donor APCs seem to exert minimal functions in this outcome as indirect cross-priming was shown to be insufficient for aGvHD onset in absence of class I MHC-expressing host APCs, a more prominent role of this pathway in the extent of tissue injury being rather suggested to impact aGvHD incidence and severity (Chakraverty and Sykes, 2007). Notably, donor monocyte-derived macrophages were the most prominent subset among leukocytes to be found in cutaneous GvHD lesions where they exerted potent T cell-stimulatory activities (Jardine et al., 2020).

In fact, no consensus was reached as to what distinct subset of haematopoietic APC is fundamental in the induction of aGvHD (Holtan et al., 2014). It is even suggested that depleting strategies would be inefficient, if not deleterious, with respects to the elimination of APCs with protective functions, instead advised to favour therapeutic approaches aimed at fine-tuning their signalling (MacDonald et al., 2013). Indeed, while fibroblasts are competent APCs in aGvHD induction (Koyama et al., 2011), their targeting could also undermine their tissue repair activities mediated by keratinocyte growth factor and R-spondin secretion (Zeiser and Blazar, 2017). In line with this, the contribution of Kupffer cells as well as splenic macrophages and DCs in the clearance of apoptotic cells, termed efferocytosis, also precludes from any universal therapeutic targeting of their APC functions (Saas et al., 2016). Indeed, as part of immunological silent phagocytosis, efferocytosis is initiated by features characteristic of dying cells, notably the exposure of phosphatidylserine on the outer leaflet of the plasma membrane, are recognized by phagocytic cells and engulfed, ultimately triggering the secretion of ant-inflammatory signals, notably IL-10 (Boada-Romero et al., 2020). Hence, its moderating functions act like an immunological break to refrain from excessive inflammation, a feature lost with inefficient efferocytosis, commonly found in the pathogenesis of autoimmune diseases resulting in the exacerbation of clinical manifestations. Among the key players involved in this tolerogenic approach of apoptotic clearance, the complement pathway through C1q and iC3b opsonisation of

apoptotic cells mediates a disbalance between IL-10 and IL-12, supporting the secretion of the former by phagocytes along with the suppression of the latter, hence installing a non-immunogenic state (Merle et al., 2015). Also, the dual engagement of the CD36 and PAFR "scavenger receptors" to oxidised phospholipids presented by apoptotic cells induces the generation of phagocytic cells with regulatory properties, displaying a IL-10^{high}/Il-12^{low} profile, hence corroborating the polarisation of the inflammatory environment towards immune silence since the ratio between IL-10 and IL-12 levels are commensurate with the extent of efferocytosis (Ferracini et al., 2013). The relevance of efferocytosis in the settings of GvHD is corroborated by therapeutic approaches consisting in the intravenous infusion of apoptotic cells, not only delaying the incidence of lethal GvHD through expansion of donor T regs dependent on splenic host macrophages (Kleinclauss et al., 2006), but also facilitating haematopoietic reconstitution without causing GvHD (De Carvalho Bittencourt et al., 2001). The existence of dual and yet, contrasting functions exerted by donor APCs also restricts the scope for a putative ubiquitous targeting of APCs. Indeed, while donor DCs were identified as critical APCs for indirect antigen presentation shortly after allogeneic BMT, evidence showed that donor B cells promoted a concomitant tolerogenic signal since their removal resulted in the enhancement of DCs presenting potency (Markey et al., 2009). Here, B cells regulatory properties would be directed at re-balancing the allogeneic reaction, their interconnection with DCs notably relying on the defective polarisation towards a CD4 Th1 response, thus curtailing the prospect for mounting robust cytotoxic activities (Moulin et al., 2000). Moreover, as demonstrated by the administration of donor-derived *ex vivo* polarised M2 macrophages which, further to migration to localised GvHD tissues, attenuated GvHD severity by suppressing T cell proliferation (Hanaki et al., 2021), the repression of such immunosuppressive subset could be deleterious. Indeed, the M1/M2 ratio of tissue infiltrating macrophages was correlated with the incidence of aGvHD (Hong et al., 2020), hence a disbalance of this ratio towards M1 classical pro-inflammatory subset could be induced and, ultimately, lead to an aggravation of aGvHD. Overall, the dichotomy existing in APCs stresses the relevance of designing therapeutic strategies aimed at fine-tuning distinct pathways and ultimately uncouple these diverging signals in favour of the establishment of stable peripheral tolerance (Figure 4).

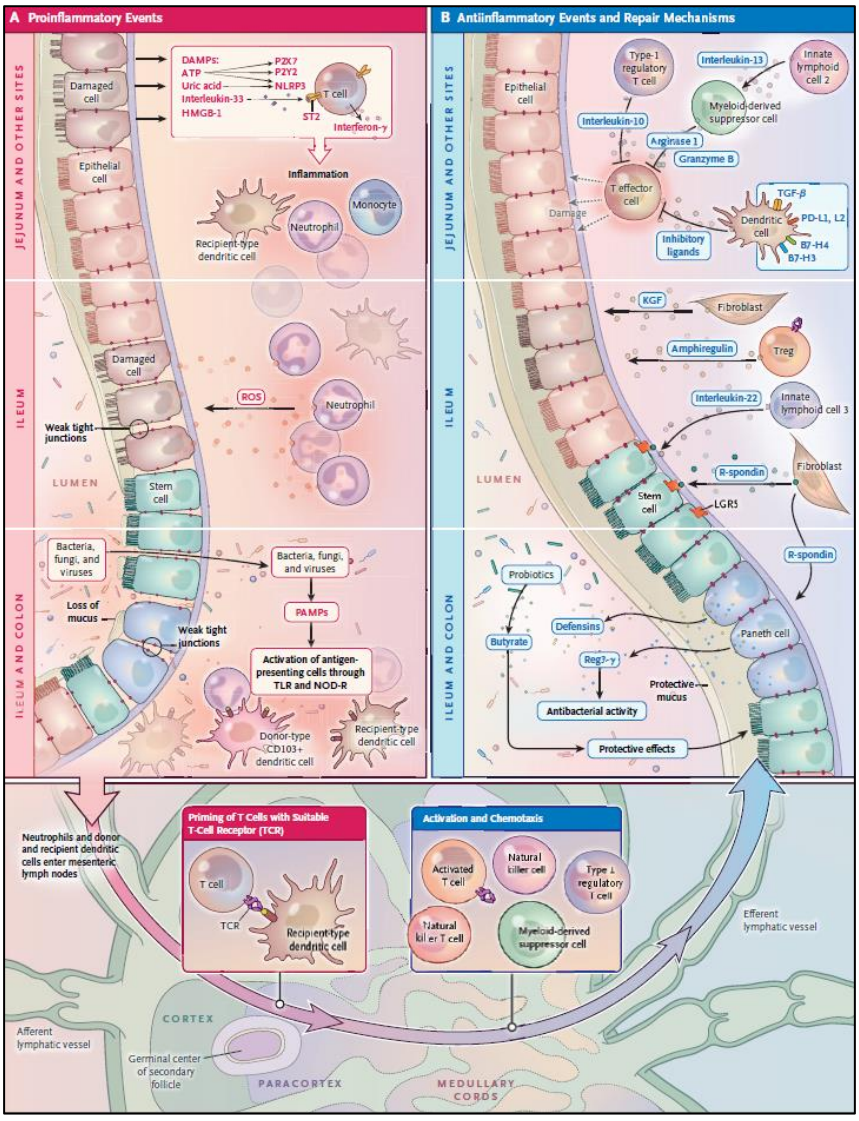

(Zeiser and Blazar, 2017)

Figure 4. Dual response brought to play throughout the early phase of aGvHD While the initial breach of the intestinal barrier integrity propagates a pro-inflammatory response, signals promoting anti-inflammatory events are also generated, including the secretion of tolerogenic soluble factors, the production of Tregs-specific chemoattractants, the support of tissue healing and repair mechanisms as well as the re-shaping of the intestinal microbiota through release of metabolites and peptides exerting anti-microbial activities.

1.2.3. Effector phase

1.2.3.1. Plurality of the effector arm of aGvHD

The local cytokine environment at the time of priming dictates the polarisation of naive T cells towards various lineages of effectors, including Tregs, Th1, Th2 and Th17 cells, which secrete distinct panels of cytokines mediating tissue-specific injuries (Henden and Hill,

2015). The dominance of INF-γ-producing Th1 subsets in aGvHD is well established and drives damages to the gastrointestinal tract, while Th2 cells, often mistakenly solely seen as a Th1 antagonist, elicit cutaneous and pulmonary pathology. In fact, this functional duality constitutes an attractive target, the injection of *in vitro* GM-CSF-derived myeloid-derived suppressor cells (MDSCs) in BMT mice models favouring the shift towards a Th2-polarised immune response critical for GvHD prevention (Messmann et al., 2015; Scheurer et al., 2021). The alteration of the cytokine environment by MDSCs is here apparent, further exacerbated in combined MDSCs/Tregs adoptive therapy with IL-10-producing Breg induction and Treg skewing at the expense of Th1/Th17 lineages, resulting in aGvHD alleviation (Park et al., 2020). The Th1/Th2 paradigm was indeed revisited with the inclusion of Th17 subsets since lethal aGvHD presenting cutaneous and pulmonary lesions was evidenced following infusion of *in vitro* IL-6/ TGF-β-differentiated Th17, with TNF-α and IL-17 as the key mediators (Carlson et al., 2009). Interestingly, the dynamic changes of Th17 cells and Tregs are inversely correlated during the onset and resolution of aGvHD, emphasising a reciprocal relationship mediated by Th17-associated cytokines altering the fate of Treg phenotype (Liu et al., 2013). Indeed, Th17 cells developmental commitment is closely linked to that of Tregs, with IL-6 identified as a critical determining factor of the balance between these two lineages by inhibiting TGF-β-induced Treg differentiation (Fu et al., 2014). This interchangeability is not restricted to the Th17/Treg axis as evidence show the existence of a mutual regulation between Th1 and Th2/Th17 cytokines which may favour one subset over another and consequently, redirect tissue targeting to specific localisations (Yi et al., 2009). As T cell activation persists, the milieu is progressively exhausted in IL-15 and thus, limits its availability for NK cell homeostasis (Simonetta et al., 2017), dismissing here a key moderator of aGvHD severity. Indeed, the infusion of IL-15 pre-activated NK cells in TCD-BMT mice suppressed aGvHD (Hüber et al., 2015). In support of this, a reduction of GvHD severity in TCD-BMT mice was attributed to donor NK cell-mediated lysis of co-injected INF-γ-producing donor Tcons and increase of the donor Tregs/Tcons ratio, an effect seemingly restricted to an early time window before GvHD induction (Olson et al., 2010). Of note, up to 14 days post-transplantation, T cells are outnumbered by IL-10-producing NK cells, however the NK:T ratio progressively declines as the time progresses (Chan et al., 2018).

Altogether, the cytokine milieu appears to exert a tight control of the outcome of the immune response by introducing a shift in the balance between suppressors and promotors of

aGvHD, the complexity of which lying in the dual functions held by certain components of the immune system, ultimately dictating the extent of tissue damage (Holtan et al., 2014) (Figure 5).

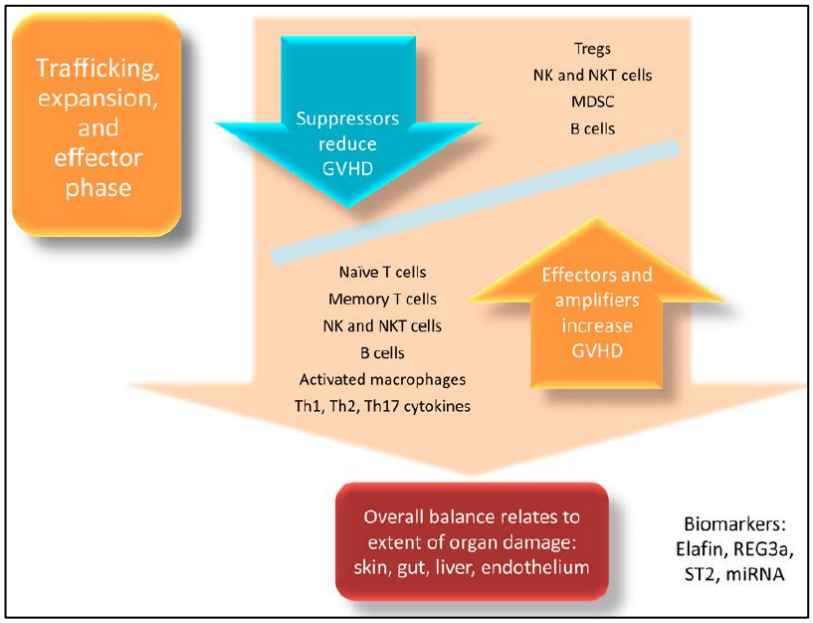

(Holtan et al., 2014)

Figure 5. The balance between tolerogenic and pro-inflammatory signals dictates the extent of tissue damage The composition of the cytokine micro-environment at the priming stage governs the polarisation into a Th1/Th17 or Treg/Th2 effector adaptive response, either resulting in localised tissue damage or aGvHD alleviation, respectively. INF-γ-producing Th1 cells mediate gastrointestinal damages while TNF-α- and IL-17-producing Th17 elicit pulmonary and cutaneous injuries. The Treg/Th17 axis is subject to interchangeability relative to IL-6 levels which preferentially supports Th17 differentiation. NK cells can increase the Treg/Tcons ratio and confer protection against aGvHD unless IL-15 availability becomes limited in case of persistent T cell activation. MDSC induce IL-10-producing Bregs which drive a shift towards a Th2 phenotype at the expense of Th1 subsets and stimulate Treg development over the Th1/Th17 axis, supporting the resolution of aGvHD. However, a possible alteration of skin and lung tissues by Th2 could still be at stake. Overall, the extent of tissue damage is closely related to a tight balance between suppressor and effectors of aGvHD interconnected with the nature of the cytokine milieu.

Alloreactive donor T cells enter target tissues through a chemokine receptor-mediated homing mechanism to perform their cytolytic functions, CD8 T cells inducing apoptosis in adjacent cells through Fas/FasL interaction, perforin/granzyme signalling and TNF-α secretion, therefore requiring cognate interaction, whereas this prerequisite is eluded in the CD4 T cell response in which TNF-α and IL-1β are the major mediators (Markey et al., 2014).

1.2.3.2. Clinical manifestations of aGvHD

The clinical manifestation of aGvHD is commonly assessed through the extent of cutaneous alterations, classically evoking the outbreak of a maculopapular rash on the face, palms, soles spreading out to the trunk with a risk of progression to diffuse erythroderma and toxic epidermal necrolysis (Strong Rodrigues et al., 2018). Indeed, TNF-α and IL-1β are reported to be among the key drivers of the premature induction of apoptosis in basal stem cell-like epidermal keratinocytes present in lesional skin resulting in the dysregulation of normal skin tissue homeostasis, impeding the sustainment of wound healing mechanisms (Hofmeister et al., 2004). Also, a breach in the skin commensal microbiota integrity could be a stake considering the antimicrobial functions exerted by TLR-expressing keratinocytes via cathelicidin and β-defensins secretion (Matejuk, 2018), here extrapolating from the dysbiotic events taking place in gut aGvHD. The third key clinical occurrence is hepatic GvHD, characterised by altered biliary epithelial tissues conducive to ductopenia, cholestasis, necroinflammation and deposition of fibrotic tissue, however no precise histopathological criteria clearly singles out a GvHD aetiology from other liver dysfunctions, hence the concomitant manifestation of skin and/or gastrointestinal GvHD is sought (Matsukuma et al., 2016). While associated with the lowest incidence, its diagnosis is all the more critical since evidence identifies hepatic aGvHD complications as a strong prognostic factor for worsened OS and higher rates of TRM in grades II-IV aGvHD, correlating the existence of previous history of hepatitis C infections and liver failures as risk factors alerting on the need for new prophylactic strategies better addressing these outcomes (Arai et al., 2015).

As soon as the involvement of classical target organs of aGvHD are identified, the differential diagnosis for kidney aGvHD should be carried out in case of acute kidney injury since it is a multifactorial complication, arising as a result of the GvHD prophylactic nephrotoxic and thrombotic medication, exposure to cryoprecipitants infused with the graft or reactivation of viruses in immunocompromised patients (Krishnappa et al., 2016). In fact, the spectrum of aGvHD affected organs is being extended, including the lungs and central nervous system although, similarly to acute kidney injury, no exclusive diagnostic criteria exists to attribute their clinical manifestations, encephalitis and idiopathic pneumonia syndrome, respectively, to an aGvHD aetiology without resorting to the identification of concurrent skin, gut or liver aGvHD (Mariotti et al., 2020). Also, aGvHD seems to be driven against the BM stromal cell environment which sets the foundation for normal functional

haematopoiesis, the outcome of the alterations introduced being graft failure caused by poor graft function (PGF) (Chen et al., 2020). Occurring in 5-27% of allogeneic HSCT recipients with aGvHD accounting for 14% of cases, PGF presents a minimum of persistent bilineage cytopenia commonly describing a thrombocytopenia with concomitant neutropenia and anaemia, which, unlike graft rejection, involves an hypoplastic BM under full donor chimerism (Imamura, 2021). Interestingly, the dysregulation of the B cell compartment seems to be a major manifestation of PGF, a lesser effect being recorded on the myeloid lineage while T lymphopoiesis appears to rather be influenced by the extent of thymic and lymphoid organ injuries (Müskens et al., 2021). Emerging evidence shows a CD4 T cell-directed destruction of the endosteal osteoblastic niche resulting in the impairment of B lymphopoiesis independent of class II MHC recognition (Shono et al., 2010). This mechanism is suggested to be fuelled by the induction of apoptotic pathways triggered by TNF-α and INF-γ, also driving dysfunctional mesenchymal stem cell activities which no longer support HSPCs renewal (Müskens et al., 2021). In line with this, the sinusoidal vascular endothelial niche undergoes apoptosis mediated by CD4 T cells through Fas/FasL interaction supposedly bringing into play TCR-class II MHC ligation, consequently failing to sustain haematopoietic reconstitution (Yao et al., 2014).

1.3. IL-15: a putative role in aGvHD

Over the past 60 years, a better insight of the intricate machinery driving aGvHD has been acquired, notably outlining more accurately how the initial breach in tissue integrity sets its foundation, a process within which IL-15 appears to hold a significant role.

Primarily produced by dendritic cells (DCs), macrophages and a variety of tissues, notably epithelial cells, endothelial cells, fibroblasts and keratinocytes, IL-15 is a major regulator of CD8 T cell and NK cell homeostasis and effector functions signalled through a receptor complex formed by the shared IL-2/15Rβ and the γC subunit (Castillo and Schluns, 2012; Stonier and Schluns, 2010). The existence of a private α receptor subunit displaying a higher affinity for IL-15, namely IL-15Rα, which, further to its association with IL-2/15Rβ/γC, enhances a distinct response providing notably a better sustainment of T cell proliferation, shed light on a specific mechanism behind the IL-15 response. Indeed, IL-15Rα/IL-15 complex found on haematopoietic cells, endogenously synthesised and shuttled to the cell surface, can interact with IL-2/15Rβ/γC on an opposing cell to stimulate it as part of a

mechanism called trans-presentation, particularly required for the promotion of CD8 T cell proliferation since they express IL-2/15Rβ/γC but not IL-15Rα. Strikingly, empty cell surface IL-15Rα are ubiquitously expressed across the lymphoid and myeloid compartment, accounting for the existence of an alternative mechanism, referred to as cis-presentation, postulated to prevail in IL-15-rich environments in which, further to its capture, the hereby formed IL-15Rα/IL-15 complex would interact with an adjacent IL-2/15Rβ/γC in an autocrine fashion. Furthermore, in circumstances where all IL-15Rα are occupied, IL-15 would transduce its signal directly through IL-2/15Rβ/γC, although exerting a weaker T cell response as opposed to an IL-15Rα-dependent pathway.

Efforts were put in scrutinising the cytokine network existing in aGvHD, notably unravelling the kinetics of plasma IL-15 production which, although exhibiting minor discrepancies with regards to the exact time course, provided a correlation between chronic systemic levels of IL-15 and the incidence of severe aGvHD. Thus, identifying IL-15 as a key effector since its production paralleled the manifestation of clinical symptoms, regardless of the intensity and nature of the conditioning regimen applied (Sakata et al., 2001; Thiant et al., 2011, 2010). The potential sources of tis cytokine are manifold, whether released as a consequence of tissue injury or secreted by macrophages and DCs in response to the acute inflammatory environment established. IL-15 is also produced by BM stromal cells in response to the profound lymphopenia commonly identified in allogeneic HSCT patients, here targeting the homeostatic status of T cell in an attempt to drive their proliferation and survival to ultimately achieve immune reconstitution (Matsuoka et al., 2013). Notably, post-transplant IL-15 administration to TCD HSCT recipients was found to enhance the recovery of $CD122^{+}CD44^{+}$ memory CD8 T cells, NK cells and NK T cells and was associated with modest GvT effect against lymphoma cells while no aggravation of GvHD in T cell-replete settings was observed, although this was dose and time dependent (Alpdogan et al., 2005). Similar recovery patterns were recorded in TCD haplo-HSCT recipients undergoing post-transplant IL-15, although showing a preferential sustainment of slow-proliferative $CD62^{+}CD44^{+}$memory-like CD8 T cell reconstitution with a higher INF-γ secretory status. This is suggested to be the main mediators of the GvT effect achieving P815 tumour resolution when combined with low-dose donor T cell infusion without significant induction of GvHD (Sauter et al., 2013). Hence, IL-15 used as an adjuvant therapy for TCD HSCT offers interesting outlook to address the high rates of disease relapse, graft failure and infections recorded in this particular context (Bertaina et al., 2017; Negrin, 2015). However,

this approach would be difficult to apply to other types of allogeneic HSCT as evidence showed that unlike IL-2, IL-15 administration resulted in lethal xenogeneic GvHD in severe-combined immunodeficient mice grafted with human peripheral blood lymphocytes (hu-PBL-SCID) paralleled with high systemic INF-γ levels, also depicting a selective expansion of memory CD8 T cells (Roychowdhury et al., 2005). Of note, IL-15 constitutes a determining regulator of the fate of autoreactive CD8 T cells by inducing a breach in the existing peripheral tolerogenic state. This was demonstrated in a K14-mOVA^{low} Tg mice by the conversion of adoptively transferred tolerant OT-I cells into functionally active INF-γ-producing effectors, resulting in the emergence of clinical hallmarks of GvHD equalling those observed in K14-mOVA^{high} Tg mice in which case endogenous IL-15 was identified as a key contributor (Miyagawa et al., 2008). In fact, these characteristic functions of IL-15 are described in therapeutic strategies aiming at rescuing the anti-tumour activity of tolerant CD8 T cells. Indeed, the tolerance of TCR^{Gag} CD8 T cells towards the hepatic Gag antigen, representing a candidate tumour antigen, in TCR^{Gag}-Tg mice was abrogated in response to exogenous IL-15 and resulted in their proliferation and acquisition of antigen responsiveness, an effect poorly reproduced with IL-2 administration (Teague et al., 2006). Supporting results involving TCR^{pmel-1} mice expressing the self/melanoma antigen gp100 towards which TCR^{pmel-1} CD8 T cells are tolerant showed that the adoptive transfer of antigen-primed TCR^{pmel-1} CD8 T cells cultured in IL-15 supported the expansion of CD44^{+}CD122^{+} central memory (T_{CM})-like CD8 T cells, which delayed tumour growth and improved survival of recipients. This is in contrast to the effect observed with IL-2, which favoured the polarisation to IL-10-producing effector memory (T_{EM})-like T cell phenotype (Klebanoff et al., 2004). The advantage conferred by IL-15-mediated expansion of tumour-reactive CD8 T cell responses over IL-2 may also find an explanation in the delay/reversal of T_{CM}-like CD8 T cell senescence evidenced by the high percentage of cells arrested in the S/G2 phase under proliferative stimulus, increased STAT5 signalling and decrease in senescence-associated markers (Weng et al., 2016).

Furthermore, IL-15 trans-presentation between donor haematopoietic IL15Rα/IL-15-producing and -bearing cells and primed donor allogeneic CD8 T cells emerged as central to the onset and mortality of aGvHD, promoting particularly the polarisation towards CD8 Tc1 cells at the expense of CD4 Th2 and CD8 Tc2 lineages, as evidenced by the increased levels of T-bet mRNA and IFN-γ (Blaser et al., 2006, 2005). This could exacerbate aGvHD, since IFN-γ is described as a key enhancer of antigen presenting functions, the surface expression of class II MHC molecules and costimulatory ligands being upregulated, but also

a mediator of tissue damage. Although posed as the predominant mechanism driving aGvHD, the abrogation of donor-derived IL-15 trans-presentation did not achieve complete recovery, but only postponed its associated mortality, thus highlighting distinct impact of the host-derived cytokine microenvironment (Blaser et al., 2006). Notably, a kinetics of IL-15 production is correlated with aGvHD severity, potentially signalling through a trans-presentation independent pathway as described in IL-15-rich settings.

Altogether, these data suggest that IL-15 represents a key component of the aGvHD pathophysiology, decisive for the breach in peripheral tolerance, and consequently, a relevant target for putative therapeutic strategies.

1.4. aGvHD prophylaxis: refining the therapeutic strategies

1.4.1. Current challenges

Pivotal in cutting down the tumour burden and ensuring proper engraftment, the preparative regimens face a major setback as they are at the root of early tissue injury, a key event setting the ground for aGvHD initiation (Nakasone et al., 2015). This prompted attempts to resort to RIC which harness the GvT effect to counterbalance the curb in chemotherapy and radiation doses and thus, sustain the elimination of malignant cells (Barrett, 2008; Sweeney and Vyas, 2019). However, the extent to which it relies on the GvT effect determines the level of immunosuppressive agents required to support HSC engraftment (Figure 6) (Gyurkocza and Sandmaier, 2014). Hence, although minimising tissue trauma, RIC is associated with higher incidence of disease relapse, interpatient variances being also reported. As a result, no standards treatment is yet at hand.

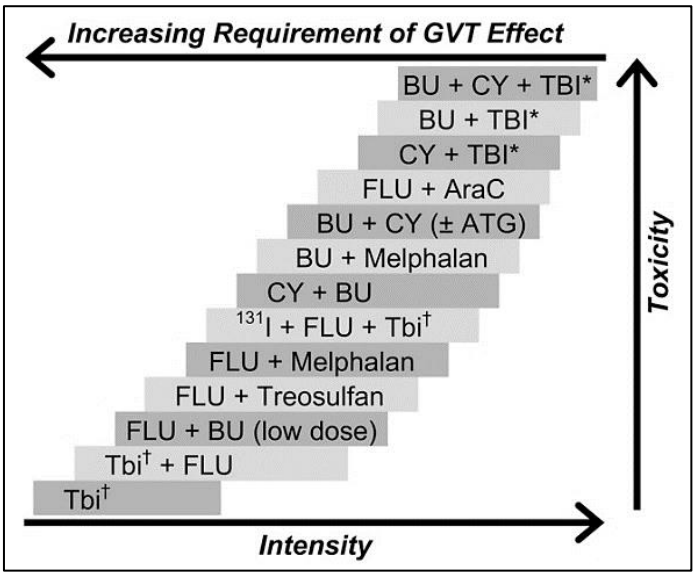

(Gyurkocza and Sandmaier, 2014)

Figure 6. Spectrum of RIC regiments displaying the extent of their immunosuppressive properties in correlation with their toxicity and reliance on the GvT effect In an attempt to minimise the extent of tissue injury incurred by chemotherapy and TBI, and thus, curtail aGvHD initiation, RIC of varying intensities were developed. The reliance on the GvT effect increases as the intensity of RIC lessens, posing however a higher risk of disease relapse.

The classical T cell-targeted immunosuppressive therapeutics encompass inhibitors of calcineurin (cyclosporine, tacrolimus), cell proliferation (methotrexate, mycophenolate mofetil) and mTOR (rapamycin, sirolimus). They suffer major drawbacks with regards to their lack of selectivity and narrow therapeutic index, conducive to off-target toxicities (Ferrara et al., 2009). Not only is it compromising the prospect for patient full recovery, but it can also potentially further propagate the aGvHD reaction. Indeed, these therapeutics induce endothelial damage and mucositis which are characteristic complications associated with TBI, correlated with the progression to grade II-IV aGvHD (Nakasone et al., 2015).

As the pathophysiology of aGvHD was better understood, therapeutic strategies directed against distinct key T cell-centred processes were implemented. This included the targeting of T cell activation by disrupting the JAK/STAT pathway-mediated transduction of pro-inflammatory cytokine signals. Alternatively, hampering their priming and trafficking by altering co-stimulatory and co-inhibitory signals and chemokine receptor-ligand binding, respectively. However, these two latter approaches adversely affect the beneficial suppressive response induced by Tregs (Blazar et al., 2012).

Indeed, a successful approach taking advantage of the distinct patterns of homeostatic support provided by low-dose IL-2 offered a promising outlook for the selective expansion of stable and functional Tregs to sustain corneal transplant survival (Tahvildari and Dana, 2019). This is based on the exclusive and abundant constitutive expression of the high affinity IL-2 receptor α (CD25) on Tregs, hence conventional T cells (Tcons) are eluded as they would require high IL-2 concentrations, a deprivation of homeostatic support further sustained as the achievement of lymphocyte recovery reinstates basal IL-7 and IL-15 levels (Matsuoka et al., 2013). The injection of ultra-low dose IL-2 in a clinical trial increased the frequency of *in vivo* Tregs from 4.8% to 11.1% which was sufficient to protect against aGvHD (Guo et al., 2021). Importantly, this mechanism seems to spare the GvT effect since no record of disease relapse in patients with active cGvHD was made while a reduction of the clinical manifestations in the liver, skin, gastrointestinal tract and lungs was observed (Elias and Rudensky, 2019). Although prolonged exposure to low-dose IL-2 appears to exert antagonistic functions and bring Tcons to an equal state of sensitivity towards IL-2 than Tregs, the concurrent administration of rapamycin seems to rescue the original homeostatic imbalance, emphasising the synergistic effect of its selective immunosuppressive targeting of Tcons resulting in the protection against skin graft rejection in mice (Pilon et al., 2014). Alternatively, low-dose IL-2 as an adjuvant to *in vitro* Treg expansion protocols represents an interesting strategy to yield sufficient numbers for adoptive therapy since they only account for 2-10% of peripheral CD4 T cells, further supported *in vivo* with the concourse of low-dose IL-2 therapy (Blazar et al., 2018). Tregs in these settings displayed a diverse degree of protection against GvHD, an effect also recorded whether infused concomitantly with Tcons at a 1:1 ratio or 2 days before at a 1:10 ratio although the Tcons-mediated GvT effect is spared (Mancusi et al., 2019). Indeed, while attempting to impede aGvHD, care must be taken to not completely obliterate the GvT effect, notably demonstrated in TCD-HSCT where increased incidence of graft failure, disease relapse and severe opportunistic infections are recorded (Li Pira et al., 2016). Thus, it is crucial to fine-tune the balance between the GvT effect and aGvHD. Delayed DLI in TCD-HSCT patients aimed to restore the GvT effect prior to host APC activation, however diverging outcomes linked to the lymphopenic state of the patient were observed, questioning the applicability of this strategy (Li et al., 2009).

Therefore, the potency of a therapeutic strategy relies on the achievement of a clear separation between the GvT effect and aGvHD. Low-dose IL-2 protocols seem to

successfully address this issue in a generic approach. The rational for a more refined method taking advantage of miHA differential tissue distribution could also offer interesting prospects in this aspect.

1.4.2. Separating GvL from aGvHD: miHA targeting

The evidence showing that the GvT effect could arise independently of GvHD led to the assumption that miHAs may be differentially expressed across tissues and that therapeutic strategies exploiting these non-self antigenic determinants could help separate GvHD response from GvT (Feng et al., 2008). Indeed, miHAs restricted to cells of the haematopoietic compartment were shown to trigger donor-derived T cell cytotoxicity against leukemic cells resulting in disease remission with minimal reactivity against host non-haematopoietic tissues, emphasising the need for the distribution profile of miHAs to be determined. This is achieved through molecular characterisation of peptides eluted from miHA-specific cytotoxic T cells, isolated either from allogeneic HSCT patients or following co-culture with skin fibroblasts, genome-wide analysis through cDNA library screening, genetic linkage study or prediction using the HapMap project which indexes common SNP variants associated with haematological malignancies (Bleakley and Riddell, 2011). The immunodominant nature of miHAs, referring to their ability to trigger an immune response, is however not taken into account. Moreover, in cases involving ubiquitously-expressed miHAs, the absence of GvHD was reported although host non-haematopoietic miHA-specific T cells were detected, suggesting that a certain threshold of reactivity must be reached for GvHD to occur (Griffioen et al., 2016)**.** Hence, in addition to its tissue distribution, the therapeutic value of a given miHA not only depends on its immunodominance but also on the intensity of the alloresponse it can elicit. This stresses the importance of evaluating the strength of the inflammatory response in *in vitro* models accounting for the physiological environment observed in the context of allogeneic HSCT, especially the early phase since the impact of the conditioning regimens on the amplification of the immune response is considerable.

1.4.2.1. Harnessing the cytotoxic potential of miHA-specific CD8 T cells to restore the GvL effect

Following the development of tissue restricted-miHA targeting therapeutic strategies, the MHC specificity of miHAs was considered to be relevant. Although class I MHC molecules are expressed on all nucleated cells, class II MHC molecules are exclusively found in the haematopoietic compartment on professional APCs, whether malignant or not, therefore providing conditions where T cells specific for class II MHC-restricted miHAs could promote the GvT effect (Warren et al., 2012).

A particular attention was given to the adoptive transfer of *ex-vivo* expanded miHA-specific $CD8^+$ T cells isolated from patients with post-transplantation relapse in order to restore the GvT response. The objective being to generate class II MHC-restricted miHA-specific cytotoxic CD8 T cells for the specific targeting of any remaining malignant haematopoietic cells, although involving a complex multistep protocol unfit for implementation in a clinical setting and unlikely to reach the expected cell yield (Warren et al., 2010). Moreover, the short *in vivo* viability of these cells negated the achievement of sustained remission, potentially arising from the appearance of IL2-dependent effector T cells throughout the *in vitro* selection and expansion process. In order to circumvent these issues, T cells genetically engineered to express a miHA-specific T cell receptor (TCR) represented a considerable advantage with respect to their efficient generation involving a short-term *in vitro* culture for the transduction of the vector of interest (Bendle et al., 2010). However, the manifestation of GvHD following the adoptive transfer of T cells expressing a transgenic ovalbumin-specific OT-I TCR in leuko-depleted mice highlighted the existence of self-reactive chimeric TCRs characterised by a mispairing between the TCR dimers. Presenting similar technical benefits, the generation of chimeric antigen receptor (CAR)-expressing T cells consisting in the miHA-specific monoclonal antibody variable regions conjugated with the CD28 transmembrane and CD3ζ domains were found to be 100fold less sensitive to exposure to the miHA than the cognate cytotoxic T cell, limiting the prospect for clinical implementation (Inaguma et al., 2014).

1.4.2.2. Tolerance induction: a safer approach?

An alternative way of taking advantage of the differential miHA tissue distribution is to drive a tolerogenic immune response towards T cells specific for miHAs presented on host non-haematopoietic cells and therefore, impair aGvHD while sustaining the GvT effect. Because class I MHC molecules are ubiquitously expressed on nucleated cells, establishing tolerance specifically towards class I MHC-restricted miHAs could repress donor-derived miHA-specific T cell activation and consequently, preserve the integrity of host non-haematopoietic tissues presenting these particular miHA. Although class I MHC molecules are also present in the haematopoietic compartment, the GvT effect would still be sustained considering the large repertoire of miHAs for which donor/recipient pairs are mismatched (Warren et al., 2012). Indeed, the existence of disparities in class II-restricted miHAs would provide the elimination of any residual malignant haematopoietic cells bearing the corresponding miHAs.

Noteworthy, the induction of tolerance represents a safer approach than establishing a targeted cytotoxicity for the exclusive removal of malignant cells using class II MHC-restricted miHA-specific T cells. Indeed, mechanisms of endogenous class II MHC presentation of peptides were reported, implying that class I MHC-restricted miHAs could potentially be also presented on class II MHC molecules, leading to a cross-reactivity causing deleterious effects on host non-haematopoietic tissue. Furthermore, as part of the well described semi-direct priming, donor APCs could be led to acquire host cell-derived full class I and II MHC-allopeptide complex following trogocytosis and thus become potential targets for class II MHC-restricted miHA-specific cytotoxic CD8 T cells, the prospect for successful engraftment being therefore severely hindered.

However, in the context of intense inflammatory environment such as that observed in aGvHD, host non-haematopoietic cells could be induced to express class II MHC molecules, thus escaping the desired tolerogenic response directed towards class I MHC-restricted miHAs and becoming potential target for aGvHD. Primarily mediated by INF-γ, this phenomenon was reported to notably occur in the intestine and liver where the functional outcomes remain to be determined (Duraes et al., 2013). It is suggested that, while they can participate in their proliferation once activated, non-haematopoietic APCs cannot efficiently prime naïve T cells, thus no clinical significance was observed. They even show suppressive functions potentially resulting from the lack of strong co-stimulatory activities, as evidenced by the absence of B7 molecules, or provision of anergic stimuli via the expression of ICOS-

L and PDL-1, although this function could be restored after treatment with IL-1β and IL-6. Therefore, it seems that the micro-environment inflammatory status dictates the functional capacity of non-haematopoietic cells to initiate a potent immune response, strictly depending on a tight balance between pro-inflammatory and tolerogenic mediators. This context is characteristic of aGvHD in which IL-1β and IL-6 constitute the predominant cytokines released during the early phase, as a consequence of conditioning-induced tissue injury. Hence, with the mitigation of early inflammation, it can be speculated that if such non-haematopoietic APC were generated in the course of aGvHD, the likelihood to trigger T cell activation would be low. And in so far as any were detected, the clinical relevance would be negligible considering the poor reactivity of these T cells, particularly in an immunological context where a certain threshold of reactivity must be met to induce a clinical effect.

In practice, such tolerogenic approach was undertaken through the *ex vivo* expansion of miHA-specific Tregs by coculture with HLA-matched host DCs following purification from leukopheresis samples using CD25-coated beads, achieving a 78% purity (Veerapathran et al., 2013). Although fully functionally characterised with respect to their suppressive activities, TGF-β production and FoxP3 expression, the stability of this phenotype was not investigated in the context of GvHD and thus, does not take into account the intense inflammatory environment elicited in the physiological conditions which could potentially alter the effector functions of these miHA-specific Tregs after adoptive transfer. Indeed, FoxP3 expression can be repressed following methylation of the FoxP3 enhancer region, leading to the abrogation of the suppressive functions of Tregs, a process mediated by the pro-inflammatory cytokine IL-6 (Lal et al., 2009). Similarly, IL-21 was shown to block the acquisition of FoxP3 expression in naïve T cells and thus, disrupt their conversion into Tregs, emphasising the unstable nature of the regulatory phenotype of these cells in the inflammatory milieu of GvHD (Bucher et al., 2009).

It emerges from these data that prospective therapeutic strategies should integrate a dual strategy. Firstly, to curtail early inflammatory events, while limiting the breach in tissue integrity. Then, to promote therapies propitious to tissue healing and regeneration. This could be achieved by targeting the priming phase of GvHD and introducing a state of tolerance. Overall, the goal is to readjust the existing equilibrium amongst promoters and suppressors of aGvHD in an effort to achieve long-term tolerance (Zeiser and Blazar, 2017). Although constrained by technical limitations, miHA-specific Tregs hold promising

potential considering the successful outcomes achieved with low-dose IL-2 protocols. It remains to be determined, however, if other cells could offer such tolerogenic signal.

1.5. B cells as APCs in acute GvHD: a potential target?

1.5.1. Emerging evidence of a role for B cells in aGvHD: which B cell targeting options hold interesting prospects?

Although GvHD is primarily defined as a T-cell-mediated event, a growing interest in the relevance of B cells emerged regarding the critical impact of their antigen-presenting and antibody-producing functions. This could be particularly important in the setting of chronic GvHD (cGvHD) (Sarantopoulos et al., 2015). Indeed, the successful implementation of the anti-CD20 chimeric antibody rituximab, a B cell depleting agent, for the management of established cGvHD prompted attempts of including rituximab also as a preventive treatment for acute GvHD. However, the reported immunoregulatory functions exerted by B cells, either through indirect expansion of Tregs or mediated by the newly described regulatory B cells (Bregs) (Clatworthy, 2011) could complicate this therapeutic approach. Bregs are still poorly phenotypically characterised, their identification relying on the detection of IL-10 production. However, the extent of the immunosuppressive functions of Bregs is now better outlined, including the impairment of the $CD8^+$ cytotoxic T cell-mediated response and the cytokine-induced inflammation as well as the promotion of Treg expansion and functions, brought about by IL-10, IL-35 and TGF-β production (C. Wortel and Heidt, 2017). The activation of Bregs results from the presence of an inflammatory milieu as a way to provide a negative feedback loop and to control its intensity, notably to oppose the pro-inflammatory cytokine IL-6, belonging to the cytokine storm produced in the initiation phase of aGvHD. Despite the therapeutic potential of Bregs, until their phenotype is better characterised and a robust protocol of Breg induction is designed, the establishment of B cell depleting strategies preserving Bregs, as well as the development of Breg-induced tolerance towards miHAs expressed on host non-haematopoietic cells remain limited (Mauri and Menon, 2015). It is worth noting however that the prophylactic potency of rituximab for the prevention of aGvHD was evidenced as its administration prior to allogeneic HSCT was correlated with a lower incidence of aGvHD, stressing here a role of B cells in early aGvHD as priming effectors (Christopeit et al., 2009; Crocchiolo et al., 2011). Hence, it appears that the timing of treatment dictates which B cell subset will be affected, either the Breg-

associated immunosuppressive response or the B cell-associated T cell priming. Notably, this latter mechanistic option also offers interesting prospects to harness the tolerogenic potential of B cells with poor antigen presenting functions, referred to as resting B cells.

Indeed, these properties of resting B cells have been demonstrated in InsHA mice expressing the haemagglutinin protein HA from the PR8 influenza virus. In this model, K^dHA-specific resting B cells, recognising the variant K^dHA, generated by peptide pulsing were shown to induce self-tolerance within K^dHA-specific naïve CD8 T cells through induction of their proliferation without acquisition of effector functions followed by their depletion, referred to as abortive activation (Fraser et al., 2006). Similarly, in a mouse model of autoimmune encephalomyelitis, resting B cells genetically engineered to express the myelin oligodendrocyte glycoprotein (MOG) provided a protective effect against the T cell-mediated demyelination by inhibiting the accumulation of autoreactive $CD8^+$ and $CD4^+$ T cell and affecting the humoral immunity, as evidenced by the reduced level of autoantibodies (Calderón-Gómez et al., 2011). Their immunoregulatory properties are also manifested through the instauration of an anergic state in $CD4^+$ T_h0 clones unable to produce IL-2, therefore impairing the acquisition of the $CD4^+$ T_h1 phenotype, which exert critical stimulatory functions in $CD8^+$ T cell activation (Gajewski et al., 1994). Further to their immunoinhibitory functions, the contribution of resting B cells to the maintenance of peripheral tolerance was highlighted, as they can promote the expansion and survival of existing Tregs through TGF-β3 secretion, a feature lost when they get activated (Shah and Qiao, 2008). Recently, the assumption that thymic B cells are only generated as a "default cell fate" from Notch-negative early thymic progenitors has been revisited, conferring resting B cells with a role in central tolerance (Yamano et al., 2015). Indeed, they were shown to migrate into the thymus where they recapitulate the phenotype of thymic B cells after a licensing process performed by $CD4^+$ SP cells and take part in the negative selection of autoreactive $CD4^+$ T cells, following the same mechanism as medullary thymic epithelial cells (mTECs) with regard to the Aire-dependent expression of tissue-restricted peripheral antigen (TRAs). The extent of thymic B cell functions was revisited, bringing into light their involvement in the generation and expansion of thymus-derived Tregs similarly to thymic DCs (Lu et al., 2015). Overall, this gives an insight into the breadth of the tolerogenic potential of resting B cells. However, the significance of the contribution of resting B cells to the thymic B cell repertoire was disputed. A study using mouse model of parabiosis showed that resting B cells were minimally recirculated to the thymus as opposed to the phenomenon observed with splenic B cells (Perera et al., 2013). Nonetheless, this does not

take into account the impact of extrinsic factors modulating the homing process. Such signalling could be induced in acute GvHD where mTECs are eliminated by alloreactive donor T cells (Dertschnig et al., 2015), as a mean of re-shaping the thymic environment.
Hence, abrogating B cell antigen presenting functions could be of clinical significance to shield from aGvHD. In addition, harnessing the tolerogenic properties harboured by resting B cells could offer patients promising prospects for long term recovery, although this has been given surprisingly little attention. Indeed, such strategy would take advantage of their peripheral immunoinhibitory potential exerted through mitigation of the CD4 T cell help and induction of Treg expansion, as well as their participation to the establishment of central T-cell tolerance. The contribution of Bregs to the mediation or amplification of this effect, as they exert similar functions, needs to be determined. In order to fully exploit these properties, the identification of the regulators involved in the transition from resting to activated B cells is essential.

1.5.2. B cells: from resting to activated state

1.5.2.1. B cell ontogeny and priming

The basic structure of an Ig, present at the surface of B cells as an antigen receptor (BCR), consists in two identical heavy (H) and light (L) chains, either κ or λ, which N-terminal domains are home to three hypervariable regions implicated in antigen recognition, termed complementarity-determining regions (CDR1-3) (Tonegawa, 1983). Initiated in the BM from HSC-derived common lymphoid progenitor cells, B cell development involves a stepwise process of V(D)J immunoglobulin (Ig) gene rearrangement within the Ig variable regions, also termed somatic recombination, yielding unique specificities at the root of BCR diversity (Wang et al., 2020). Each V (variable), D (diversity), and J (joining) gene segment is flanked by recombination signal sequences (RSSs) consisting of an heptamer and nonamer motif with an intervening 12- or 23-bp spacer, defined as 12RSS and 23RSS, respectively, recognized by recombination activating gene (RAG) proteins (RAG1 and RAG2) (Roth, 2014). In accordance with the 12/23 rule, a 12RSS/23RSS synaptic complex is formed, followed by DNA nicking at the heptamer/coding flank border and subsequent double stranded DNA break, ultimately generating a covalently sealed hairpin coding end and a blunt signal joint (Schatz and Ji, 2011). The random loss of nucleotides at the junctional interface and thus, imprecise joining end, introduces additional diversity to that yielded with

the combinatorial diversity across the various V, D and J segments, further expanded with the inclusion of short non-templated nucleotides by terminal deoxynucleotidyl transferase to coding ends (TdT) (Jung and Alt, 2004). When a productive IgH locus VDJ rearrangement is completed on one allele, a pre-BCR comprising a μH chain paired with VpreB and λ5 surrogate light chains is displayed at the B cell surface to take part in a checkpoint regulating IgH allelic exclusion and progression to IgL loci VJ rearrangement (Winkler and Martensson, 2018). This mechanism ensures a monoallelic encoding of the IgH chain, also applied to IgL loci rearrangement in addition to which isotype exclusion restricts to either a IgLκ or IgLλ chain, here securing the production of a BCR of unique specificity (Mårtensson et al., 2010). The fate of immature B cells expressing a mature BCR is manifold as they are screened for self-reactivity in the BM environment in order to perpetuate effective central tolerance (Melchers, 2015). Autoreactive B cells undergo central clonal deletion by apoptosis or enter into an anergic state accounting for 30-40% of transitional B cells (Nemazee, 2017). Alternatively, this fate can be rescued through receptor editing in an attempt to alter BCR specificity into becoming self-ignorant, here not only reducing the frequency of autoreactive B cells but also reinforcing the diversification of the antibody repertoire (Luning Prak et al., 2011). Lastly, non-autoreactive immature B cells producing adequate BCR tonic signal differentiate into transitional B cells which acquire markers associated with a mature phenotype, notably IgD, CD21 and CD23, ultimately exported to secondary lymphoid organs where their maturation is initiated further to antigen encounter (Pelanda and Torres, 2012).

Consequently, germinal centres (GCs) in B cell follicles form, a process mediated by follicular DCs (FDCs) displaying intact antigens captured via deposition of circulating immune complexes on FcγRIIB or C3d-coated antigens on CD21 (Batista and Harwood, 2009). Further to BCR-mediated antigen retrieval and engagement in the class II MHC presenting process, resting B cells migrate at the interface between the follicular border and T cell zone where they receive cognate signals from CD4 helper T cells initiating a process of BCR affinity maturation (Zhang et al., 2016). Hence, an interclonal competition exists at the V(D)J level between naïve B cell precursors across the diverse BCR repertoire in a “T cell-centric” model involving the preferential selection of B cells presenting high surface levels of peptide-MHC II complexes (Yeh et al., 2018). Indeed, the discrimination between GC B cells of varied affinities does not seem to be strictly dependent on the strength of BCR tonic signal, rather evoking a model where it is their ability to capture high antigen contents which dictates whether they can outcompete other subsets for follicular CD4 helper T cells

(Allen et al., 2007). The segregation of the GC into two anatomically distinct compartments ensues, notably a dark zone primarily containing compact clusters of highly proliferative B cells, known as centroblasts, where somatic hypermutation (SHM) are introduced in the variable regions of the BCR along with antibody isotype class-switching (Tsai et al., 2019). They subsequently enter the light zone as centrocytes where an intraclonal selection between SHM variants of identical clone origin occurs, ultimately favouring rare B cell clones with the highest BCR affinity (Yeh et al., 2018). A fraction of SHM B cell variants is retained in the GC and re-enter the dark zone to undergo iterative cycles of somatic hypermutations before returning to the light zone for selection by, here emphasizing the dynamic nature of germinal centre reactions (Mesin et al., 2016). This interzonal migration relies on the sequential ability of GC B cells to endocytose antigens deposited on FDCs and present them to GC-resident follicular CD4 helper T cells for selection (Victora and Mesin, 2014). Alternatively, there are driven to transit out of the GC as plasma cells (PCs), returning to the BM to drive the effector arm of the humoral immunity via antibody production, or memory B cells (MBCs), migrating back to secondary peripheral organs to scan for antigens and mount secondary responses (Lau and Brink, 2020). A dichotomy seems to exist in their differentiation programs as PCs exit the GC through the dark zone while MBCs directly egress from the light zone, the later emergence of PCs suggested to facilitate further accumulations of mutations introducing higher antigen affinities compared to MBCs (Suan et al., 2017). These subsets eventually replace IgM-producing short-lived extrafollicular plasma cells yielded in a GC-independent fashion, thus eluding SHM mechanisms, supporting immediate relatively low-affinity humoral responses (Akkaya et al., 2019).

1.5.2.2. Modulators of the BCR-activation threshold

Naive peripheral circulating naïve B cells, referred to as resting B cells, are indeed poor antigen presenting cells, associated with tolerogenic properties, due to the absence of co-stimulatory activities, further acquired after activation by primed $CD4^+$ T cells through CD40-CD40L/CD154 signalling (Rodríguez-Pinto, 2005). They express a BCR complex, formed by the membrane-bound immunoglobulin molecule (IgM, IgD) and the Igα-Igβ heterodimer transmembrane signalling components, also called CD79α-CD79β, containing the immunoreceptor tyrosine-based activation motif (ITAM) transducing the signal for BCR activation following antigen encounter, organized in an autoinhibited form as oligomers (Yang and Reth, 2010a, 2010b). The proposed dissociation-activation model leading to BCR

activation involving the rearrangement into monomeric clusters and subsequent conformational changes exposing the ITAM-containing domains to the protein kinases Lyn and Syk does not exclude the presence of active BCR monomers essential for the provision of the tonic survival signal, mediated through the PI3 kinase signalling pathway, critical for the survival of resting B cells in absence of antigenic response (Srinivasan et al., 2009) (Figure 7).

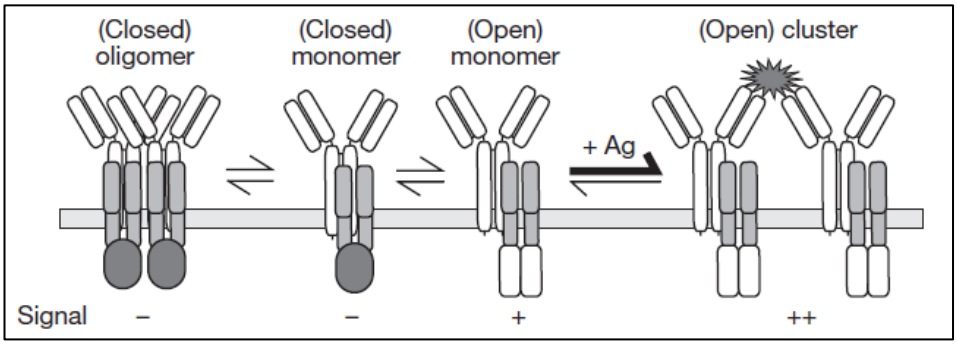

(Yang and Reth, 2010b)

Figure 7. From resting to activated B cell: dissociation-activation model of the BCR Further to antigen ligation, BCR in closed autoinhibited oligomer conformation dissociate into monomeric structures, exposing ITAM-containing domains to Lyn and Syk to transduce the signal for BCR activation.

While suggested to generate redundant immune functions since they display identical unique antigen specificity triggering signalling through shared Igα-Igβ heterodimers, emerging data shed light on distinct regulatory events mediated by IgD and IgM. Indeed, data identified IgD^{+}/IgM^{low} B cell subsets as anergic, proposed to shunt undesired autoreactive B cells differentiation into short-lived plasma cells since IgD is less efficient at sensing monovalent endogenous antigens *in vivo* as IgM while mounting appropriate immune responses against infectious agents (Gutzeit et al., 2018). Also, this discrepancy could be explained by the existence of differential nanocluster size, number and organisation relative to their association with co-receptors, potentially modulating the BCR signal strength or fine-tuning distinct downstream components of the signalling cascade (Noviski et al., 2018).

The threshold for BCR activation is indeed tightly regulated by response regulator components, determining the fate of the immune response, all the more crucial as it draws a line between immune escape and autoimmunity.

Among these is CD22 which provides a negative feedback loop upon antigen engagement with the BCR, initiating its co-localisation and phosphorylation of immunoreceptor tyrosine-based inhibition motifs (ITIM) by Lyn. This is followed by the recruitment of SH2 domain-containing protein tyrosine phosphatase 1 (SHP-1) subsequently dephosphorylating BCR signalling transducers, notably the Igα-Igβ heterodimer transmembrane signalling components and Syk, ultimately raising the threshold for BCR activation (Enterina et al., 2019) (Figure 8).

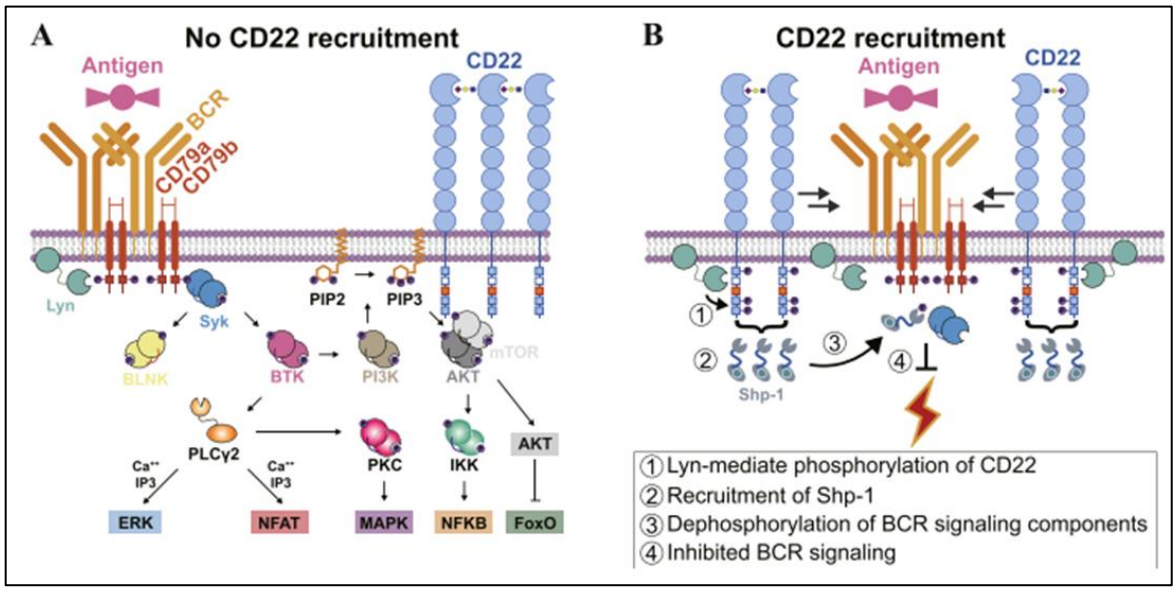

(Enterina et al., 2019)

Figure 8. Role of CD22 in the modulation of the BCR signalling: direct BCR targeting CD22 acts as an inhibitory BCR co-receptor by dephosphorylating BCR signalling transducers. CD22 co-localises with the BCR further to antigen engagement and phosphorylates ITIM-containing domains. SHP-1 is recruited and subsequently dephosphorylates Igα-Igβ heterodimers and Syk resulting in heightened BCR threshold, ultimately hampering BCR activation.

In addition to directly modulating BCR phosphorylation, SHP-1 also exerts a broader dephosphorylation, not only of downstream components of the signalling cascade, notably Vav-1and BLNK, but also of the membrane adaptor protein CD19, which, as part of the complex it forms with the complement receptor type 2 (CR2) CD21, is a critical stimulatory regulator of BCR activation (Walker and Smith, 2008) (Figure 9).

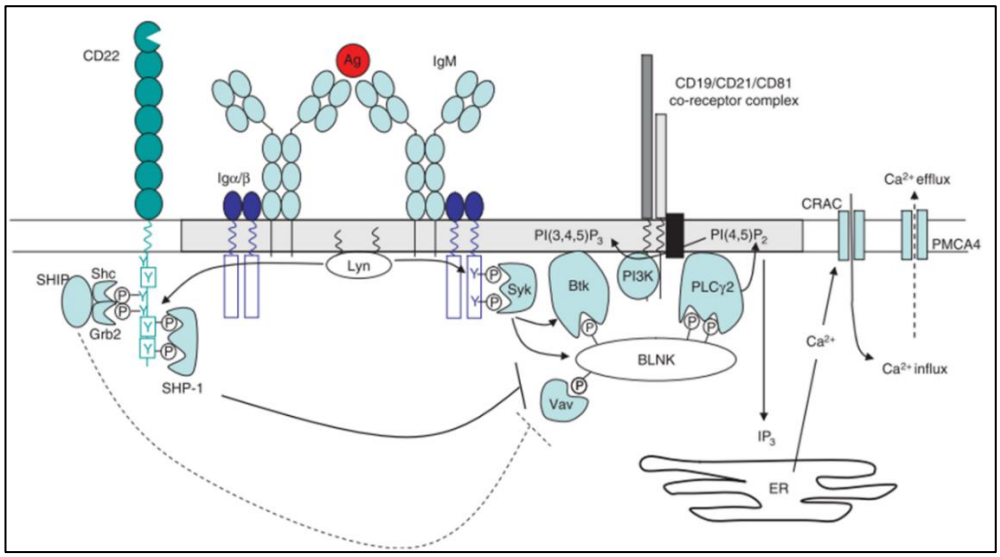

(Walker and Smith, 2008)

Figure 9. Role of CD22 in the modulation of the BCR signalling: broader targeting CD22 transduces an inhibitory signal extending to downstream components of the signalling cascade initiated by the BCR as well as to the positive response regulator CD19/CD21 complex.

On resting B cells, CD22 is present in distinct independent nanoclusters at a density similar to IgM while IgD is the most densely clustered molecule (Gasparrini et al., 2016). Thus, a differential sensitivity to the inhibitory functions of CD22 may be at stake between IgM and IgD, their association with CD22 suggested to be contingent to its ability to access the BCR (Noviski et al., 2018). Here, the difference in cluster density could be a determining factor in this outcome.

Although long considered solely as a branch of the innate host defense, the interconnexion of the complement system with the adaptive arm of the immunity is now established (Dunkelberger and Song, 2010). C3d is one of the central components involved in this interplay through the signal mediated by the CD19/CD21 complex acting synergistically with the BCR. Indeed, when C3d-coated antigens bound to CD21 cross-link the BCR, CD19 is brought in close vicinity which potentiates the signal transduced by Lyn (Figure 10), not only lowering the threshold of BCR activation but also scaling up antigen engagement in the class II MHC processing pathway (Cherukuri et al., 2001; Poe et al., 2001; Toapanta and Ross, 2006). C3d-coated antigens co-ligating the BCR are preferentially presented over those lacking this interaction, denoting 100-fold increased efficiency, here ensuring the specificity of the immune response (Zsef Prechl et al., 2002).

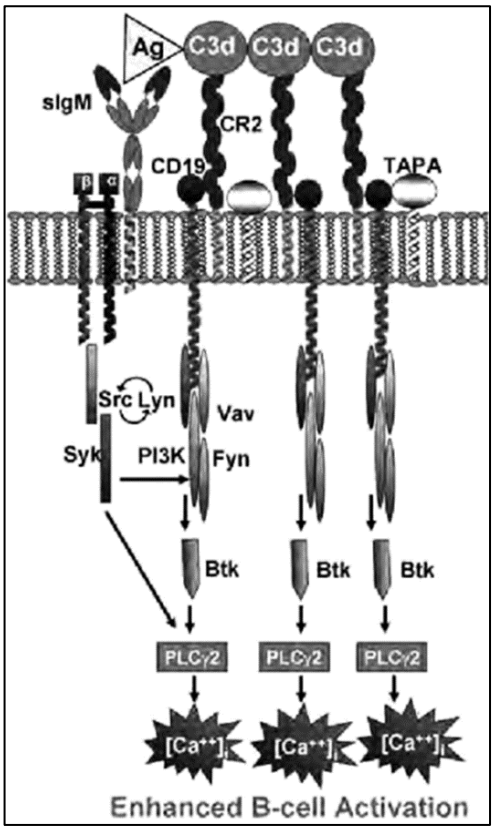

(Toapanta and Ross, 2006)

Figure 10. Role of C3d and the CD19/CD21 complex in the modulation of the BCR signalling The CD19/CD21 complex acts as a potentiator of BCR signalling when C3d-coated antigens bound to CD21 through C3d crosslink the BCR. CD19 moves in close proximity with the BCR where its association with Lyn potentiate the recruitment and activity of Syk and PI3K which ultimately enhance BCR activation.

C3d is a by-product of a proteolytic cascade within an intricate system of plasma and membrane-associated proteins (Figure 11), either initiated by C1q interaction with antibodies in immune complexes (classical pathway), capture of pathogenic carbohydrate structures on PAMPs by mannose-binding lectin (MBL) (lectin pathway) or through spontaneous hydrolysis of C3 (alternative pathway) (Lubbers et al., 2017). They all converge to the generation of the C3 convertase (C4b2a/C3bBb), cleaving C3 in downstream components exerting chemoattractant properties (C3a/C5a), targeted lysis through formation of the membrane attack complex (MAC) and phagocytosis of opsonised particles (C3b/iC3b/C3d) (Gros, 2011; Lubbers et al., 2017).

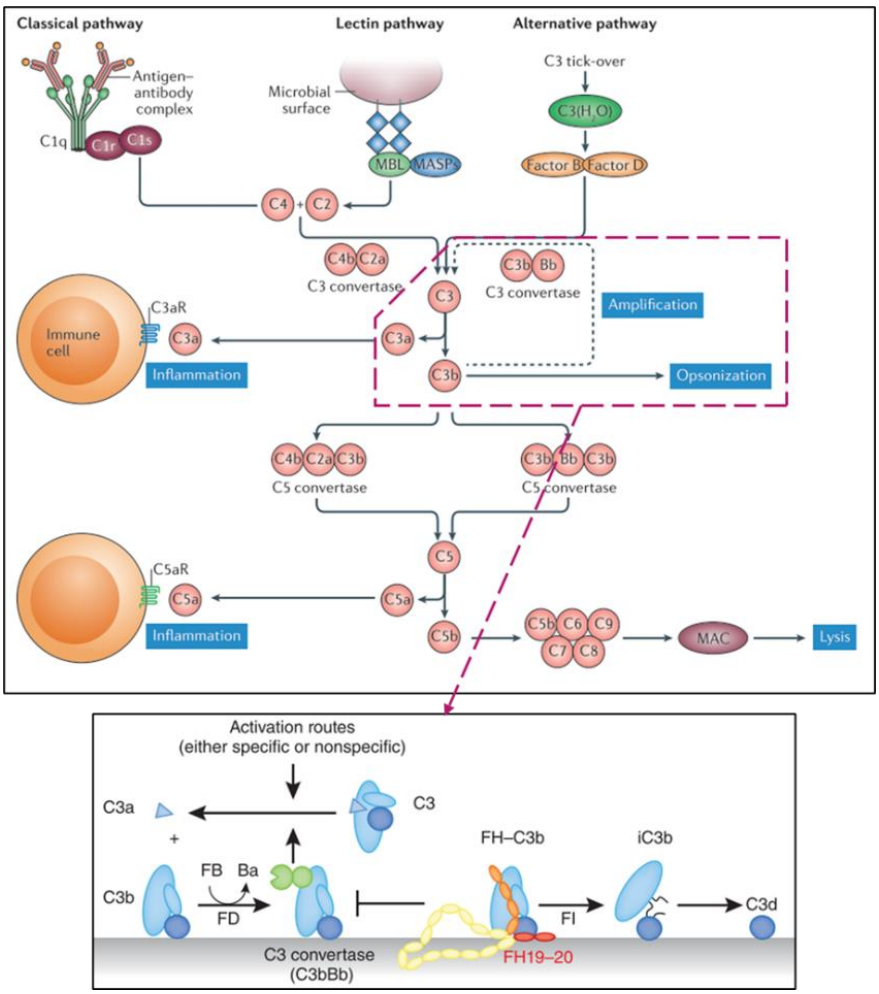

(Gros, 2011; Trouw et al., 2017)

Figure 11. The three pathways of the complement system and C3d generation The complement pathway can be initiated further to binding of C1q to immune complexes (classical pathway), recognition of carbohydrates on the surface of PAMPs (lectin pathway) or spontaneous hydrolysis of C3 (alternative pathway). They all converge to the formation of the C3 convertase which, further down the proteolytic cascade, generates anaphylatoxins (C3a, C5a), the MAC complex and opsonins (C3b/iC3b/C3d).

The synergistic potential of C3d was demonstrated in a collagen-induced arthritis (CIA) mice model where immunisation with C3d-bound type II collagen efficiently initiated inflammatory arthritis, substituting for the conventional mycobacterial components of the Freund's adjuvant, a mechanism strictly linked to the CD19/CD21 complex and resulting enhancement of antigen presentation to CD4 helper T cells (Del Nagro et al., 2005). Similarly, the exacerbation of demyelination in experimental autoimmune encephalomyelitis was reported with the adjunction of C3d-coated MOG, drawing upon the facilitation of germinal centre formation in draining lymph nodes which supports the shift to adaptive autoimmunity (Jégou et al., 2007). Failure to direct C3d-coated antigen to CD21 abrogates these functions as demonstrated with the adjunction of the complement factor H-

related protein-3 (FHR-3) which, by altering the tertiary structure of C3d proteins consecutive to its association, hinders their engagement with CD21 (Buhlmann et al., 2016). Interestingly, C3d-tagged antigens can be captured by CD21 in a BCR-independent way, irrespective of epitope specificity, and endocytosed to then co-localise with compartments associated with the endocytic pathway of class II MHC presentation (Hess et al., 2000). In fact, this mechanism was demonstrated in resting B cells to efficiently elicit T cell activation in a class II MHC-restricted fashion, strictly dependent on T cell help to upregulate CD86 expression on B cells, here suggesting that failure to receive such support would instead drive a tolerogenic response (Boackle et al., 1998) (Figure 12). Also, these data indicate that prior B cell activation is not a prerequisite for C3d-coated antigens to be internalised by CD21. Hence, resting B cells, regardless of their specificity, could present a large repertoire of antigens towards which a tolerogenic response would be propagated. However, this state could be reverted further to BCR cross-linking since antigen specificity is prioritised (Zsef Prechl et al., 2002), driving resting B cells into becoming potent APCs.

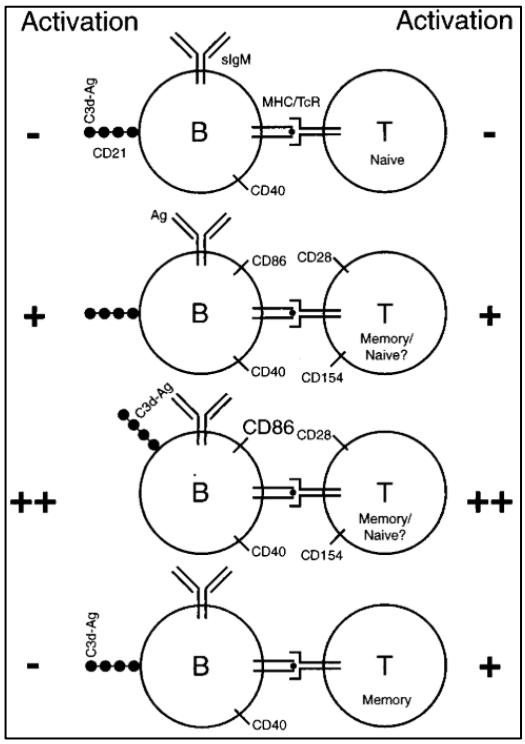

(Boackle et al., 1998)

Figure 12. Model of C3d-directed antigen presentation by B cells: differential outcomes B cell activation is amplified when C3d drive BCR-bound antigens to CD21 as compared to a CD21-independent antigen engagement with the BCR (2nd and 3rd rows). C3d-coated antigen uptake independent of BCR cross-linking mediate poor or tolerogenic signals depending on the provision of T cell help for the acquisition of co-stimulatory molecules (1st and 4th rows).

Hence, it can be speculated that fine-tuning the signal potentiated by CD19/CD21 could give the upper hand to determine B cells fate. It would provide a strategic approach to sustain a resting state of B cells and take full advantage of their tolerogenic properties. This could be achieved either indirectly, through CD22 targeting in order to shift the equilibrium dictating BCR activation towards inhibition, here overriding the CD19/CD21-induced potentiation. Or directly, by engaging a CD21-mediated antigen capture facilitated by C3d independent BCR cross-linking.

The key challenge to fully investigate this approach and correlate the findings with the settings of aGvHD is to design a model that integrates the histocompatibility background as well as the inflammatory environment characteristic of that observed in severe grades aGvHD. This would provide an insight on whether B cells are brought to play in the priming phase and to what extent the tolerogenic properties of resting B cells could be exploited.

1.6. *In vitro* models of histocompatibility: limitations of current mixed lymphocyte reactions

The major concern is to use an *in vitro* model which best reflects the clinical settings of aGvHD. However, the existing models, based on the principle of the mixed lymphocyte reaction (MLR), essentially consist of the use of isolated allogeneic T cell populations, derived from two different blood samples, where the outcome of the immune response is assessed by evaluating the magnitude of their proliferation (DeWolf et al., 2016). As a consequence, they present a major drawback since the complex intercommunication between the components of the immune system, including the production of cytokines and cellular interactions, is not integrated while elementary in the pathogenesis of aGvHD. Hence, any therapeutic approaches assessed through these models raise concerns with regards to their implementation in clinical settings as the effects observed might be artificially created. Other models partly overcome this barrier. Notably, those involving peripheral blood mononuclear cells (PBMCs) as responders to represent the donor-derived immune system. They are used in conjunction with distinct stimulatory cell populations, commonly splenocytes (Beilhack et al., 2005), DCs or macrophages differentiated from PBMC-derived monocytes (Kulakova et al., 2010; Jardine et al., 2020) isolated from a secondary donor source which replicate the host tissues expressing host-specific self-antigens absent from the donor repertoire. Here, the advantage resides in the avoidance of

treatment with mitomycin C or irradiation to block stimulator cell proliferation, which is a procedure commonly used in standard MLRs involving PBMCs (Sairafi et al., 2016) or isolated T cell populations (Lim et al., 1998). Although standard MLR was designed to precisely measure the outcome of the reaction triggered by the responder population, it also alters the stimulatory capabilities of the irradiated or mitomycin-treated population. While PBMC-based responders integrate a larger panel of immune cells, including B and T cells, NK cells and monocytes, the MLR misses out on the presumed contribution of DCs, neutrophils and other granulocytes in the cellular and cytokine network making up aGvHD. Thus, it underestimates, amongst others, the apoptotic arm of aGvHD since tissue apoptosis can lead to the generation of apoptotic bodies and extracellular vesicle recruiting the aforementioned phagocytic cells for clearance, further fuelling the inflammation (Caruso and Poon, 2018). Moreover, the exclusion of B cells from the pool of stimulators may be prejudicial considering the growing interest in their role as APCs in the initiation of aGvHD.
It could be argued that the use of primary cells as stimulators could be associated with numerous limitations. Indeed, the lack of reproducibility and the existing variability between donors, risking the MLR not to be robust enough to provide consistent and reliable results, could ultimately lead to biased interpretations. In place of PBMC-derived monocytes, the stimulator cells could be derived from the Thp-1 monocytic tumour cell line which, because of its genetic homogeneity, confers the distinct advantage of maintaining a stable phenotype and, as a result, providing reproducible responses (Chanput et al., 2014). The use of immortalised cell lines is however disputed, attributing them with a different degree of sensitivity than primary cells which could lead to artificial responses not reproducible *in vivo*. Indeed, although macrophages derived from the Thp-1 cell line using PMA were shown to exert similar features as their PBMC counterparts with regard to the expression pattern of cell surface markers, morphological characteristics (granularity, presence of lysosomes, cytoplasmic volume) as well as functional properties (cytokine and nitric oxide production, phagocytosis of opsonized particles and resistance to apoptosis) (Daigneault et al., 2010), the immune response triggered by the responders might not reflect the one occurring in the course of aGvHD. Thus, any findings generated with Thp-1 monocytes would be hardly transferrable into *in vivo* settings.
While the cellular composition of MLRs has been the subject of many variations, the inclusion of a particular inflammatory status at its induction was rarely addressed. Indeed, only the presence of allogeneic components represented by the stimulators and responders is accounted for in the standard MLR. However, this could constitute a caveat when

modelling aGvHD settings considering the initial intense inflammatory environment established further to pre-conditioning and aGvHD prophylaxis at the foundation of its initiation phase (Holtan et al., 2014; Kuba and Raida, 2018).

1.7. Research aims

The present study aims at evaluating the putative role of B cells as APCs in the pathophysiology of aGvHD, focusing on the regulatory properties of the CD19/CD21 complex, and evaluate the extent of the tolerogenic potential of resting B cells in the context of allogeneic HSCT. K^dHA-specific resting B cells were shown to induce abortive activation of K^dHA-specific naïve CD8 T cells in InsHA mice (Fraser et al., 2006). Also, resting B cells presenting MOG-derived epitopes via their class II MHC molecules protected against demyelination in EAE (Calderón-Gómez et al., 2011). However, what remains to be determined is whether the tolerogenic functions of resting B cells would be sustained in an intense inflammatory environment such as that observed in aGvHD. In order to address this issue, a MLR integrating IL-15, a critical component identified in early phases post-HSCT, will be designed and optimised. The identification of an immunological readout identifying the cytotoxic effector response is critical to address the research questions raised in the present study. First, to assess whether reducing the surface expression of the CD19/CD21 complex hinders the establishment of the allogeneic reaction, here addressing the role of B cells in the onset of aGvHD. Then, to identify a way to fine-tune the CD19/CD21 complex so that antigen capture is directed through CD21 in a context of low or high surface CD19/CD21 complex expression, here addressing whether resting B cells inducing tolerance towards a large repertoire of antigens can be yielded. Overall, this study will give an insight on whether resting B cells could be introduced as a new clinical asset for the prevention or management of acute GvHD. A promising application would be to selectively target non-haematopoietic miHAs to preserve the GvT effect and thus, maximise the prospect for long-term survival and disease remission. Here, a differential tolerance based on the tissue distribution of miHAs would be established. The implementation of such therapeutic strategies is all the more urgent for partially HLA-mismatched donor/recipient pairs. Indeed, despite being associated with higher rates of graft failures, aGvHD incidence and progression to severe grades, these will constitute the main alternative HSC source due to the scarcity of HLA-matched unrelated donors (Kekre and Antin, 2014).

Chapter 2

Material and Methods

2.1. Human blood samples

A total of 16 human buffy coat samples collected from healthy individuals were provided by the National Health Service Blood and Transplant (NHSBT, Colindale, London, UK). It supplies research laboratories with biologic material unfit for therapeutic application, ensuring that the ethics requirements are fulfilled through the informed consent given by the donors regarding the use of their blood for training, education and ethically approved research (National Health Service Blood and Transplant, 2015).

2.2. Cell preparation

The blood samples were collected into sodium heparin tubes (6mL BD Vacutainer, Becton Dickinson, Franklin Lakes, New Jersey, USA) and treated with 10 volumes of red blood cell lysis buffer (R&D System, Minneapolis, USA) per volume of blood, a total of 3mL for each donor being processed, for 7 minutes at 37°C then washed with PBS. Cell viability was checked by trypan blue exclusion (Sigma-Aldrich, Saint-Louis, Missouri, USA) on the CellDrop automated cell counter (DeNovix, Wilmington, Delaware, USA) recording on average 95% viability. Overall, 40 x 10^6 cells were yielded, either brought to 2 x 10^6 cells/mL in complete RPMI-1640 (Life Technologies, Carlsbad, California, USA), supplemented with 10% FBS (Life Technologies, Carlsbad, California, USA) and 1% penicillin/streptomycin (GE Healthcare, Little Chalfont, Buckinghamshire, UK) or resuspended in 500µL PBS for further CFSE staining (BD Horizon, BD Biosciences, East Rutherford, New Jersey, USA). The major concern being to eliminate any trace of serum proteins which could interfere with the incorporation of the CFSE pro-dye in the cells since it interacts with amine groups. Then, 500µL of a 10µM CFSE labelling solution was added to the cell suspension, achieving a final concentration of 5µM CFSE for 40 x 10^6 cells/mL, incubated 3 minutes at 37°C in the dark. The reaction was quenched and washed twice with 10 volumes of RPMI-1640, the resulting cell pellet being resuspended at 2 x 10^6 cells/mL in RPMI-1640. The differential CFSE staining was designed to help discriminate between the responders, unstained, and the stimulators, CFSE labelled, when the MLR was set up (Figure 13). The stability of CFSE staining in the 3-day culture was verified against CFSE-unstained blood.

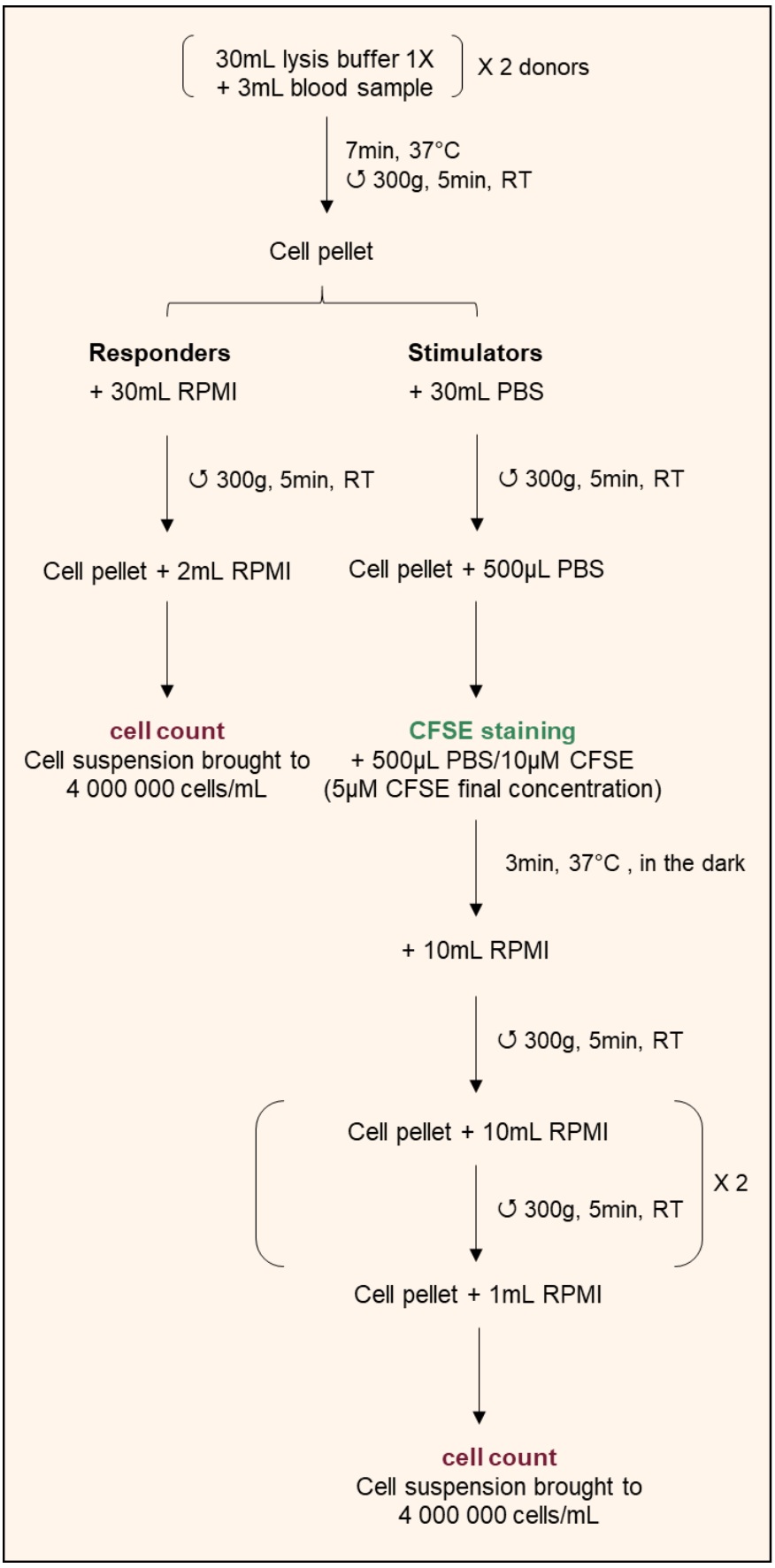

Figure 13. Protocol implemented for the preparation of the responders and stimulators

2.3. Optimisation of the Stim/Resp ratio and IL-15 concentration of the Mixed Lymphocyte Reaction

The MLR was first optimised for the Stim/Resp ratio and IL-15 concentration. The stimulators were not CFSE-stained for this work, they were prepared following the same protocol as the responders as detailed in Figure 13. These preliminary data were generated before CFSE staining was included for the discrimination between stimulators and responders. First, the MLR was carried out following a Stim/Resp ratio of 1:2, 1:5 or 1:10 in 500µL/24-flat bottom wells (1 x 10^6 cells/well). Then, the MLR set up with the validated Stim/Resp ratio was supplemented with 5, 10 or 100ng/mL IL-15 (Sigma-Aldrich, Saint-Louis, Missouri, USA). The outcome of the reaction was examined at Day 3 of incubation at 37°C, 5% CO_2, by measuring surface expression of CD86 and HLA-DR by flow cytometry. The resulting fold-change in CD86 and HLA-DR levels yielded between the MLR and the corresponding responder controls was calculated to determine which parameter provided the largest assay window. A Day 6 readout for the conditions showing an increase in signal at Day 3 was performed to see whether a wider assay window could be obtained.

2.4. Setup of the Mixed Lymphocyte reaction

The MLR was carried out following a StimCFSE/Resp ratio of 1:10 in 500µL/24-flat bottom wells (1 x 10^6 cells/well) and supplemented with 5ng/mL IL-15, further referred to as M15 in the results section. The outcome of the reaction was examined at Day 3 of incubation at 37°C, 5% CO_2. 50ng/mL Epratuzumab (Biovision, Milpitas, California, USA) or/and 50ng/mL C3d (Sigma-Aldrich, Saint-Louis, Missouri, USA) were added to R15 and M15 concomitantly at the start of the reaction. The supernatants were harvested and stored at -20°C for further quantification of Granzyme b, IL-10 and TNFα production by ELISA. B cell, CD4 T cell and CD8 T cell surface marker expression levels were determined by flow cytometry.

2.5. Quantification of Granzyme b, IL-10 and TNF-α production by ELISA

Granzyme b, IL-10 and TNF-α levels in culture supernatants were measured using the DuoSet ELISA kit (R&D Systems, Minneapolis, Minnesota, USA) following the manufacturer's instructions. Briefly, polystyrene plastic microplates (COSTAR 96) were coated with anti- Granzyme b or IL-10 capture antibody overnight at 4°C, blocked for 1h at room temperature with 10% BSA solution, then 50µL of supernatant, with the adjusted dilution, and standards, realised in duplicates, were added for an overnight incubation at 4°C. The bound proteins were detected by the biotin-conjugated antibodies, incubated 2h at room temperature, then, protected from light, coupled with the HRP for 20 minutes at room temperature. The complexes formed were revealed after 20 minutes incubation at room temperature with TMB substrate solution, the reaction being stopped by addition of sulfuric acid. The reading was carried out at both 450nm and 570nm to account for non-specific emissions on SPECTROstar Nano (BMG Labtech, Aylesbury, England). The data were generated with MARS software (BGM Labtech, Aylesbury, England).

2.6. Live/dead cell exclusion: fixable viability stain

The staining was carried out on 1 x 10^6 cells/mL, therefore a whole well was used, the cells being first washed in 2mL PBS since the proteins contained in RPMI-1640 could alter the reactivity of the dye, then resuspended in 1mL of 1µg/mL FVS staining solution (FVS780, BD Biosciences, East Rutherford, New Jersey, USA) and incubated 15 minutes in the dark at room temperature, any remaining free dye being quenched by washing twice with 2mL staining buffer (BD Biosciences, East Rutherford, New Jersey, USA). The cells were finally brought up to a 200µL suspension in staining buffer. The analysis was carried out on the BD LSRFortessa X-20 (Becton, Dickinson and Company, BD Biosciences, San Jose, California, USA), FVS being detected using the APC-Cy^7 channel, data acquisition was performed with the BD FACS DIVA software (BD FACSDiva v8.0) and the graphs and data were generated with the FCSalyzer software (version 0.9.18-alpha; Sven Mostböck). Dead cells generated in the MLR were used as an internal control to set the threshold for FVS positivity. They are identified as FSC^{low}/FSC^{high} and gated on $CFSE^+$ to distinguish them from debris.

2.7. Surface marker staining and gating strategy

2.7.1. Protocol used for the optimisation of the MLR

The staining was carried out on 5 x 10^5 cells/100µL with antibody concentrations used at recommended manufacturer's instructions. 10µL of the APC-conjugated selection marker CD19 in combination with 10uL of either PE-conjugated CD86 or HLA-DR (BD Biosciences, East Rutherford, New Jersey, USA) were added to the cells and incubated for 20 minutes in the dark at room temperature. FMO controls were added to determine where to set the gates to distinguish negative from positive populations. The cells were washed with PBS and resuspended in 200µL staining buffer (BD Biosciences, East Rutherford, New Jersey, USA). The analysis was carried out on the CyAn ADP (Beckman Coulter, Pasadena, California, USA). The Summit software (Summit v4.3) was used for data acquisition and graphs and data generation. The lymphocytes were identified on a SSC-A/FSC-A dot plot as the FSC^{low}/SSC^{low} population and the B cells identified as $CD19^+$ cells. The assessment of HLA-DR and CD86 expression levels was performed by recording the MFI of HLA-DR and the $\%CD86^+$ B cells.

2.7.2. Protocol used for the optimised MLR

The staining was carried out on 5 x 10^5 cells/100µL with antibody concentrations used at recommended manufacturer's instructions. 10µL of the corresponding combination of the APC-conjugated selection markers, CD19, CD4 or CD8, with either PE-conjugated CD86, HLA-DR, CD21 or CD25, CD40L, CTLA-4 or CD2, CD29, TCR, respectively (BD Biosciences, East Rutherford, New Jersey, USA) was added to the cells and incubated for 20 minutes in the dark at room temperature. The cells were washed with PBS and resuspended in 200µL staining buffer (BD Biosciences, East Rutherford, New Jersey, USA). The analysis was carried out on the BD LSRFortessa X-20 (Becton, Dickinson and Company, BD Biosciences, San Jose, California, USA). The PE-conjugated antibodies were selected for the measurements of changes in the expression levels of markers, as this fluorophore is one of the most stable and brightest reagents available for flow cytometry. Data acquisition was performed with the BD FACS DIVA software (BD FACSDiva v8.0), the graphs and data were generated with the FCSalyzer software (version 0.9.18-alpha; Sven Mostböck). The lymphocytes were identified on a SSC-A/FSC-A dot plot as the

FSC^{low}/SSC^{low} population. Then, a double gating combining CFSE with either CD19 (B cells), CD4 (CD4 T cells) or CD8 (CD8 T cells) was used to select either responder B cells ($CD19^{+}/CFSE^{-}$), responder CD4 T cells ($CD4^{+}/CFSE^{-}$) or responder CD8 T cells ($CD8^{+}/CFSE^{-}$). 1000 events were collected for each population. The MFI was recorded for all markers except CD86 for which the $\%CD86^{+}$ responder B cells was chosen and CD25, CD40L and CTLA-4 for which the $\%CD25^{+}$, $\%CD40L^{+}$ and $\%CTLA\text{-}4^{+}$ responder CD4 T cells were chosen. The MFI of CD19 on responder B cells was also assessed. However, no isotype control was used since the whole population expresses CD19 and that a shift in total MFI is investigated. PE-conjugated IgG2α and IgG1κ isotype controls were added in place of the corresponding PE-conjugated marker in order to determine where to set the gate to distinguish negative from positive populations. They account for non-specific background staining resulting from binding to Fc receptors. CS&T beads (Becton, Dickinson and Company, BD Biosciences, San Jose, California, USA) were used to ensure quality control of the flow cytometer's optics, electronics and fluidics. Optimal instrument setup was performed to minimise spectral overlap between fluorochromes. Unstained cells were used to account for the intrinsic autofluorescence of the lymphocytes and set the detector voltages. OneComp eBeads™ (ThermoFisher Scientific, Waltham, Massachusetts, United States) were used to correct any potential background spillover of fluorophores into secondary detectors (Supplementary figure 1). Briefly, the beads were either unstained (Supplementary figure 1B) or single-stained (Supplementary figure 1C) with 1uL CD3 FITC, CD19 APC or HLA-DR PE, identified in the P1 gate (Supplementary figure 1A). After 15min in the dark at RT incubation, the beads are washed with PBS and resuspended in 200µL staining buffer. A compensation matrix was generated (Supplementary Figure 1D) and the compensation was applied.

2.8. Statistical analysis

Statistical analysis was carried when a minimum of 3 experimental repeats are obtained for each readout. For each experimental approach, two or more independent categorical data were compared for one dependent continuous variable, hence a one-way analysis of variance (one-way ANOVA) was used for data processing. Statistical analysis and corresponding graphs were generated with Prism (version 7; GraphPad Software). Repeated-measures one-way analysis of variance (RM one-way ANOVA) was used to account for uncontrolled experimental variabilities, here embodied by the diversity of HLA- and miHA-mismatches

at stake for each experiment because of the diversity of blood sources, hence each pairing involves different histocompatibility disparities and the ensuing immune response could fluctuate from one experiment to another with regards to its strength. The reliance on repeated measures was validated by testing for the effectiveness of the matching ($p<0.005$). The Shapiro-Wilk normality test was run in order to verify that the data follow a Gaussian distribution, a prerequisite for the application of RM one-way ANOVA, if passed, the sphericity is assumed since the present study depends on matching rather than repeated measures, and post-hoc analysis is carried out with Sidak method. The data that failed the Shapiro-Wilk normality test use the Friedman non-parametric test followed by the Dunn's multiple comparison test. The $p<0.05$ was considered as significant, the data being reported as the means ± SEM.

2.9. Ethics

The present research fully complies with the ethics requirements as stated by the University of Westminster research ethics committee (ethics application reference: ETH1617-1175)

Chapter 3

Results

3.1. Introduction

Over the past 60 years, a better understanding of the underlying mechanisms constituting the backbone of acute GvHD has been acquired. Particularly, the critical and yet tight balance existing between promotors fuelling the allogeneic reaction and suppressors dampening it was outlined. This is opening new prospects for the establishment of therapeutic strategies which potential for long term recovery relies on the dual and combinatory impact of the alleviation of the initial cytokine storm and introduction of a tolerogenic signal. The perspective of separating the GvT effect from GvHD by taking advantage of the differential tissue distribution of miHA could indeed fulfil this prerequisite by directing a tolerogenic response towards mismatched HLA and host non-haematopoietic, mismatched miHA. Thus, the protection of host tissues from acute GvHD would be promoted while the GvT effect would be indirectly sustained through targeting of haematopoietic mismatched-miHA, stressing that class I MHC-restricted miHA would be of great interest for this application. The development of miHA-specific Tregs sought to fulfil this strategy, however yielding inconclusive results with respect to the cumbersome procedure to generate them as well as the unstable nature of their phenotype and specificity further to adoptive transfer. Interestingly, B cells received scarce attention despite their tolerogenic potential when in a resting state. However, a better characterisation of their contribution as antigen presenting cells to aGvHD pathophysiology has to be addressed. The objective would not only be to validate the relevance of B cells as therapeutic targets, but also to assess whether these tolerogenic functions would be overwhelmed in the intense inflammatory environment that is prevailing in aGvHD.

It is therefore essential to investigate this particular aspect in a MLR which integrates key components of the events contributing to aGvHD onset so that the effects observed are better aligned with distinct aspects of the pathological settings. It will ensure a better reliability of the effects observed when assessing the relevance of the therapeutic potency of abrogating B cell antigen presenting functions and additional impact associated with the preservation of their resting state for possible clinical applications. Hence, this MLR could serve as a cell-based assay platform used in drug discovery to assess the potency of compounds and help in the decision-making process for progression to next stages of validation.

The current MLRs fail to account for these particular settings. Indeed, they elude the existing complex cellular and cytokine network generated as a result of conjugate formation, but also underestimating the predominant role of the initial inflammatory milieu prevailing in the

onset of aGvHD. Therefore, the present study aims to address this drawback and come up with the implementation of a MLR which includes IL-15 as a core component since it was demonstrated to be abundantly secreted in the early phase to correct the lymphopenic state, supposedly exacerbated by its release from injured tissues or secretion by macrophages and DCs in response to the acute inflammation.

The key challenge here is to design a model that integrates the HLA disparities as well as the inflammatory environment prevailing in aGvHD. IL-15 systemic plasma levels being correlated with the incidence of severe grades, it constitutes the core of this newly designed MLR such that any findings give an insight into their applicability in clinical settings. The emphasis is put on deciphering to what extent B cells are involved in the onset of aGvHD as APCs, a feature poorly addressed in the literature.

The duality of B cells in their signalling as APCs, at the crossroad between immune activation and tolerance induction, constitutes an attractive aspect in the case of aGvHD. This is relevant either in the disruption of the capacity of B cells to present antigens and thus, passively hinder the onset of aGvHD. Or conversely, in the harnessing of their tolerogenic properties, here actively sustaining an anergic state protecting host tissues from unwanted cytotoxic killing. This latter holds interesting prospects for long term recovery with regards to the selective shielding of host non-haematopoietic miHAs for the preservation of the GvT effect. Hence, this chapter addresses the plausibility of these strategies. Also, it provides an insight on whether B cells occupy a central role in the priming phase of aGvHD. Given the prominent regulatory activities of the CD19/CD21 complex with respect to the potentiation of BCR signalling, not only through the reduction of its activation threshold but also in the amplification of antigen processing for class II MHC presentation (Cherukuri et al., 2001; Poe et al., 2001; Toapanta and Ross, 2006), it logically represented an ideal target for the induction of a resting state. The anti-CD22 antibody epratuzumab is relevant for this prospect since, further to CD22 ligation, it provokes the internalisation and also trogocytosis of the CD19/CD21 complex (Dörner et al., 2015), overall resulting in its diminished representation on the surface of B cells. The mechanistic impact of epratuzumab was indeed well described with regards to the phenotypic changes incurred to B cells, however its functional impact has never been clearly addressed. Given the reduced surface expression of the CD19/CD21 complex and BCR, it could be anticipated that the hereby generated B cells would be unresponsive. This aspect will be investigated in the MLR. Although this strategy would fulfil the first hypothesis,

that is the passive hindrance of aGvHD initiation, it is not clear whether these resting B cells would spontaneously propagate a tolerogenic signal. Indeed, the anticipated obstruction of antigen uptake would mitigate the specificity of the anergic signal associated with resting B cells, hence a way to circumvent the reliance on the BCR in this mechanism must be found. A way to do so could be to redirect antigen uptake to CD21, a process which, independent of co-ligation with the BCR, can ultimately drive T cells in an anergic state via a class II MHC-restricted way due to the failure to acquire co-stimulatory receptors (Hess et al., 2000). Ultimately, resting B cells displaying a wide antigen repertoire towards which a tolerogenic state would be established could be yielded. However, this strategy is double edged, the desired tolerance possibly thwarted by the exaggerated prevalence of C3d, potentially reviving B cells out of their resting state. The strength of C3d-coated antigen adjunction was indeed evidenced as efficient at breaking anergy (Del Nagro et al., 2005), hence posing C3d as a crucial trigger to set off the immune response. Following the same reasoning, it could be feasible that C3d mediates divergent responses relative to the extent of CD19/CD21 surface density expression. Thus, it could represent a limiting factor for the redirection of antigens to the CD21-mediated class II MHC presentation, consequently mitigating the chances to propagate a tolerogenic state. Here two issues need to be addressed. Firstly, the risk of breaking the resting state of B cells and thus, failing to keep them away from the pool of APCs involved in T cell priming. And also, the obstruction of C3d-coated antigen internalisation via CD21, hampering the prospect for the constitution of a repertoire of tolerated antigens. Therefore, C3d adjunction was applied in two contexts, one where B cells are unmodified and thus, have the potential to participate in the alloreaction, and another where the surface expression of the CD19/CD21 complex is reduced in an attempt to maintain B cells unresponsive.

What remains to be determined however is whether the attempt to put a hold on the initiation of aGvHD is not interfered with by bystander APCs which would substitute for the incompetence of B cells in this matter. Also, it raises the question around the stability of the resting state in such an overwhelming inflammatory environment, potentially compromising the prospect for harnessing their tolerogenic potential. Our MLR will help to get an insight on these issues. Indeed, it integrates a complex cellular network accounting for the interplay between the various immune components at stake and resulting cytokine production together with inflammatory settings, characteristic of severe grades aGvHD through the inclusion of IL-15.

3.2. Model development: two-way mixed lymphocyte reaction supplemented with IL-15

3.2.1. Rational for the integration of IL-15 as a core component of the MLR

One of the major drawbacks of current models is the failure to integrate pre-existing inflammatory settings whereas these are characteristic features of aGvHD (Ball and Egeler, 2008; Holtan et al., 2014). It is all the more crucial as it will ensure a better reliability of the effects observed. Indeed, the intense inflammatory milieu hereby reproduced potentially adds more weight to the tight balance between suppressors and promotors of aGvHD in favour of the latter, challenging the strength of the tolerogenic response induced by resting B cells.

Considering the wide diversity of the cytokine environment, the selection of the most representative or relevant to the pathogenesis of aGvHD is critical. Based on the literature, IL-15 and the leading components of the cytokine storm, TNF-α, IL-1 and IL-6, came out as particularly pertinent for this prospect. Indeed, high systemic IL-15 levels were correlated with the incidence of severe aGvHD (Sakata et al., 2001; Thiant et al., 2011, 2010). While tissue injury and secretion by macrophages and DCs in response to the acute inflammation can exacerbate IL-15 plasma levels, the post-HSCT lymphopenic state provides a strong trigger for IL-15 production by BM stromal cells to support homeostatic T cell proliferation and sustain immune reconstitution (Matsuoka et al., 2013). Post-transplant IL-15 is in fact a promising strategy in TCD HSCT to correct the high rates of disease relapse, graft failure and infections commonly arising in these settings (Alpdogan et al., 2005; Bertaina et al., 2017; Negrin, 2015; Sauter et al., 2013). In other contexts, however, IL-15 is a key driver of the breach in peripheral tolerance (Miyagawa et al., 2008), a potential harnessed to rescue anti-tumour activities in tolerant CD8 T cells (Klebanoff et al., 2004; Teague et al., 2006). On the other hand, TNF-α, IL-1β and IL-6 are shown to facilitate homing to target tissues and activation of host APCs (Ball and Egeler, 2008). Moreover, the role of IL-1β and TNF-α in causing tissue lesions is well described (Carlson et al., 2009; Du and Cao, 2018; Hofmeister et al., 2004; Markey et al., 2014; Müskens et al., 2021; Tu et al., 2016), notably involving Th17 which polarization requires IL-1β and IL-6 (Jankovic et al., 2013). Altogether, it appears that IL-15 and the lead cytokines TNF-α, IL-1β and IL-6 exert distinct functions, these latter being greatly involved in directing the effector response whereas IL-

15 stands out in the priming stage. The aim of this study being to investigate whether B cells could modulate the direct allorecognition portrayed in the MLR, IL-15 represents the most relevant option. All the more so considering that PB cells are in a quiescent state, readily reversable by IL-15 if appropriate TCR engagement is provided (Dooms et al., 1998). TNF-α, IL-1β and IL-6 were shown to be produced in the MLR (Bishara et al., 1998; Jordan and Ritter, 2002), however, their involvement in responder T cell proliferation was not required when PBMCs are used as stimulators, suggested to be due to their superior antigen presenting functions over isolated cells (Leenaerts et al., 1992). Hence, the MLR used in this study may not represent an appropriate model to test the impact of TNF-α, IL-1β and IL-6.

Interestingly, the literature is scare on IL-15 in MLR settings. A study however showed that IL-15 is not produced despite evidence of T cell proliferation attributed to IL-2, its involvement being even refuted since blocking the shared IL-2/IL-15R γC subunit failed to show further anti-proliferative effect than that obtained with the inhibition of the private IL-2Rα subunit (Praditpornsilpa et al., 2003). However, IL-15 mediates alloreactive CD8 T cell proliferation through trans-presentation of endogenously produced 15Rα/IL-15 (Blaser et al., 2006, 2005), which could account for this outcome. In spite of that, the presence of empty cell surface IL-15Rα on most cells was emphasized, suggested to represent a state where IL-15 expression has not yet been triggered (Stonier and Schluns, 2010). Hence, trans-presentation seems to be tightly regulated according to the magnitude of the inflammatory environment. The binding of soluble IL-15 to empty IL-15Rα was demonstrated to be unlikely in BMT mice recipients of mixed BM cells efficiently producing either IL-15 or IL-15Rα as they displayed similar survival trend as those receiving one type separately (Blaser et al., 2006). However, it was shown that the strict requirement for trans-presentation to be endogenously mediated could be bypassed if the level of secreted IL-15 was abundant enough to bind all IL-15Rα molecules (Stonier and Schluns, 2010). These are circumstances presumably encountered in the settings of severe aGvHD where prolonged systemic plasma IL-15 levels make up the host cytokine microenvironment (Sakata et al., 2001; Thiant et al., 2011, 2010), the breadth of which being commensurate with the extent of tissue damage. Ultimately, it would further fuel the immune response in an allospecific fashion since 15Rα/IL-15 transduces its signal to primed T cells. Here, IL-15 adjunction in the MLR seeks to replicate this aspect.

3.2.2. Cellular and cytokine environment in MLRs

The robustness of the newly-established MLR (Figure 14) lies in the inclusion of unmanipulated buffy coat samples obtained from two healthy individuals, only red blood cell lysis being carried out to rule out transfusion reactions, for both the stimulators and responders. Here, the inclusion of B cells, T cells, NK cells, DCs, monocytes, neutrophils and other granulocytes allows to integrate the complex interplay existing between these components, both in terms of cellular interactions and cytokines produced, thus representing a step forward to better model part of the events contributing to aGvHD onset. A comprehensive understanding of the cellular and cytokine environment at stake in the MLR is essential to help in the interpretation of the experimental outcomes generated in the present study. It can be in part extrapolated from studies characterising blood product composition as well as the current knowledge accumulated in the MLR field.

A comparative leukocyte count between peripheral blood and buffy coat revealed similar distribution profiles for each individual subset, also emphasising a predominance of neutrophils (60%) and lymphocytes (30%) over monocytes, eosinophil and basophils (<10%) (Teetson et al., 1983). As for DCs, they represent a minority, only accounting for 0.25-0.84% of PB leukocytes and 0.60-1.69% of PBMCs (Hasskamp et al., 2005). Precisely, T cells account for 55.2% of the lymphocyte population in PBMCs, with a CD4:CD8 ratio of 1.44, including 22.1% naïve T cells, 12.6% T_{CM}, 35.9% T_{EM} and 21.7% terminally differentiated T cells, considerably surpassing B cells (15.5%) and NK cells (10.1%) (Sairafi et al., 2016).

As the most represented subset, commonly found to account for 50% to 70% of peripheral leukocytes (Mayadas et al., 2014), the influence that neutrophils would exert with respect to their short lifespan needs to be anticipated. Indeed, while having a 8h half-life in periphery, not exceedingly increased *in-vivo* as less than a 24h half-life was reported, neutrophils were shown to readily die over a 24h blood storage partly explained by altered cholesterol levels (Bonilla et al., 2020). Although buffy coats are processed fresh for the MLR setup, the 3-day incubation period, exceeding the average 6-8h peripheral half-life (Blanter et al., 2021), could in fact replicate neutrophils death as depicted in stored blood. At the end of their life, neutrophils undergo spontaneous death via apoptosis and are degraded by resident macrophages resolving the inflammation (Geering and Simon, 2011). However, a failure to process apoptotic neutrophils in a timely manner leads to a shift towards secondary necrosis,

involving the release of DAMPs further to plasma membrane disintegration and nuclear content exfiltration, instead fuelling the inflammation (Chatfield et al., 2018; Iba et al., 2013). Since macrophages are the key mediators in the phagocytosis of apoptotic neutrophils, it is essential to envisage whether such mechanism is conceivable in the MLR. *In vivo*, macrophages derive from tissue infiltrating circulating monocytes, a replenishment of skin $CD14^+$ macrophages 12 days post-HSCT from peripheral $CD14^+$ recovered 4 days prior to this illustrating this property (Coillard and Segura, 2019). The recruitment of monocytes to local inflamed tissues is in fact a well described event, whether dependent on CCR2 to mobilize bone marrow-derived monocytes or LFA-1 to support extravasation of circulating monocyte into tissues (Kratofil et al., 2017). *In vitro*, established protocols integrate distinct cytokine cocktails to polarise monocytes towards selected macrophage phenotypes, notably GM-CSF/IFN-γ/LPS and M-CSF/IL-4/IL-13 driving pro- (M1) or anti-inflammatory (M2) subsets, respectively (Orekhov et al., 2019). Monocyte-derived macrophages are usually yielded after 5-9 days of culture with these protocols, occasionally involving a stepwise addition of GM-CSF or M-CSF first completed at a later stage with the full set of cytokines (Nielsen et al., 2020; Rey-Giraud et al., 2012; Zarif et al., 2016). The completion of macrophage differentiation from monocytes in our MLR remains unlikely. Not only is it limited by the low frequency of monocytes in the buffy coat (<10%) (Teetson et al., 1983), but also it would not be adequately supported in a short-term incubation time, 3 days, which is preferred in this study. Hence, the phagocytosis of apoptotic neutrophils, described as being macrophage-driven (Geering and Simon, 2011), appears improbable, indicating a most probable switch to necrotic death (Chatfield et al., 2018; Iba et al., 2013). Here, the MLR could include a background inflammatory status derived from neutrophil necrosis and, considering the ubiquitous expression of PRRs, notably TLRs, across the leukocyte compartment (El-Zayat et al., 2019), a broad repercussion on all leukocytes at stake in the MLR could be expected. Neutrophils are among the first cells to reconstitute following a 10-20-day pancytopenia post-HSCT and evidence shows that they have a role in the establishment of an inflammatory microenvironment feeding into aGvHD pathogenesis (Tecchio and Cassatella, 2020). Hence, despite the uncontrollable nature of neutrophils death in the MLR, their inclusion represents an important aspect.

This unspecific inflammation accounted for, direct alloreaction of intact mismatched MHC-allopeptide complexes would allegedly be supported by responder naïve T cells since they are identified as the key drivers of aGvHD initiation (Chen et al., 2007; Sairafi et al., 2016), representing 22.1% of the T cell population (Sairafi et al., 2016). Unlike B cells and

monocytes, the involvement of the existing pool of DCs as APCs in this process would be minor considering the low DC frequency in PB (Hasskamp et al., 2005). The generation of monocyte-derived DCs is described in established protocols using a GM-CSF/IL-4-driven stimulation over a 7-day course (Marzaioli et al., 2020). However, the completion of DC differentiation would be unlikely in our MLR. The small monocyte fraction in the buffy coat as well as the preferred short culture time, 3-days, would not adequately support such process. Yet, IL-15-based short-term protocols are published. Either broken down into a first 48h generation of DCs with GM-CSF/IL-15 followed by maturation for 24h with a TLR7/8 agonist-based cocktail, yielding competent DCs exerting more potent T cell stimulatory capacity than DCs matured with TNF-α, IL-1β, IL-6 and PGE2 (Anguille et al., 2009). Or, similarly, consisting in 28h of GM-CSF/IL-15/R848-based DC derivation and subsequent maturation with a culture in IFN-γ/TNF-α/PGE2 for 20h, producing DCs potentiating efficient anti-leukemic T cell functions (Van Acker et al., 2018). Here the timeframe for completion better aligns with the 3-day M15. What's more, the cytokine kinetic profile at stake in standard MLRs revealed a 24h post-induction peak of IL-1 and TNF-α followed at 72h by IL-6, although presumably spontaneously released irrespective of the allogeneic context (Bishara et al., 1998). In line with this, the 24h-peak of TNF-α was similarly evidenced, however also denoting a slow kinetic for IFN-γ only starting at day 3 (Jordan and Ritter, 2002). These cytokines could in fact feed into the maturation process of DCs if yielded by IL-15 in M15 as TNF-α, IL-1β and IL-6 are part of such *in vitro* protocols (Anguille et al., 2009). Also, the intrinsic inflammatory properties harnessed by IL-15 could facilitate this mechanism. Indeed, co-cultures of IL-15-activated PB and monocytes indirectly induced their secretion of TNF-α as part of a cross-talk with NK cells, these later in turn producing IFN-γ as activated monocytes cross-present membrane-bound IL-15 (González-Álvaro et al., 2006). Of note, in addition to impacting the cytokine environment, IL-15 also promotes the acquisition of phenotypic profiles characteristic of potent APCs. Indeed, IL-15 was shown to not only strongly induce HLA-DR and CD86 upregulation on monocytes, but also to bring the expression levels of other co-stimulatory molecules, notably CD86, CD80 and CD40, to those found on DCs derived with a standard GM-CSF/IL-4/TNF-a for 7 days (Saikh et al., 2001).

3.2.3. Setup of the model

The setup of the newly-designed two-way MLR is presented in Figure 14.

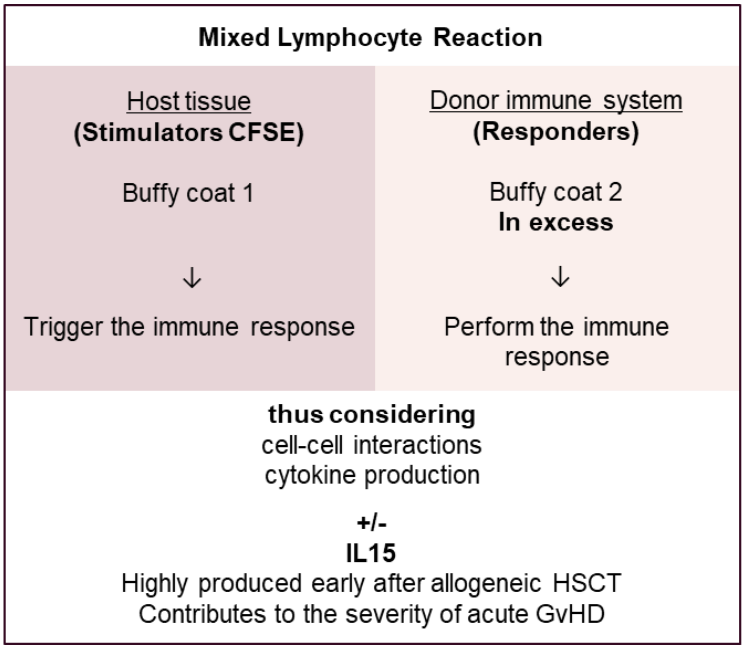

Figure 14. Setup of the newly-designed MLR Unmanipulated buffy coats obtained from two healthy individuals are mixed together to replicate the host tissues (stimulators) expressing self-antigens recognised as foreign by the donor-derived immune system (responders). The MLR is setup up at a Stim/Resp ratio of 1:10 and supplemented with 5ng/mL IL-15 as it was shown to be central to the afferent and priming phases of aGvHD and correlates with the incidence of severe clinical grades. The differential CFSE labelling of the stimulators allows the unequivocal selection of the responders since the focus is on the outcome of the immune response at the donor level. The phenotypic status of both responder B ($CD19^+/CFSE^-$) and CD8 T cells ($CD8^+/CFSE^-$) is determined at the end of the 3-day incubation period at 37°C, 5% CO_2 by flow cytometry for CD21, HLA-DR and CD86 (B cells) or TCR, CD2 and CD29 (CD8 T cells). The MFI is recorded for all markers except CD86 for which the $\%CD86^+$ B cells is chosen. Also, supernatants are collected and frozen at -20°C for further granzyme b and IL-10 levels quantification by ELISA.

The methodology and hypothetical outcomes presented in Figure 15 were designed to determine whether IL-15 is critical for the onset of the immune response or exert a substantial role in its escalation.

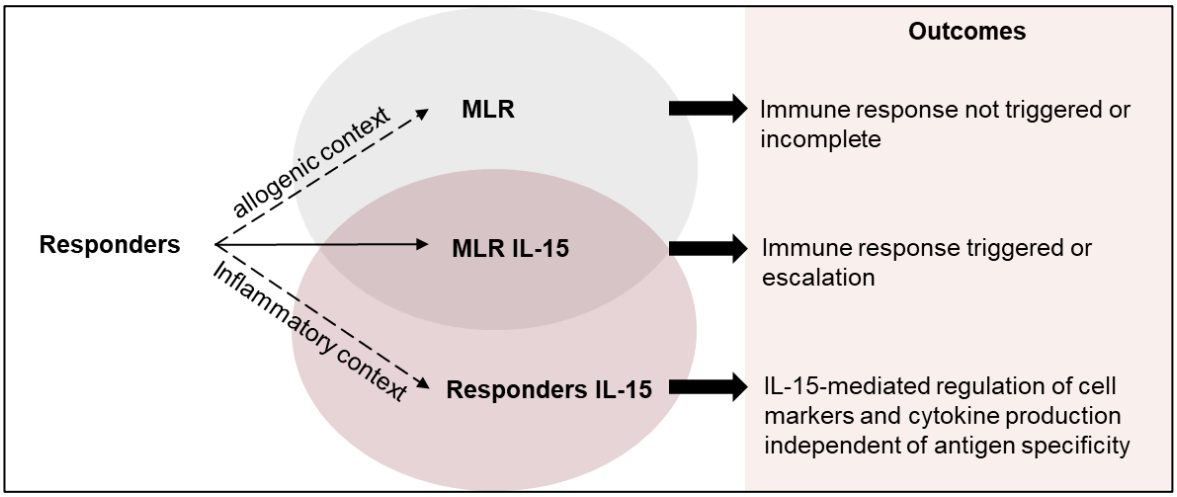

Figure 15. Methodology and hypothetical outcomes emerging from the different contexts designed to uncover the role of the inflammation induced by IL-15 The aim of this study is to elucidate whether the inflammatory environment established by IL-15 is a prerequisite for the initiation of the immune reaction, or if it solely contributes to its escalation. The MLR supplemented with IL-15 (M15) is used to model this context. An unstimulated MLR (M) will help determine the outcome of the reaction elicited by the allogeneic context in a milieu devoid of pre-existing inflammatory cues and thus, whether or not the presence of allogeneic components only is enough to trigger an immune response. Responders stimulated with IL-15 (R15) will help identify IL-15-mediated regulation of selected cell markers and effector cytokines independent of antigen specificity. The background expression profile of these markers and cytokine levels will be defined using unstimulated responders (R).

3.2.3.1. Optimisation of the assay parameters and considerations for data acquisition

3.2.3.1.1. Optimisation of the Stim/Resp ratio and IL-15 concentration

The assay parameters were optimized for the stimulator to responder ratio (Figure 16) and IL-15 concentration (Figure 17). They were validated when CD86 and HLA-DR expression levels provided an acceptable assay window with the corresponding responder control. CD86 and HLA-DR were selected as validation markers since they represent central readouts for the characterisation of phenotypic changes in B cells further to CD19/CD21 complex modulation.

3.2.3.1.1.1. Optimisation of the Stim/Resp ratio

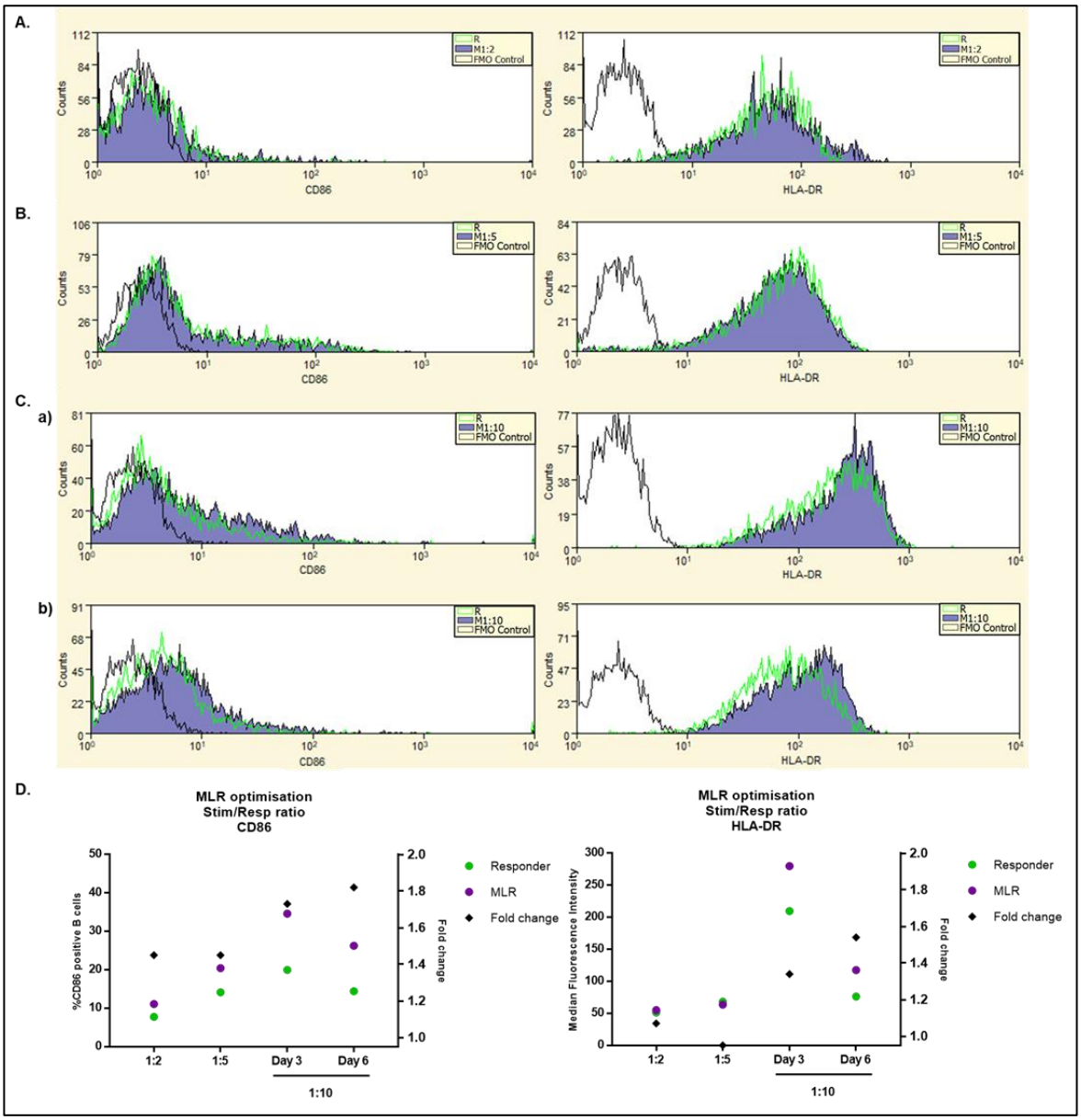

Figure 16. MLR optimisation: Stim/Resp ratio Stim/Resp ratios of **A)** 1:2 (n=1) or **B)** 1:5 (n=1) in a 3-day MLR and **C)** 1:10 (n=1) in a **a)** 3-day and **b)** 6-day MLR were setup in 500µL/24-flat bottom wells (1 x 10^6 cells/well). Flow cytometry profiles of the MLRs and respective responder controls were overlaid together with a FMO control (clear peak). Gating on $CD19^+$ B cells (1000 events recorded) within the lymphocyte population (FSC^{med}/SSC^{low}), **D)** the % $CD86^+$ B cells and MFI of HLA-DR were plotted along with the calculated fold change between the MLRs and respective responder controls. The analysis was carried out on the CyAn ADP (Beckman Coulter, Brea, California, United States) and the data acquired with the Summit software (Summit V4.4.00 Build 2500). The histograms were generated with the Summit software (Summit V4.4.00 Build 2500) and the data plotted with Prism (version 7; GraphPad Software).

The 3-day MLR set up following a 1:10 Stim/Resp ratio (Figure 16Ca and D) generated the highest signal window with a 1.73-fold change in CD86 expression compared to a 1.45-fold increase obtained with either a 1:2 (Figure 16A and D) or 1:5 ratio (Figure 16B and D). HLA-DR ratio was similar in the 1:2 (Figure 16A and D) and 1:5 (Figure 16B and D) ratio, contrasting with the 1.34-fold increase yielded with the 1:10 ratio (Figure 16Ca and D). The 1:10 Stim/Resp ratio seems therefore to comply with the desired validation criteria for the cellular composition of the MLR. An extended timepoint at day 6 of culture (Figure 16Cb and D) was tested to see if the assay window could be further increased. Although a slight raise for both CD86 and HLA-DR levels was denoted, reaching a 1.82- and 1.54-fold change, respectively, as compared to day 3, a decrease in the signal was also recorded. Here, a breach in plasma membrane integrity could be at stake since the loss of surface receptors is a characteristic consequence of membrane damage and ensuing repair mechanisms (Ammendolia et al., 2021). Long term incubation for B cells whole blood culture may not be adequate to maintain their viability and thus, any interpretation of data generated at day 6 may not be reliable.

Altogether, a 3-day culture and 1:10 Stim/Resp ratio are validated parameters for the setup of the MLR.

3.2.3.1.1.2. Optimisation of IL-15 concentration

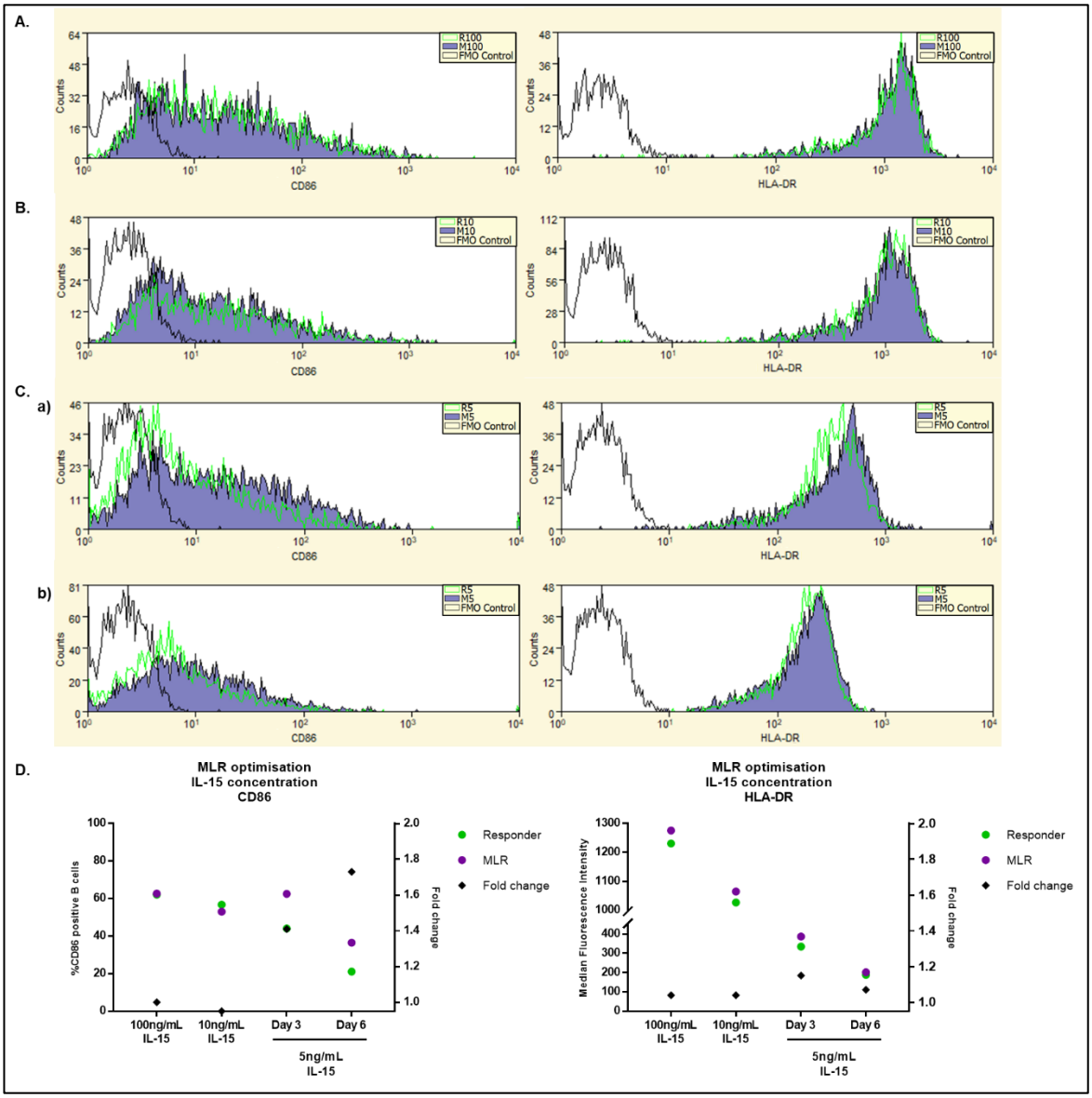

Figure 17. MLR optimisation: IL-15 concentration Using a Stim/Resp ratio of 1:10, the MLR was supplemented with IL-15 at A) 100ng/mL (n=1) or B) 10ng/mL (n=1) and incubated for 3 days, or C) 5ng/mL (n=1) for a a) 3-day and b) 6-day incubation time in 500µL/24-flat bottom wells (1 x 10^6 cells/well). Flow cytometry profiles of the MLRs and respective responder controls were overlaid together with a FMO control (clear peak). Gating on $CD19^+$ B cells (1000 events recorded) within the lymphocyte population (FSC^{med}/SSC^{low}), **D)** the % $CD86^+$ B cells and MFI of HLA-DR were plotted along with the calculated fold change between the MLRs and respective responder controls. The analysis was carried out on the CyAn ADP (Beckman Coulter, Brea, California, United States) and the data acquired with the Summit software (Summit V4.4.00 Build 2500). The histograms were generated with the Summit software (Summit V4.4.00 Build 2500) and the data plotted with Prism (version 7; GraphPad Software).

The supplementation of the hereby optimised 1:10 Stim/Resp ratio MLR with IL-15 at 100ng/mL (Figure 17A and D) or 10ng/mL (Figure 17B and D) resulted in minor differences in CD86 and HLA-DR expressions with the responder control, despite the notable upregulation of both markers imputable to IL-15 only. In contrast, at 5ng/mL, a signal window is particularly visible with CD86, recording a 1.41-fold-change (Figure 17C.a and D), whereas HLA-DR only provided a slight upregulation in the MLR as denoted by the 1.15-fold change. Thus, IL-15 used at 5ng/mL seems to comply with the desired validation criteria for the introduction of an initial inflammatory environment in the MLR. It is worth noting that IL-15 induces a dose-dependent increase in CD86 and HLA-DR expression. Here again, an extended timepoint at day 6 of culture (Figure 17C.b and D) was tested to see if the assay window could be further increased, relying on the homeostatic functions exerted by IL-15 to potentially help sustain B cell integrity. A 1.73-fold increase in the CD86 signal window is recorded, contrasting with the absence of a substantial change in HLA-DR expression levels. However, a similar decrease in the signal is apparent, suggesting that the proposed loss of surface markers may still be occurring despite IL-15 adjunction.

Based on the optimisation data, Il-15 used at 5ng/mL is validated for the setup of the MLR.

Only one instance of the experiments used for assay optimisation was done. However, they only constitute preliminary data aimed at giving enough confidence to select parameters for further assay development. Ultimately, the optimisation process validated a 3-day MLR using a 1:10 Stim/Resp ratio and 5ng/mL IL-15 supplementation as key parameters offering optimum assay conditions with respect to CD86 and HLA-DR expression levels. This model is further referred to as M15.

3.2.3.1.2. Considerations for the discrimination between stimulators and responders

The optimisation of the assay parameters was carried out on the whole B cell population, irrespective of any distinction between stimulators and responders. However, this study focuses on the immune response at the donor level, more specifically on responder B, CD4 and CD8 T cells. A stimulator to responder ratio of 1:10 was chosen thus, as the responders are in excess, the outcome of the reaction will primarily be reflective of their alloreactivity.

This notwithstanding, as a mean to confidently link the experimental observations to the responders only, a differential labelling will be carried out in order to discriminate between responders and stimulators. Whether this improves the signal remains to be determined.

3.2.3.1.3. Considerations for doublet cell exclusion

The outcome of MLRs is the generation of activated responders further to direct allorecognition of stimulator APCs. Conventionally, events deviating from the linear correlation between FSC-A and FSC-H are excluded from data analysis as they may not represent single cells. The increase in FSC-A could indeed denote two cells going through the interrogation point at the same time. Indeed, a rare lymphocyte population expressing both a TCR and BCR identified in the blood of patients with Type I diabetes revealed to be contaminated with T-and B- cell conjugates (Stadinski and Huseby, 2020). In contrast, the integration of doublet cells as a parameter to monitor the proliferation of activated T cells since it is accompanied by an increase in size reflected on the FSC suggested that doublet cell exclusion could be counterproductive (Böhmer et al., 2011). In the present study, the focus is made on the activation of responder B, CD4 and CD8 T cells in the MLR. Excluding doublets could thus be made at the expense of these cells and the data would be biased.

Nevertheless, the proportion of doublet-like cells in our model was determined. The standard singlet/doublet profile for the lymphocytes within the optimised MLR was graphed by plotting the FSC-A and FSC-H together (Figure 18). This will allow to determine the extent of cells outside the linear scale, that is presenting a higher FSC-A compared to the main population, commonly identified as doublets. It can be noted that the fraction of this cell subset accounts for less than 5% of the unstimulated responders (Figure 18A) and MLR (Figure 18B) while it reaches 10% when IL-15 supplementation is applied on the responders (Figure 18C) and MLR (Figure 18D). Although it cannot be ascertained, the extra 5% of cells identified in the standard doublet cell population of the IL-15-stimulated responders and MLR could represent activated cells.

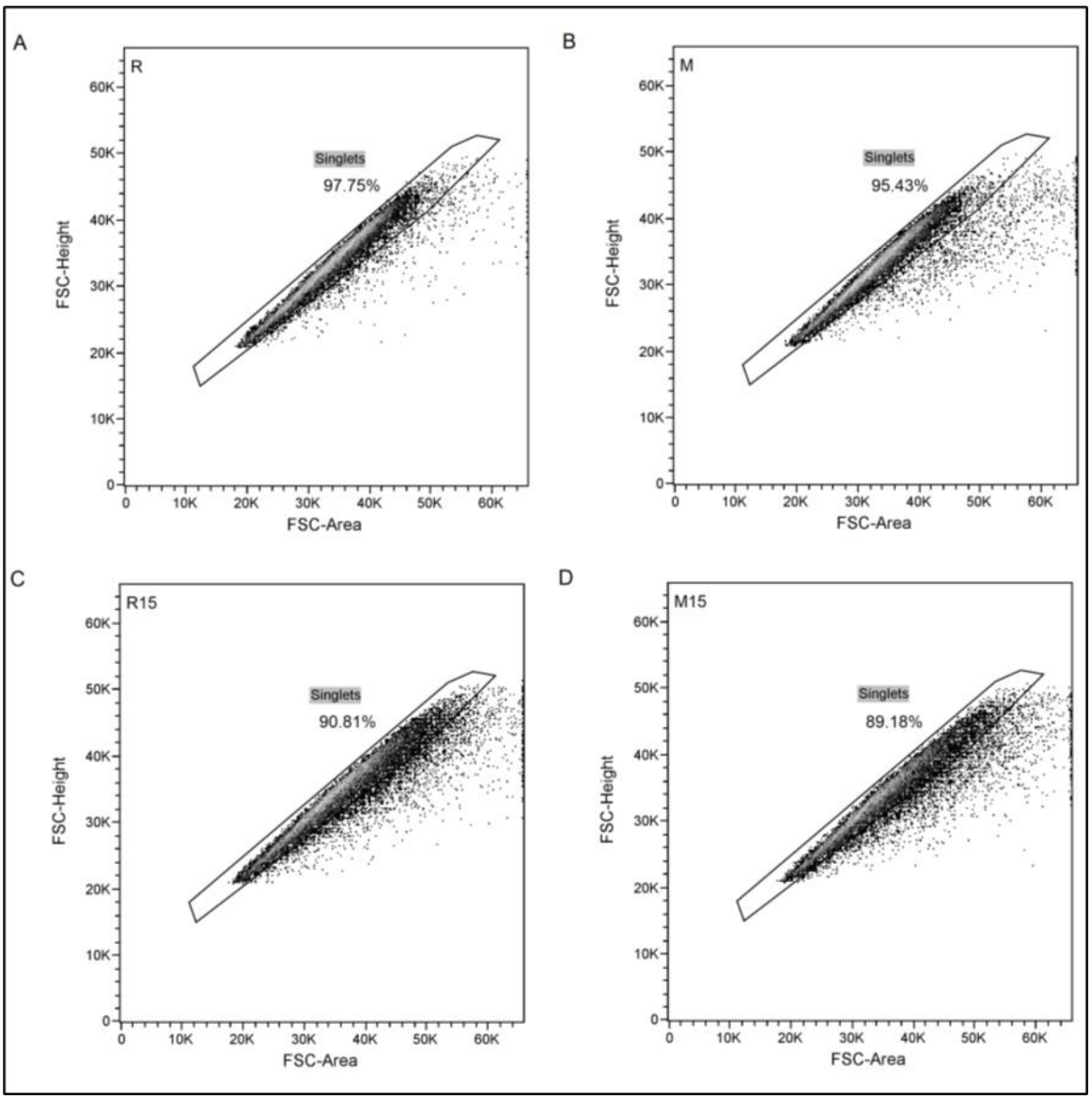

Figure 18. Standard singlet/doublet profile of the optimised MLR and controls The standard singlet/doublet profile of the optimised 3-day MLR (Stim/Resp ratio of 1:10 in 500µL/24-flat bottom wells (1 x 10^6 cells/well) supplemented with 5ng/mL IL-15) is graphed to determine the extent of cells commonly identified as doublets. The standard gating for doublet cell exclusion was carried out on the lymphocyte population (gated on a SSC/FSC dot plot as FSCmed/SSClow) by plotting the FSC-A and FSC-H to retrieve the %cells within the linear scale, identified as singlets. This was done for unstimulated **A)** responders (R) and **B)** MLR (M) as well as IL-15-stimulated **C)** responders (R15) and **D)** MLR (M15) in order to determine whether an increase in the doublet cell-like population in the optimised MLR can be found. Data acquisition was carried out on the CyAn ADP (Beckman Coulter, Brea, California, United States) The graphs and data are generated with the FCSalyzer software (version 0.9.18-alpha; Sven Mostböck). These graphs were generated from the data obtained in the optimisation experiment presented in Figure 17.

3.2.3.2. Validation of the stability and reliability of CFSE labelling applied to the MLR

The present study is strictly relying on the selective focus on the responders, this model includes CFSE-labelled stimulators to exclude them from the analysis. Although care is taken to offset the risk associated with CFSE toxicity by bringing the concentration (5µM CFSE) and exposure (3 minutes) to a minimum, a potential deterioration of the cell's physiological functions cannot be fully ruled out, potential hampering the activation or interfering with the expression levels of activation-associated cellular markers (Lašt'ovička et al., 2009) of the responders if they were to be CFSE labelled. Furthermore, the purpose of the stimulators being merely to sustain appropriate presentation of the mismatched HLAs/miHAs, such drawback would have marginal impact on the overall outcome of the response. All the more so given that the integrity of the extracellular structure is preserved since CFSE diffuses passively through the membrane into the cytoplasm where it is irreversibly anchored.

Despite these precautions, it is essential that the strategy adopted can be confidently used, therefore the pertinence of CFSE labelling must be validated (Figure 19).
Firstly, the intrinsic stability of CFSE staining applied to this particular protocol is verified against unstained blood (Figure 19A) to rule out an eventual spontaneous loss of fluorescence attributable to a natural decay. Since only one population of CFSE-stained cells is visible, it is validated.
Then, the application of CFSE labelling to the MLR over the 3-day incubation period for the discrimination between responders and stimulators is validated by setting up a MLR following a StimCFSE/RespCFSE ratio of 1:10, both samples being CFSE-stained, in 500µL/24-flat bottom wells, supplemented or not with 5ng/mL IL-15 (Figure 19B). Its reliability will thus be verified to rule out an eventual proliferation of the StimCFSE resulting in the generation of a new population harbouring a dimmed fluorescence as they receive half the initial CFSE content from one generation to another, potentially overlapping with the peak of unstained responders, hence, posing a risk to misconstrue responders for newly generated stimulators. Here, no secondary peak is noticeable, testifying of the absence of proliferation of either of the 2 populations, hence no doubt can rise when gating on the responder B or CD8 T cells in our analysis as they represent true initial responders.

Lastly, the model relying on a StimCFSE/Resp ratio of 1:10, it needs to be assured that it is experimentally respected and consistent throughout our study, thus their relative distribution is verified within the lymphocyte population (Figure 19C). Altogether, the stimulators account for 11.53% (n_M=15) and 11.16% (n_{M15}=16) of the lymphocytes, ensuring then that the data collected from different experiment can be confidently discussed against one another.

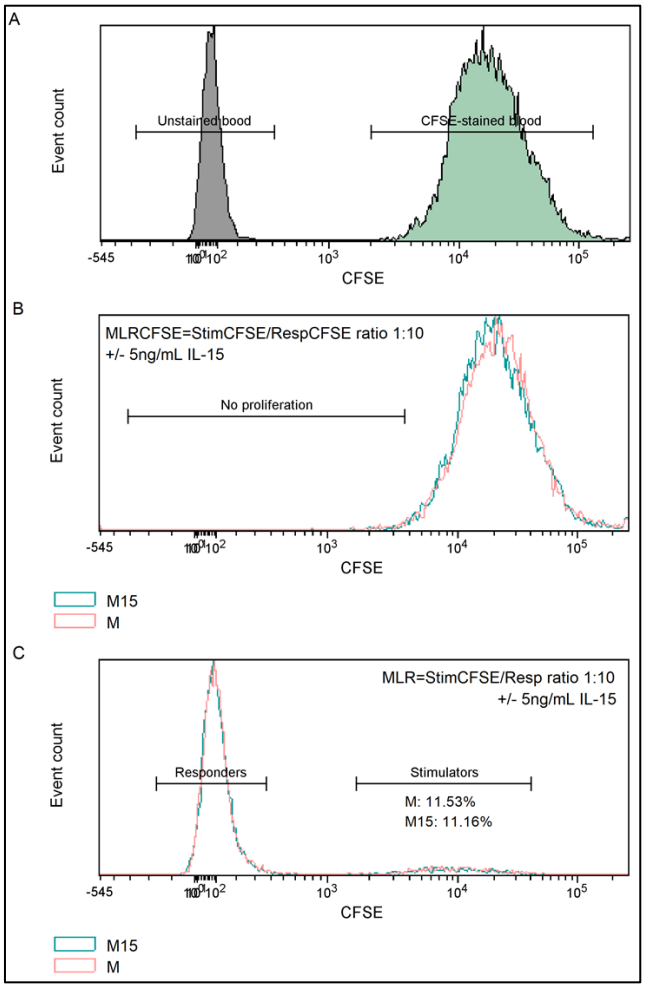

Figure 19. Validation of the stability and reliability of CFSE labelling A 3-day MLR was carried out following a StimCFSE/Resp or StimCFSE/RespCFSE ratio of 1:10 in 500µL/24-flat bottom wells (1 x 10^6 cells/well) supplemented (M15) or not (M) with 5ng/mL IL-15.**A)** The stability of CFSE staining within the lymphocyte population gated on a SSC/FSC (FSC^{med}/SSC^{low}) dot plot is verified against unstained blood over a 3-day incubation period (n=6), as well as **B)** its reliability with regards to a potential proliferation of StimCFSE within [StimCFSE/RespCFSE]M (n=3) or [StimCFSE/RespCFSE]M15 (n=3) **C)** The StimCFSE/Resp ratio in M (n=15) and M15 (n=16) is verified against the 1:10 theoretical ratio. The analysis is carried out on the BD LSRFortessa X-20 (Becton, Dickinson and Company, BD Biosciences, San Jose, California, USA). Data acquisition is performed with the BD FACS DIVA software (BD FACSDiva v8.0) and the graphs and data are generated with the FCSalyzer software (version 0.9.18-alpha; Sven Mostböck).

In conclusion, the application of CSE labelling to this model is validated, any acquired data can be confidently analysed without including technical bias. The absence of proliferation is unexpected, although short incubation time compared to 5-7 days of cell culture in standard MLR could explain this observation.

3.2.3.3. Gating strategy

The gating strategy used for the present study is presented in Figure 20.

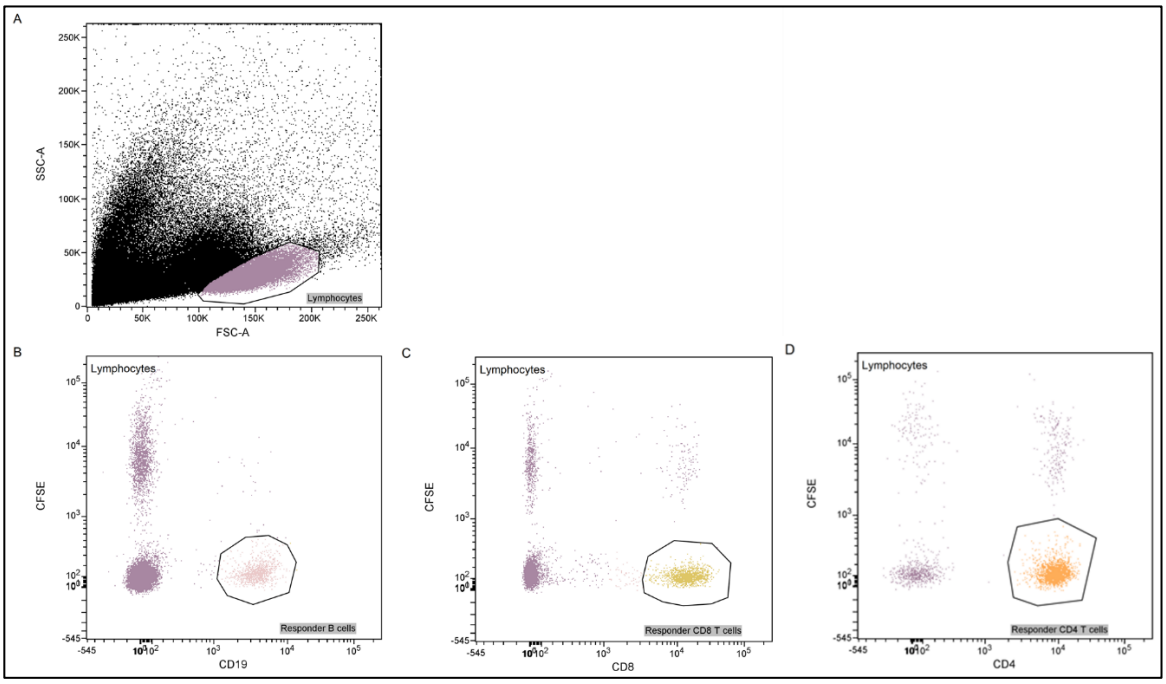

Figure 20. Gating strategy for the selection of responder B and CD8 T cells A 3-day MLR was carried out following a StimCFSE/Resp ratio of 1:10 in 500µL/24-flat bottom wells (1 x 10^6 cells/well) supplemented (M15) with 5ng/mL IL-15. Gating on the **A)** lymphocytes (FSC^{med}/SSC^{low}, purple), the responder B (pink), CD8 T cells (yellow) and CD4 T cells (orange) are identified through the differential CFSE labelling plotted together with CD19 (B cells), CD8 (CD8 T cells) or CD4 (CD4 T cells) by selecting the **B)** $CD19^+/CFSE^-$, **C)** $CD8^+/CFSE^-$ or **D)** $CD4^+/CFSE^-$ populations respectively (1000 events recorded). Data acquisition was carried out on the BD LSRFortessa X-20 with the BD FACS DIVA software (BD FACSDiva v8.0) and the graphs were generated with the FCSalyzer software (version 0.9.18-alpha; Sven Mostböck).

The differential CFSE labelling of the stimulators allows the unequivocal selection of $CFSE^-$ responders. Precisely, the phenotypic status of both responder B ($CD19^+/CFSE^-$) and CD8 T cells ($CD8^+/CFSE^-$) is determined at the end of the 3-day incubation period by flow cytometry. The gating strategy (Figure 20) involves a first selection of the lymphocytes on the SSC-A/FSC-A dot plot which allows the discrimination between populations in a heterogeneous samples based on their size (FSC-A) and granularity/internal complexity (SSC-A) (Figure 20A). The lymphocytes are 6-9µm in diameter and have a low granularity content, therefore they display a (FSC^{med}/SSC^{low}, purple) profile (purple population). Then, a double gating of CFSE plotted against either CD19 (B cells) (Figure 20B), CD8 (CD8 T cells) (Figure 20C) or CD4 (CD4 T cells) (Figure 20D) is carried out to identify responder B cells ($CD19^+/CFSE^-$, pink population), responder CD8 T cells ($CD8^+/CFSE^-$, yellow population) or responder CD4 T cells ($CD4^+/CFSE^-$, orange population), respectively.

3.2.3.4. Determination of the extent of cell death within the lymphocytes

The induction of cell death inherent to the MLR, all the more likely in an intense inflammatory environment induced by IL-15, could be detrimental to the accuracy of the data collected since dead cells could unspecifically bind the staining antibodies, hence potentially shifting the results towards false positivity. Thus, the extent of cell death in M15 is assessed by differentially labelling the necrotic cells using fixable viability stain (FVS). The loss of membrane integrity is characteristic of cells death and, since it has become permeable, the dye will be able to passively diffuse into the cytoplasm where it will be irreversibly anchored. As a results, dead cells are identified as FVS^+. The gating strategy used to determine the extent of cell death in the MLR with and without IL-15 is presented Figure 21.

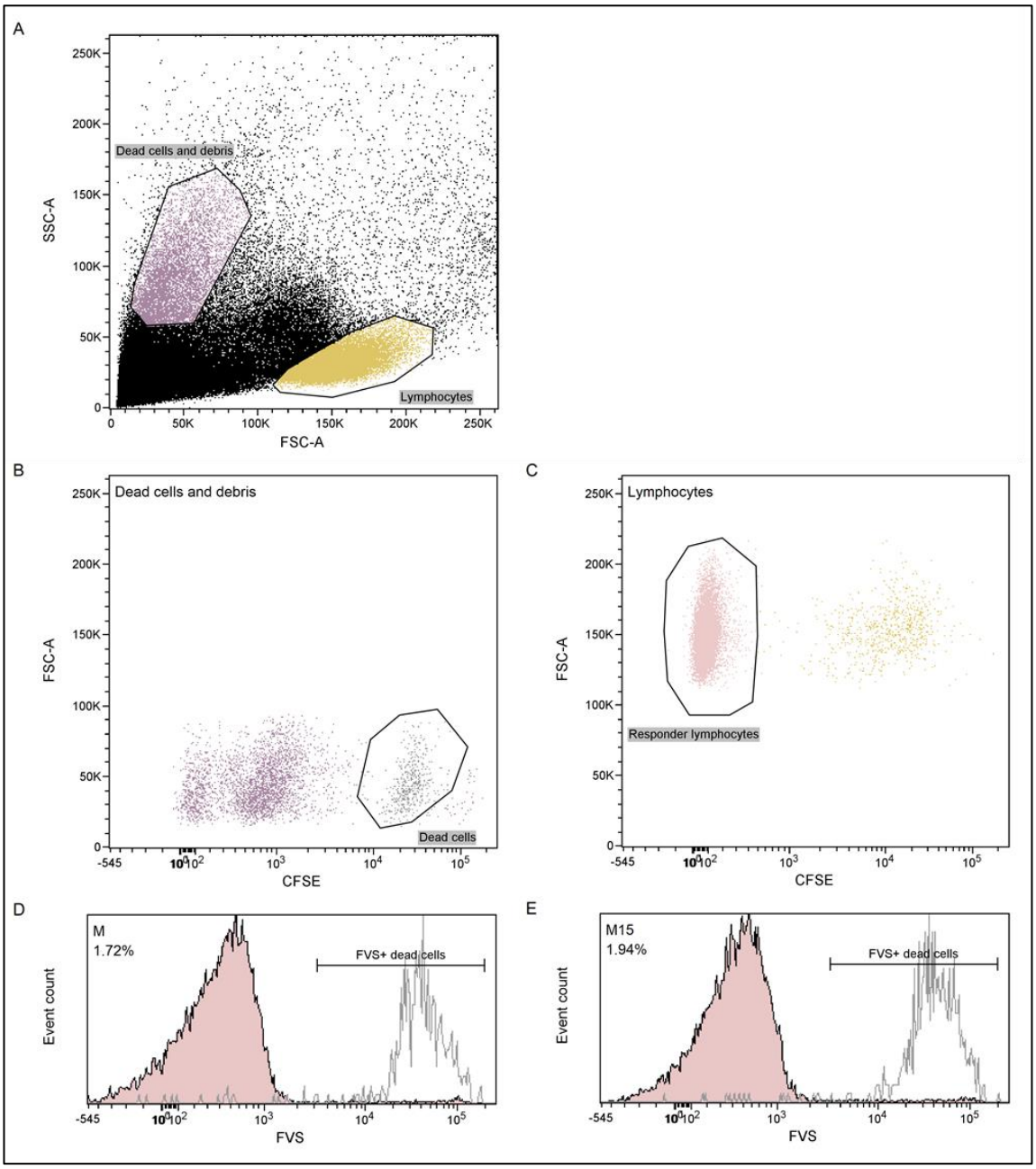

Figure 21. Determination of the extent of cell death with FVS live/dead cell discrimination A 3-day MLR was carried out following a StimCFSE/Resp ratio of 1:10 in 500µL/24-flat bottom wells (1 x 10^6 cells/well) supplemented (M15) or not (M) with 5ng/mL IL-15. FVS staining was performed as per the methods section. **A)** Gating on the lymphocytes (FSC^{med}/SSC^{low}; yellow) or the dead cells/debris (purple), a further characterisation based on CFSE labelling allows the selection of the **B)** dead cells (grey), which have retained CFSE, or **C)** responder lymphocytes (pink; 1000 events recorded), CFSE-unstained, the extent of cell death in the responder lymphocytes (pink) within D) M (n=4) and E) M15 (n=4) verified against the dead cells used (grey) as an internal control setting the threshold for FVS positivity, allowing the discrimination between live and dead cells. Data acquisition was carried out on the BD LSRFortessa X-20 with the BD FACS DIVA software (BD FACSDiva v8.0) and the graphs were generated with the FCSalyzer software (version 0.9.18-alpha; Sven Mostböck).

A threshold of positivity must be set so as to clearly define what level of FVS fluorescence intensity characterises dead cells. The MLR uses buffy coats which, after 3 days, will involve a large pool of dead cells which can be used as internal controls for FVS positivity. The most characteristic feature of dead cells is pyknosis, which results from chromatin condensation in the nucleus, resulting in increased SSC. Also, their size is considerably shrunk, appearing as small clumps, consequently dead cells display lower FSC than viable cells. Thus, dead cells are found on the far-left side of the SSC-A/FSC-A dot plot. A gate was drawn around the population displaying these characteristics, although it is an approximate estimation since this zone also contains a fair number of debris (Figure 21A). Therefore, in order to be more selective, a further discrimination based on CFSE labelling (Figure 21B; grey) was performed on the reasoning that, although presenting alterations to their membrane, the dead cells will have retained CFSE since it cannot diffuse out of the cells. The debris, however, would only present artefacts of CFSE-associated fluorescence if any, therefore the dead cells are defined by a positive CFSE staining.

Cell viability within the responder lymphocytes was assessed irrespective of the subset involved, no specific selection of responder B cells, CD4 T cells or CD8 T cells was performed since an overall estimate of the extent of cell death is needed. Hence, following the gating strategy established to differentiate responder from stimulator lymphocytes, a first selection of the lymphocytes on the FSC/SSC dot plot by gating on the FSC^{med}/SSC^{low} (Figure 21A; yellow) population was carried out, within which the responders are selected as $CFSE^-$ cells (Figure 21C; pink).

On average, less than 2% (μ_M=1.72%; μ_{M15}=1.94%) (Figure 21D and 21E) of the responder lymphocytes account for dead cells.

However, it is worth noting that the population located between the lymphocytes and the dead cells/debris contains cells which have started the apoptosis/necrosis process (Figure 22).

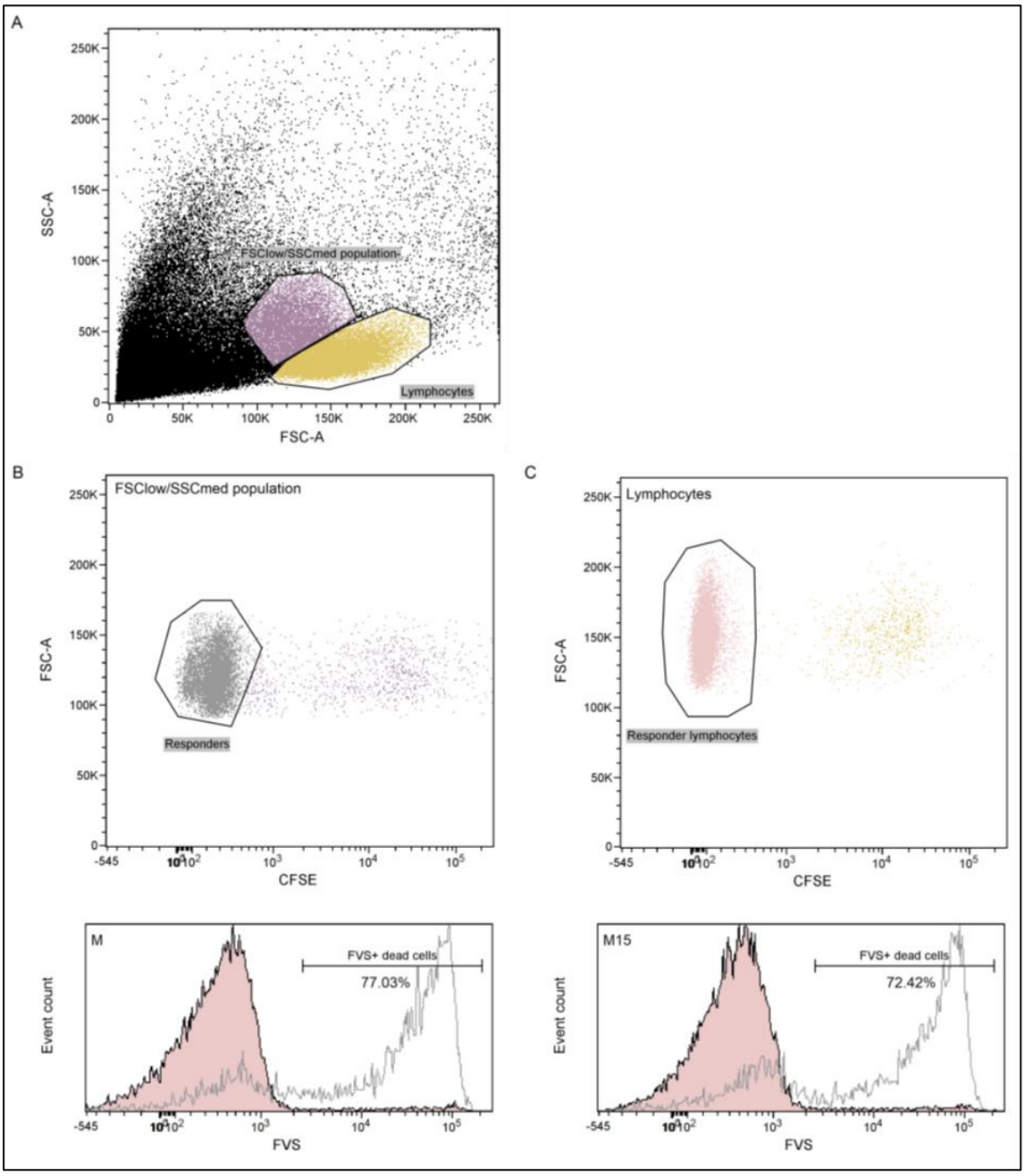

Figure 22. Comparison of the FVS expression profile between the responder lymphocytes and the FCS^{low}/SSC^{med} population A 3-day MLR was carried out following a StimCFSE/Resp ratio of 1:10 in 500µL/24-flat bottom wells (1 x 10^6 cells/well) supplemented (M15) or not (M) with 5ng/mL IL-15. FVS staining was performed as per the methods section. **A)** Gating on the lymphocytes (FSC^{med}/SSC^{low}; yellow) or the **FCS^{low}/SSC^{med}** population (purple), a further characterisation based on CFSE labelling allows the selection of the responder cells for the **B) FCS^{low}/SSC^{med}** population (grey) and **C)** lymphocytes (pink; 1000 events recorded), both CFSE-unstained. The FVS expression profile of the responder lymphocytes (pink) and **FCS^{low}/SSC^{med}** population (grey) D) M (n=4) and E) M15 (n=4) were overlaid together. The threshold of FVS positivity was set using the dead cells as described in Figure 21. Data acquisition was carried out on the BD LSRFortessa X-20 with the BD FACS DIVA software (BD FACSDiva v8.0) and the graphs were generated with the FCSalyzer software (version 0.9.18-alpha; Sven Mostböck).

The apoptotic/necrotic cells have a reduced size (lower FSC) along with a more complex internal structure (higher SSC), however no to the same extent as the dead cells. This could account for the initiation of pyknosis. An average of 77.03% (Figure 22D) and 72.42% (Figure 22E) of the FSC^{low}/SSC^{med} population is FVS^{+}. Although a fraction of this population is FVS^{-} and thus, would still appear viable, they would not be integrated within the population gated for data analysis. Indeed, they do not display FSC/SSC parameters characteristic of the lymphocyte population. Indeed, the activated cells would show an increase in the size, the opposite being observed here. It could be argued that the remaining fraction of FVS^{-} cells represents a transitory state, expected to shift towards a full FVS^{+} profile with a longer incubation time.

It is accepted that a high level of cell death takes place in the MLR. Notably, this is due to the short lifespan of neutrophils, not exceeding 24h (Bonilla et al., 2020; Blanter et al., 2021), which undergo spontaneous death via apoptosis, further progressing to secondary necrosis if not phagocytosed (Iba et al., 2013; Chatfield et al., 2018). It can be assumed that after 3 days of culture, these dead neutrophils would constitute the major part of the dead cells and debris identified on the far-left part of the FSC/SSC dot plot. The FSC^{low}/SSC^{med} population could be a collection of monocytes and lymphocytes entering cell death. Hence, while only less than 2% of the responder lymphocytes are identified as dead, it should not be assumed that it accounts for the whole lymphocyte population within the MLR. This fraction only relates to the lymphocyte population identified as FSC^{med}/SSC^{low}, which is the standard practice for gating on lymphocytes in whole blood/buffy coat samples.

The decision to not routinely include live/dead cell exclusion with FVS was based on the assumption that the fraction of dead cells was minor and, as a result, would not interfere with data analysis since an eventual unspecific binding of staining reagent would be inconsequential. However, this could lead to difficult interpretation of the data in case of minor changes considered statistically significant. Indeed, the distinction between true variations due to the allogeneic reaction or unspecific staining of the dead cells would be challenging to do. If such situation is encountered in the present study, care will be taken with data interpretation.

2.2.3.5. Determination of the outcome of the reaction in M15: selection of immunological readouts

3.2.3.5.1. Characterisation of B and T cell phenotypes: panel design

The aim is to get an insight on the phenotypic status of key drivers of the allogeneic response. It includes B cells since their APC functions is the focus of the present study, but also CD4 T cells considering their supporting functions, and CD8 T cells considering their crucial part taken in the cytotoxic effector response. This will allow to distinguish what functions and cell subsets are modulated and, ultimately, identify potential targets for therapeutic strategies. Here, the question of whether B cells as APCs can drive a tolerogenic signal hampering the cytotoxic effector response will be addressed.

3.2.3.5.1.1. B cell phenotype

####### 3.2.3.5.1.1.1. CD19/CD21 complex

The emphasis being put on the modulation of the CD19/CD21 complex for the sustainment of tolerogenic signals and diversion of antigen uptake away from the classical pathway, both these receptors are assessed for surface expression.

####### 3.2.3.5.1.1.2. HLA-DR and CD86

The expression pattern of markers deemed as hallmark of antigen presenting potency are examined, including the class II MHC component HLA-DR, producing signal 1 through provision of allopeptide interaction with the TCR, constitutively expressed on B cells, and the co-stimulatory ligand CD86, delivering signal 2 through engagement with CD28 on the T cell for efficient activation.

3.2.3.5.1.2. CD4 T cell phenotype

3.2.3.5.1.2.1. CD25

Described in aGvHD and linked to both pro-inflammatory and regulatory mechanisms, the expression pattern of CD25 on CD4 T cells, the high affinity private IL-2Rα, is investigated. Indeed, elevated frequencies of $CD25^+$ CD4 T cells in the donor graft are correlated with the incidence of aGvHD (Stanzani et al., 2004). On the other hand, blockade of the p55 subunit of IL-2Rα using the humanized monoclonal antibody daclizumab as a prophylactic treatment for aGvHD did not mitigate its incidence. Also, other clinical endpoints, such as severity, mortality and NRM were not affected by daclizumab, but this treatment resulted in delayed Treg reconstitution (Locke et al., 2017). The fact that Tregs constitutively express CD25 unlike Tcons could explain this effect, a discrepancy which is at the core of low-dose IL-2 therapy potency (Matsuoka et al., 2013). $CD4^+CD25^+Foxp3^+$ Tregs make up around 5% of human PB CD4 T cells (Baatar et al., 2007), hence they would constitute a minor population in our study. Regardless, the existence of a Treg response will not be ruled out since naïve Tcons can be driven to express Foxp3 under conditions of suboptimal provision of hight affinity ligands or co-stimulatory signals, generating induced Tregs (iTregs) (Schmitt and Williams, 2013).

3.2.3.5.1.2.2. CD40L

CD40L, expressed on activated CD4 T cells, interacts with CD40 on opposing APCs, resulting in the upregulation of co-stimulatory molecules, notably class II MHC molecules and CD86, in turn enhancing T cell activation (Appleman et al., 2001). Blockade of CD40L induces tolerant CD4 T cells towards host alloantigens, hence preserving the GvT effect, ultimately reducing GvHD in a more efficient way than blocking CD28 (Briones et al., 2011). An inhibition of Th1 proliferation and associated cytokine production, consequently interfering with host-allospecific cytotoxic CD8 T cell generation, was identified as the mode of action of anti-CD40L antibodies in aGvHD mice models (Tamada et al., 2002). Hence, assessing CD40L levels on CD4 T cells will help give an insight on the direction taken by the immune reaction, either activation or tolerance induction.

3.2.3.5.1.2.3. CTLA-4

Activated CD4 T cells upregulate surface CTLA-4, a negative immune checkpoint regulator displaying higher affinity than CD28 for CD86, thus generating a competition which results in either T cell activation or anergy (Buchbinder and Desai, 2016). The administration of abatacept, a humanised CTLA-4-Ig fusion protein, proved to be effective in reducing GvHD incidence not only by interfering with the CD28/CD86 signal but also by increasing PD-1 expression on T cells (Thangavelu and Blazar, 2019). The accumulation of inhibitory regulators such as CTLA-4 and PD-1 contributes to the sustainment of an immunosuppressive environment which, in a context of chronic persistent antigen exposure, can lead to exhaustion (Yi et al., 2010). Here again, a trend showing the direction taken by the immune reaction could be extrapolated from the levels of CTLA-4 expression on CD4 T cells recorder in our model.

3.2.3.5.1.3. CD8 T cell phenotype

3.2.3.5.1.3.1. TCR

The modulation of TCR expression will give an insight on the propensity for antigen recognition.

3.2.3.5.1.3.2. CD2

The potentiation of CD8 T cell activation is determined by focussing on CD2. Further to its engagement with CD58 (LFA3) on the opposing APCs or target cells, CD2 represents a crucial enhancer of TCR signalling, even reported to break the anergic state of CD8 T cells lacking the conventional stimulatory receptor CD28, bearing in mind that such conditions are not the prerequisite for the completion of CD2-mediated signalling (Leitner et al., 2015). Located at the interface between the T cells and their cognate APCs or target cells, referred to as the immunological synapse (IS), CD2 facilitates the enrichment of co-stimulatory molecules in close vicinity with the TCR/class I or II MHC-allopeptide complex in the central supramolecular activation complex (cSMAC) (Binder et al., 2020). It also provides an extended adhesion area favouring interactions between the cellular conjugates through the existence of CD2/CD58 (LFA3) clusters arranged in a corolla pattern in regions at its periphery, sustaining scanning activities of the cell surface for co-stimulatory complexes

(Demetriou et al., 2019). These are subsequently captured and recruited to the corolla where TCR signalling is initiated, decreasing the threshold of TCR activation. CD2 expression levels are thus correlated with the intensity of TCR signalling, hence incarnating here a role as a quantitative checkpoint governing the fate of T cells (Figure 23).

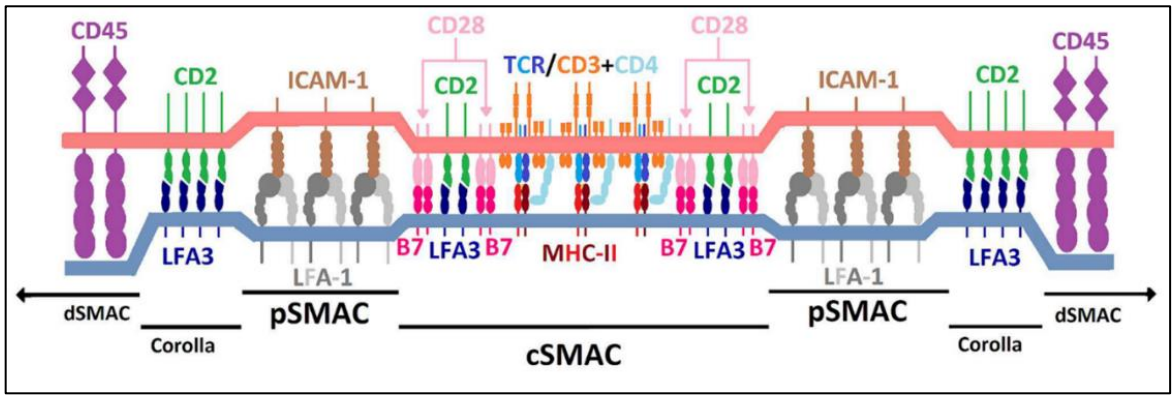

(Binder et al., 2020)

Figure 23. Distribution and role of CD2 in the immunological synapse (IS) CD2 potentiate enhanced TCR signalling. CD2 localised in the cSMAC facilitates the enrichment of co-stimulatory molecules in close proximity with the TCR. In a peripherical region of the IS, arranged in a corolla pattern, CD2 forms clusters with CD58 (LFA3) exposed on opposing APCs or target cells enhancing scanning activities for class I or II MHC-allopeptide complexes and co-stimulatory ligands.

Moreover, CD2 engages in reinforcing CD8 T cells adhesion avidity for their selective class I MHC-restricted antigen, posing indeed as a key mediator for optimal conjugate formation with their target cells, critical for the completion of potent cytotoxic effector functions (Bierer et al., 1989).

3.2.3.5.1.3.3. CD29

A particular emphasis is put on the expression of CD29, the integrin β1 subunit which, further to association with the corresponding α subunit, forms heterodimeric dimers making up the very late activation antigen (VLA). It belongs to a family of adhesion receptors, the most studied being the α4β1 integrin VLA-4, found to exert co-stimulatory properties dependent on CD28 engagement, potentiating T cells activation subsequent to recruitment to the pSMAC (Kim et al., 2010; Mittelbrunn et al., 2004). Moreover, the cytotoxic status of CD8 T cells, characterised by selective INF-γ production and intensification of granzyme b-mediated effector functions, was linked to CD29 expression (Nicolet et al., 2020). Its

implication in CD8 T cell degranulation events following connexion to extracellular matrix proteins, triggering the activation of focal adhesion kinases re-arranging the microtubular network (Doucey et al., 2003), is seemingly at the core of this effect. Hence, the dual levels at which CD29 acts will help get a broader picture of CD8 T cell physiological status at stake in the present model.

3.2.3.5.2. Effector response

The intricate cytokine network governing the physiopathology of aGvHD depicts its timeline into three well defined phases. Thus, from the initial cytokine storm, disseminated as a result of the breach in tissue integrity brought about by the myeloablative and conditioning regimens, expanding into a wave driving the emergence of the cytotoxic effector arm, and ultimately exerting target tissue apoptosis through a diverse array of mediators (Henden and Hill, 2015) (Figure 24).

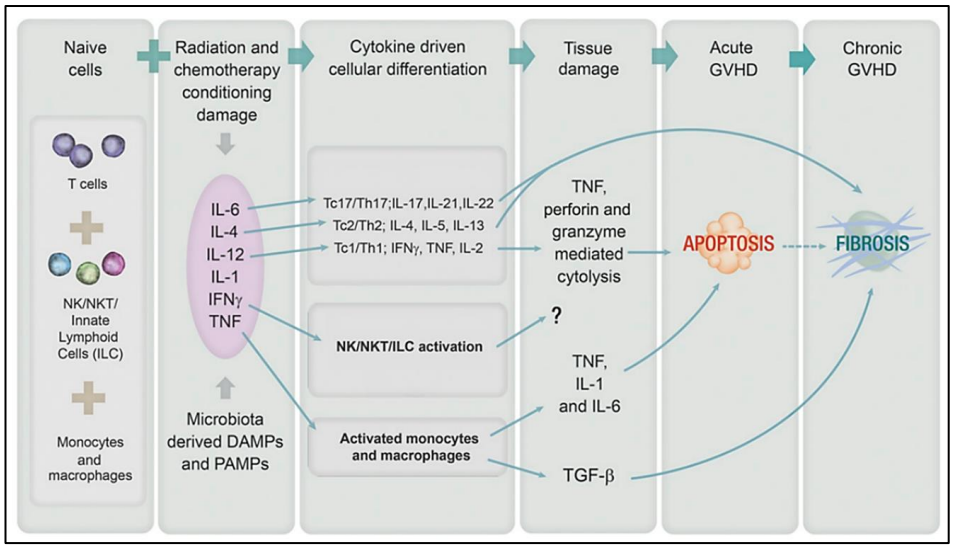

(Henden and Hill, 2015)

Figure 24. Cytokine network governing the timeline of aGvHD pathophysiology The cytokine environment drives the progression through the different phases of aGvHD pathophysiology. The initiation phase is mainly characterised by the propagation of the cytokine storm, comprising TNF-α, IL-1β and IL-6, in response to tissue damage consecutive to the toxicity induced by the chemotherapy and radiation pre-conditioning regiment. The priming stage involves a cytokine-driven differentiation of naïve T cells towards Th1, Th2, and Th17 cell subsets determining the localisation and extent of tissue-injury identified in the effector phase. End-organ damage is elicited by Tc1/Th1 through apoptosis mediated by TNF-α or in a perforin/granzyme cytolytic pathway requiring cognate TCR-MHC interaction.

Hence, the selection of cytokines characteristic of distinct time windows represents an interesting strategy to adopt in an attempt to reveal what stage the MLR particularly portrays, whether it spans the cytotoxic outcome being of notable interest.

3.2.3.5.2.1. Cytotoxic response: Granzyme b

The present study proposes that the induction of resting B cells along with the re-direction of antigen uptake to the CD19/CD21 complex via C3d supplementation holds tolerogenic potential. It is thus crucial to attest of the propagation of these signals, that is whether or not the alleviation of the cytotoxic response takes place. Hence, a way to quantitively measure this outcome must be identified, one pre-requisite being that the marker chosen does not have overlapping functions from one phase of immune response to another. Based on these requirements, resorting to the assessment of granzyme b secretion constitutes an optimal approach. It is described as being primarily of CD8 T cell origin in aGvHD since the CD4 T cells demonstrated, if any, only to a lesser degree a potency in mediating this pathway, bearing in mind that the pathogenesis of aGvHD manifests itself via alternative routes, notably through Fas/FasL interaction or INF-γ and TNF-α production (Du and Cao, 2018). The latter, although quantifiable, would be hardly distinguishable from earlier phases, hence attributing any correlation between the targeted alteration of B cells antigen presenting activities and the cytotoxic effector phase, defined by INF-γ and TNF-α levels, involves a considerable bias.

Granzyme b, together with perforin, is stored in cytolytic granules which, upon conjugate formation, discharge their content within the synaptic cleft separating the cytotoxic T cell from its target, further crossing the membrane into the cytosol through pores formed by perforin (Boivin et al., 2009). However, this long held dogma is challenged, suggesting an endocytic uptake out of which granzyme b is released in a perforin-dependent way, ultimately inducing apoptosis by eliciting the caspase pathway or mitochondrial membrane destabilisation (Lieberman, 2003) (Figure 25).

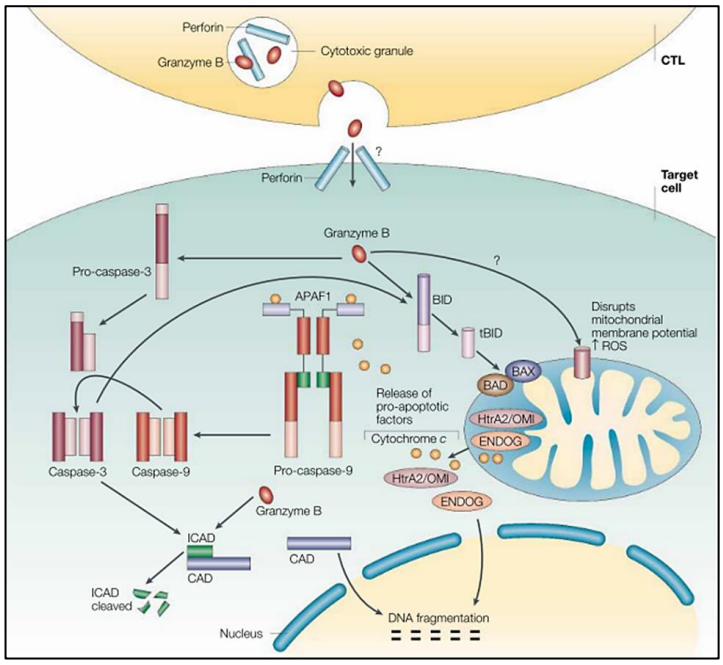

(Lieberman, 2003).

Figure 25. Granzyme b-mediated apoptosis of target cells Granzyme b discharged by the cytotoxic T cell in the synaptic cleft enters the target cell through pores formed by perforin or via endocytic uptake followed by a perforin-dependent release in the cytosol. Granzyme b then induces apoptosis by promoting the caspase cascade by cleaving caspase-3 into pro-caspase-3, or by disrupting the mitochondrial membrane which causes the leakage of the pro-apoptotic molecule cytochrome-c.

Importantly, the persistent increase in granzyme b serum levels following allogeneic HSCT was shown to be predictive of the incidence of aGvHD, establishing a correlation with its severity. It thus suggests that granzyme b would be a powerful marker to track the progression of aGvHD in these settings (Kircher et al., 2009). This confirms the pertinence of selecting granzyme b in our study.

3.2.3.5.2.2. Immunosuppressive response: IL-10

The implementation of the B cell depleting agent rituximab early after allogeneic HSCT yielding a high incidence of aGvHD has suggested that the withdrawal of B cells with immunosuppressive properties was achieved, thus shedding light on the potential role of Bregs (Clatworthy, 2011). The aim of the present study revolving around the dysregulation of the balance governed by promoters and suppressors of aGvHD in favour of the latter through the induction of resting B cells and redirection of their tolerogenic properties, it was of particular interest to determine whether such subset would be actively involved in the propagation of tolerogenic signal. Although efforts were made into the phenotypic

characterisation of Bregs, no consensus was found to this date on a set of markers exclusively identifying them. This questioned whether Bregs are even a distinct lineage, rather emerging from the whole pool of B cells as a result of the inflammatory stimuli surrounding them, hence leaving as the sole option to resort to their functional hallmark, that is their ability to produce the regulatory cytokine IL-10 (C. M. Wortel and Heidt, 2017). However, IL-10 is not restrictively of Breg origin, as a matter of fact it is ubiquitously secreted within the lymphoid and myeloid compartment as a negative feedback loop in a way to counterbalance any excessive immune response (Saraiva and O'Garra, 2010), therefore the challenge lies, if IL-10 levels are found to fluctuate in our model, in singling out the subset of cells at stake.

3.2.3.5.2.3. TNF-α

TNF-α is particularly represented throughout GvHD pathophysiology (Figure 22). Notably, TNF-α is one of the most commonly described components of the cytokine storm during the initiation phase of aGvHD (Kuba and Raida, 2018). Also, TNF-α is among the cytokines produced by primed T cells, further fuelling the allogeneic reaction (Ball and Egeler, 2008). Finally, TNF-α induces tissue injury as part of the effector phase (Markey et al., 2014). Hence, the determination of TNF-α levels would allow to follow the unravelling of the inflammatory environment within our model, the identification of the particular phase depicted being however challenging to achieve.

3.2.4. Impact of IL-15 supplementation on the MLR

3.2.4.1. Experimental strategy

The present study aims to address whether IL-15 is critical for the initiation of aGvHD or if its role lies primarily in the escalation of the inflammation. Although being a simplified system, the MLR supplemented with IL-15 was designed to model this context. The methodology applied to characterise the key drivers in M15 is presented Figure 26. The extent of discrepancies in surface marker expression and cytokine levels between R, the background status, and M, R15 and M15 is evaluated. The extent of the reaction in M15 attributable to the inflammatory environment established by IL-15 (M→M15) or the presence of allogeneic components (R15→M15) will indicate whether one parameter is

predominant in driving the recorded changes within M15 (R→M15) or if both are interrelated, in which case two scenarios are envisaged. Indeed, the outcome of the immune response could be a consequence of a synergistic effect further intensifying the inflammation observed in either contexts separately, or reveal an interdependence where both the presence of allogeneic components and IL-15 is required to elicit a reaction.

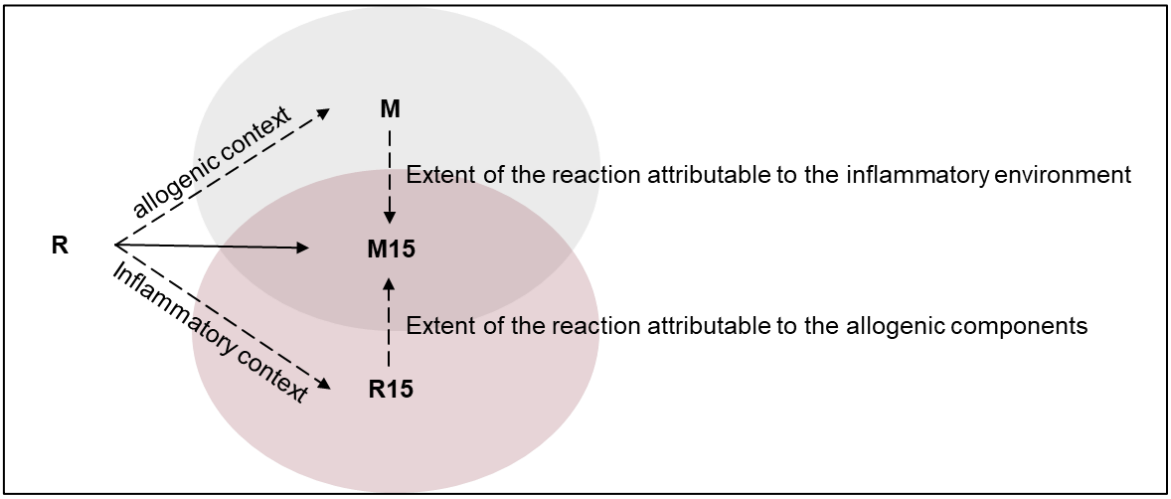

Figure 26. Methodology applied to identify the key players involved in the outcome of the allogeneic reaction in the newly designed *in vitro* model of histocompatibility The extent of the contribution within M15 of the inflammatory environment established by IL-15 and allogeneic context will be determined by comparing the surface marker expression and cytokine levels recorded with those obtained with R15 and M, respectively. This will reveal whether one parameter is a predominant driver of the reaction, or if both are interrelated, resulting in a synergistic effect escalating the inflammation or interdependence setting as a pre-requisite the co-existence of both parameters.

3.2.4.2. Responder B, CD8 and CD4 T cell phenotype

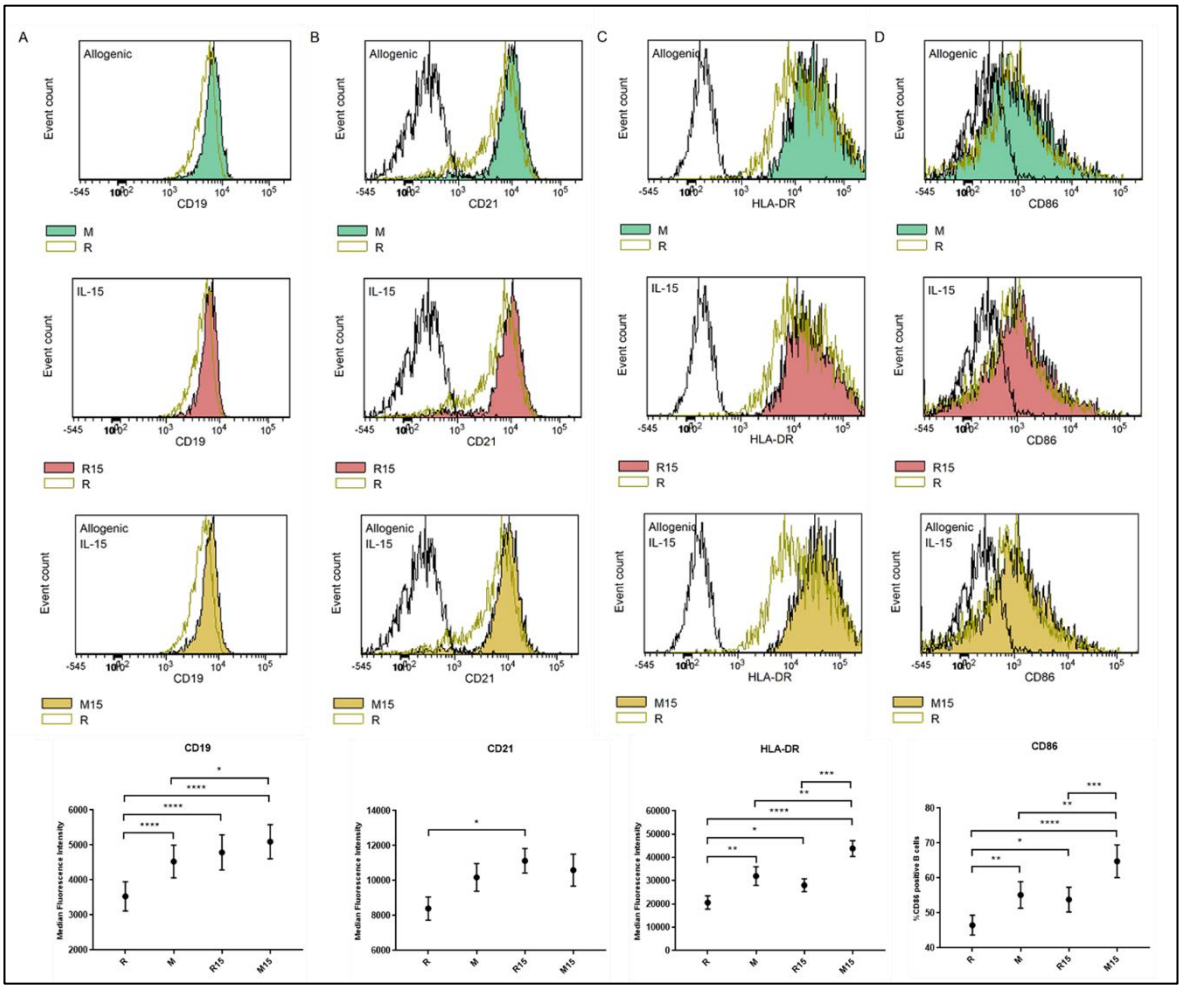

Figure 27. Impact of IL-15 on responder B cell phenotype A 3-day MLR was carried out following a StimCFSE/Resp ratio of 1:10 in 500µL/24-flat bottom wells (1 x 10^6 cells/well) supplemented (M15) or not (M) with 5ng/mL IL-15, including responders supplemented (R15) or not (R) with 5ng/mL IL-15. The MFI of **A)** CD19 (n=11) **B)** CD21 (n=8) **C)** HLA-DR (n=6) and **D)** %$CD86^+$ cells (n=9) on $CD19^+/CFSE^-$ responder B cells (1000 events recorded) gated within the lymphocyte population (FSC^{med}/SSC^{low}) were recorded. Data acquisition was carried out on the BD LSRFortessa X-20 with the BD FACS DIVA software (BD FACSDiva v8.0) and the graphs were generated with the FCSalyzer software (version 0.9.18-alpha; Sven Mostböck). Flow cytometry profiles representative of the experiments were overlaid together with the isotope control (clear peak). Statistical analysis was carried out with Prism (version 7; GraphPad Software) with the data reported as the means ± SEM (*p<0.05; **p<0.01; ***p<0.001; ****p<0.0001).

Regardless of the context involved, a substantial rise in CD19 (Figure 27A) expression is brought about. It reaches a 1.28-fold increase within an allospecific environment (μ_R=3535; μ_M=4527; p<0.0001) and 1.35-fold increase with IL-15 (μ_R=3535; μ_{R15}=4788; p<0.0001). Both these contexts combined yield a 1.44-fold upregulation (μ_R=3535; μ_{M15}=5096; p<0.0001), involving a synergistic effect at the root of which IL-15 appears to have the upper hand (μ_M=4527; μ_{M15}=5096; p<0.05) although, in spite of this ascendancy, the inclusion of an allogeneic aspect in CD19 upregulation cannot be excluded.

Interestingly, the modulation of CD21 (Figure 27B) expression is in sharp contrast with CD19, only showing a significant 1.25-fold upregulation in response to IL-15 (μ_R=8400; μ_{R15}=11132; p<0.05). The presence of allogeneic components, whatever the inflammatory environment, exerts little influence although the upward trend observed in the allogeneic context (μ_R=8400; μ_M=10183) is not reflected when combined with IL-15 (μ_{R15}=11132; μ_{M15}=10598). Furthermore, the loss of correlation in CD21 surface levels inputted by IL-15 when the allogeneic context is at stake (μ_R=8400; μ_{M15}=10598) could point to a downmodulation of CD21, keeping in mind that it would be minor since no significant drop stands out.

Interestingly, while a 1.55- and 1.36-fold upregulation of HLA-DR (Figure 27C) expression can be noticed when in the sole presence of allogeneic cells (μ_R=20650; μ_M=32009; p<0.01) and IL-15 (μ_R=20650; μ_{R15}=28087; p<0.05), respectively, providing a significant outcome, it is the synergistic effect between these two contexts which brings about the strongest response, increasing by 2-fold HLA-DR surface levels (μ_R=20650; μ_{M15}=43855; p<0.0001). This emphasizes here a marked shift towards a HLA-DR^{high} B cell population. When isolating the single engagement of the alloreaction (μ_{R15}=28087; μ_{M15}=43855; p<0.001) or inflammation (μ_M=32009; μ_{M15}=43855; p<0.01), neither stands out particularly, achieving a 1.51- and 1.37-fold rise in HLA-DR surface expression, respectively. Here, only the effect initially recorded in both contexts independently is retrieved, emphasising a cumulative effect.

An analogous trend is observed with CD86 (Figure 27D) expression, here presenting as well a strong correlation with the presence of allogeneic cells (μ_R=46.50%; μ_M=55.17%; p<0.01) and IL-15 (μ_R=46.50%; μ_{R15}=53.84%; p<0.05), achieving a 1.19- and 1.16-fold increase in responder CD86$^+$ B cells, respectively. Both contexts equally take part in the synergistic

outcome (μ_R=46.50%; μ_{M15}=64.78%; p<0.0001) in which a 1.39-fold upregulation is noted. Indeed, this is evidenced by the similar contribution of the alloresponse (μ_{R15}=53.84%; μ_{M15}=64.78%; p<0.001) and inflammation (μ_M=55.17%; μ_{M15}=64.78%; p<0.01) to this trend, accounting for 1.20- and 1.17-fold change, respectively.

The acquisition of significant assay windows imputable to the allogeneic reaction for CD86 and HLA-DR testifies of the successful optimisation procedure carried out to validate the Stim/Resp ratio (Figure 16) and IL-15 concentration (Figure 17). However, it can be noted that the use of CFSE staining to exclude the stimulators from the analysis has changed the fold ranges initially obtained during assay development. Indeed, it seemed to have shortened the assay window for CD86 (1.73 vs 1.19 in M; 1.41 vs 1.20 in M15) and increased it for HLA-DR (1.34 vs 1.55 in M; 1.15 vs 1.51 in M15). HLA-DR appears to be a more sensitive marker of the allogeneic reaction than CD86. Hence, the 10% stimulators making up the MLR seems to have an influence of the final data, despite representing a minor fraction of the cellular environment. However, as only one instance of the optimisation experiments was performed, a careful interpretation of these differences should be done.

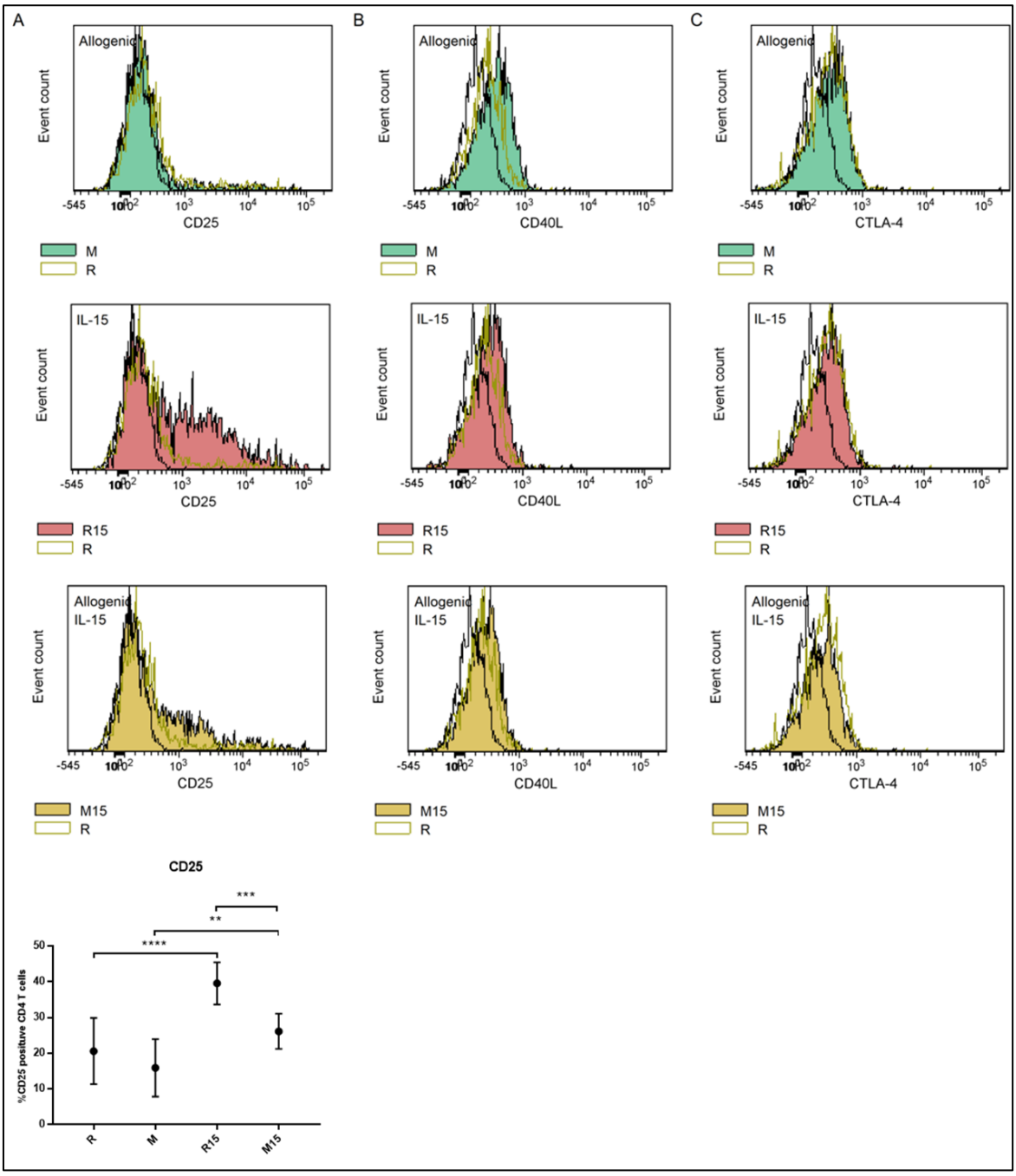

Figure 28. Impact of IL-15 on responder CD4 T cell phenotype A 3-day MLR was carried out following a StimCFSE/Resp ratio of 1:10 in 500µL/24-flat bottom wells (1 x 10^6 cells/well) supplemented (M15) or not (M) with 5ng/mL IL-15, including responders supplemented (R15) or not (R) with 5ng/mL IL-15. The **A)** %C25$^+$ (n=5) **B)** %CD40L$^+$ (n=2) and **C)** %CTLA-4$^+$ (n=2) on CD4$^+$/CFSE$^-$ responder CD4 T cells (1000 events recorded) gated within the lymphocyte population (FSC^{med}/SSC^{low}) was recorded. Data acquisition was carried out on the BD LSRFortessa X-20 with the BD FACS DIVA software (BD FACSDiva v8.0) and the graphs were generated with the FCSalyzer software (version 0.9.18-alpha; Sven Mostböck). Flow cytometry profiles representative of the experiments were overlaid together with the isotope control (clear peak). Statistical analysis was carried out with Prism (version 7; GraphPad Software) with the data reported as the means ± SEM (*p<0.05; **p<0.01; ***p<0.001; ****p<0.0001).

Noteworthy, a 1.9-fold upregulation of responder $CD25^+$ CD4 T cells imputed by IL-15 is recorded (μ_R=20.62%; μ_{R15}=39.59%; $p<0.0001$) (Figure 28A). However, the inclusion of allogeneic components within this milieu induces a 0.66-fold drop in this subset (μ_{R15}=39.59%; μ_{M15}=26.16%; $p<0.01$). Here, the fraction of $CD25^+$ CD4 T cells is reaching a similar level range as that found in the initial background status (μ_R=20.62%; μ_{M15}=26.16%). Although no correlation is found, a slight decrease in responder $CD25^+$ CD4 T cells can be observed in the allogeneic context devoid of IL-15 (μ_R=20.62%; μ_M=15.92%). Consequently, the effect of IL-15 on the allogeneic reaction generates a 1.64-fold increase in the subset of responder $CD25^+$ CD4 T cells (μ_M=15.92%; μ_{M15}=26.16%), here only reflecting the effect of IL-15 as seen in the context independent of antigen specificity.

As for CD40L (Figure 28B) and CTLA-4 (Figure 28C), the data indicate that the responder CD4 T cells do not show any detectable levels at a basal status. It also appears that IL-15 has no effect on CD40L and CTLA-4 expression, a similar outcome being observed within an allogeneic context whether or not an IL-15-rich milieu is present. However, the interpretation of the data obtained for CD40L and CTLA-4 must be cautiously drawn since only two experiments were carried out instead of the 3 instances, as usually required for *in vitro* studies.

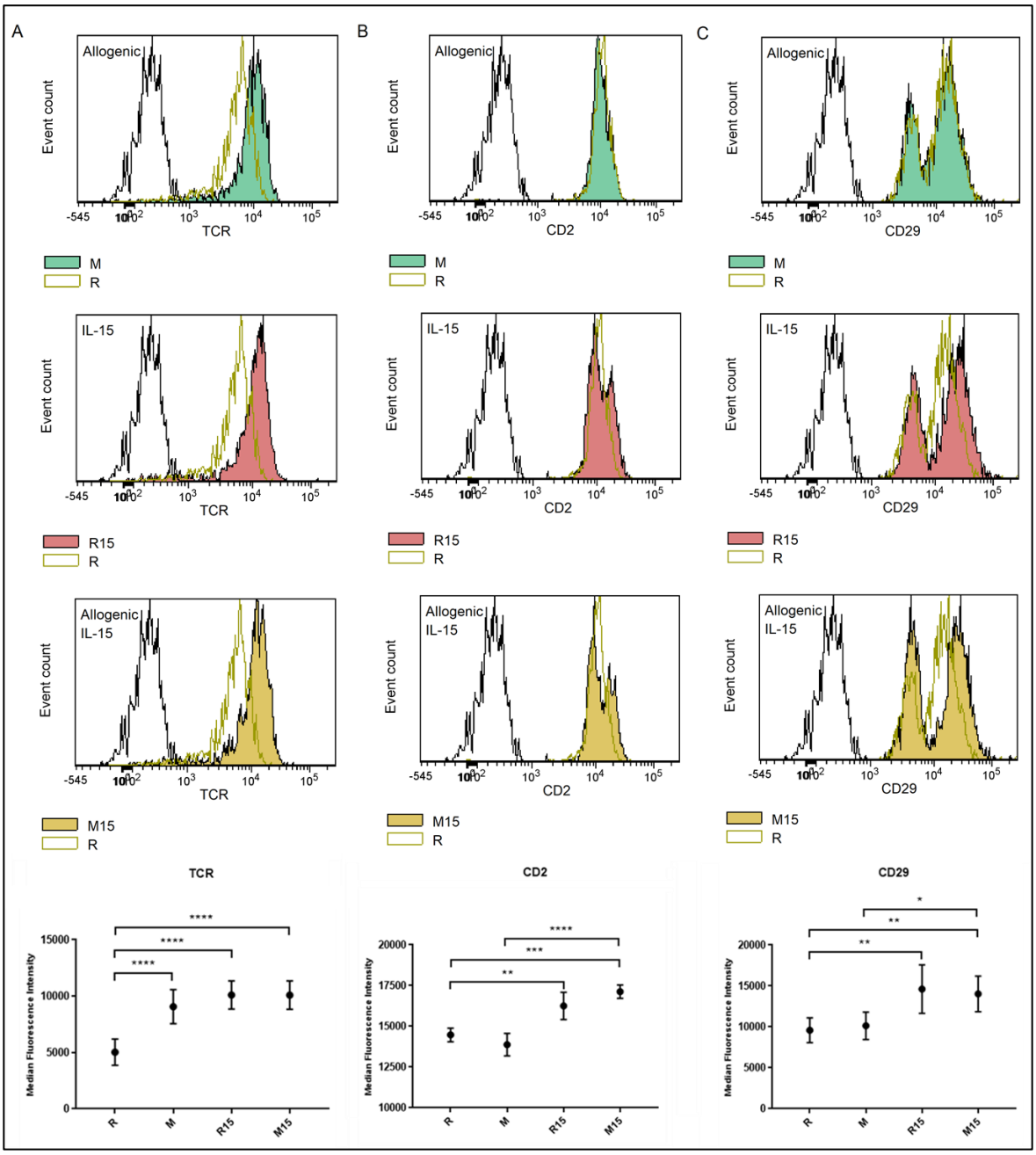

Figure 29. Impact of IL-15 on responder CD8 T cell phenotype A 3-day MLR was carried out following a StimCFSE/Resp ratio of 1:10 in 500µL/24-flat bottom wells (1 x 10^6 cells/well) supplemented (M15) or not (M) with 5ng/mL IL-15, including responders supplemented (R15) or not (R) with 5ng/mL IL-15. The MFI of **A)** TCR (n=6) **B)** CD2 (n=6) and **C)** CD29 (n=6) on $CD8^+/CFSE^-$ responder CD8 T cells (1000 events recorded) gated within the lymphocyte population *(*FSC^{med}/SSC^{low}) was recorded. Data acquisition was carried out on the BD LSRFortessa X-20 with the BD FACS DIVA software (BD FACSDiva v8.0) and the graphs were generated with the FCSalyzer software (version 0.9.18-alpha; Sven Mostböck). Flow cytometry profiles representative of the experiments were overlaid together with the isotope control (clear peak). Statistical analysis was carried out with Prism (version 7; GraphPad Software) with the data reported as the means ± SEM (*p<0.05; **p<0.01; ***p<0.001; ****p<0.0001).

Whether at the allospecific (μ_R=5030; μ_M=9066; p<0.0001) or inflammatory level (μ_R=5030; μ_{R15}=10107; p<0.0001), a sharp upregulation of TCR (Figure 29A) surface expression, up to 1.8- and 2-fold respectively, is achieved, similarly observed when both parameters are accounted for (μ_R=5030; μ_{M15}=10096; p<0.0001), reaching a 2-fold change. Thus, it appears that no cumulative effect is materialized here quantitatively, nor is a sole repercussion of IL-15 envisaged although it seems to potentiate a strongest increase. Thus, it could be speculated that a plateau in TCR surface expression is reached, the allospecificity of which most likely established since the allogeneic context on its own triggers its elevation, IL-15 possibly accelerating this process.

While all CD8 T cells express CD2 (Figure 29B), a 1.1-fold rise in surface density expression imputable to IL-15 (μ_R=14475; μ_{R15}=16255; p<0.01) is recorded, interestingly denoting the formation of a secondary subset not clearly distinct from the initial population. This indicates that only a fraction of CD8 T cells is responsive to IL-15 as opposed to a general effect that would result in the shift of the entire population. A comparable modulation is observed when a possible synergy with the allogeneic response was sought, reaching a 1.18-fold increase. (μ_R=14475; μ_{M15}=17129; p<0.001). Here, although slightly higher, it mainly stems from the presence of IL-15 (μ_M=13881; μ_{M15}=17129; p<0.0001). Thus, no significant impact of the allogeneic reaction itself can be assumed here. Since no alteration in CD2 expression profile is observed in the allogeneic context only (μ_R=14475; μ_M=13881), it can be asserted that IL-15 is the predominant factor in the shaping of CD2 modulation.

A trend analogous to that of CD2 applies to CD29 (Figure 29C) profile expression, that is the repercussion of IL-15 on CD29 upregulation by 1.52-fold (μ_R=9597; μ_{R15}=14619; p<0.01), comparable to the 1.47-fold change observed when an allogeneic component was introduced within this inflammatory milieu (μ_R=9597; μ_{M15}=14037; p<0.01). No particular effect attributable to the allogeneic reaction (μ_{R15}=14619; μ_{M15}=14037) seems to take place. Given that CD29 is immutable in the sole presence of allogeneic components (μ_R=9597; μ_M=10136) and that only the addition of IL-15 (μ_M=10136; μ_{M15}=14037; p<0.05) results in a significant difference, it is apparent that IL-15 is the sole regulator at stake here.

3.2.4.3. Effector response: granzyme b, IL-10 and TNF-α production

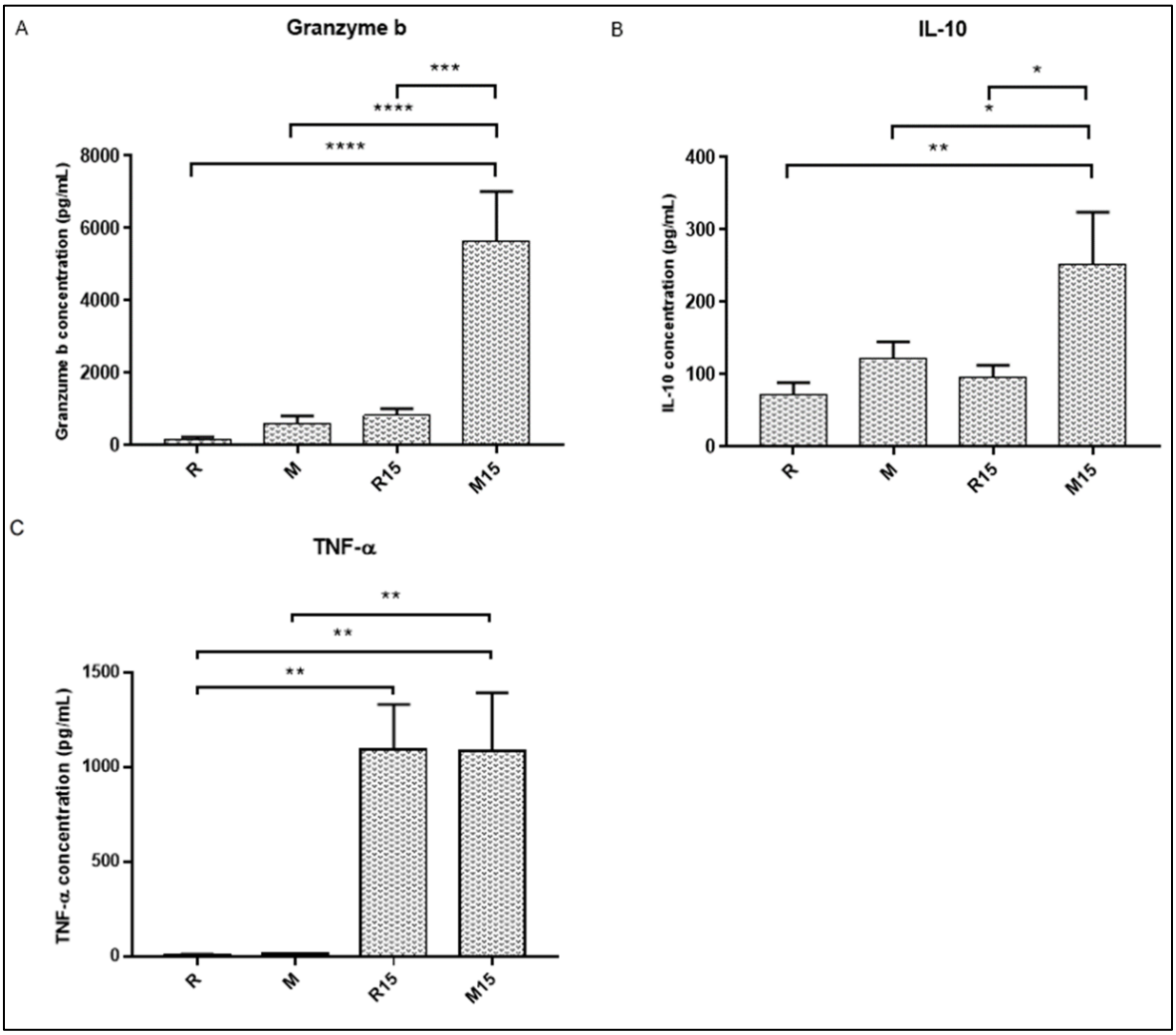

Figure 30. Impact of IL-15 on the effector response A 3-day MLR was carried out following a StimCFSE/Resp ratio of 1:10 in 500µL/24-flat bottom wells (1 x 10^6 cells/well) supplemented (M15) or not (M) with 5ng/mL IL-15, including responders supplemented (R15) or not (R) with 5ng/mL IL-15. The production of **A)** granzyme b (n=8), **B)** IL-10 (n=5) and **C)** TNF-α (n=4) in frozen supernatants was measured by ELISA. Data acquisition was carried out on the SPECTROstar Nano (BMG Labtech, Aylesbury, England) and the data were generated with MARS software (BGM Labtech, Aylesbury, England). Statistical analysis was carried out with Prism (version 7; GraphPad Software) with the data reported as the means ± SEM (*p<0.05; **p<0.01; ***p<0.001; ****p<0.0001).

It clearly stands out that only the allogeneic context combined with IL-15 (μ_R=171.56pg/mL; μ_{M15}=5.66ng/mL; p<0.0001) shows a significant escalation in Granzyme b (Figure 30A) production, more than 30 times higher than the background status. This trend is similarly denoted when analysing the part taken by each component separately, whether exclusively linked to the allogeneic (μ_{R15}=824.81pg/mL; μ_{M15}=5.66ng/mL; p<0.001) or inflammatory (μ_M=615.84pg/mL; μ_{M15}=5.66ng/mL; p<0.0001) milieu, characterised by a 6.86-fold and 9.19-fold incrementation respectively. Hence, it evidently emphasises that the synergy observed is not solely attributed to a cumulative effect but is indeed generating a singular outcome, revealing of their interdependence.

Likewise, whereas IL-10 (Figure 30B) levels attributable to the presence of allogeneic components (μ_R=72.25pg/mL; μ_M=121.45pg/mL) or IL-15 (μ_R=72.25pg/mL; μ_{R15}=96.87pg/mL) do not reflect any particular variations, they seem however self-explanatory of the 3.49-fold augmentation observed when both these parameters are accounted for (μ_R=72.25pg/mL; μ_{M15}=252.49pg/mL; p<0.01). Hence, following the pattern observed with granzyme b, the synergy emphasised here does not show a cumulative effect nor an ascendent trend where one of the factors investigated would exert a distinct effect, predominant on the other. They rather show a mutual reciprocity, the contribution of the allogeneic reaction equally significant (μ_{R15}=96.87pg/mL; μ_{M15}=252.49pg/mL; p<0.05) as that of IL-15 (μ_M=121.45pg/mL; μ_{M15}=252.49pg/mL), achieving a 2.61-fold and 2.08-fold increase, respectively.

Unlike granzyme-b and IL-10, TNF-α (Figure 30C) is highly responsive to IL-15 stimulation, denoting an 81.76-fold increase in TNF-α secretion (μ_R=13.43pg/mL; μ_{R15}=1,098ng/mL; p<0.01). The allogeneic context, whether enriched in IL-15 (μ_{R15}=1.098ng/mL; μ_{M15}=1.087ng/mL) or not (μ_R=13.43pg/mL; μ_M=15.19pg/mL), does not impact TNF-α levels. Hence, only the impact of IL-15 stimulation on TNF-α secretion is visible here.

3.2.4.4. Summary

The data generated in this chapter gave us the opportunity to extract the effects inherent to each context individually, with respect to M and R15, on the markers investigated, allowing us to draw a trend on their eventual synergistic outcomes, represented by M15, whether this influences the course of the immune response as depicted by the nature of the inflammatory environment is highlighted (Figure 31).

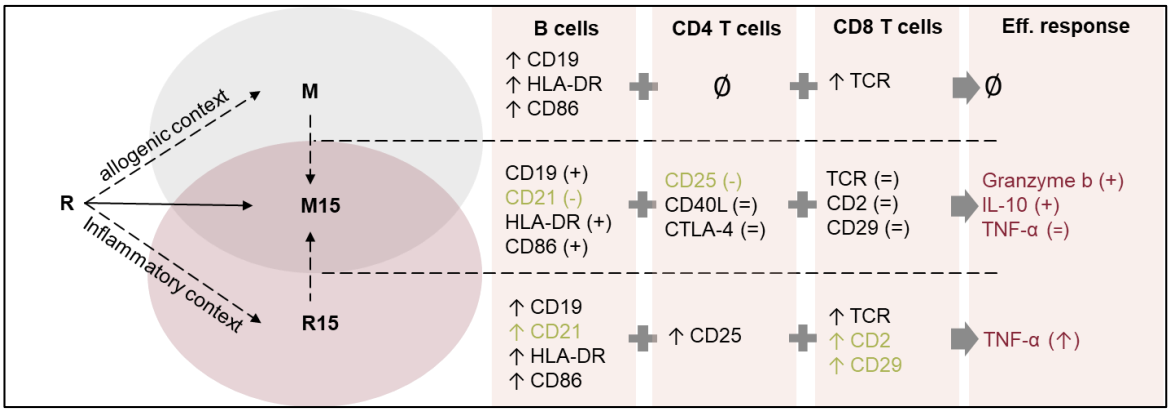

Figure 31. Summary of the effects inherent to M and R15 individually and their synergistic impact, represented by M15, on the outcome of the immune reaction Only B cell, CD4 and CD8 T cell markers for which a trend exists (upregulation: ↑; downregulation: ↓) in M or R15 individually are included. The outcome of the combination of M and R15, represented by M15, is expressed according to the resulting trend, either promoting a positive (+) or negative (-) synergistic effect, no synergy (=) or no effect at all (Ø). In green are identified the markers which trend reflects a distinct divergence.

3.3. Fine-tuning B cell activation: targeting the CD19/CD21 complex with epratuzumab and C3d

3.3.1. Epratuzumab

3.3.1.1. Rational for the inclusion of epratuzumab

The strategy adopted in the present study to dictate the fate of B cells into the induction of a resting state is twofold. Firstly, to shift the balance existing between the signals transduced by antagonistic BCR response regulators in favour of an inhibitory feedback. This would raise the threshold for BCR activation and thus, hinder the completion of antigen uptake and processing for presentation. The second strategy being to divert antigen engagement through an alternative pathway failing to provide adequate co-stimulatory activities, here betting on the potential to harness tolerogenic properties.

The humanised monoclonal anti-CD22 antibody epratuzumab induces in less than 1h, independent of antigen engagement, the mobilisation of CD22 into lipid rafts neighbouring the BCR, co-localising with CD79α (Sieger et al., 2013). Subsequently, it precipitates the dephosphorylation of downstream BCR signal transducers, notably Syk and PLCγ2, ultimately hindering B cell activation. Concurrently, epratuzumab triggers the internalisation of the BCR complex along with CD19 and CD21 and, alternatively, exert the physical surface downregulation of these components through a process referred to as trogocytosis (Dörner et al., 2015) (Figure 32). It brings into play the transfer of cell surface material onto the membrane of FcγR-bearing cells, notably monocytes, here emphasizing the implication of the Fc domain of epratuzumab since such mechanism was absent with the use of the F(ab')2 fragment of epratuzumab.

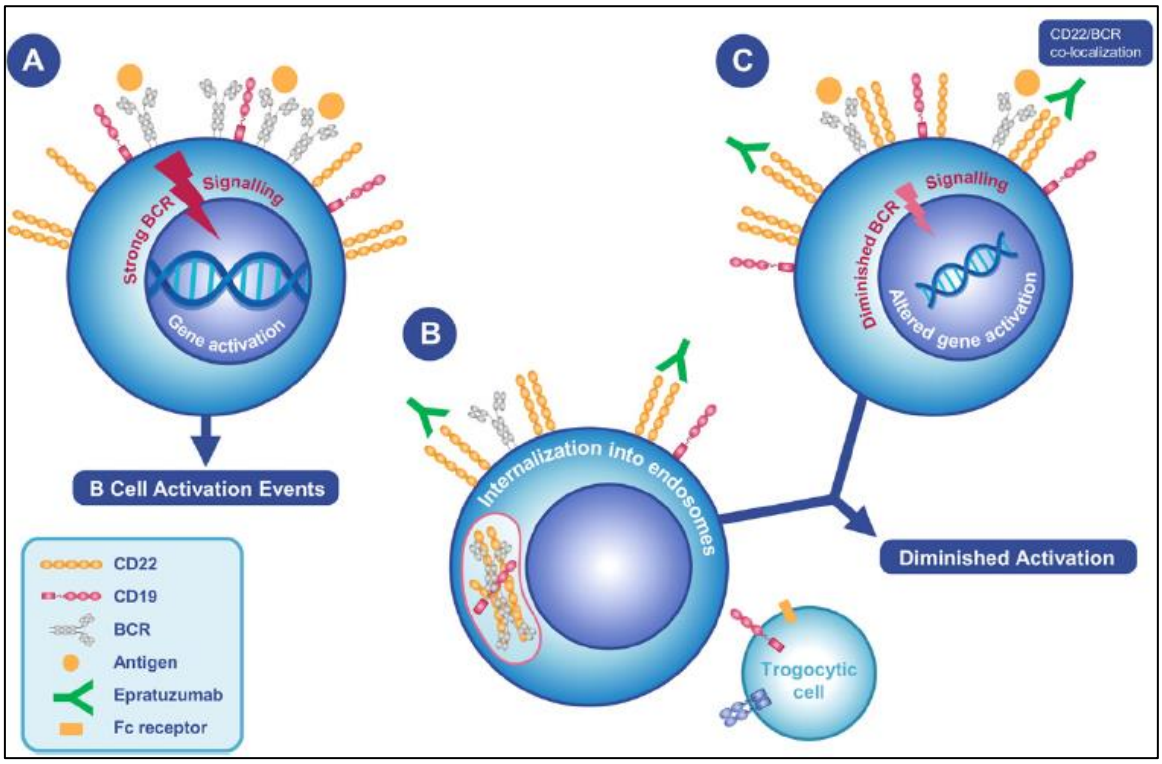

(Dörner et al., 2015)

Figure 32. Inhibition of B cell activation by the humanised monoclonal anti-CD22 antibody epratuzumab: mode of action Epratuzumab induces the generation of hyporesponsive B cells through sustained inhibitory signals and reduction in cell surface expression of the BCR response regulator CD19/CD21 complex through internalisation or trogocytosis.

While evidence shows that endocytosed CD22 can shuttle glycan ligand-based cargo to endosomal compartments and recycle back to the cell surface with its binding groove empty, contrasting outcomes arise when the anti-CD22 antibody RFB4 is involved (O'Reilly et al., 2011). Indeed, it rather depicts a joint recycling/redistribution of the CD22/anti-CD22 antibody RFB4 complex to the membrane. This mechanism was corroborated in a study testing 5 antibodies recognizing overlapping or distinct CD22 epitopes, showing that internalised anti-CD22 antibodies promptly recycled to the surface and thus, underwent minimal degradation in lysosomes, except when extensive recycling occurred (Ingle and Scales, 2013). Although epratuzumab-mediated CD22 turnover has not been the subject of such investigations, it is reasonably assumed that it would adopt similar processes. Indeed, epratuzumab exerts high binding affinity to CD22 across a wide range of acidic pH's characteristics of sorting endosomes and lysosomes, thus refuting a possible dissociation of epratuzumab from CD22 (Ereño-Orbea et al., 2017). Hence, the persistence of epratuzumab on the cell surface could not only sustain prolonged inhibitory signals but also even fuel the completion of trogocytic events. Alternatively, the absence of detectable surface CD22

recorded for an extended period of time in Huki mice, up to 57 days after epratuzumab injection followed by a recovery to baseline expression by day 84, was proposed to be caused by the residual serum persistence of epratuzumab systematically engaging CD22, ruling out a potential involvement of trogocytosis in this effect (Özgör et al., 2016).

Unlike rituximab which promotes B cell depletion through either antibody-dependent cellular cytotoxicity (ADCC) or complement-dependent cytotoxicity (CDC), epratuzumab generates hyporesponsive B cells by providing a sustained inhibitory signal mediated by the intensification of CD22 signalling, together with a reduction of surface CD19/CD21 complex expression (Dörner et al., 2015), Here, the advantage lies in the benefit of this resting state as opposed to solely depleting B cells

Hence, epratuzumab represents an ideal candidate to fulfil the first requirement of the present study.

3.3.1.2. Technical considerations

Epratuzumab is commonly used at 10µg/mL in *in vitro* experimental studies (Lumb et al., 2016; Sieger et al., 2013). At this concentration, CD22, CD19 and CD21 are reduced by 50%, 52% and 70%, respectively, however, similar effects are recorded for CD19 and CD22 when epratuzumab is used at lower concentrations (Rossi et al., 2013) (Figure 33). CD21 supposedly follows the same trend. According to this study, 50ng/mL epratuzumab is the lowest concentration at which such identical profiles are yielded.

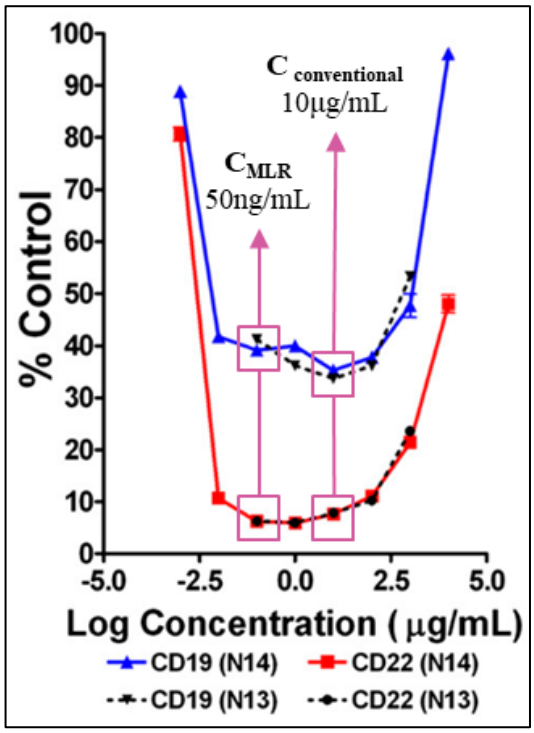

(Rossi et al., 2013)

Figure 33. Profile of CD19 and CD22 reduction obtained with epratuzumab concentrations ranging from 1ng/mL to 100µg/mL The 10µg/mL epratuzumab concentration conventionally used in experimental studies provides similar reductions in CD19 and CD22 to 50ng/mL, which is selected for the MLR.

Hence, since care is taken not to unbalance the milieu at stake in the MLR, the lowest concentration providing optimal decrease in surface expression levels of CD19 and CD21 is selected. Based on the CD19 and CD22 reduction profile (Rossi et al., 2013), a concentration of 50ng/mL clearly fulfils this prerequisite.

The effect of epratuzumab signalling is not tightly linked to an allogeneic context since the reduction in CD22, CD19 and CD21 is observed without BCR engagement (Sieger et al., 2013). Consequently, the distinction with an allospecific outcome, indicative of whether a more targeted response is triggered as opposed to a sole broad consequence of the loss of surface CD19/CD21 complex, should be accounted for in the present study. To this aim, control conditions including the impact of epratuzumab on responders supplemented with IL-15 ($R15_{Epratuzumab}$), which represents the inflammatory environment of our model without the allogeneic component, is included. Ultimately, the identification of an eventual alteration of the allogeneic response within these conditioned environments from its original course will help evaluate the strength of the signal transduced.

3.3.2. C3d

3.3.2.1. Rational for the inclusion of C3d

While epratuzumab is used to drive B cells in a state of unresponsiveness, the chances that they can exert tolerogenic properties are limited since the acquisition of antigen specificity is a pre-requisite. The induction of self-tolerance within K^dHA-specific naïve CD8 T cells required K^dHA-specific resting B cells (Fraser et al., 2006). Similarly, the protection against T cell-mediated demyelination in EAE required resting B cells presenting MOG-derived epitopes via their class II MHC molecule (Calderón-Gómez et al., 2011). Given that epratuzumab would disrupt their capacity to capture and present antigen, no tolerogenic signal would be supported. A way to circumvent this issue would be to drive antigen uptake, irrespective of any specificity, through CD21 with the concourse of C3d. Here, it would provide the "switch on" signal for tolerance induction. In such a context, the immunopeptidome towards which resting B cells could potentiate their immunosuppressive response would be extensive (Boackle et al., 1998; Zsef Prechl et al., 2002). This strategy could however be double-edged considering that C3d supplementation is documented as being instead the critical missing factor at the root of disease onset, hence C3d adjunction could be counterproductive. Nonetheless, the hyporesponsive state induced by epratuzumab could set the line between these two outcomes, tilting the balance towards tolerance. To test this hypothesis, C3d adjunction will be performed in our model in presence and absence of epratuzumab, providing an insight on whether CD19/CD21 surface level expression, associated with a resting state, could be a determining factor which dictates the direction taken by the immune response, emphasising here the dual effect of C3d.

Hence C3d supplementation within these two contexts would fulfil the second requirement of the present study.

3.3.2.2. Technical considerations

While the adjuvant power of C3d was the subject of few investigations, it was used in a CIA mouse model (Del Nagro et al., 2005) and MOG/C3d fusion protein construct (Jégou et al., 2007), thus no standard C3d concentration is available for *in vitro* experimental studies. However, physiological C3d serum levels in patients with systemic lupus erythematosus (SLE) were determined, ranging from 129-291ng/mL (Krauledat et al., 1985), providing here reference values in disease settings. The aim of the present study being only to divert antigen uptake towards CD21 in an effort to favour tolerance over activation, it can be speculated that pathogenic levels would antagonise this effect, hence bringing down the concentration to 50ng/mL, more than half the lowest value recorded in SLE, would account for this problem.

Since epratuzumab exerts its effects 30-45 minutes following induction (Dörner et al., 2015) and achieve complete response within a few hours (Rossi et al., 2013), the generation of hyporesponsive B cells ($M15_{Epratuzumab}$) will occur prior to any engagement of C3d with antigens would take place, this temporality ensuring that it is the impact of C3d adjunction on hyporesponsive B ($M15_{Epratuzumab/C3d}$) cells that is particularly investigated. This, however, raises the questions as to whether the extent of CD19/CD21 complex surface density determines the nature of the signal transduced by C3d, hence the effect of C3d adjunction on unmodified B cells (M15+C3d) is investigated.

Although C3d signalling is tightly linked to an allogeneic context, similar controls as those included for epratuzumab are used to rule out any unspecific effect. Therefore, based on the same reasoning, the impact of C3d on responders supplemented with IL-15 (R15+C3d) is carried out in order to confirm that its activity is restricted to the allogeneic context.

Altogether, this strategy will provide an insight on the strength of the tolerogenic signal propagated by the hereby generated resting B cells. On a broader perspective, it will also give the opportunity to evaluate the extent to which the CD19/CD21 complex participate in B cells antigen presenting potency within the priming phase of aGvHD, if any commitment at this level is noticed on behalf of B cells, since the model designed here attempts to reflect the inflammatory environment described in patients presenting severe grade aGvHD. The key challenge lies indeed in the intense inflammatory milieu at stake in aGvHD which could

supersede the strategy taken to sustain a resting state in B cells, questioning the pertinence of a hypothetical therapeutic implementation in clinical practice.

3.3.3. Experimental strategy

The targeting of the CD19/CD21 complex on responder B cells was divided into 3 core investigations, each providing a detailed understanding of the mechanistic impact of epratuzumab and C3d supplementation, whether on unresponsive or unmodified B cells (Figure 34).

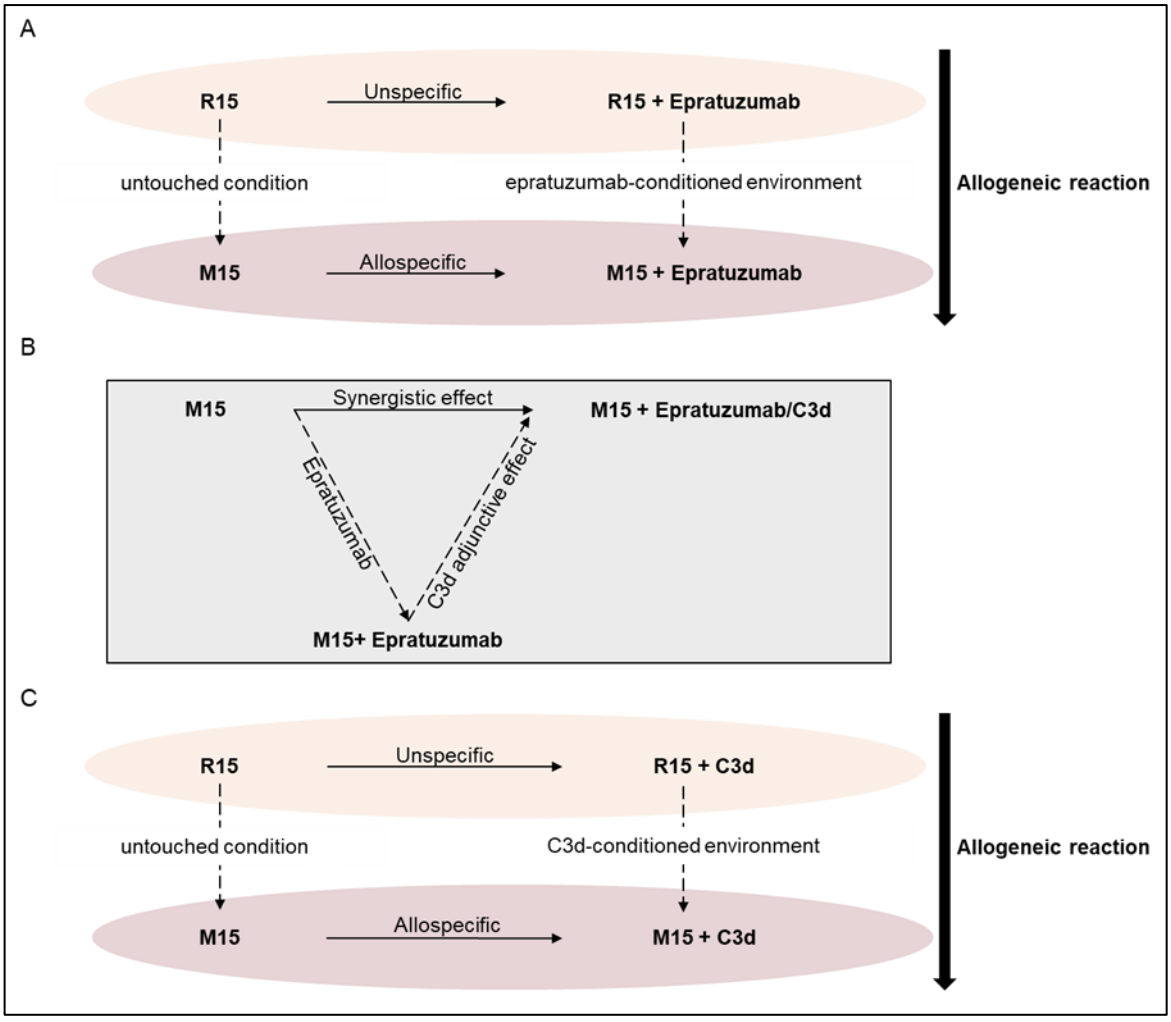

Figure 34. Methodology applied to identify the key players involved in the outcome of the allogeneic reaction A) Induction of unresponsive B cells with epratuzumab B) C3d supplementation on epratuzumab-induced unresponsive B cells C) C3d supplementation on unmodified B cells

Epratuzumab exerts reduction in CD22, CD19 and CD21 without BCR engagement. A distinction with an allogeneic outcome indicative of a more targeted response must be made. These distinct features will be isolated by evaluating its unspecific ($R15_{Epratuzumab}$) and allospecific ($M15_{Epratuzumab}$) effects (Figure 34A), whether or not the elicitation of the alloreaction within the epratuzumab-conditioned milieu ($M15_{Epratuzumab}$) diverges from its typical course in unmodified conditions (M15) is investigated.

Then, the adjunctive or synergistic effect of C3d on epratuzumab-induced unresponsive B cells ($M15_{+Epratuzumab/C3d}$) is examined so as to identify a potential diversion of the immune response from that triggered by epratuzumab only ($M15_{Epratuzumab}$), hence attributable to the direction of C3d-coated antigens away from classical processing and presentation (Figure 34B).

Finally, analogous to the reasoning governing the isolation of the intrinsic and incidental consequences of epratuzumab application, the above-mentioned mechanism is sought in unmodified B cells. This will provide an insight as to whether the initial status of B cells, at the core of which prevails the described surface reduction in CD19/CD21 complex, is a determining factor for the direction taken by the C3d-mediated signalling (Figure 34C) as evidence show a dual, yet, contrasting effect, either potentiating BCR activation or inversely promoting tolerance.

The distribution of CD21 throughout the lymphocyte compartment up until now sparks an open debate over its exclusiveness to B cells (Braun, 1998). It indeed adopts an ubiquitous pattern as arising evidence correlates T cells predisposition for CD21 expression with pathophysiological settings, a subset attributed with the capability to strengthen cellular adhesion in SLE or facilitate Epstein-Barr virus entry into T cells (Levy et al., 1992; Smith et al., 2020). Thus, it needs to be assured that the existence of such phenotype is ruled out in our model before any assertion can be drawn on the signalling transduced by unresponsive B cells when C3d adjunction is investigated. Although representing a minor fraction of the events involved in aGvHD onset, the inclusion of IL-15 could induce such events considering its critical role in the progression to severe aGvHD.

Taking advantage of the omnipresence of CD21 on the surface of B cells to set a threshold value for the determination of the extent of its prevalence on non-B cells (Figure 35), it

appears that CD21 solely pertains to B cells. This expression profile is unaffected by the immune response characterised in the MLR as mirroring the IL-15-centred progression to severe aGvHD.

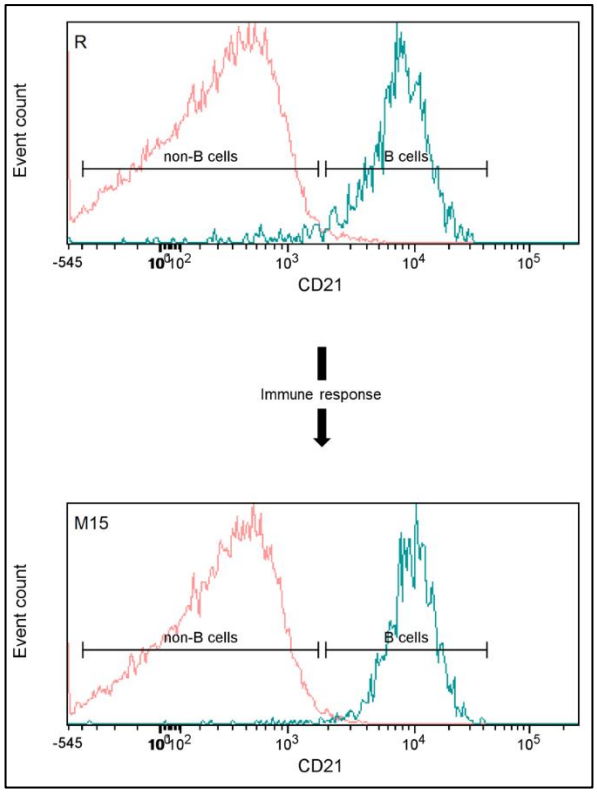

Figure 35. Evolution of CD21 expression profile in non-responder B cells in M15 A 3-day MLR was carried out following a StimCFSE/Resp ratio of 1:10 in 500µL/24-flat bottom wells (1 x 10^6 cells/well) supplemented with 5ng/mL IL-15 (M15), including untouched responders (R). Gating on the lymphocytes, (FSC^{med}/SSC^{low}), non-responder B cells were selected as $CD19^-/CFSE^-$ cells and responder B cells as $CD19^+/CFSE^-$ cells. Flow cytometry profiles of CD21 expression in R (top histogram) and M15 (bottom histogram show the extent of CD21 expression acquired during the alloreaction in a milieu rich in IL-15. Data acquisition was carried out on the BD LSRFortessa X-20 with the BD FACS DIVA software (BD FACSDiva v8.0) and the graphs were generated with the FCSalyzer software (version 0.9.18-alpha; Sven Mostböck).

Since no overlapping mechanism can emanate from C3d adjunction, strictly restricted to B cells, any modulation of CD8 T cells phenotypic characteristics will be a consequence of the signalling propagated by B cells as a downstream target of C3d-coated antigen co-engagement with CD21, the unresponsive or untouched state in which B cells are maintained revealing of the direction taken by the immune response.

3.3.4. Induction of an unresponsive state in B cells: Epratuzumab

3.3.4.1. Responder B and CD8 T cell phenotype

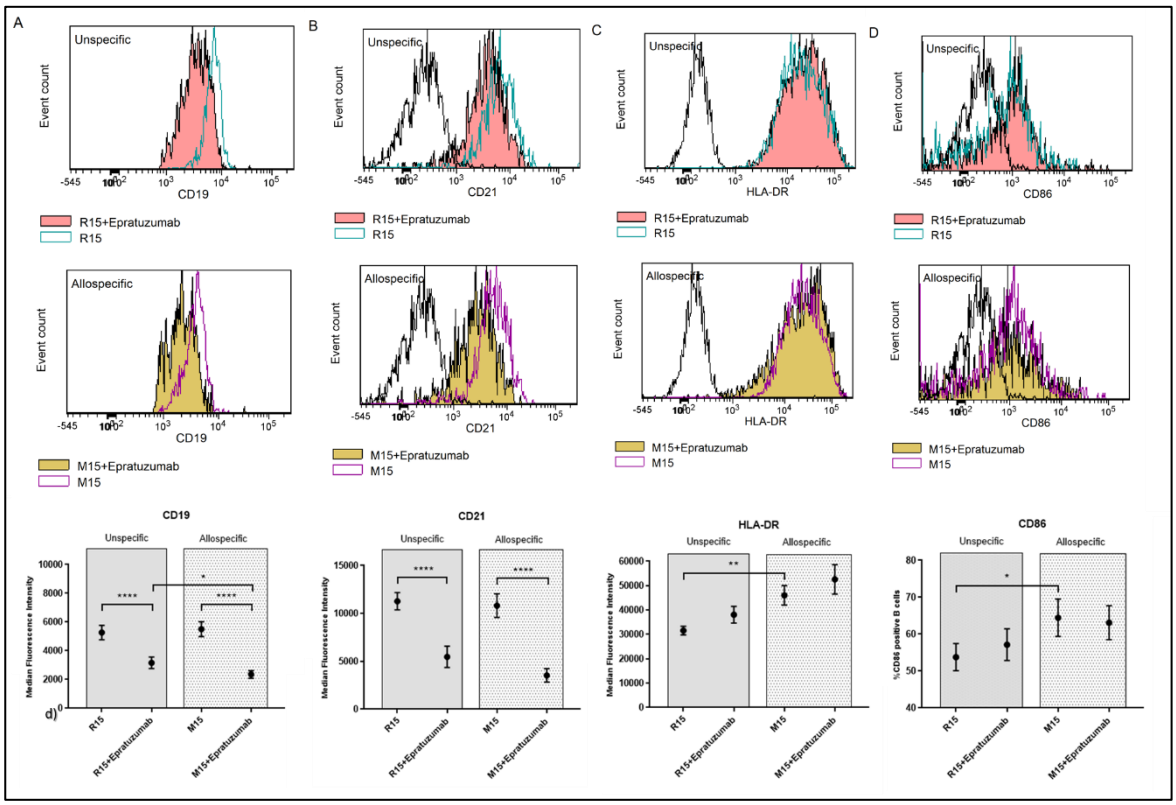

Figure 36. Impact of epratuzumab on responder B cell phenotype A 3-day MLR was carried out following a StimCFSE/Resp ratio of 1:10 in 500µL/24-flat bottom wells (1 x 10^6 cells/well) supplemented with 5ng/mL IL-15 and treated ($M15_{Eptauzumab}$) or not (M15) with 50ng/mL epratuzumab, including responders supplemented with 5ng/mL IL-15 and treated ($R15_{Eptauzumab}$) or not (R15) with 50ng/mL epratuzumab. The MFI of **A)** CD19 (n=9) **B)** CD21 (n=6) **C)** HLA-DR (n=8) and **D)** $\%CD86^+$ cells (n=7) on $CD19^+/CFSE^-$ responder B cells (1000 events recorded) gated within the lymphocyte population (FSC^{med}/SSC^{low}) were recorded. Data acquisition was carried out on the BD LSRFortessa X-20 with the BD FACS DIVA software (BD FACSDiva v8.0) and the graphs were generated with the FCSalyzer software (version 0.9.18-alpha; Sven Mostböck). Flow cytometry profiles representative of the experiments were overlaid together with the isotope control (clear peak). Statistical analysis was carried out with Prism (version 7; GraphPad Software) with the data reported as the means ± SEM (*p<0.05; **p<0.01; ***p<0.001; ****p<0.0001).

The efficacy of epratuzumab is clearly apparent here, as denoted by the dramatic 1.66- and 2.06-fold unspecific reduction in CD19 (μ_{R15}=5268; $\mu_{R15+Epratuzumab}$=3165; $p<0.0001$) (Figure 36A) and CD21 (μ_{R15}=11272; $\mu_{R15+Epratuzumab}$=5466; $p<0.0001$) (Figure 36B) surface expression respectively. Here, a stronger effect on CD21 is emphasized. Only CD19 modulation showed an allospecific outcome with a 1.34-fold decrease ($\mu_{R15+Epratuzumab}$=3165; $\mu_{M15+Epratuzumab}$=2360; $p<0.05$). Conversely, while CD21 internalisation further to C3d-coated antigen uptake could be argued for its loss, it seems here to only be imputed to the inherent features of epratuzumab ($\mu_{R15+Epratuzumab}$=5466; $\mu_{M15+Epratuzumab}$=3535).

HLA-DR (Figure 36C) does not seem to be directly modulated by epratuzumab, neither unspecifically (μ_{R15}=31569; $\mu_{R15+Epratuzumab}$=38087) nor allospecifically (μ_{M15}=46039; $\mu_{M15+Epratuzumab}$=52565). It appears however to be a downstream target of the immune response altered within the epratuzumab-conditioned environment as evidenced by the failure to identify the allogeneic reaction ($\mu_{R15+Epratuzumab}$=38087; $\mu_{M15+Epratuzumab}$=52565) although a distinguishable 1.46-fold upregulation is recorded in unmodified conditions (μ_{R15}=31567; μ_{M15}=46039; $p<0.01$).

A similar trend is observed with CD86 (Figure 36D). That is, an unresponsiveness to epratuzumab, whether in a context devoid of allogeneic components (μ_{R15}=53.80%; $\mu_{R15+Epratuzumab}$=57.15%) or including this aspect (μ_{M15}=64.46%; $\mu_{M15+Epratuzumab}$=63.12%). And yet, a loss of the 1.2-fold upregulation observed in unmodified conditions (μ_{R15}=53.80%; μ_{M15}=64.46%; $p<0.05$) is recorded within the epratuzumab-conditioned environment ($\mu_{R15+Epratuzumab}$=57.15%; $\mu_{M15+Epratuzumab}$=63.12%).

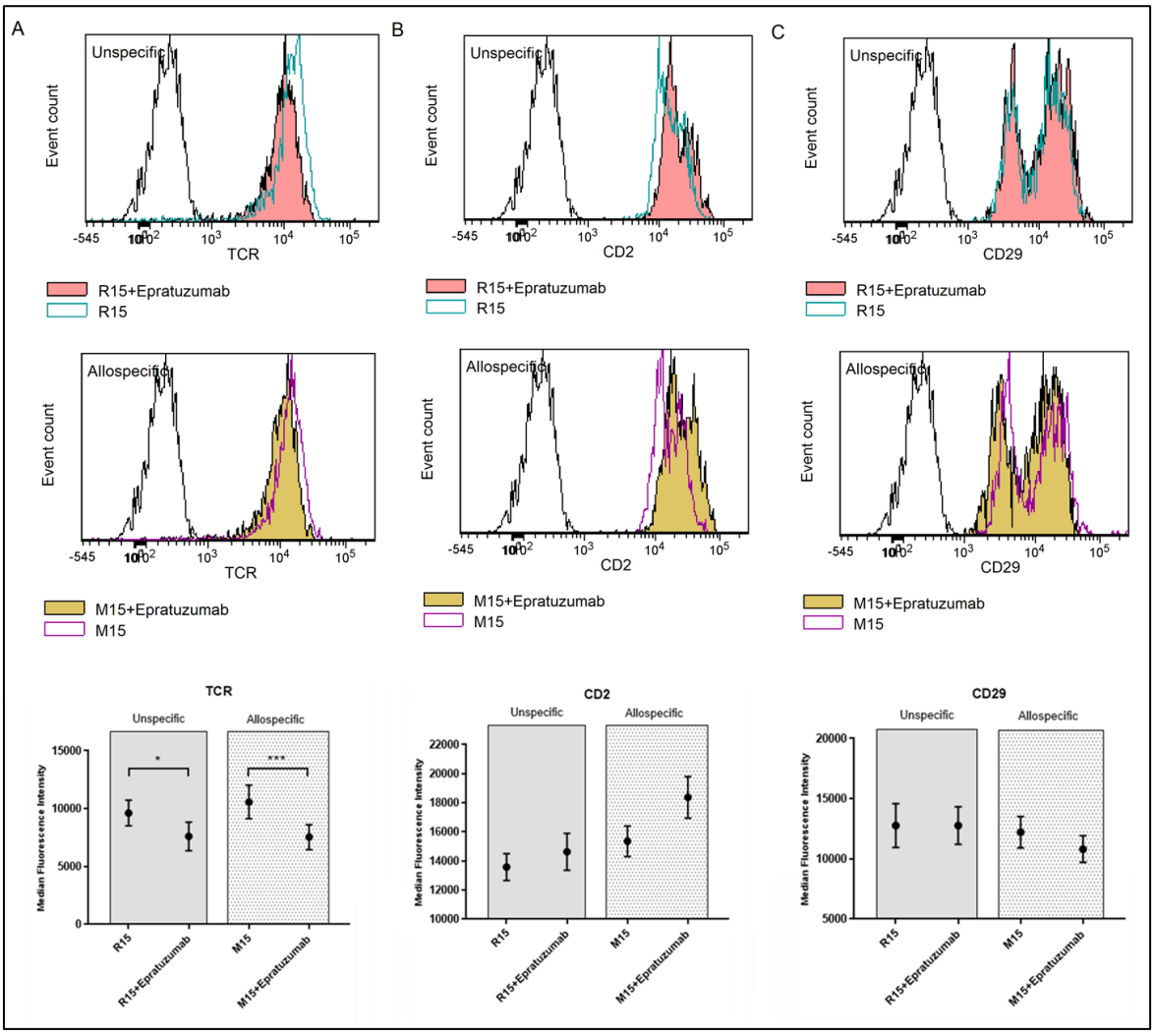

Figure 37. Impact of epratuzumab on responder CD8 T cell phenotype A 3-day MLR was carried out following a StimCFSE/Resp ratio of 1:10 in 500µL/24-flat bottom wells (1 x 106 cells/well) supplemented with 5ng/mL IL-15 and treated ($M15_{Epratuzumab}$) or not (M15) with 50ng/mL epratuzumab, including responders supplemented with 5ng/mL IL-15 and treated ($R15_{Epratuzumab}$) or not (R15) with 50ng/mL epratuzumab. The MFI of **A)** TCR (n=7) **B)** CD2 (n=5) and **C)** CD29 (n=9) on $CD8^{+}/CFSE^{-}$ responder CD8 T cells (1000 events recorded) gated within the lymphocyte population (FSC^{med}/SSC^{low}) was recorded. Data acquisition was carried out on the BD LSRFortessa X-20 with the BD FACS DIVA software (BD FACSDiva v8.0) and the graphs were generated with the FCSalyzer software (version 0.9.18-alpha; Sven Mostböck). Flow cytometry profiles representative of the experiments were overlaid together with the isotope control (clear peak). Statistical analysis was carried out with Prism (version 7; GraphPad Software) with the data reported as the means ± SEM (*p<0.05; **p<0.01; ***p<0.001; ****p<0.0001).

Surprisingly, whereas CD22 is exclusively expressed on B cells, epratuzumab induces a 1.27-fold decrease in TCR (Figure 37A) expression unspecifically (μ_{R15}=9624; $\mu_{R15+Epratuzumab}$=7601; $p<0.05$). This trend is also observed in the allogeneic context (μ_{M15}=10575; $\mu_{M15+Epratuzumab}$=7538; $p<0.0001$), with a 1.4-fold decrease. This is only reflective of the intrinsic properties of epratuzumab since no significant outcome arises from the allogeneic reaction itself ($\mu_{R15+Epratuzumab}$=7601; $\mu_{M15+Epratuzumab}$=7538), similarly observed when epratuzumab is lacking (μ_{R15}=9624; μ_{M15}=10575).

Conversely, epratuzumab does not seem to propagate its effect on CD2 (Figure 37B) expression unspecifically (μ_{R15}=13582; $\mu_{R15+Epratuzumab}$=14635), nor is a notable discrepancy arising within the allogeneic context uncovered (μ_{M15}=15361; $\mu_{M15+Epratuzumab}$=18376). The allogeneic reaction remains unaffected since, similarly to unmodified conditions (μ_{R15}=13582; μ_{M15}=15361), no correlation is found in the variation in CD2 surface levels within the epratuzumab-conditioned environment ($\mu_{R15+Epratuzumab}$=14635; $\mu_{M15+Epratuzumab}$=18376).

An analogous trend is recorded with CD29 (Figure 37C), that is the absence of regulation induced by epratuzumab either unspecifically (μ_{R15}=12770; $\mu_{R15+Epratuzumab}$=12775) or allospecifically (μ_{M15}=12771; $\mu_{M15+Epratuzumab}$=10871). No diversion in the outcome of the alloreaction is detectable ($\mu_{R15+Epratuzumab}$=12775; $\mu_{M15+Epratuzumab}$=10871) as it is likewise unidentifiable within untouched conditions (μ_{R15}=12770; μ_{M15}=12271).

3.3.4.2. Effector response: granzyme b and IL-10 production

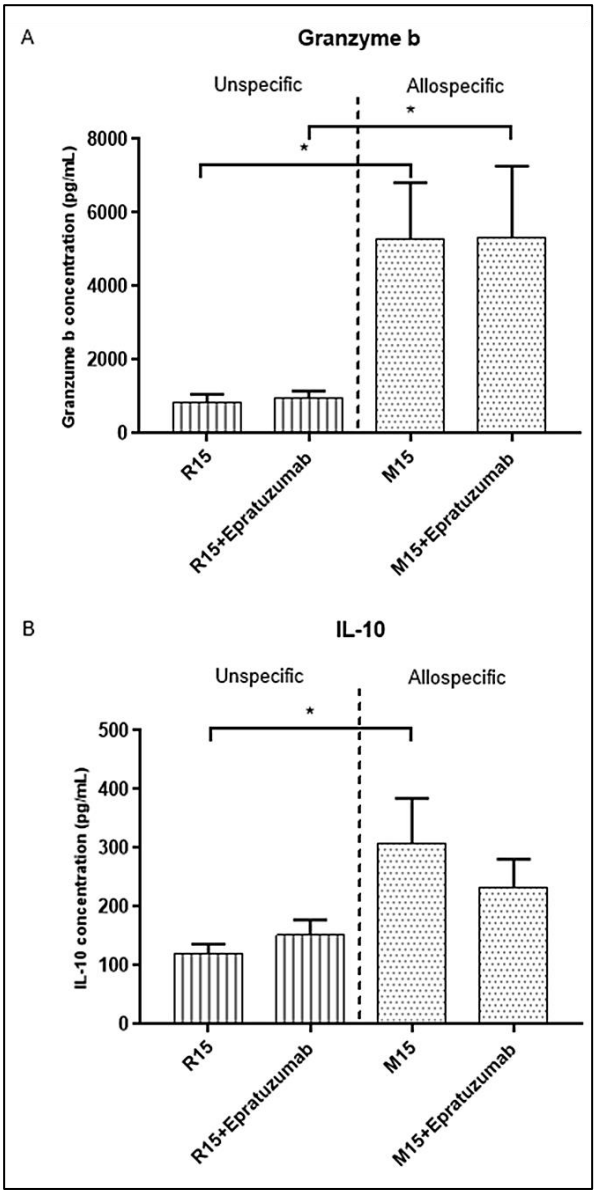

Figure 38. Impact of epratuzumab on the effector response A 3-day MLR was carried out following a StimCFSE/Resp ratio of 1:10 in 500µL/24-flat bottom wells (1 x 10^6 cells/well) supplemented with 5ng/mL IL-15 and treated ($M15_{Eptauzumab}$) or not (M15) with 50ng/mL epratuzumab, including responders supplemented with 5ng/mL IL-15 and treated ($R15_{Epratuzumab}$) or not (R15) with 50ng/mL epratuzumab. The production of **A)** granzyme b (n=7) and **B)** IL-10 (n=5) in frozen supernatants was measured by ELISA**.** Data acquisition was carried out on the SPECTROstar Nano (BMG Labtech, Aylesbury, England) and the data were generated with MARS software (BGM Labtech, Aylesbury, England). Statistical analysis was carried out with Prism (version 7; GraphPad Software) with the data reported as the means ± SEM (*p<0.05; **p<0.01; ***p<0.001; ****p<0.0001).

The outcome of the reaction as depicted by Granzyme b (Figure 38A) production remains unchanged. The aftermath of epratuzumab is inexistant allospecifically (μ_{M15}=5.29ng/mL; $\mu_{M15+Epratuzumab}$=5.33ng/mL) and no variation in the course of the allogeneic reaction is uncovered, yielding a 5.49-fold ($\mu_{R15+Epratuzumab}$=971.36pg/mL; $\mu_{M15+Epratuzumab}$=5.33ng/mL; $p<0.05$) and 6.29-fold (μ_{R15}=840.57pg/mL; μ_{M15}=52.88ng/mL; $p<0.05$) incrementation, hence comparable in their strength.

As for IL-10 production (Figure 38B), it stands out that no unspecific influence of epratuzumab occurs (μ_{R15}=121.04pg/mL; $\mu_{R15+Epratuzumab}$=151.4pg/mL), nor are critical disparities observed allospecifically (μ_{M15}=308.16pg/mL; $\mu_{M15+Epratuzumab}$=233.6pg/mL), although it seems that the allogeneic reaction initially identified with a 2.5-fold incrementation (μ_{R15}=121.04pg/mL; μ_{M15}=308.16pg/mL; $p<0.05$) has disappeared $\mu_{R15+Epratuzumab}$=151.4pg/mL; $\mu_{M15+Epratuzumab}$=233.6pg/mL).

3.3.4.3. Summary of the effects of epratuzumab

The data generated in this chapter gave us the opportunity to extract the effects inherent to epratuzumab, unspecific or allospecific, on the markers investigated, and see their outcome on the alloreaction. Hence they allow to determine whether a milieu where unresponsive B cells are prevalent still maintains the course of the immune response, as depicted by the extent of the cytotoxic response represented by granzyme b production, or rather alters it (Figure 39).

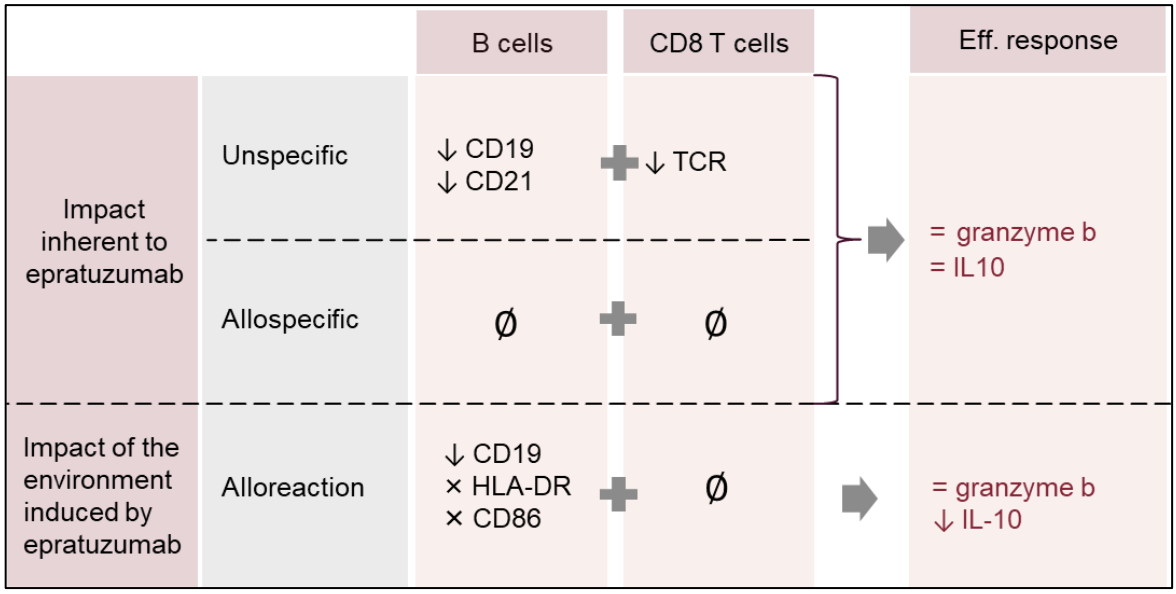

Figure 39. Summary of the effects inherent to epratuzumab and its outcome on the alloreaction Only B cell and CD8 T cell markers for which a trend exists (upregulation: ↑; downregulation: ↓) are included, unless there is a total absence of effect on a subset (∅). Similarly, only diverging trends in B cell and CD8 T cell markers as products of the alloreaction in the milieu conditioned with epratuzumab are given, including in addition to those previously mentioned the loss of the allogeneic-induced regulation of the markers (×). The outcome of the response on the inflammatory environment is indicated in terms of increased (↑), decreased (↓) or unchanged (=) production. All trends are expressed in comparison with unmodified conditions.

3.3.5. Driving antigens to the CD19/CD21 complex in unresponsive B cells: Epratuzumab and C3d supplementation

3.3.5.1. Responder B and CD8 T cell phenotype

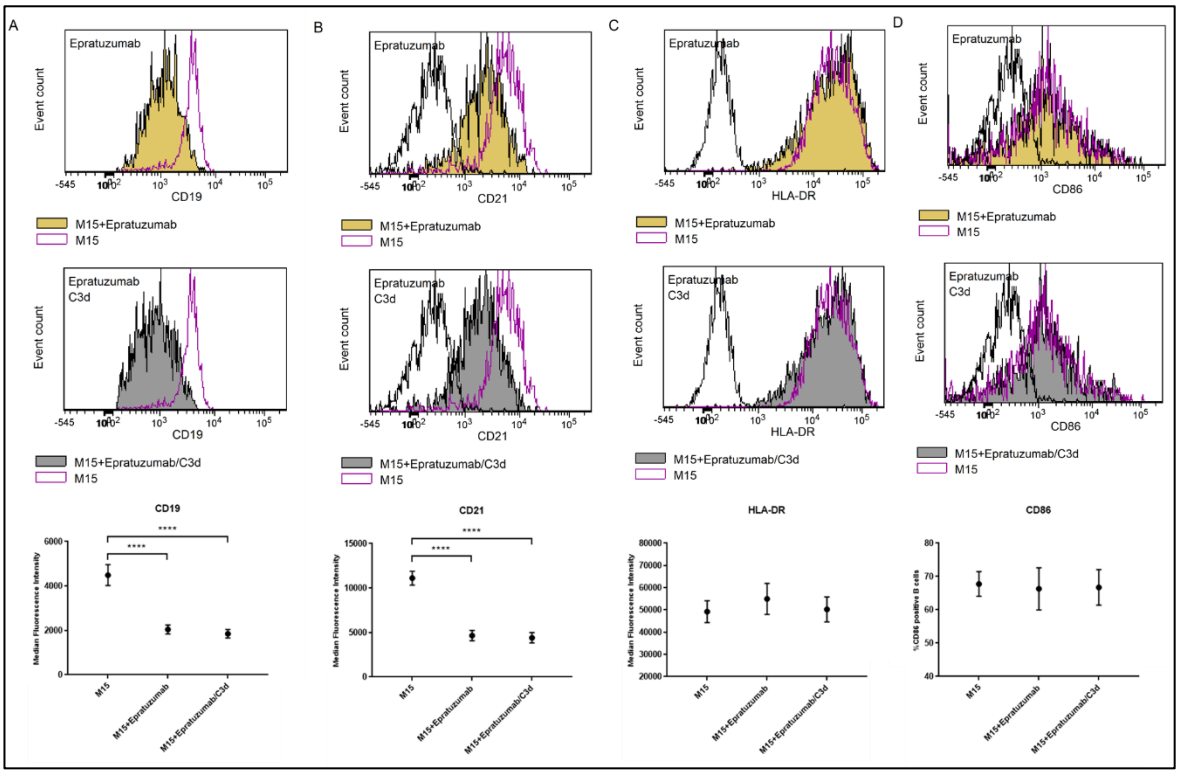

Figure 40. Impact of epratuzumab/C3d on responder B cell phenotype A 3-day MLR was carried out following a StimCFSE/Resp ratio of 1:10 in 500µL/24-flat bottom wells (1 x 10^6 cells/well) supplemented with 5ng/mL IL-15 and either untouched (M15) or treated with 50ng/mL epratuzumab with ($M15_{Epratuzumab+C3d}$) or without ($M15_{Epratuzumab}$) 50ng/mL C3d. The MFI of **A)** CD19 (n=10) **B)** CD21 (n=8) **C)** HLA-DR (n=9) and **D)** $\%CD86^+$ cells (n=6) on $CD19^+/CFSE^-$ responder B cells (1000 events recorded) gated within the lymphocyte population *(*FSC^{med}/SSC^{low}) were recorded. Data acquisition was carried out on the BD LSRFortessa X-20 with the BD FACS DIVA software (BD FACSDiva v8.0) and the graphs were generated with the FCSalyzer software (version 0.9.18-alpha; Sven Mostböck). Flow cytometry profiles representative of the experiments were overlaid together with the isotope control (clear peak). Statistical analysis was carried out with Prism (version 7; GraphPad Software) with the data reported as the means ± SEM (*p<0.05; **p<0.01; ***p<0.001; ****p<0.0001).

Although recording a 2.43-fold drop in CD19 expression (μ_{M15}=4489; $\mu_{M15+Epratuzumab/C3d}$=1848; p<0.0001) (Figure 40A), this putative synergistic effect only reflects the original downregulation imputed to epratuzumab (μ_{M15}=4489; $\mu_{M15+Epratuzumab}$=2042; p<0.0001), the absence of any adjunctive effect of C3d ($\mu_{M15+Epratuzumab}$=2042; $\mu_{M15+Epratuzumab/C3d}$=1848) attesting of it.

The same profile is obtained for CD21 (Figure 40B), that is a failure to yield any adjuvant event with C3d ($\mu_{M15+Epratuzumab}$=4654; $\mu_{M15+Epratuzumab/C3d}$=4412), the 2.52-fold reduction reported in the combined environment (μ_{M15}=11114; $\mu_{M15+Epratuzumab/C3d}$=4412; p<0.0001) only attributable to the efficacy exerted by epratuzumab (μ_{M15}=11114; $\mu_{M15+Epratuzumab}$=4654; p<0.0001).

Finally, C3d adjunction is inconsequential with respect to HLA-DR (μ_{M15}=49233; $\mu_{M15+Epratuzumab/C3d}$=50251 (Figure 40C) and CD86 (μ_{M15}=67.75%; $\mu_{M15+Epratuzumab/C3d}$=66.72) (Figure 38D) expressions, failing to promote any differential response from epratuzumab, whether for HLA-DR (μ_{M15}=49233; $\mu_{M15+Epratuzumab}$=54979) or CD86 (μ_{M15}=67.75%; $\mu_{M15+Epratuzumab}$=66.31%).

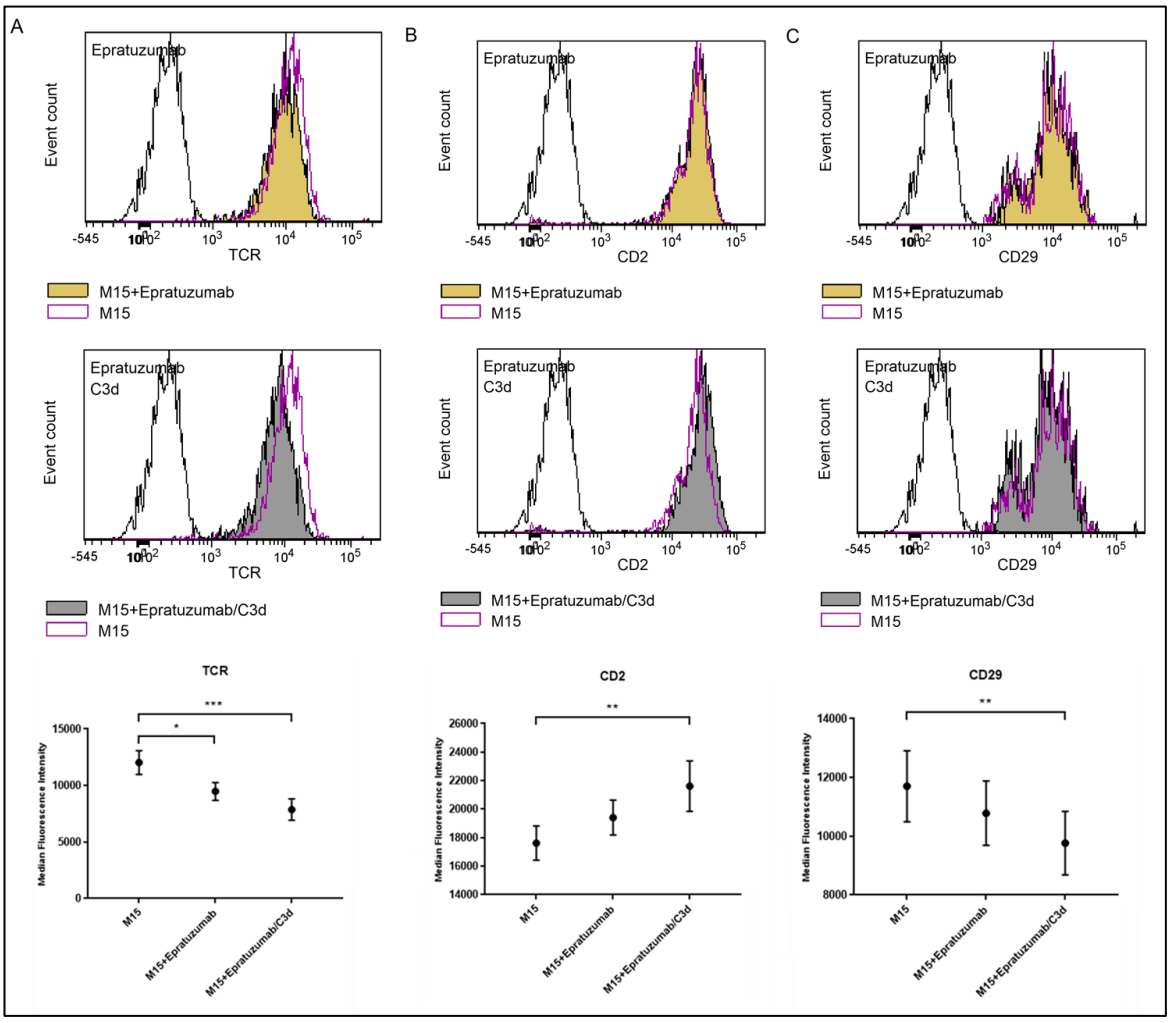

Figure 41. Impact of epratuzumab/C3d on responder CD8 T cell phenotype A 3-day MLR was carried out following a StimCFSE/Resp ratio of 1:10 in 500µL/24-flat bottom wells (1 x 10^6 cells/well) supplemented with 5ng/mL IL-15 and either untouched (M15) or treated with 50ng/mL epratuzumab with ($M15_{Epratuzumab+C3d}$) or without ($M15_{Epratuzumab}$) 50ng/mL C3d. The MFI of **A)** TCR (n=8) **B)** CD2 (n=6) and **C)** CD29 (n=6) on $CD8^+/CFSE^-$ responder CD8 T cells (1000 events recorded) gated within the lymphocyte population (FSC^{med}/SSC^{low}) was recorded. Data acquisition was carried out on the BD LSRFortessa X-20 with the BD FACS DIVA software (BD FACSDiva v8.0) and the graphs were generated with the FCSalyzer software (version 0.9.18-alpha; Sven Mostböck). Flow cytometry profiles representative of the experiments were overlaid together with the isotope control (clear peak). Statistical analysis was carried out with Prism (version 7; GraphPad Software) with the data reported as the means ± SEM (*p<0.05; **p<0.01; ***p<0.001; ****p<0.0001).

The recorded 1.53-fold reduction in TCR (Figure 41A) expression within the context involving C3d combination (μ_{M15}=12025; $\mu_{M15+Epratuzumab/C3d}$=7866, $p<0.001$) seems only attributable to epratuzumab (μ_{M15}=12025; $\mu_{M15+Epratuzumab}$=9480, $p<0.05$) since no significant variation imputable to the supplementation with C3d is brough to light ($\mu_{M15+Epratuzumab}$=9480; $\mu_{M15+Epratuzumab/C3d}$=7866).

However, a contrasting modulation of CD2 (Figure 41B) and CD29 (Figure 41C) is observed. Indeed, a modest 1.19-fold downregulation of CD29 resulting from the synergistic effect of epratuzumab and C3d (μ_{M15}=11700; $\mu_{M15+Epratuzumab/C3d}$=9767, $p<0.01$) emerges, a trend not observed with epratuzumab only (μ_{M15}=11700; $\mu_{M15+Epratuzumab}$=10784). CD2 within the same context features a 1.23-fold increase (μ_{M15}=17615; $\mu_{M15+Epratuzumab/C3d}$=21614, $p<0.01$), also solely linked to its combination with epratuzumab (μ_{M15}=17615; $\mu_{M15+Epratuzumab}$=19408).

3.3.5.2. Effector response: granzyme b and IL-10 production

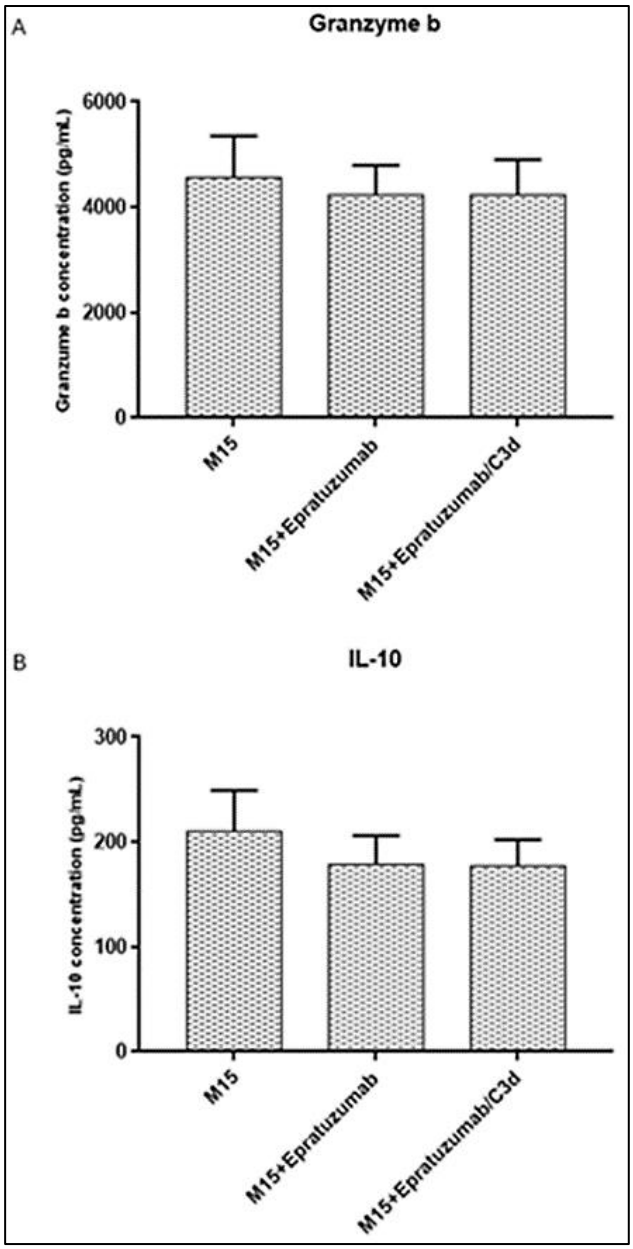

Figure 42. Impact of epratuzumab/C3d on the effector response A 3-day MLR was carried out following a StimCFSE/Resp ratio of 1:10 in 500µL/24-flat bottom wells (1 x 10^6 cells/well) supplemented with 5ng/mL IL-15 and either untouched (M15) or treated with 50ng/mL epratuzumab with ($M15_{Epratuzumab+C3d}$) or without ($M15_{Epratuzumab}$) 50ng/mL C3d. The production of **A)** granzyme b (n=8) and **B)** IL-10 (n=6) in frozen supernatants was measured by ELISA**.** Data acquisition was carried out on the SPECTROstar Nano (BMG Labtech, Aylesbury, England) and the data were generated with MARS software (BGM Labtech, Aylesbury, England). Statistical analysis was carried out with Prism (version 7; GraphPad Software) with the data reported as the means ± SEM (*p<0.05; **p<0.01; ***p<0.001; ****p<0.0001).

Manifestly, the immune response persisted through its course without suffering any alteration stemming from C3d combination, granzyme b (μ_{M15}=4.57ng/mL; $\mu_{M15+Epratuzumab/C3d}$=4.23ng/mL) (Figure 42A) and IL-10 (μ_{M15}=209.49pg/mL; $\mu_{M15+Epratuzumab/C3d}$=177.12pg/mL) (Figure 42B) productions displaying as little variability as with epratuzumab only (μ_{M15}=4.57ng/mL; $\mu_{M15+Epratuzumab}$=4.22ng/mL and (μ_{M15}=209.49pg/mL; $\mu_{M15+Epratuzumab/C3d}$=177.12pg/mL, respectively).

3.3.5.3. Summary of the effects of C3d

The data generated in this chapter gave us the opportunity to extract the adjunctive effect of C3d on the investigated markers in a milieu where unresponsive B cells are prevailing. Thus, this will allow to determine whether the desired redirection of C3d-coated antigens to CD21-mediated uptake for class II MHC presentation effectively took place and, if so, altered the course of the immune response depicted by the extent of granzyme b production, or leaves it unchanged (Figure 43).

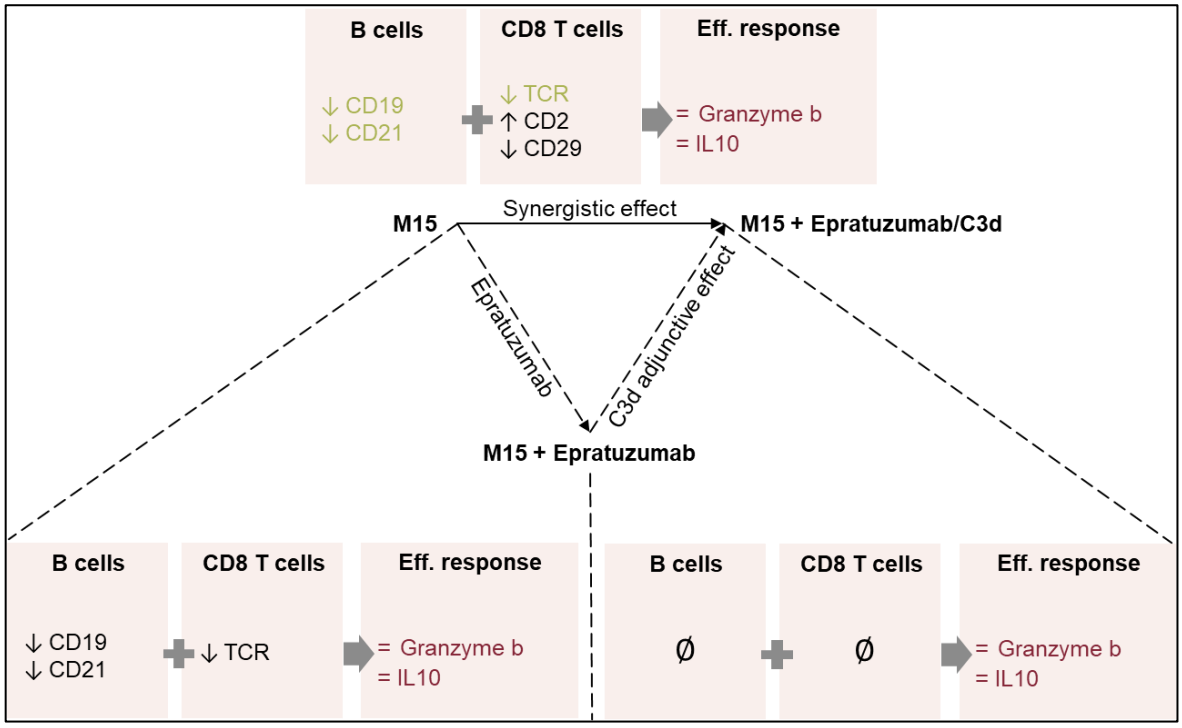

Figure 43. Summary of the adjunctive effect of C3d on unresponsive B cells Only B cell and CD8 T cell markers for which a trend exists (upregulation: ↑; downregulation: ↓) are included, unless there is an absence of effect on a subset (∅). The outcome of the response on the inflammatory environment is indicated in terms of increased (↑), decreased (↓) or unchanged (=) production. All trends are expressed in comparison with the condition lacking the component considered. In green are the markers that show the trends which reflect the effects inherent to epratuzumab.

3.3.6. Driving antigens to the CD19/CD21 complex in unmodified B cells: C3d supplementation

3.3.6.1. Responder B and CD8 T cell phenotype

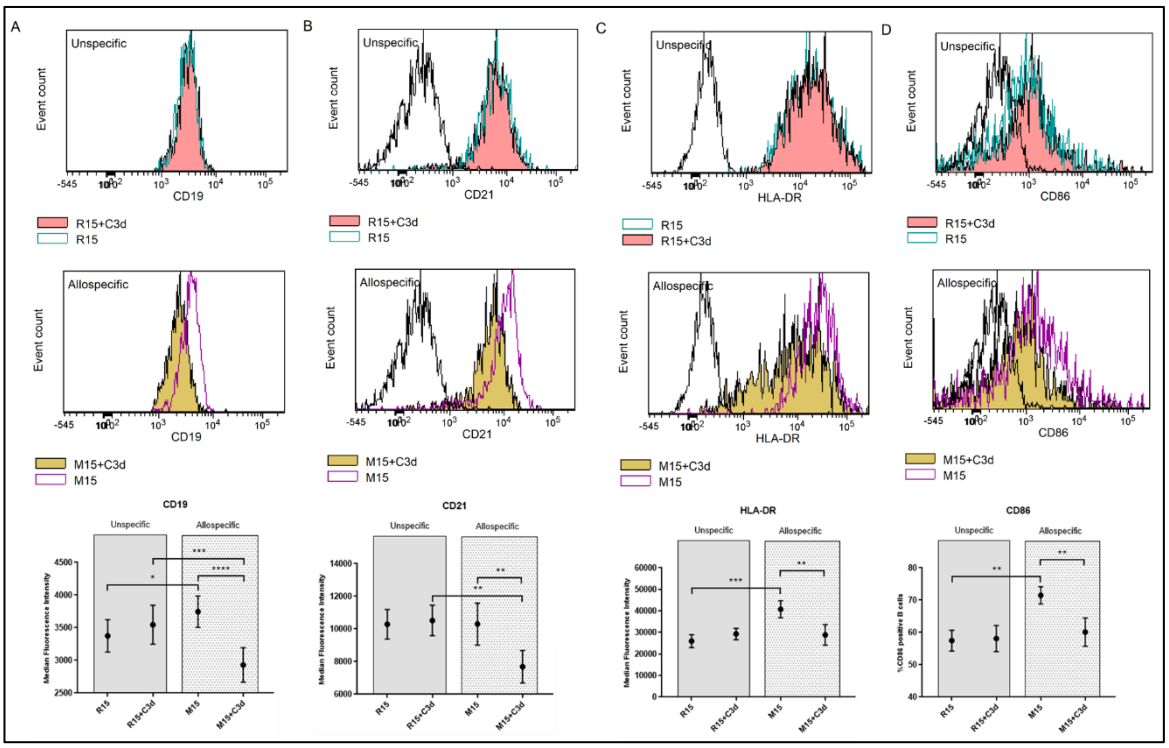

Figure 44. Impact of C3d on responder B cell phenotype A 3-day MLR was carried out following a StimCFSE/Resp ratio of 1:10 in 500µL/24-flat bottom wells (1 x 10^6 cells/well) supplemented with 5ng/mL IL-15 and treated ($M15_{C3d}$) or not (M15) with 50ng/mL C3d, including responders supplemented with 5ng/mL IL-15 and treated ($R15_{C3d}$) or not (R15) with 50ng/mL C3d. The MFI of **A)** CD19 (n=7) **B)** CD21 (n=6) **C)** HLA-DR (n=6) and **D)** $\%CD86^+$ cells (n=7) on $CD19^+/CFSE^-$ responder B cells (1000 events recorded) gated within the lymphocyte population (FSC^{med}/SSC^{low}) were recorded. Data acquisition was carried out on the BD LSRFortessa X-20 with the BD FACS DIVA software (BD FACSDiva v8.0) and the graphs were generated with the FCSalyzer software (version 0.9.18-alpha; Sven Mostböck). Flow cytometry profiles representative of the experiments were overlaid together with the isotope control (clear peak). Statistical analysis was carried out with Prism (version 7; GraphPad Software) with the data reported as the means ± SEM (*p<0.05; **p<0.01; ***p<0.001; ****p<0.0001).

What clearly stands out is that C3d adjunction solely acts on the CD19/CD21 complex through an allospecific fashion, as neither of these markers show a substantial change within an unspecific context. CD19 (μ_{R15}=3376; $\mu_{R15+C3d}$=3546) (Figure 44A) and CD21 (μ_{R15}=10288; $\mu_{R15+C3d}$=10518) (Figure 44B) are indeed stable as opposed to the 1.28- (μ_{M15}=3746; $\mu_{M15+C3d}$=2931; $p<0.0001$) and 1.34-fold (μ_{M15}=10301; $\mu_{M15+C3d}$=7688; $p<0.01$) recorded reduction, respectively, imputed to the presence of allogenic components. The 1.37-fold downregulation in CD21 expression generated by the alloreaction ($\mu_{R15+C3d}$=10518; $\mu_{M15+C3d}$=7688; $p<0.01$) is only reflective of the allospecificity of C3d, otherwise inexistant in untreated conditions (μ_{R15}=10288; μ_{M15}=10301). The 1.21-fold drop noted in CD19 levels imputable to the allogenic reaction within a C3d supplemented milieu ($\mu_{R15+C3d}$=3546; $\mu_{M15+C3d}$=2931; $p<0.001$) is in sharp contrast with the original 1.11-fold upregulation (μ_{R15}=3376; μ_{M15}=3746; $p<0.05$).

This absence of unspecific repercussion of C3d in HLA-DR (μ_{R15}=25959; $\mu_{R15+C3d}$=29300) (Figure 44C) and CD86 (μ_{R15}=57.47%; $\mu_{R15+C3d}$=58.12%) (Figure 44D) is apparent here. Its distinct propensity for a selective targeting of allogeneic components is however indisputable, triggering a 1.41- (μ_{M15}=40789; $\mu_{M15+C3d}$=28836; $p<0.01$) and 1.19-fold (μ_{M15}=71.51%; $\mu_{M15+C3d}$=60.11%; $p<0.01$) reduction in HLA-DR and CD86 expressions, respectively. Furthermore, whereas the allogeneic reaction itself is revealed by an upregulation of HLA-DR and CD86 by 1.57- (μ_{R15}=25959; μ_{M15}=40789; $p<0.001$) and 1.24-fold (μ_{R15}=57.47%; μ_{M15}=71.51%; $p<0.01$), respectively, this trend is clearly abrogated with C3d adjunction, whether at the HLA-DR ($\mu_{R15+C3d}$=29300; $\mu_{M15+C3d}$=28836) or CD86 ($\mu_{R15+C3d}$=58.12%; $\mu_{M15+C3d}$=60.11%) level.

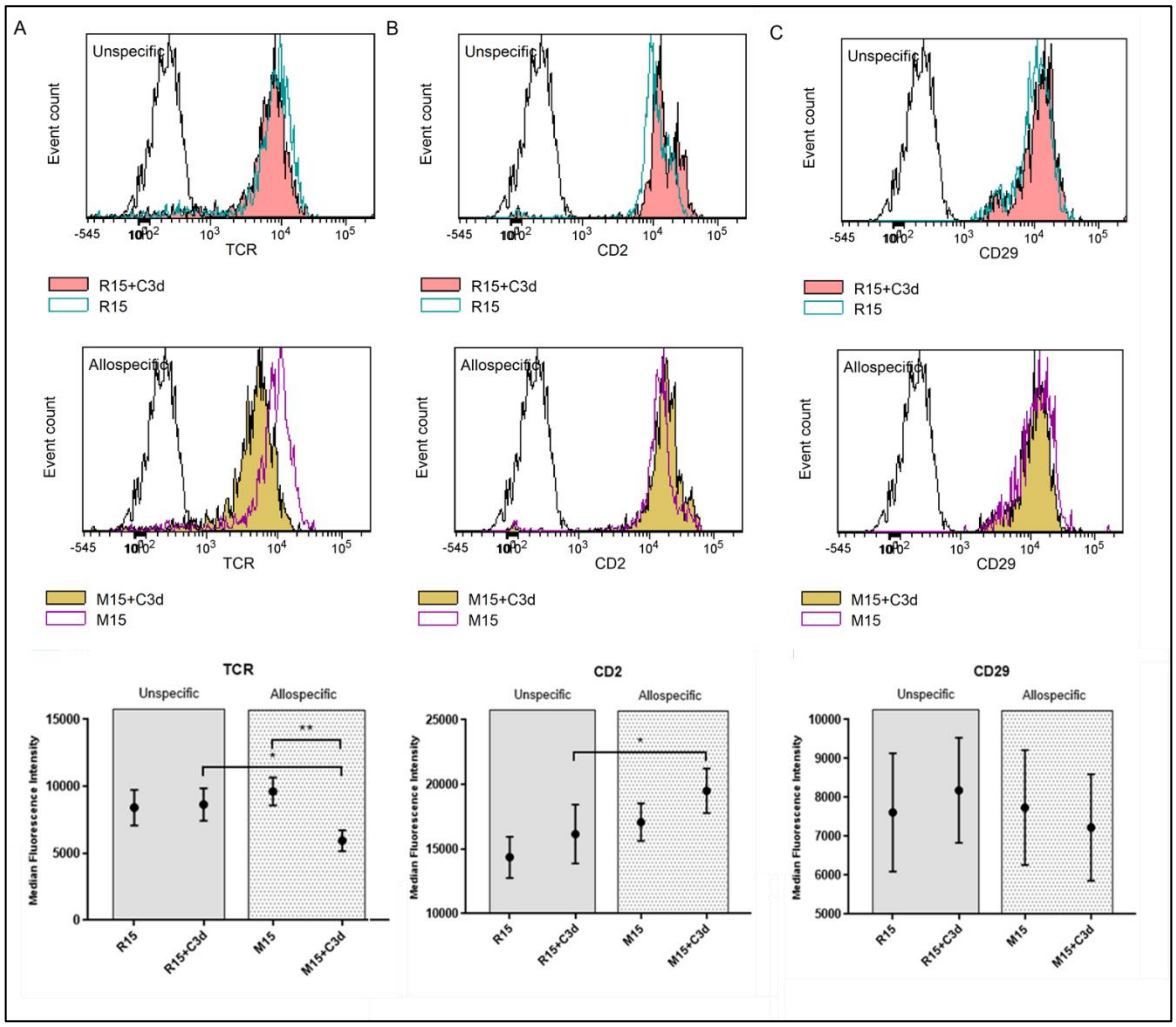

Figure 45. Impact of C3d on responder CD8 T cell phenotype A 3-day MLR was carried out following a StimCFSE/Resp ratio of 1:10 in 500µL/24-flat bottom wells (1 x 10^6 cells/well) supplemented with 5ng/mL IL-15 and treated ($M15_{C3d}$) or not (M15) with 50ng/mL C3d, including responders supplemented with 5ng/mL IL-15 and treated ($R15_{C3d}$) or not (R15) with 50ng/mL C3d. The MFI of A) TCR (n=8) B) CD2 (n=6) and C) CD29 (n=6) on $CD8^+/CFSE^-$ responder CD8 T cells (1000 events recorded) gated within the lymphocyte population (FSC^{med}/SSC^{low}) was recorded. Data acquisition was carried out on the BD LSRFortessa X-20 with the BD FACS DIVA software (BD FACSDiva v8.0) and the graphs were generated with the FCSalyzer software (version 0.9.18-alpha; Sven Mostböck). Flow cytometry profiles representative of the experiments were overlaid together with the isotope control (clear peak). Statistical analysis was carried out with Prism (version 7; GraphPad Software) with the data reported as the means ± SEM (*p<0.05; **p<0.01; ***p<0.001; ****p<0.0001).

Whereas the absence of unspecific modulation characterises both TCR (μ_{R15}=8415; $\mu_{R15+C3d}$=8644) (Figure 45A) and CD2 (μ_{R15}=14363; $\mu_{R15+C3d}$=16158) (Figure 45B), the aftermath of C3d adjunction appears to exhibit a differential outcome allospecifically, denoting a sharp 1.62-fold inflection in TCR (μ_{M15}=9618; $\mu_{M15+C3d}$=5947; $p<0.01$) expression while CD2 does not fluctuate substantially (μ_{M15}=17087; $\mu_{M15+C3d}$=19507). The 1.45-fold drop in TCR expression attributed to the allogenic reaction within a C3d-rich environment ($\mu_{R15+C3d}$=8644; $\mu_{M15+C3d}$=5947; $p<0.05$) appears to only be imputable to the allospecific shift impelled by C3d. Since a quantitative plateau is reached for TCR in unmodified conditions (μ_{R15}=8415; μ_{M15}=9618), isolating a distinct effect of the presence of allogeneic components is infeasible. However, it seems to hold a more preponderant role with regards to CD2 expression as denoted by the 1.21-fold incrementation ($\mu_{R15+C3d}$=16158; $\mu_{M15+C3d}$=19507; $p<0.05$) otherwise lacking in a context devoid of C3d (μ_{R15}=14363; μ_{M15}=17087). Here, it supports the reasoning that C3d solely does not sustain particular functions but it is rather the allogeneic reaction which, in its course within this milieu, is driven to upregulate CD2.

Interestingly here, CD29 (Figure 45C) is not affected in any way by C3d adjunction, whether unspecifically (μ_{R15}=7614; $\mu_{R15+C3d}$=8181) or allospecifically (μ_{M15}=7819; $\mu_{M15+C3d}$=7227). It neither reflects an intrinsic engagement of the alloreaction unique to the C3d-rich milieu ($\mu_{R15+C3d}$=8181; $\mu_{M15+C3d}$=7227) which could have contrasted with the absence of such distinction in untouched conditions (μ_{R15}=7614; μ_{M15}=7819). Thus, the immutable CD29 levels evidenced here are only the product of the inflammatory environment established by IL-15.

3.3.6.2. Effector response: granzyme b and Il-10 production

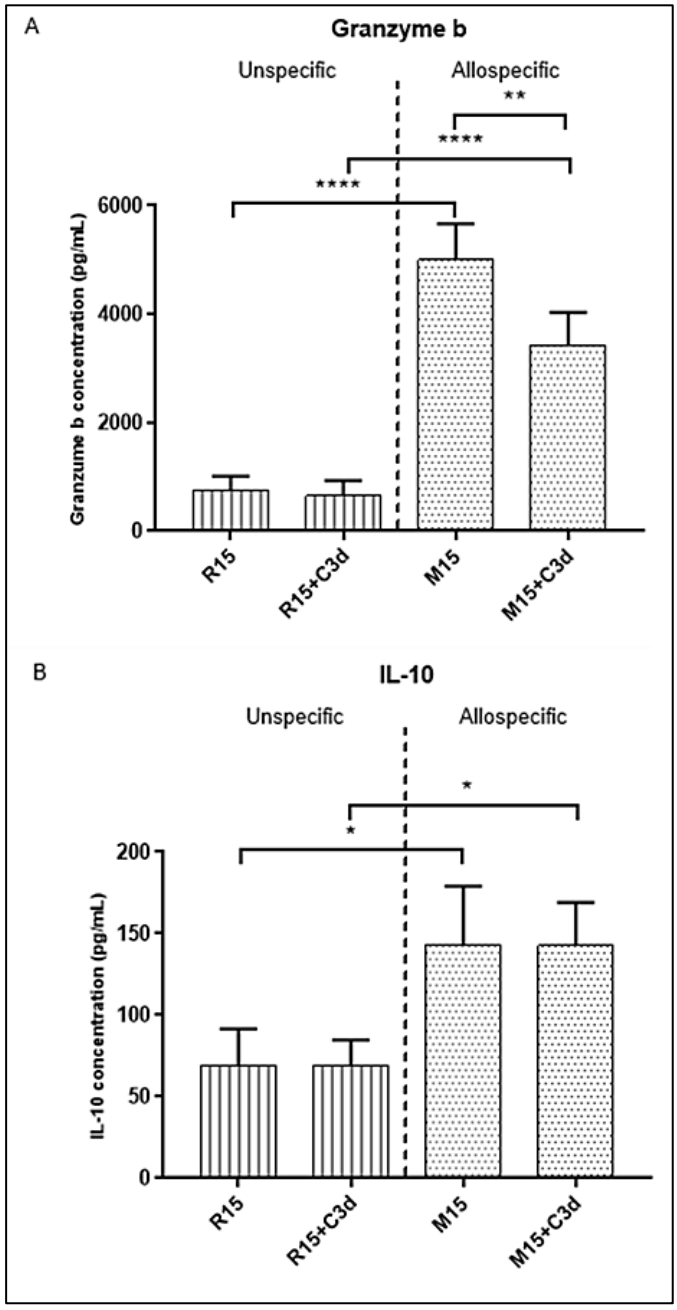

Figure 46. Impact of C3d on the effector response A 3-day MLR was carried out following a StimCFSE/Resp ratio of 1:10 in 500µL/24-flat bottom wells (1 x 10^6 cells/well) supplemented with 5ng/mL IL-15 and treated ($M15_{C3d}$) or not (M15) with 50ng/mL C3d, including responders supplemented with 5ng/mL IL-15 and treated ($R15_{C3d}$) or not (R15) with 50ng/mL C3d. The production of **A)** granzyme b (n=5) and **B)** IL-10 (n=6) in frozen supernatants was measured by ELISA**.** Data acquisition was carried out on the SPECTROstar Nano (BMG Labtech, Aylesbury, England) and the data were generated with MARS software (BGM Labtech, Aylesbury, England). Statistical analysis was carried out with Prism (version 7; GraphPad Software) with the data reported as the means ± SEM (*p<0.05; **p<0.01; ***p<0.001; ****p<0.0001).

The outstanding event emerging from our data is the significant allospecific 1.46-fold decrease in granzyme b production (μ_{M15}=50ng/mL; $\mu_{M15+C3d}$=34.31ng/mL; $p<0.01$) (Figure 46A), exonerated from unspecific aftereffects (μ_{R15}=752.76pg/mL; $\mu_{R15+C3d}$=647.86pg/mL). However, the allogeneic reaction prevailing within the C3d-rich environment remains clearly identified, recording a 5.3-fold incrementation ($\mu_{R15+C3d}$=647.86pg/mL; $\mu_{M15+C3d}$=34.31ng/mL; $p<0.0001$), still contrasting with the 6.6-fold escalation in unmodified conditions (μ_{R15}=752.76pg/mL; μ_{M15}=50ng/mL; $p<0.0001$).

This outcome is achieved independently of IL-10 production as evidenced by its immutable profile when an allospecific impact of C3d was sought (μ_{M15}=142.88pg/mL; $\mu_{M15+C3d}$=142.66pg/mL) (Figure 46B), the allogeneic reaction similarly distinguished within the unmodified (μ_{R15}=69.33pg/mL; μ_{M15}=142.88pg/mL; $p<0.05$) and C3d-rich milieu (μ_{R15}=69.48pg/mL; μ_{M15}=142.66pg/mL; $p<0.05$).

3.3.6.3. Summary of the effects of C3d on the alloreaction where B cells are unmodified

The data generated in this chapter gave us the opportunity to extract the effects inherent to C3d, unspecific or allospecific, on the markers investigated, and see their outcome on the alloreaction where B cells are unmodified. Thus, determining whether the desired redirection of C3d-coated antigen to CD21-mediated uptake for class II MHC presentation effectively took place and, if so, altered the course of the immune response, as depicted by the extent of the cytotoxic response represented by granzyme b production, or leaves it unchanged (Figure 47).

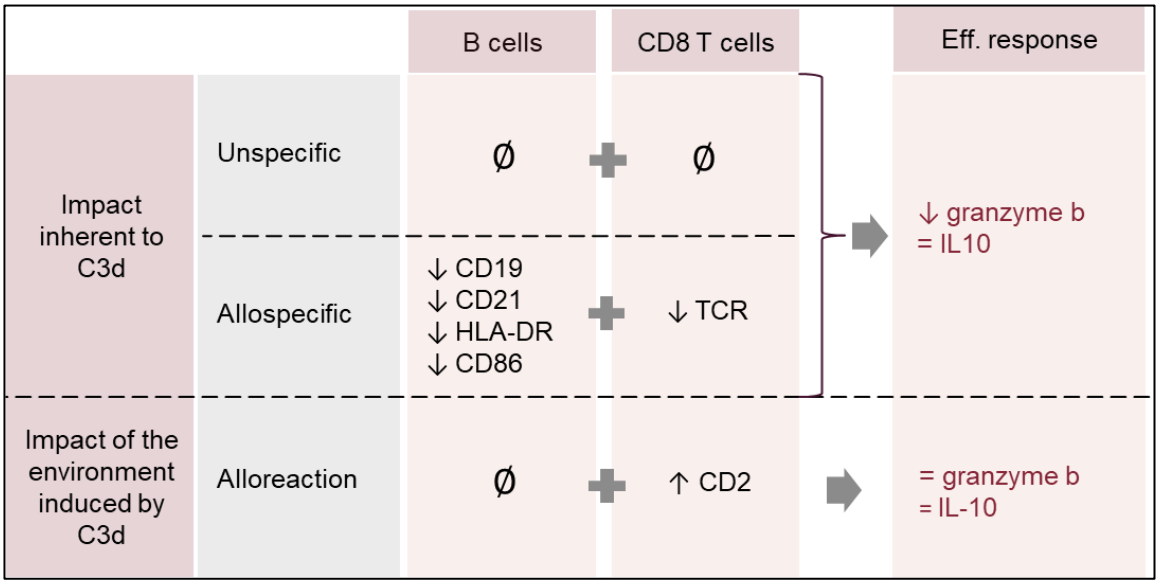

Figure 47. Summary of the effects inherent to C3d and its outcome on the alloreaction where B cells are unmodified Only B cell and CD8 T cell markers for which a trend exists (upregulation: ↑; downregulation: ↓) are included, unless there is a total absence of effect on a subset (∅). Similarly, only diverging trends in B cell and CD8 T cell markers as products of the alloreaction in the milieu conditioned with C3d are given, including in addition to those previously mentioned the loss of the allogeneic-induced regulation of the markers (✕). The outcome of the response on the inflammatory environment is indicated in terms of increased (↑), decreased (↓) or unchanged (=) production. All trends are expressed in comparison with unmodified conditions. In green are the markers that show the trend which is reflection of the allospecific effect of C3d.

Chapter 4

Discussion

The fate of resting B cells is governed by the BCR response regulator CD19/CD21 complex, setting the foundation of the dichotomy in their functions as APCs, at the crossroad between tolerance induction and immune activation. Identifying a way to fine-tune the CD19/CD21 complex to uncouple these functionalities holds interesting prospects in the settings of aGvHD, a lethal complication post-allogeneic HSCT. The establishment of novel therapies in this area is critical since no standard aGvHD prophylactic strategy is yet at hand whereas allogeneic HSCT remains the exclusive therapy for a wide range of haematological malignancies. This aspect of B cells is barely addressed in the literature, nor is their role in aGvHD onset. The present study will thus attempt to give an insight as to whether such functions could be derived as well as their relevance to aGvHD, ultimately setting the foundation for future research.

We proposed that reducing the surface expression of the CD19/CD21 complex with the anti-CD22 antibody epratuzumab could disrupt B cells antigen presenting capacity by mitigating their responsiveness to allopeptides. We also introduced concomitant C3d adjunction as a way to re-direct antigens towards the CD21-mediated class II MHC presentation and build a diverse peripheral repertoire of tolerated antigens based on evidence that eluding BCR co-ligation fails to drive the acquisition of features characteristic of potent APCs. This strategy faces two challenges, not only the potential breach in the B cell resting state as C3d is described as the limiting factor driving the shift from anergy to immune activation, but also the inaptitude to efficiently target C3d-coated antigens to CD21 on B cells displaying low surface density of the CD19/CD21 complex. To test these hypotheses, we devised a two-way MLR using raw human buffy coats and IL-15 as a core component as it is one of the key drivers of GvHD pathogenesis, potentially challenging the stability of the resting state of B cells derived in our experimental approach.

We found that C3d adjunction on unmodified MLRs hampered the effector response by 1.46-fold as measured by granzyme b production, associated with a sharp reduction in CD21 and CD19 expression. Chronically engaged C3d-coated antigens in SLE patients were shown to induce CD21 and CD19 internalisation leading to their reduction from the surface of B cells, suggested to be the result of increased turnover of these receptors (Hasegawa et al., 2001; Inaoki et al., 1997). Considering the prevalence of C3d in the MLR, this scenario could parallel our experimental observations. In line with this, our data indicate that the impact of C3d is tightly linked to the presence of allogeneic components since the level of

CD21 and CD19 expression was unchanged in responder cells, confirming that C3d on its own does not engage this pathway. This would support the assumption that peptides are produced in the MLR and further complexed with C3d, ultimately binding CD21. However, the outcome contrasts with the well-described role of C3d in breaking tolerance in autoimmune diseases (Del Nagro et al., 2005; Jégou et al., 2007). Our data even show a decrease in HLA-DR and CD86 expression, suggesting a shift away from a phenotype characteristic of potent APCs. This effect is however reported in the context of CD21 targeting by C3d-coated antigens independent of BCR co-engagement (Boackle et al., 1998). It would indicate that B cells are not involved in the acquisition of the effector response depicted in the MLR. B cells displaying low-affinity BCR strictly rely on C3d co-ligation to sustain efficient activation (Mongini et al., 2002). The MLR involves naïve B cells which have not undergone affinity maturation in GCs, thus it is most likely that such B cells are involved. If host-derived antigen capture by the BCR had taken place, C3d adjunction would have facilitated B cell activation. As expected, indirect allorecognition is not represented in the MLR. The upregulation of B cell markers recorded in the MLR without IL-15 would rather be attributed to DAMPS release further to neutrophil necrosis (Chatfield et al., 2018; Iba et al., 2013; Land, 2015) as this short-live population represented up to 70% of the MLR. This observation is difficult to correlate with other studies since most MLRs involve isolated B, T, PBMCs or macrophages and DCs derived from monocytes used as adherent stimulators.

Surprisingly, C3d adjunction in epratuzumab-treated MLR had not influence on the outcome of the effector response. Our data show a decrease in CD19 and CD21 expression characteristic of the intrinsic properties of epratuzumab, although not quite to same extent to the reductions obtained using same concentrations in another study (Rossi et al., 2013). $CD21^{-/low}$ B cells enriched in patients with CVID and RA were shown to fail to get activated, induce [Ca2+] influx or proliferate further to BCR and CD40 triggering (Isnardi et al., 2010). $CD21^{-/low}$ B cells in primary Sjogren's syndrome were similarly refractory to this stimuli (Saadoun et al., 2013). This unresponsiveness indicates that $CD21^{-/low}$ B cells may be anergic. On the other hand, the enhancement of CD19 expression in $CD21^{-}/CD35^{-}$ mice was sufficient to augment the BCR-induced [Ca2+] response when challenged with *Streptococcus pneumonia* infection (Haas et al., 2009). Similarly, CD19 overexpression was shown to be enough to break the tolerance in mice expressing the soluble hen egg lysozyme model autoantigen together with its cognate receptors (Inaoki et al., 1997). These data would indicate that the anergic state could be rescued by excessive CD19 expression.

In the MLR, epratuzumab yields $CD19^{low}/CD21^{low}$ B cells. It could be speculated that the anergic state described to be associated with $CD21^{low}$ expression would be sustained. Thus, it would appear that the outcome of C3d-coated antigen engagement depends on the degree of CD19/CD21 expression. This would also demonstrate a distinct aspect of the functional impact exerted by epratuzumab at the cell level. The inclusion of epratuzumab in SLE standard therapy resulted in the reduction of IgM serum levels, although showing diverging outcomes with respect to the impact on disease activity (Clowse et al., 2017; Gottenberg et al., 2018). Here, the impact of epratuzumab on the effector response does not indicate what mechanism was involved. The induction of an anergic state in B cells could be explaining these events. These failure to proliferate, differentiate and produce antibodies are the characteristic consequences of anergy (Yarkoni et al., 2010).

Unexpectedly, the MLR failed to generate proliferative cells despite yielding a considerable effector response as depicted with the substantial production of granzyme b. MLRs are standard assays originally developed to predict the risk of GvHD reactions (Lim et al., 1988; Sairafi et al., 2016; Visentainer et al., 2002) where T cell proliferation is the most common immunological readout (DeWolf et al., 2016). Evidence showing that proliferating CD8 T cells failed to exert effector functions demonstrated that these events could be uncoupled (Hernández et al., 2002). T cells in synovial fluid from patients with juvenile idiopathic arthritis showed features of activated cells, notably CD69, HLA-DR, CD25 and CD71 independently of proliferation, suggested to be caused by alterations in the microenvironment, here hypoxia (Black et al., 2002). IL-15 is preponderant in the MLR. Its role in T cell homeostasis (Castillo and Schluns, 2012) is well described, notably in the correction of the lymphopenic state post-HSCT (Matsuoka et al., 2013), but also in the breach of immunological tolerance (Miyagawa et al., 2008; Teague et al., 2006). The implication of IL-15 in this inhibition would be surprising. However, it is suggested that the extent of IL-15 levels determines a threshold at which proliferation is promoted. Notably, while 50ng/mL IL-15 induced T cell proliferation, the use of 5ng/mL failed to do so (Teague et al., 2006). The MLR uses this particular concentration. However, there is no evidence that the effector functions would still be sustained in spite of that. In anti-CD3-stumlated T cells, 10^{-8}M IL-15 treatment independent of TCR engagement resulted in acquisition of intracellular granzyme b expression before T cell proliferation started at day 3 of culture (Tamang et al., 2006). The outcome of the MLR is assessed at day 3. However, the possibility that TCR engagement does not occur is unlikely as IL-15 on responders only did

not cause granzyme b production. Autophagy is a mechanism regulating the direction of cytoplasmic substrates to lysosomes for degradation (Merkley et al., 2018). The ATG5-mediated inhibition of autophagy resulted in greater accumulation of granzyme b in CD8 T cells conferring them a stronger cytotoxic profile while proliferation was significantly reduced (Oravecz-Wilson et al., 2021). However, IL-15 was described to stimulate autophagy in NKT cells involving TBK-binding protein 1 and support their survival (Zhu et al., 2018). Hence, a mechanism through which IL-15 would inhibit autophagy and uncouple granzyme b production from proliferation would be unlikely.

Despite this unexpected outcome, the MLR integrates events characteristic of the establishment of the immune reaction in addition to granzyme b production. Notably, the 0.66-fold drop in $CD25^+$ CD4 T cells. This phenomenon most likely stems from the cleavage of CD25 as a downstream event of the alloreactive response. It is commonly described in autoimmune diseases such as type I diabetes (Downes et al., 2014) or systemic lupus erythematosus (Zhang et al., 2018). Hence, plasma soluble CD25 concentration constitutes a relevant biomarker to monitor disease progression, as it correlates with the extent of the inflammation. Also, granzyme b production is paralleled with a 3.49-fold increase in IL-10 levels. High IL-10 serum levels are reported in clinical aGvHD and found to correlate with the onset of aGvHD, suggested to represent a compensatory mechanism where IL-10 acts as a negative feedback loop (Abraham et al., 2017). Thus, similarly to granzyme b, IL-10 in our MLR could be used as a readout to follow the course of the allogeneic reaction. IL-10 protein expression was shown to be significantly increased in a MLR bringing into play a concurrent stimulation by MHC H-2d and H-2k which resulted in partial inhibition of T cell proliferation (Zhou et al., 2014). Here, it was suggested that the existence of a competition between lymphocytes of different specificities could curtail the strength of the immune response. This context is encountered in our MLR since the blood of random donors are mixed together without any consideration for HLA matching. The extent of the HLA disparities at stake is presumably large and thus, the introduction of a competition between T cells is plausible and could be the source of IL-10 production in the MLR. What stands out is the crucial role of IL-15 in triggering these events, supporting the reasoning detailed in the present study that the inclusion of an inflammatory environment at the initiation of the MLR is critical. Importantly, the inflammation induced by IL-15 supplementation promoted a 2-, 1.1- and 1.52-fold upregulation in TCR, CD2 and CD29 surface levels on CD8 T cells, respectively. The literature in the expression profile

of these markers in MLR models is surprisingly scarce, thus the discussion of this data proves challenging. However, it could be speculated that IL-15 primes CD8 T cells into a state of better preparedness for antigen encounter. Indeed, CD2 is an important enhancer of TCR signalling through remodelling of the IS, facilitating the enrichment of co-stimulatory signals and conjugate formation (Demetriou et al., 2019; Binder et al., 2020). CD29 expression identifies CD8 T cells with an active cytotoxic potential notably in the production of granzyme b (Nicolet et al., 2020). Finally, the increase in TCR would sustain better scanning capabilities. However, while TCR downmodulation is a well-accepted consequence of its engagement with class I or II MHC-allopeptide (Liu et al., 2000), it came as a surprise to see levels similar to those induced by IL-15. A distinct dynamic referred to as TCR replenishment could account for this observation. It describes a recovery system further to prolonged exposure to high dose cognate ligand, revealed when TCR engagement terminates (Schrum et al., 2003). Such context could be at stake in the MLR consequently to the direct allorecognition. Indeed, the initial fast response to the preponderant presence of HLA-mismatched epitopes is only short-lived (Benichou and Thomson, 2009), thus TCR engagement would cease, enabling recovery of TCR basal levels.

The use of *in vitro* models in the pre-clinical development of new therapeutic strategies is valuable. The MLR remains however a reductive platform, hence care must be taken when extrapolating any effects observed to a clinical perspective. Indeed, the MLR focusses on a restricted stage which has been simplified in terms of spatio-temporal framework and so, eludes characteristic features of aGvHD, notably tissue infiltration and the key role of host-non hematopoietic cells as APCs (Koyama and Hill, 2016). In addition, despite being the central theme of this study, the priming stage is extremely simplified as it excludes the intricate reactions prevailing in secondary lymphoid organs as exemplified by GC reactions, critical for the development of effective B cell responses. Also, keeping in mind that aGvHD is not a linear, sequential unravelling of isolated events, but rather a combination of overlapping and contrasting effects altering the fate of the immune response, here referring to the tight balance between promoters and suppressors of aGvHD (Holtan et al., 2014). It is therefore challenging to reproduce this differential dynamic into a MLR which only gives a glimpse of a distinct, disconnected, stage. Besides, HLA-matched or HLA-partially matched HSCT, resorting notably to the inclusion of HLA haploidentical donors, is standard practice in clinic (Kekre and Antin, 2014). The MLR designed in this study presumably involves a wide variety of HLA disparities since blood from random donors are mixed

together without concerns for HLA matching. Here, it is rather a proof of concept based on observations made in the field of aGvHD which is tested, the effort being put in the inclusion of a key factor identified as critical in aGvHD pathogenesis, IL-15 (Sakata et al., 2001; Thiant et al., 2011, 2010), to try and emulate more physiological conditions. Based on the protection against aGvHD conferred by pre-transplant administration with rituximab (Christopeit et al., 2009; Crocchiolo et al., 2011), the question that the MLR addressed is whether B cells fine-tuning B cells functions would alter the direct allorecognition despite their restricted role in indirect allorecognition as class II MHC-expressing APCs. In fact, the MLR only depicts the direct alloresponse (Afzali et al., 2008), it thus represents a relevant model to test this hypothesis.

In addition, no readout allowing to determine the activation status of the cells has been performed. Whereas increased HLA-DR and CD86 expressions is indicative of better potency as APCs, they do not clearly establish that antigen presentation effectively occurred. Only conjectures can be made in this aspect. However, the use of C3d greatly helped in giving directions. Here, downstream components of BCR and TCR signalling, such as SIK (Ackermann et al., 2015) or ZAP-70 (Hwang et al., 2020) could be used to accurately assess the extent of B and T cell activation.

Also, although the specificity of epratuzumab was established by recording distinct features characteristic of its impact, that is the reduction of CD19 and CD21, the decrease in TCR expression raises question as to the presence of unspecific aspects. Another mechanism explaining the reduction in B cell surface markers is trogocytosis, involving the transfer of cell surface material onto the membrane of FcγR-bearing cells, notably monocytes, hence involving the Fc domain of epratuzumab. The full range of consequences arising from trogocytosis are not clearly established, raising concerns about the physiological processes it could perturb. It could introduce a bias in experimental studies attempting to decipher the functional role of cells in a complex environment, as it is in our model, and bring about off-target effects. Whether T cells are affected in the process is unclear. It could be tested by using the $F(ab)_2$ fragment of epratuzumab as it was shown to effectively drive CD22 co-localisation and BCR-complex internalisation. Here, a $F(ab)_2$ control would be more suited to the MLR used in this study than an isotype control which would be more suited to cultures involving isolated unique subsets (Giltiay et al., 2017; Lumb et al., 2016).

Lastly, the presence of neutrophils, and the inflammation they induce, makes it hard to distinguish allogeneic- and IL-15- specific effects. Notably, the increase in TCR expression is induced on the whole CD8 T cell population whereas up to 10% of these cells should be

involved in the alloreaction (Koyama and Hill, 2016). The B cells follow the same trend. The use of PBMCs may help in distinguishing these effects.

Our findings suggest that anergic B cells could be induced by epratuzumab. Moreover, C3d adjunction on resting B cells, not yet engaged in the allogeneic reaction, could drive a tolerogenic response where the cytotoxic T cells would become anergic. Despite this encouraging result, it must be mentioned that the allogeneic reaction was not completely abrogated. This would imply that the antigen-specific tolerogenic resting B cells generated would only provide a limited protection. In fact, the repertoire of antigens presented, although supposedly varied since the specificity of the BCR is eluded, may only represent a fraction of the entire pool generated following direct allorecognition. However, further investigations need to be performed to confirm these hypotheses. Anergy is an active repressive state where engagement with the TCR is not accompanied by the provision of CD28/CD86 co-stimulatory interaction with APCs (Chappert and Schwartz, 2010). Here, the addition of an anti-CD28 antibody could restore the loss of granzyme B production observed in the MLR supplemented with C3d.

These findings constitute interesting preliminary data on the potential of targeting CD19/CD21 complex to fine-tune B cells into driving a tolerogenic potential. In addition, the MLR established seems to constitute an interesting platform to test the potency of selected compounds.

Chapter 5

Conclusion

The occurrence of aGvHD constitutes a substantial barrier to a routine implementation of allogeneic HSCT and yet, no definite therapeutic strategy received a unanimous agreement. Its foundation lying on a complex network of promotors and suppressors of the inflammation, the alteration of this balance in favour of a shift towards the instauration of a tolerogenic state offers promising outlook to achieve long term recovery post allogeneic HSCT. With this perspective in mind, the present study attempted to develop a strategy centred on the targeting of B cells as APCs in the onset of aGVHD. Only here, we focused on their regulatory properties as APCs via harnessing of their tolerogenic potential. The reshaping of their functions to fit our purpose was only made possible by fine tuning the CD19/CD21 complex using C3d as a mediator on resting B cell. Further to this, a significant decrease in granzyme b production was recorded, although not completely abrogated, here suggesting that tolerogenic B cells were derived

If C3d supplementation were to be administered to patients undergoing allogeneic HSCT, it would have to be shortly after infusion of the graft cells, when the initial cytotoxic killing of host tissues as part of direct presentation occurred, releasing further to their degradation antigenic components which would then be coated with C3d for redirection to B cells through CD21. However, considering that C3d is also described as a key trigger at the root of the initiation of autoimmune diseases, breaking the anergic state, it would hold serious concerns with respect to its safety. All the more so that off-target effects were observed in our model, hence rejecting the potential of implementing such protocols in clinical practice. What holds therapeutic value are the resulting tolerogenic resting B cell. Hence, instead of inducing this subset *in vivo*, it could be generated *in vitro* for future administration to patients. An earlier temporality could be considered since these cells would already be antigen competent, even concomitantly with the infusion of the graft cells, here constituting the arm of adoptive therapy.

The recent findings highlighting the contribution of resting B cells to the thymic B cell repertoire (Yamano et al., 2015) and therefore, to the diversity of central tolerance, holds promising prospects for the conversion of mismatched HLAs and non-haematopoietic miHAs into self-antigens to become ignored by the donor immune system, thus achieving long term recovery post allogeneic HSCT. This mechanism is disputed, attributing only a minor role to resting B cells in this process since they were shown to poorly recirculate to the thymus of parabiotic mice (Perera et al., 2013), however it could be that the impact of extrinsic factors on the homing process of resting B cells was not considered in this model

and that such mediators are induced in the settings of allogeneic HSCT, facilitating then the circulation of resting B cells to the thymus (Dertschnig et al., 2015).

This emphasises how crucial the establishment of models reflecting the settings of aGvHD are. Our newly designed *in vitro* model of histocompatibility attempted to recreate the inflammatory settings characteristics of severe grades aGvHD with the inclusion of IL-15. Although having its limitations with respect, notably, to the exclusion of the migration of immune cells to the lymph nodes and associated homing process, it constitutes a relevant platform for the evaluation of the therapeutic potency of selected compounds, as carried out in the present study. Here, epratuzumab did not alter the effector response, thus its application for the prevention of aGvHD onset seems limited. This would in fact provide a first glance with respect to their relevance in aGvHD. As established earlier, the generation of tolerogenic resting B cells with C3d supplementation carried out in our model is not transferable as it is into clinical practice. However, the mere fact that these cells propagated their signal in spite of the intense inflammatory environment prevailing in our model attests of their strength and stability, thus the adoptive transfer of these cells in patients presenting such a context looks promising in terms of their functional robustness.

This study was built around the pathogenesis of aGvHD, however the application of the induction of tolerogenic B cells with C3d could also extent to solid organ transplantation as the basics for rejection mechanisms are shared.

Despite this successful achievement, more needs to be done to get a detailed picture of the immune response at stake in our model so as to get a better understanding of the mechanisms at the root of the tolerogenic signal induced by resting B cells fashioned by C3d supplementation.

Chapter 6

References

Abraham, S., Guo, H., Choi, J. G., Ye, C., Thomas, M. B., Ortega, N., Dwivedi, A., Manjunath, N., Yi, G., & Shankar, P. (2017). Combination of IL-10 and IL-2 induces oligoclonal human CD4 T cell expansion during xenogeneic and allogeneic GVHD in humanized mice. Heliyon, 3(4), e00276.

Ackermann, J.A., Nys, J., Schweighoffer, E., McCleary, S., Smithers, N., Tybulewicz, V.L.J., 2015. Syk Tyrosine Kinase Is Critical for B Cell Antibody Responses and Memory B Cell Survival. J. Immunol. 194, 4650–4656.

Afzali, B., Lombardi, G., Lechler, R.I., 2008. Pathways of major histocompatibility complex allorecognition. Curr. Opin. Organ Transplant. 13, 438–444.

Akkaya, M., Kwak, K., Pierce, S.K., 2019. B cell memory: building two walls of protection against pathogens. Nat. Rev. Immunol. 2019 204 20, 229–238.

Al-Adra, D.P., Anderson, C.C., 2011. Mixed chimerism and split tolerance: Mechanisms and clinical correlations. Chimerism 2, 89.

Al-Homsi, A.S., Roy, T.S., Cole, K., Feng, Y., Duffner, U., 2015. Post-Transplant High-Dose Cyclophosphamide for the Prevention of Graft-versus-Host Disease. Biol. Blood Marrow Transplant. 21, 604–611.

Allen, C.D.C., Okada, T., Cyster, J.G., 2007. Germinal-center organization and cellular dynamics. Immunity 27, 190–202.

Alpdogan, O., Eng, J.M., Muriglan, S.J., Willis, L.M., Hubbard, V.M., Tjoe, K.H., Terwey, T.H., Kochman, A., Van Den Brink, M.R.M., 2005. Interleukin-15 enhances immune reconstitution after allogeneic bone marrow transplantation. Blood 105, 865–873.

*Ammendolia, D.A., Bement, W.M. & Brumell, J.H. (2021). Plasma membrane integrity: implications for health and disease. BMC Biol **19,** 71.*

Anguille, S., Smits, E.L.J.M., Cools, N., Goossens, H., Berneman, Z.N., Van Tendeloo, V.F.I., 2009. Short-term cultured, interleukin-15 differentiated dendritic cells have potent immunostimulatory properties. J. Transl. Med. 7, 1–16.

Appleman, L J, Tzachanis, · D, Grader-Beck, · T, Van Puijenbroek, A A F L, Boussiotis, V A, Appleman, Leonard J, Tzachanis, D., Grader-Beck, T., Van Puijenbroek, Andre A F L, Boussiotis, Vassiliki A, 2001. Helper T cell anergy: from biochemistry to cancer pathophysiology and therapeutics. J Mol Med 78, 673–683.

Arai, Y., Kanda, J., Nakasone, H., Kondo, T., Uchida, N., Fukuda, T., Ohashi, K., Kaida, K., Iwato, K., Eto, T., Kanda, Y., Nakamae, H., Nagamura-Inoue, T., Morishima, Y., Hirokawa, M., Atsuta, Y., Murata, M., 2015. Risk factors and prognosis of hepatic acute GvHD after allogeneic hematopoietic cell transplantation. Bone Marrow Transplant. 2016 511 51, 96–102.

Araki, R., Uda, M., Hoki, Y., Sunayama, M., Nakamura, M., Ando, S., Sugiura, M., Ideno, H., Shimada, A., Nifuji, A., Abe, M., 2013. Negligible immunogenicity of terminally differentiated cells derived from induced pluripotent or embryonic stem cells. Nature 494, 100–104.

Baatar, D., Olkhanud, P., Sumitomo, K., Taub, D., Gress, R., & Biragyn, A. (2007). Human peripheral blood T regulatory cells (Tregs), functionally primed CCR4+ Tregs and unprimed CCR4- Tregs, regulate effector T cells using FasL. Journal of immunology (Baltimore, Md. : 1950), 178(8), 4891–4900.

Ball, L.M., Egeler, R.M., 2008. Acute GvHD: pathogenesis and classification. Bone Marrow Transplant. 41, S58–S64.

Barnes, D.W.H., Corp, M.J., Louth, J.F., Neal, F.E., 1956. Treatment of Murine Leukaemia with X Rays and Homologous Bone Marrow. Br. Med. J. 2, 626.

Barrett, A.J., 2008. Understanding and harnessing the graft-versus-leukaemia effect. Br. J. Haematol. 142, 877–888.

Batista, F.D., Harwood, N.E., 2009. The who, how and where of antigen presentation to B

cells. Nat. Rev. Immunol. 2008 91 9, 15–27.

Baumeister, S.H.C., Rambaldi, B., Shapiro, R.M., Romee, R., 2020. Key Aspects of the Immunobiology of Haploidentical Hematopoietic Cell Transplantation. Front. Immunol. 11, 191.

Beilhack, A., Schulz, S., Baker, J., Beilhack, G. F., Wieland, C. B., Herman, E. I., Baker, E. M., Cao, Y. A., Contag, C. H., & Negrin, R. S. (2005). In vivo analyses of early events in acute graft-versus-host disease reveal sequential infiltration of T-cell subsets. Blood, 106(3), 1113–1122.

Bendle, G.M., Linnemann, C., Hooijkaas, A.I., Bies, L., de Witte, M.A., Jorritsma, A., Kaiser, A.D.M., Pouw, N., Debets, R., Kieback, E., Uckert, W., Song, J.-Y., Haanen, J.B.A.G., Schumacher, T.N.M., 2010. Lethal graft-versus-host disease in mouse models of T cell receptor gene therapy. Nat. Med. 16, 565–570.

Benichou, G., Thomson, A.W., 2009. Direct versus indirect allorecognition pathways: On the right track. Am. J. Transplant. 9, 655-656.

Bertaina, A., Andreani, M., 2018. Molecular Sciences Review Major Histocompatibility Complex and Hematopoietic Stem Cell Transplantation: Beyond the Classical HLA Polymorphism. J. Mol. Sci 19, 621.

Bertaina, A., Pitisci, A., Sinibaldi, M., Algeri, M., 2017. T Cell-Depleted and T Cell-Replete HLA-Haploidentical Stem Cell Transplantation for Non-malignant Disorders. Curr. Hematol. Malig. Rep. 12, 68–78.

Bierer, B.E., Sleckmann, B.P., Ratnofsky, S.E., Burakoff, S.J., 1989. The biologic roles of CD2, CD4, and CD8 in T-cell activation. Annu. Rev. Immunol.7, 579-599.

Billingham, R.E., 1966. The biology of graft-versus-host reactions. Harvey Lect. 62, 21–78.

Binder, C., Cvetkovski, F., Sellberg, F., Berg, S., Paternina Visbal, H., Sachs, D.H., Berglund, E., Berglund, D., 2020. CD2 Immunobiology. Front. Immunol.11, 1090.

Bishara, A., Malka, R., Brautbar, C., Barak, V., Cohen, I., Kedar, E., 1998. Cytokine production in human mixed leukocyte reactions performed in serum-free media. J. Immunol. Methods 215, 187–190.

Black, A.P.B., Bhayani, H., Ryder, C.A.J., Gardner-Medwin, J.M.M., Southwood, T.R., 2002. T-cell activation without proliferation in juvenile idiopathic arthritis. Arthritis Res. 4, 177.

Blanter, M., Gouwy, M., Struyf, S., 2021. Studying Neutrophil Function in vitro: Cell Models and Environmental Factors. J. Inflamm. Res. 14, 141–162.

Blaser, B.W., Roychowdhury, S., Kim, D.J., Schwind, N.R., Bhatt, D., Yuan, W., Kusewitt, D.F., Ferketich, A.K., Caligiuri, M.A., Guimond, M., 2005. Donor-derived IL-15 is critical for acute allogeneic graft-versus-host disease. Blood 105, 894–901.

Blaser, B.W., Schwind, N.R., Karol, S., Chang, D., Shin, S., Roychowdhury, S., Becknell, B., Ferketich, A.K., Kusewitt, D.F., Blazar, B.R., Caligiuri, M.A., 2006. Trans-presentation of donor-derived interleukin 15 is necessary for the rapid onset of acute graft-versus-host disease but not for graft-versus-tumor activity. Blood 108, 2463–9.

Blazar, B.R., MacDonald, K.P.A., Hill, G.R., 2018. Immune regulatory cell infusion for graft-versus-host disease prevention and therapy. Blood 131, 2651.

Blazar, B.R., Murphy, W.J., Abedi, M., 2012. Advances in graft-versus-host disease biology and therapy. Nat. Rev. Immunol. 12, 443–58.

Bleakley, M., Heimfeld, S., Loeb, K.R., Jones, L.A., Chaney, C., Seropian, S., Gooley, T.A., Sommermeyer, F., Riddell, S.R., Shlomchik, W.D., 2015. Outcomes of acute leukemia patients transplanted with naive T cell-depleted stem cell grafts. J. Clin. Invest. 125, 2677–2689.

Bleakley, M., Riddell, S.R., 2011. Exploiting T cells specific for human minor histocompatibility antigens for therapy of leukemia. Immunol. Cell Biol. 89, 396–407.

Boackle, S.A., Morris, M.A., Holers, V.M., Karp, D.R., 1998. Complement Opsonization Is

Required for Presentation of Immune Complexes by Resting Peripheral Blood B Cells. J. Immunol. 161, 6537-6543.

Boada-Romero, E., Martinez, J., Heckmann, B.L., Green, D.R., 2020. The clearance of dead cells by efferocytosis. Nat. Rev. Mol. Cell Biol. 21,398-414.

Boardman, D.A., Jacob, J., Smyth, L.A., Lombardi, G., Lechler, R.I., 2016. What Is Direct Allorecognition? Curr. Transplant. Reports 3, 275.

Böhmer, R.M., Bandala-Sanchez, E., Harrison, L.C., 2011. Forward light scatter is a simple measure of T-cell activation and proliferation but is not universally suited for doublet discrimination. Cytom. Part A 79A, 646–652.

Boivin, W.A., Cooper, D.M., Hiebert, P.R., Granville, D.J., 2009. Intracellular versus extracellular granzyme B in immunity and disease: Challenging the dogma. Lab. Investig.89, 1195-1220.

Bonilla, M.C., Fingerhut, L., Alfonso-Castro, A., Elmontaser Mergani, A., Schwennen, C., Köckritz-Blickwede, M. Von, de Buhr, N., 2020. How Long Does a Neutrophil Live?—The Effect of 24 h Whole Blood Storage on Neutrophil Functions in Pigs. Biomedicines 8.278

Braun, M., 1998. Human B and T lymphocytes have similar amounts of CD21 mRNA, but differ in surface expression of the CD21 glycoprotein. Int. Immunol. 10, 1197–1202.

Buchbinder, E. I., & Desai, A. (2016). CTLA-4 and PD-1 Pathways: Similarities, Differences, and Implications of Their Inhibition. American journal of clinical oncology, 39(1), 98–106.

Bucher, C., Koch, L., Vogtenhuber, C., Goren, E., Munger, M., Panoskaltsis-Mortari, A., Sivakumar, P., Blazar, B.R., 2009. IL-21 blockade reduces graft-versus-host disease mortality by supporting inducible T regulatory cell generation. Blood 114, 5375–5384.

Buhlmann, D., Eberhardt, H.U., Medyukhina, A., Prodinger, W.M., Figge, M.T., Zipfel, P.F., Skerka, C., 2016. FHR3 Blocks C3d-Mediated Coactivation of Human B Cells. J. Immunol. 197, 620-629.

Calderón-Gómez, E., Lampropoulou, V., Shen, P., Neves, P., Roch, T., Stervbo, U., Rutz, S., Kühl, A.A., Heppner, F.L., Loddenkemper, C., Anderton, S.M., Kanellopoulos, J.M., Charneau, P., Fillatreau, S., 2011. Reprogrammed quiescent B cells provide an effective cellular therapy against chronic experimental autoimmune encephalomyelitis. Eur. J. Immunol. 41, 1696-1708

Carlson, M.J., West, M.L., Coghill, J.M., Panoskaltsis-Mortari, A., Blazar, B.R., Serody, J.S., 2009. In vitro–differentiated TH17 cells mediate lethal acute graft-versus-host disease with severe cutaneous and pulmonary pathologic manifestations. Blood 113, 1365.

Caruso, S., Poon, I.K.H., 2018. Apoptotic Cell-Derived Extracellular Vesicles: More Than Just Debris. Front. Immunol. 9, 1486.

Castillo, E.F., Schluns, K.S., 2012. Regulating the immune system via IL-15 transpresentation. Cytokine 59, 479–90.

Chakraverty, R., Sykes, M., 2007. The role of antigen-presenting cells in triggering graft-versus-host disease and graft-versus-leukemia. Blood 110, 9.

Chan, Y.L.T., Zuo, J., Inman, C., Croft, W., Begum, J., Croudace, J., Kinsella, F., Maggs, L., Nagra, S., Nunnick, J., Abbotts, B., Craddock, C., Malladi, R., Moss, P., 2018. NK cells produce high levels of IL-10 early after allogeneic stem cell transplantation and suppress development of acute GVHD. Eur. J. Immunol. 48, 316.

Chanput, W., Mes, J.J., Wichers, H.J., 2014. THP-1 cell line: An in vitro cell model for immune modulation approach. Int. Immunopharmacol. 23, 37–45.

Chappert, P., Schwartz, R.H., 2010. Induction of T cell anergy: integration of environmental cues and infectious tolerance. Curr. Opin. Immunol. 22, 552.

Chatfield, S.M., Thieblemont, N., Witko-Sarsat, V., 2018. Expanding Neutrophil Horizons:

New Concepts in Inflammation. J. Innate Immun. 10, 422–431.

Chen, B.J., Deoliveira, D., Cui, X., Le, N.T., Son, J., Whitesides, J.F., Chao, N.J., 2007. Inability of memory T cells to induce graft-versus-host disease is a result of an abortive alloresponse. Blood 109, 3115.

Chen, J., Wang, H., Zhou, J., Feng, S., 2020. Advances in the understanding of poor graft function following allogeneic hematopoietic stem-cell transplantation. Ther. Adv. Hematol. 11, 2040620720948743.

Cherukuri, A., Cheng, P.C., Pierce, S.K., 2001. The Role of the CD19/CD21 Complex in B Cell Processing and Presentation of Complement-Tagged Antigens. J. Immunol. 167.

Choo, S.Y., 2007. The HLA system: Genetics, immunology, clinical testing, and clinical implications. Yonsei Med. J. 48, 11–23.

Christopeit, M., Schütte, V., Theurich, S., Weber, T., Grothe, W., Behre, G., 2009. Rituximab reduces the incidence of acute graft-versus-host disease. Blood 113, 3130–1.

Clatworthy, M.R., 2011. Targeting B Cells and Antibody in Transplantation. Am. J. Transplant. 11, 1359–1367.

Clowse, M.E.B., Wallace, D.J., Furie, R.A., Petri, M.A., Pike, M.C., Leszczyński, P., Neuwelt, C.M., Hobbs, Kathryn, Keiserman, Mauro, Duca, Liliana, Kalunian, K.C., Galateanu, C., Bongardt, S., Stach, C., Beaudot, C., Kilgallen, B., Gordon, C., Batalov, A., Bojinca, M., Djerassi, R., Duca, L., Horak, P., Kolarov, Z., Milasiene, R., Monova, D., Otsa, K., Pileckyte, M., Popova, T., Radulescu, F., Rashkov, R., Rednic, S., Repin, M., Stoilov, R., Tegzova, D., Vezikova, N., Vitek, P., Zainea, C., East, F., Baek, H., Chen, Y., Chiu, Y., Cho, C., Chou, C., Choe, J., Huang, C., Kang, Y., Kang, S., Lai, N., Lee, S., Park, W., Shim, S., Suh, C., Yoo, W., Armengol, H.A., Zapata, F.A., Santiago, M.B., Cavalcanti, F., Chahade, W., Costallat, L., Keiserman, M., Alcala, J.O., Remus, C.R., Roimicher, L., Abu-Shakra, M., Agarwal, V., Agmon-Levin, N., Kadel, J., Levy, Y., Mevorach, D., Paran, D., Reitblat, T., Rosner, I., Shobha, V., Sthoeger, Z., Zisman, D., Ayesu, K., Berney, S., Box, J., Busch, H., Buyon, J., Carter, J., Chi, J., Clowse, M., Collins, R., Dao, K., Diab, I., Dikranian, A., El-Shahawy, M., Gaylis, N., Grossman, J., Halpert, E., Huff, J., Jarjour, W., Kao, A., Katz, R., Kennedy, A., Khan, M., Kivitz, A., Kohen, M., Lawrence-Ford, T., Lawson, J., Levesque, M., Lowenstein, M., Majjhoo, A., Mcarthur, R., McLain, D., Merrill, J., Murillo, A., Neucks, S., Niemer, G., Noaiseh, G., Parker, C., Pantojas, C., Pattanaik, D., Petri, M., Pickrell, P., Reveille, J., Roman-Miranda, A., Rothfield, N., Sankoorikal, A., Sayers, M., Singhal, A., Snyder, A., Striebich, C., Vo, Q., von Feldt, J., Wallace, D., Wasko, M., Young, C., Adelstein, S., Hall, S., Littlejohn, G., Nicholls, D., Suranyi, M., Amoura, Z., Bannert, B., Behrens, F., Perez, L.C., Chakravarty, K., Gonzales, F.D., Davies, K., Doria, A., Emery, P., Fernández-Nebro, A., Govoni, M., Hachulla, E., Hellmich, B., Houssiau, F., Malaise, M., Margaux, J., Maugars, Y., Muñoz-Fernández, S., Navarro, F., Ordi-Ros, J., Pellerito, R., Pena-Sagredo, J., Roussou, E., Schmidt, R.E., Ucar-Angulo, E., Viallard, J.F., Westhovens, R., Worm, M., Yee, C.S., Nayiager, S., Reuter, H., Spargo, C., Bazela, B., Brzosko, M., Chudzik, D., Gasztonyi, B., Geher, P., Ionescu, R., Jeka, S., Kemeny, L., Kiss, E., Kotyla, P., Kovacs, L., Kovalenko, V., Kucharz, E., Kwiatkowska, B., Leszczynski, P., Levchenko, E., Lysenko, G., Majdan, M., Mihailov, C., Nalotov, S., Nedelciu, M., Pavel, M., Raskina, T., Rebrov, B., Rezus, E., Semen, T., Smakotina, S., Stanislavchuk, M., Stanislav, M., Szombati, I., Szucs, G., Udrea, G., Zajdel, J., Zon-Giebel, A., Bonfiglioli, R., Bustamante, R., Klumb, E., Ramirez, G.M., Neiva, C., Olguin, M., Gonzaga, J.R., Scotton, A., Ayala, S.S., Ximenes, A., Sharma, R., Srikantiah, C., Aelion, J., Aranow, C., Baker, M., Chadha, A., Chao, J., Chatham, W., Chow, A., Clay, C., Cohen-Gadol, S., Conaway, D., Denburg, J., Escalante, A., Espinoza, L., Fiechtner, J., Fortin, I., Fraser, A., Furie, R., Gladman, D., Goddard, D., Goldberg, M., Gonzalez-Rivera, R., Gorman, J., Griffin, R., Haaland, D., Halter,

D., Hemaiden, A., Hobbs, K., Joshi, V., Lim, S., Kalunian, K., Karpouzas, G., Khraishi, M., Lafyatis, R., Lee, S., Lidman, R., Lue, C., Mohan, M., Mease, P., Mehta, C., Mizutani, W., Nami, A., Nascimento, J., Neuwelt, C., Pappas, J., Pope, J., Porges, A., Roane, G., Rosenberg, D., Ross, S., Saadeh, C., Scoville, C., Sherrer, Y., Solomon, M., Surbeck, W., Valenzuela, G., Waller, P., Alten, R., Baerwald, C., Bienvenu, B., Bombardieri, S., Braun, J., Dival, L., Espinosa, G., Fernandez, I.F., Gomez-Reino, J., Hiepe, F., Hopkinson, N., Isenberg, D., Jacobi, A., Jorgensen, C., Guern, V. Le, Paul, C., Pego-Reigosa, J.M., Heredia, J.R., Rubbert-Roth, A., Sabbadini, M., Schroeder, J., Schwarting, A., Spieler, W., Valesini, G., Wollenhaupt, J., Mendoza, A.Z., Zouboulis, C., 2017. Efficacy and Safety of Epratuzumab in Moderately to Severely Active Systemic Lupus Erythematosus: Results From Two Phase III Randomized, Double-Blind, Placebo-Controlled Trials. Arthritis Rheumatol. 69, 362–375.

Coillard, A., Segura, E., 2019. In vivo differentiation of human monocytes. Front. Immunol. 10, 1907.

Crocchiolo, R., Castagna, L., El-Cheikh, J., Helvig, A., Fürst, S., Faucher, C., Vazquez, A., Granata, A., Coso, D., Bouabdallah, R., Blaise, D., 2011. Prior rituximab administration is associated with reduced rate of acute GVHD after in vivo T-cell depleted transplantation in lymphoma patients. Exp. Hematol. 39, 892–896.

Daigneault, M., Preston, J.A., Marriott, H.M., Whyte, M.K.B., Dockrell, D.H., Gordon, S, Taylor, P., Murphy, J., Summer, R., Wilson, A., Kotton, D., Fine, A., Alblas, A. van oud, Furth, R. van, Landsman, L., Jung, S., Mosser, D., Edwards, J., Gordon, S, Gordon, SB, Irving, G., Lawson, R., Lee, ME, Read, R., Murao, S., Gemmell, M., Callaham, M., Anderson, N., Huberman, E., Olsson, I., Gullberg, U., Ivhed, I., Nilsson, K., Fleit, H., Kobasiuk, C., Kohro, T., Tanaka, T., Murakami, T., Wada, Y., Aburatani, H., Park, E., Jung, H., Yang, H., Yoo, M., Kim, C., Collins, S., Rovera, G., O'Brien, T., Diamond, L., Schwende, H., Fitzke, E., Ambs, P., Dieter, P., Gantner, F., Kupferschmidt, R., Schudt, C., Wendel, A., Hatzelmann, A., Dockrell, D., Lee, M, Lynch, D., Read, R., Marriott, H., Ali, F., Read, R., Mitchell, T., Whyte, M., Vandivier, R., Fadok, V., Hoffmann, P., Bratton, D., Penvari, C., Marriott, H., Bingle, C., Read, R., Braley, K., Kroemer, G., Sokol, R., Hudson, G., James, N., Frost, I., Wales, J., Bainton, D., McCullough, K., Basta, S., Knotig, S., Gerber, H., Schaffner, R., Kradin, R., McCarthy, K., Preffer, F., Schneeberger, E., Haarst, J. van, Hoogsteden, H., Wit, H. de, Verhoeven, G., Havenith, C., de, G.M.-P., Belaud-Rotureau, M., Voisin, P., Leducq, N., Belloc, F., Cohn, Z., Benson, B., Steinbach, F., Thiele, B., Henning, L., Azad, A., Parsa, K., Crowther, J., Tridandapani, S., Liu, H., Perlman, H., Pagliari, L., Pope, R., Munn, D., Beall, A., Song, D., Wrenn, R., Throckmorton, D., Wewers, M., Rennard, S., Hance, A., Bitterman, P., Crystal, R., MacMicking, J., Xie, Q., Nathan, C., Heo, S., Ju, S., Lee, S., Park, S., Choe, S., Pham, T., Brown, B., Dobson, P., Richardson, V., Mantovani, A., Sica, A., Sozzani, S., Allavena, P., Vecchi, A., Stein, M., Keshav, S., Harris, N., Gordon, S, Berges, C., Naujokat, C., Tinapp, S., Wieczorek, H., Hoh, A., Stout, R., Jiang, C., Matta, B., Tietzel, I., Watkins, S., Geissmann, F., Jung, S., Littman, D., Desjardins, M., Huber, L., Parton, R., Griffiths, G., Toyomura, T., Murata, Y., Yamamoto, A., Oka, T., Sun-Wada, G., Pitt, A., Mayorga, L., Stahl, P., Schwartz, A., Hackam, D., Rotstein, O., Zhang, W., Demaurex, N., Woodside, M., Cohn, Z., Fedorko, M., Hirsch, J., Nichols, B., Bainton, D., Farquhar, M., Burchett, S., Weaver, W., Westall, J., Larsen, A., Kronheim, S., Smith, S., Fenwick, P., Nicholson, A., Kirschenbaum, F., Finney-Hayward, T., Gessani, S., Testa, U., Varano, B., Marzio, P. Di, Borghi, P., Nahori, M., Fournie-Amazouz, E., Que-Gewirth, N., Balloy, V., Chignard, M., Lepe-Zuniga, J., Klostergaard, J., Netea, M., Nold-Petry, C., Nold, M., Joosten, L., Opitz, B., Surewicz, K., Aung, H., Kanost, R., Jones, L., Hejal, R., Hume, D., Mangan, D., Welch, G., Wahl, S., Perlman, H., Pagliari, L., Georganas, C., Mano,

T., Walsh, K., Sabroe, I., Read, R., Whyte, M., Dockrell, D., Vogel, S., 2010. The Identification of Markers of Macrophage Differentiation in PMA-Stimulated THP-1 Cells and Monocyte-Derived Macrophages. PLoS One 5, e8668.

De Carvalho Bittencourt, M., Perruche, S., Contassot, E., Fresnay, S., Baron, M.H., Angonin, R., Aubin, F., Hervé, P., Tiberghien, P., Saas, P., 2001. Intravenous injection of apoptotic leukocytes enhances bone marrow engraftment across major histocompatibility barriers. Blood 98, 224–230.

Deeg, H.J., 2021. Chimerism, the Microenvironment and Control of Leukemia. Front. Immunol. 12, 629.

Dehn, J., Spellman, S., Hurley, C.K., Shaw, B.E., Barker, J.N., Burns, L.J., Confer, D.L., Eapen, M., Fernandez-Vina, M., Hartzman, R., Maiers, M., Marino, S.R., Mueller, C., Perales, M.-A., Rajalingam, R., Pidala, J., 2019. Selection of unrelated donors and cord blood units forhematopoietic cell transplantation: guidelines from the NMDP/CIBMTR. Blood 134, 924.

Del Nagro, C.J., Kolla, R. V., Rickert, R.C., 2005. A Critical Role for Complement C3d and the B Cell Coreceptor (CD19/CD21) Complex in the Initiation of Inflammatory Arthritis. J. Immunol. 175, 5379–5389.

Demetriou, P., Abu-Shah, E., McCuaig, S., Mayya, V., Valvo, S., Korobchevskaya, K., Friedrich, M., Mann, E., Lee, L.Y., Starkey, T., Kutuzov, M.A., Afrose, J., Siokis, A., Investigators, O.I.C., Meyer-Hermann, M., Depoil, D., Dustin, M.L., 2019. CD2 expression acts as a quantitative checkpoint for immunological synapse structure and T-cell activation. bioRxiv 589440.

Dertschnig, S., Hauri-Hohl, M.M., Vollmer, M., Holländer, G.A., Krenger, W., 2015. Impaired thymic expression of tissue-restricted antigens licenses the de novo generation of autoreactive CD4+ T cells in acute GVHD. Blood 125, 2720–2723.

DeWolf, S., Shen, Y., Sykes, M., 2016. A new window into the human alloresponse. Transplantation.100, 1639-49.

Dooms, B., Desmedt, M., Vancaeneghem, S., Rottiers, P., Goossens, V., Fiers, W., Grooten, J., 1998. Quiescence-inducing and antiapoptotic activities of IL-15 enhance secondary CD4(+) T cell responsiveness to antigen. J. Immunol. 161, 2141–2150.

Dörner, T., Shock, A., Goldenberg, D.M., Lipsky, P.E., 2015. The mechanistic impact of CD22 engagement with epratuzumab on B cell function: Implications for the treatment of systemic lupus erythematosus. Autoimmun. Rev. 14, 1079–1086.

Doucey, M.A., Legler, D.F., Faroudi, M., Boucheron, N., Baumgaertner, P., Naeher, D., Cebecauer, M., Hudrisier, D., Rüegg, C., Palmer, E., Valitutti, S., Bron, C., Luescher, I.F., 2003. The β1 and β3 integrins promote T cell receptor-mediated cytotoxic T lymphocyte activation. J. Biol. Chem. 278, 26983–26991.

Du, W., Cao, X., 2018. Cytotoxic Pathways in Allogeneic Hematopoietic Cell Transplantation. Front. Immunol.9, 2979.

Duffner, U.A., Maeda, Y., Cooke, K.R., Reddy, P., Ordemann, R., Liu, C., Ferrara, J.L.M., Teshima, T., 2004. Host dendritic cells alone are sufficient to initiate acute graft-versus-host disease. J. Immunol. 172, 7393–7398.

Dunkelberger, J.R., Song, W.C., 2010. Complement and its role in innate and adaptive immune responses. Cell Res. 20, 34–50.

Duraes, F. V., Thelemann, C., Sarter, K., Acha-Orbea, H., Hugues, S., Reith, W., 2013. Role of major histocompatibility complex class II expression by non-hematopoietic cells in autoimmune and inflammatory disorders: facts and fiction. Tissue Antigens 82, 1–15.

El-Zayat, S.R., Sibaii, H., Mannaa, F.A., 2019. Toll-like receptors activation, signaling, and targeting: an overview. Bull. Natl. Res. Cent. 2019 431 43, 1–12.

Elias, S., Rudensky, A.Y., 2019. Therapeutic use of regulatory T cells for graft-versus-host disease. Br. J. Haematol. 187, 25.

Embgenbroich, M., Burgdorf, S., 2018. Current concepts of antigen cross-presentation. Front. Immunol. 9, 1643.

Enterina, J.R., Jung, J., Macauley, M.S., 2019. Coordinated roles for glycans in regulating the inhibitory function of CD22 on B cells. Biomed. J.4, 218-232.

Ereño-Orbea, J., Sicard, T., Cui, H., Mazhab-Jafari, M.T., Benlekbir, S., Guarné, A., Rubinstein, J.L., Julien, J.P., 2017. Molecular basis of human CD22 function and therapeutic targeting. Nat. Commun. 2017 81 8, 1–11.

Eriguchi, Y., Takashima, S., Oka, H., Shimoji, S., Nakamura, K., Uryu, H., Shimoda, S., Iwasaki, H., Shimono, N., Ayabe, T., Akashi, K., Teshima, T., 2012. Graft-versus-host disease disrupts intestinal microbial ecology by inhibiting Paneth cell production of α-defensins. Blood 120, 223–31.

EW, P., JA, H., PJ, M., A, W., M, M., T, G., B, S., E, M., A, S., C, A., 2001. Major-histocompatibility-complex class I alleles and antigens in hematopoietic-cell transplantation. N. Engl. J. Med. 345, 1794–1800.

Feng, X., Hui, K.M., Younes, H.M., Brickner, A.G., 2008. Targeting minor histocompatibility antigens in graft versus tumor or graft versus leukemia responses. Trends Immunol. 29, 624–32.

Ferracini, M., Rios, F.J.O., Pecenin, M., Jancar, S., 2013. Clearance of apoptotic cells by macrophages induces regulatory phenotype and involves stimulation of CD36 and platelet-activating factor receptor. Mediators Inflamm. 2013:950273

Ferrara, J.L.M., Levine, J.E., Reddy, P., Holler, E., 2009. Graft-versus-host disease. Lancet 373, 1550–61.

Fleischhauer, K., 2019. Selection of matched unrelated donors moving forward: From HLA allele counting to functional matching. Hematol. (United States) 2019, 532–538.

Fleischhauer, K., Shaw, B.E., 2017. HLA-DP in unrelated hematopoietic cell transplantation revisited: challenges and opportunities. Blood 130, 1089–1096.

Fraser, J.M., Janicki, C.N., Raveney, B.J.E., Morgan, D.J., 2006. Abortive activation precedes functional deletion of CD8+ T cells following encounter with self-antigens expressed by resting B cells in vivo. Immunology 119, 126–133.

Fu, J., Heinrichs, J., Yu, X.Z., 2014. Helper T-cell differentiation in graft-versus-host disease after allogeneic hematopoietic stem cell transplantation. Arch. Immunol. Ther. Exp. (Warsz). 62, 277–301.

Fürst, D., Neuchel, C., Tsamadou, C., Schrezenmeier, H., Mytilineos, J., 2019. HLA Matching in Unrelated Stem Cell Transplantation up to Date. Transfus. Med. Hemotherapy.46, 326-336.

Gajewski, T.F., Lancki, D.W., Stack, R., Fitch, F.W., 1994. "Anergy" of TH0 helper T lymphocytes induces downregulation of TH1 characteristics and a transition to a TH2-like phenotype. J. Exp. Med. 179, 481–91.

Gale, R.P., Fuchs, E.J., 2016. Is there really a specific graft-versus-leukaemia effect? Bone Marrow Transplant. 2016 5111 51, 1413–1415.

Gasparrini, F., Feest, C., Bruckbauer, A., Mattila, P.K., Müller, J., Nitschke, L., Bray, D., Batista, F.D., 2016. Nanoscale organization and dynamics of the siglec CD22 cooperate with the cytoskeleton in restraining BCR signalling. EMBO J. 35, 258.

Geering, B., Simon, H.U., 2011. Peculiarities of cell death mechanisms in neutrophils. Cell Death Differ. 2011 189 18, 1457–1469.

Giltiay, N. V., Shu, G.L., Shock, A., Clark, E.A., 2017. Targeting CD22 with the monoclonal antibody epratuzumab modulates human B-cell maturation and cytokine production in response to Toll-like receptor 7 (TLR7) and B-cell receptor (BCR) signaling. Arthritis Res. Ther. 19, 1–18.

González-Álvaro, I., Domínguez-Jiménez, C., Ortiz, A.M., Núñez-González, V., Roda-Navarro, P., Fernández-Ruiz, E., Sancho, D., Sánchez-Madrid, F., 2006. Interleukin-

15 and interferon-gamma participate in the cross-talk between natural killer and monocytic cells required for tumour necrosis factor production. Arthritis Res. Ther. 8:R88.

González, F., Boué, S., Carlos Izpisúa Belmonte, J., 2011. Methods for making induced pluripotent stem cells: reprogramming à la carte. Nat. Rev. 12, 231–242.

Gore, A., Li, Z., Fung, H.-L., Young, J., Agarwal, S., Antosiewicz-Bourget, J., Canto, I., Giorgetti, A., Israel, M., Kiskinis, E., Lee, J.-H., Loh, Y.-H., Manos, P.D., Montserrat, N., Panopoulos, A.D., Ruiz, S., Wilbert, M., Yu, J., Kirkness, E.F., Belmonte, J.C.I., Rossi, D.J., Thomson, J., Eggan, K., Daley, G.Q., Goldstein, L.S.B., Zhang, K., 2011. Somatic coding mutations in human induced pluripotent stem cells. Nature 471, 63.

Gottenberg, J.E., Dörner, T., Bootsma, H., Devauchelle-Pensec, V., Bowman, S.J., Mariette, X., Bartz, H., Oortgiesen, M., Shock, A., Koetse, W., Galateanu, C., Bongardt, S., Wegener, W.A., Goldenberg, D.M., Meno-Tetang, G., Kosutic, G., Gordon, C., 2018. Efficacy of Epratuzumab, an Anti-CD22 Monoclonal IgG Antibody, in Systemic Lupus Erythematosus Patients With Associated Sjögren's Syndrome: Post Hoc Analyses From the EMBODY Trials. Arthritis Rheumatol. 70, 763–773.

Griffioen, M., van Bergen, C.A.M., Falkenburg, J.H.F., 2016. Autosomal Minor Histocompatibility Antigens: How Genetic Variants Create Diversity in Immune Targets. Front. Immunol. 7, 1–9.

Gros, P., 2011. In self-defense. Nat. Struct. Mol. Biol. 18, 401–402.

Guha, P., Morgan, J.W., Mostoslavsky, G., Rodrigues, N.P., Boyd, A.S., 2013. Lack of Immune Response to Differentiated Cells Derived from Syngeneic Induced Pluripotent Stem Cells. Cell Stem Cell 12, 407–412.

Guo, W.W., Su, X.H., Wang, M.Y., Han, M.Z., Feng, X.M., Jiang, E.L., 2021. Regulatory T Cells in GVHD Therapy. Front. Immunol. 12, 2374.

Gupta, A.O., Wagner, J.E., 2020. Umbilical Cord Blood Transplants: Current Status and Evolving Therapies. Front. Pediatr. 8:570282.

Gutzeit, C., Chen, K., Cerutti, A., 2018. The enigmatic function of IgD: some answers at last. Eur. J. Immunol. 48, 1101–1113.

Gyurkocza, B., Sandmaier, B.M., 2014. Conditioning regimens for hematopoietic cell transplantation: one size does not fit all. Blood 124, 344–53.

Haas, K.M., Poe, J.C., Tedder, T.F., 2009. CD21/35 Promotes Protective Immunity to Streptococcus pneumoniae through a Complement-Independent but CD19-Dependent Pathway That Regulates PD-1 Expression. J. Immunol. 183, 3661–3671.

Hanaki, R., Toyoda, H., Iwamoto, S., Morimoto, M., Nakato, D., Ito, T., Niwa, K., Amano, K., Hashizume, R., Tawara, I., Hirayama, M., 2021. Donor-derived M2 macrophages attenuate GVHD after allogeneic hematopoietic stem cell transplantation. Immunity, Inflamm. Dis. 9, 1489–1499.

Hasegawa, M., Fujimoto, M., Poe, J.C., Steeber, D.A., Tedder, T.F., 2001. CD19 Can Regulate B Lymphocyte Signal Transduction Independent of Complement Activation. J. Immunol. 167, 3190–3200.

Hasskamp, J.H., Zapas, J.L., Elias, E.G., 2005. Dendritic cell counts in the peripheral blood of healthy adults. Am. J. Hematol. 78, 314–315.

He, C., Heeger, P.S., 2004. CD8 T cells can reject major histocompatibility complex class I-deficient skin allografts. Am. J. Transplant 4, 698–704.

Henden, A.S., Hill, G.R., 2015. Cytokines in Graft-versus-Host Disease. J. Immunol. 194, 4604–4612.

Hernández, J., Aung, S., Marquardt, K., Sherman, L.A., 2002. Uncoupling of proliferative potential and gain of effector function by CD8(+) T cells responding to self-antigens. J. Exp. Med. 196, 323–333.

Hess, M.W., Schwendinger, M.G., Eskelinen, E.-L., Pfaller, K., Pavelka, M., Dierich, M.P.,

Prodinger, W.M., 2000. Tracing uptake of C3dg-conjugated antigen into B cells via complement receptor type 2 (CR2, CD21). Blood 95, 2617–2623.

Hock, K., Mahr, B., Schwarz, C., Wekerle, T., 2015. Deletional and regulatory mechanisms coalesce to drive transplantation tolerance through mixed chimerism. Eur. J. Immunol. 45, 2470–2479.

Hofmeister, C.C., Quinn, A., Cooke, K.R., Stiff, P., Nickoloff, B., Ferrara, J.L.M., 2004. Graft-versus-host disease of the skin: Life and death on the epidermal edge. Biol. Blood Marrow Transplant. 10, 366–372.

Holtan, S.G., Pasquini, M., Weisdorf, D.J., 2014. Acute graft-versus-host disease: a bench-to-bedside update. Blood 124, 363–373.

Holtan, S.G., Verneris, M.R., Schultz, K.R., Newell, L.F., Meyers, G., He, F., DeFor, T.E., Vercellotti, G.M., Slungaard, A., MacMillan, M.L., Cooley, S.A., Blazar, B.R., Panoskaltsis-Mortari, A., Weisdorf, D.J., 2015. Circulating Angiogenic Factors Associated with Response and Survival in Patients with Acute Graft-versus-Host Disease: Results from Blood and Marrow Transplant Clinical Trials Network 0302 and 0802. Biol. Blood Marrow Transplant. 21, 1029–1036.

Hong, Y.Q., Wan, B., Li, X.F., 2020. Macrophage regulation of graft-vs-host disease. World J. Clin. Cases 8, 1793.

Hüber, C.M., Doisne, J.M., Colucci, F., 2015. IL-12/15/18-preactivated NK cells suppress GvHD in a mouse model of mismatched hematopoietic cell transplantation. Eur. J. Immunol. 45, 1727–1735.

Hwang, J.R., Byeon, Y., Kim, D., Park, S.G., 2020. Recent insights of T cell receptor-mediated signaling pathways for T cell activation and development. Exp. Mol. Med. 2020 525 52, 750–761.

Iba, T., Hashiguchi, N., Nagaoka, I., Tabe, Y., Murai, M., 2013. Neutrophil cell death in response to infection and its relation to coagulation. J. Intensive Care 1, 1–10.

Imado, T., Iwasaki, T., Kitano, S., Satake, A., Kuroiwa, T., Tsunemi, S., Sano, H., 2010. The protective role of host Toll-like receptor-4 in acute graft-versus-host disease. Transplantation 90, 1063–1070.

Imamura, M., 2021. Impaired Hematopoiesis after Allogeneic Hematopoietic Stem Cell Transplantation: Its Pathogenesis and Potential Treatments. Hemato 2021, Vol. 2, Pages 43-63 2, 43–63.

Inaguma, Y., Akahori, Y., Murayama, Y., Shiraishi, K., Tsuzuki-Iba, S., Endoh, A., Tsujikawa, J., Demachi-Okamura, A., Hiramatsu, K., Saji, H., Yamamoto, Y., Yamamoto, N., Nishimura, Y., Takahashi, T., Kuzushima, K., Emi, N., Akatsuka, Y., 2014. Construction and molecular characterization of a T-cell receptor-like antibody and CAR-T cells specific for minor histocompatibility antigen HA-1H. Gene Ther. 21, 575–584.

Inaoki, M., Sato, S., Weintraub, B.C., Goodnow, C.C., Tedder, T.F., 1997. CD19-regulated signaling thresholds control peripheral tolerance and autoantibody production in B lymphocytes. J. Exp. Med. 186, 1923–1931.

Ingle, G.S., Scales, S.J., 2013. DropArray™, a Wall-Less 96-Well Plate for Uptake and Immunofluorescence Microscopy, Confirms CD22 Recycles.

Isnardi, I., Ng, Y.S., Menard, L., Meyers, G., Saadoun, D., Srdanovic, I., Samuels, J., Berman, J., Buckner, J.H., Cunningham-Rundles, C., Meffre, E., 2010. Complement receptor 2/CD21− human naive B cells contain mostly autoreactive unresponsive clones. Blood 115, 5026.

Jagasia, M., Arora, M., Flowers, M.E.D., Chao, N.J., McCarthy, P.L., Cutler, C.S., Urbano-Ispizua, A., Pavletic, S.Z., Haagenson, M.D., Zhang, M.-J., Antin, J.H., Bolwell, B.J., Bredeson, C., Cahn, J.-Y., Cairo, M., Gale, R.P., Gupta, V., Lee, S.J., Litzow, M., Weisdorf, D.J., Horowitz, M.M., Hahn, T., 2012. Risk factors for acute GVHD and

survival after hematopoietic cell transplantation. Blood 119, 296–307.

Jankovic, D., Ganesan, J., Bscheider, M., Stickel, N., Weber, F.C., Guarda, G., Follo, M., Pfeifer, D., Tardivel, A., Ludigs, K., Bouazzaoui, A., Kerl, K., Fischer, J.C., Haas, T., Schmitt-Gräff, A., Manoharan, A., Müller, L., Finke, J., Martin, S.F., Gorka, O., Peschel, C., Ruland, J., Idzko, M., Duyster, J., Holler, E., French, L.E., Poeck, H., Contassot, E., Zeiser, R., 2013. The Nlrp3 inflammasome regulates acute graft-versus-host disease. J. Exp. Med. 210, 1899–1910.

Jardine, L., Cytlak, U., Gunawan, M., Reynolds, G., Green, K., Wang, X.N., Pagan, S., Paramitha, M., Lamb, C.A., Long, A.K., Hurst, E., Nair, S., Jackson, G.H., Publicover, A., Bigley, V., Haniffa, M., Simpson, A.J., Collin, M., 2020. Donor monocyte–derived macrophages promote human acute graft-versus-host disease. J. Clin. Invest. 130, 4574.

Jégou, J.-F., Chan, P., Schouft, M.-T., Griffiths, M.R., Neal, J.W., Gasque, P., Vaudry, H., Fontaine, M., 2007. C3d Binding to the Myelin Oligodendrocyte Glycoprotein Results in an Exacerbated Experimental Autoimmune Encephalomyelitis. J. Immunol. 178, 3323–3331.

Jiang, H., Fu, D., Bidgoli, A., Paczesny, S., 2021. T Cell Subsets in Graft Versus Host Disease and Graft Versus Tumor. Front. Immunol. 12:761448.

Joffre, O.P., Segura, E., Savina, A., Amigorena, S., 2012. Cross-presentation by dendritic cells. Nat. Rev. Immunol. 2012 128 12, 557–569.

Jordan, W.J., Ritter, M.A., 2002. Optimal analysis of composite cytokine responses during alloreactivity. J. Immunol. Methods 260, 1–14.

Jung, D., Alt, F.W., 2004. Unraveling V(D)J Recombination: Insights into Gene Regulation. Cell 116, 299–311.

Kanakry, C.G., Fuchs, E.J., Luznik, L., 2016. Modern approaches to HLA-haploidentical blood or marrow transplantation. Nat. Rev. Clin. Oncol. 13, 10.

Kawai, T., Akira, S., 2011. Toll-like receptors and their crosstalk with other innate receptors in infection and immunity. Immunity 34, 637–650.

Kekre, N., Antin, J.H., 2014. Hematopoietic stem cell transplantation donor sources in the 21st century: choosing the ideal donor when a perfect match does not exist. Blood 124, 334–343.

Kekre, N., Antin, J.H., 2016. Cord blood versus haploidentical stem cell transplantation for hematological malignancies. Semin. Hematol.53, 98-102.

Kennedy, D.W., Abkowitz, J.L., 1997. Kinetics of Central Nervous System Microglial and Macrophage Engraftment: Analysis Using a Transgenic Bone Marrow Transplantation Model. Blood 90, 986–993.

Khera, N., Zeliadt, S.B., Lee, S.J., 2012. Economics of hematopoietic cell transplantation. Blood 120, 1545–1551.

Kim, T.K., Billard, M.J., Wieder, E.D., McIntyre, B.W., Komanduri, K. V., 2010. Co-engagement of α4β1 integrin (VLA-4) and CD4 or CD8 is necessary to induce maximal Erk1/2 phosphorylation and cytokine production in human T cells. Hum. Immunol. 71, 23–28.

Kircher, B., Schumacher, P., Nachbaur, D., 2009. Granzymes A and B serum levels in allo-SCT. Bone Marrow Transplant. 43, 787–791.

Klebanoff, C.A., Finkelstein, S.E., Surman, D.R., Lichtman, M.K., Gattinoni, L., Theoret, M.R., Grewal, N., Spiess, P.J., Antony, P.A., Palmer, D.C., Tagaya, Y., Rosenberg, S.A., Waldmann, T.A., Restifo, N.P., 2004. IL-15 enhances the in vivo antitumor activity of tumor-reactive CD8+ T Cells. Proc. Natl. Acad. Sci. U. S. A. 101, 1969.

Kleinclauss, F., Perruche, S., Masson, E., de Carvalho Bittencourt, M., Biichle, S., Remy-Martin, J.P., Ferrand, C., Martin, M., Bittard, H., Chalopin, J.M., Seilles, E., Tiberghien, P., Saas, P., 2006. Intravenous apoptotic spleen cell infusion induces a

TGF-beta-dependent regulatory T-cell expansion. Cell Death Differ. 13, 41.

Koyama, M., Hill, G.R., 2016. Alloantigen presentation and graft-versus-host disease: fuel for the fire. Blood 127, 2963–70.

Koyama, M., Hill, G.R., 2021. Mouse Models of Antigen Presentation in Hematopoietic Stem Cell Transplantation. Front. Immunol. 12, 3716.

Koyama, M., Kuns, R.D., Olver, S.D., Raffelt, N.C., Wilson, Y.A., Don, A.L.J., Lineburg, K.E., Cheong, M., Robb, R.J., Markey, K.A., Varelias, A., Malissen, B., Hämmerling, G.J., Clouston, A.D., Engwerda, C.R., Bhat, P., MacDonald, K.P.A., Hill, G.R., 2011. Recipient nonhematopoietic antigen-presenting cells are sufficient to induce lethal acute graft-versus-host disease. Nat. Med. 2011 181 18, 135–142.

Kratofil, R.M., Kubes, P., Deniset, J.F., 2017. Monocyte conversion during inflammation and injury. Arterioscler. Thromb. Vasc. Biol. 37, 35–42.

Krauledat, P.B., Krapf, F.E., Manger, B., Kalden, J.R., 1985. Evaluation of plasma C3d and immune complex determinations in the assessment of disease activity of patients with rheumatoid arthritis, systemic lupus erythematosus, and spondylitis ancylopoetica. Rheumatol. Int. 5, 97–101.

Krishnappa, V., Gupta, M., Manu, G., Kwatra, S., Owusu, O.T., Raina, R., 2016. Acute Kidney Injury in Hematopoietic Stem Cell Transplantation: A Review. Int. J. Nephrol. 2016. 5163789

Kuba, A., Raida, L., 2018. Graft versus host disease: from basic pathogenic principles to DNA damage response and cellular senescence. Mediators Inflamm. 2018, 9451950.

Kulakova, N., Urban, B., McMichael, A. J., & Ho, L. P. (2010). Functional analysis of dendritic cell-T cell interaction in sarcoidosis. Clinical and experimental immunology, 159(1), 82–86.

Kumari, R., Palaniyandi, S., Hildebrandt, G.C., 2019. Microbiome: An Emerging New Frontier in Graft-Versus-Host Disease. Dig. Dis. Sci. 64, 669–677.

Lal, G., Zhang, N., van der Touw, W., Ding, Y., Ju, W., Bottinger, E.P., Reid, S.P., Levy, D.E., Bromberg, J.S., 2009. Epigenetic regulation of Foxp3 expression in regulatory T cells by DNA methylation. J. Immunol. 182, 259–273.

Land, W.G., 2015. The Role of Damage-Associated Molecular Patterns in Human Diseases: Part I - Promoting inflammation and immunity. Sultan Qaboos Univ. Med. J. 15, e9.

Lašťovička, J., Budinský, V., Špíšek, R., Bartůňková, J., 2009. Assessment of lymphocyte proliferation: CFSE kills dividing cells and modulates expression of activation markers. Cell. Immunol. 256, 79–85.

Lau, A.W., Brink, R., 2020. Selection in the germinal center. Curr. Opin. Immunol. 63, 29–34.

Leenaerts, P.L., Ceuppens, J.L., Van Damme, J., Michielsen, P., Waer, M., 1992. Evidence that stimulator cell-derived IL-6 and IL-1 are released in the mixed lymphocyte culture but are not requisite for responder T cell proliferation. Transplantation 54, 1071–1078.

Leitner, J., Herndler-Brandstetter, D., Zlabinger, G.J., Grubeck-Loebenstein, B., Steinberger, P., 2015. CD58/CD2 Is the Primary Costimulatory Pathway in Human CD28 − CD8 + T Cells. J. Immunol. 195, 477–487.

Leung, C.S.K., 2015. Endogenous Antigen Presentation of MHC Class II Epitopes through Non-Autophagic Pathways. Front. Immunol. 6, 464.

Levy, E., Ambrus, J., Kahl, L., Molina, H., Tung, K., Holers, V.M., 1992. T lymphocyte expression of complement receptor 2 (CR2/CD21): A role in adhesive cell-cell interactions and dysregulation in a patient with systemic lupus erythematosus (SLE). Clin. Exp. Immunol. 90, 235–244.

Li, J.-M., Giver, C.R., Lu, Y., Hossain, M.S., Akhtari, M., Waller, E.K., 2009. Separating graft-versus-leukemia from graft-versus-host disease in allogeneic hematopoietic stem

cell transplantation. Immunotherapy 1, 599–621.

Li Pira, G., Di Cecca, S., Montanari, M., Moretta, L., Manca, F., 2016. Specific removal of alloreactive T-cells to prevent GvHD in hemopoietic stem cell transplantation: rationale, strategies and perspectives. Blood Rev. 30, 297–307.

Lieberman, J., 2003. The ABCs of granule-mediated cytotoxicity: New weapons in the arsenal. Nat. Rev. Immunol.

Liesveld, J.L., Rothberg, P.G., 2008. Mixed chimerism in SCT: conflict or peaceful coexistence? Bone Marrow Transplant. 2008 425 42, 297–310.

Lim, J.Y., Ryu, D. Bin, Lee, S.E., Park, G., Choi, E.Y., Min, C.K., 2015. Differential Effect of MyD88 Signal in Donor T Cells on Graft-versus-Leukemia Effect and Graft-versus-Host Disease after Experimental Allogeneic Stem Cell Transplantation. Mol. Cells 38, 966.

Lim, S.H., Patton, W.N., Jobson, S., Gentle, T.A., Baynham, M., Franklin, I.M., Boughton, B.J., 1988. Mixed lymphocyte reactions do not predict severity of graft versus host disease (GVHD) in HLA-DR compatible, sibling bone marrow transplants. J. Clin. Pathol. 41, 1155.

Lin, C.M., Gill, R.G., 2016. Direct and indirect allograft recognition: Pathways dictating graft rejection mechanisms. Curr. Opin. Organ Transplant.21, 40-44.

Little, A., Green, A., Harvey, J., Hemmatpour, S., Latham, K., E Marsh, S.G., Poulton, K., Sage, D., Little, A.-M., and, H., 2016. BSHI Guideline: HLA matching and donor selection for haematopoietic progenitor cell transplantation. Int. J. Immunogenet. 43, 263.

Liu, H., Rhodes, M., Wiest, D. L., & Vignali, D. A. (2000). On the dynamics of TCR:CD3 complex cell surface expression and downmodulation. Immunity, 13(5), 665–675.

Liu, Y., Cai, Y., Dai, L., Chen, G., Ma, X., Wang, Y., Xu, T., Jin, S., Wu, X., Qiu, H., Tang, X., Li, C., Sun, A., Wu, D., Liu, H., 2013. The expression of Th17-associated cytokines in human acute graft-versus-host disease. Biol. Blood Marrow Transplant. 19, 1421–1429.

Locke, F. L., Pidala, J., Storer, B., Martin, P. J., Pulsipher, M. A., Chauncey, T. R., Jacobsen, N., Kröger, N., Walker, I., Light, S., Shaw, B. E., Beato, F., Laport, G. G., Nademanee, A., Keating, A., Socie, G., & Anasetti, C. (2017). CD25 Blockade Delays Regulatory T Cell Reconstitution and Does Not Prevent Graft-versus-Host Disease After Allogeneic Hematopoietic Cell Transplantation. Biology of blood and marrow transplantation: journal of the American Society for Blood and Marrow Transplantation, 23(3), 405–411.

Lu, F.-T., Yang, W., Wang, Y.-H., Ma, H.-D., Tang, W., Yang, J.-B., Li, L., Ansari, A.A., Lian, Z.-X., 2015. Thymic B cells promote thymus-derived regulatory T cell development and proliferation. J. Autoimmun. 61, 62–72.

Lubbers, R., van Essen, M.F., van Kooten, C., Trouw, L.A., 2017. Production of complement components by cells of the immune system. Clin. Exp. Immunol.188, 183-194.

Lumb, S., Fleischer, S.J., Wiedemann, A., Daridon, C., Maloney, A., Shock, A., Dörner, T., 2016. Engagement of CD22 on B cells with the monoclonal antibody epratuzumab stimulates the phosphorylation of upstream inhibitory signals of the B cell receptor. J. Cell Commun. Signal. 10, 143–51.

Luning Prak, E.T., Monestier, M., Eisenberg, R.A., 2011. B cell receptor editing in tolerance and autoimmunity. Ann. N. Y. Acad. Sci. 1217, 96.

MacDonald, K.P., Shlomchik, W.D., Reddy, P., 2013. Biology of Graft-versus-Host Responses: Recent Insights. Biol. Blood Marrow Transplant. 19, S10.

Mancusi, A., Piccinelli, S., Velardi, A., Pierini, A., 2019. CD4+FOXP3+ Regulatory T Cell Therapies in HLA Haploidentical Hematopoietic Transplantation. Front. Immunol. 10, 2901.

Marino, J., Paster, J., Benichou, G., 2016a. Allorecognition by T Lymphocytes and Allograft Rejection. Front. Immunol. 7, 582.

Marino, J., Paster, J., Benichou, G., 2016b. Allorecognition by T lymphocytes and allograft rejection. Front. Immunol. 7, 582.

Mariotti, J., Penack, O., Castagna, L., 2020. Acute Graft-versus-Host-Disease Other Than Typical Targets: Between Myths and Facts. Biol. Blood Marrow Transplant.27, 115-124.

Markey, K. a., Macdonald, K.P. a, Hill, G.R., 2014. The biology of graft-versus-host disease : experimental systems instructing clinical practice. Blood 124, 354–362.

Markey, K.A., Banovic, T., Kuns, R.D., Olver, S.D., Don, A.L.J., Raffelt, N.C., Wilson, Y.A., Raggatt, L.J., Pettit, A.R., Bromberg, J.S., Hill, G.R., MacDonald, K.P.A., 2009. Conventional dendritic cells are the critical donorAPC presenting alloantigen after experimental bone marrow transplantation. Blood 113, 5644–5649.

Mårtensson, I.L., Almqvist, N., Grimsholm, O., Bernardi, A.I., 2010. The pre-B cell receptor checkpoint. FEBS Lett. 584, 2572–2579.

Marzaioli, V., Canavan, M., Floudas, A., Wade, S.C., Low, C., Veale, D.J., Fearon, U., 2020. Monocyte-Derived Dendritic Cell Differentiation in Inflammatory Arthritis Is Regulated by the JAK/STAT Axis via NADPH Oxidase Regulation. Front. Immunol. 11, 1406.

Matejuk, A., 2018. Skin Immunity. Arch. Immunol. Ther. Exp. (Warsz).66, 45-54.

Mathewson, N.D., Jenq, R., Mathew, A. V, Koenigsknecht, M., Hanash, A., Toubai, T., Oravecz-Wilson, K., Wu, S.-R., Sun, Y., Rossi, C., Fujiwara, H., Byun, J., Shono, Y., Lindemans, C., Calafiore, M., Schmidt, T.M., Honda, K., Young, V.B., Pennathur, S., van den Brink, M., Reddy, P., 2016. Gut microbiome–derived metabolites modulate intestinal epithelial cell damage and mitigate graft-versus-host disease. Nat. Immunol. 17, 505–513.

Matsukuma, K.E., Wei, D., Sun, K., Ramsamooj, R., Chen, M., 2016. Diagnosis and differential diagnosis of hepatic graft versus host disease (GVHD). J. Gastrointest. Oncol. 7, S21.

Matsuoka, K.I., Koreth, J., Kim, H.T., Bascug, G., McDonough, S., Kawano, Y., Murase, K., Cutler, C., Ho, V.T., Alyea, E.P., Armand, P., Blazar, B.R., Antin, J.H., Soiffer, R.J., Ritz, J., 2013. Low-dose interleukin-2 therapy restores regulatory T cell homeostasis in patients with chronic graft-versus-host disease. Sci. Transl. Med. 5, 179ra43.

Matsuoka, S., Hashimoto, D., Kadowaki, M., Ohigashi, H., Hayase, E., Yokoyama, E., Hasegawa, Y., Tateno, T., Chen, X., Aoyama, K., Oka, H., Onozawa, M., Takeda, K., Akashi, K., Teshima, T., 2020. Myeloid differentiation factor 88 signaling in donor T cells accelerates graft- versus-host disease. Haematologica 105, 226–234.

Mauri, C., Menon, M., 2015. The expanding family of regulatory B cells. Int. Immunol. 27, 479–86.

Mayadas, T.N., Cullere, X., Lowell, C.A., 2014. The Multifaceted Functions of Neutrophils. Annu. Rev. Pathol. 9, 181.

Mayani, H., Wagner, J.E., Broxmeyer, H.E., 2019. Cord blood research, banking, and transplantation: achievements, challenges, and perspectives. Bone Marrow Transplant. 2019 551 55, 48–61.

Medinger, M., Tichelli, A., Bucher, C., Halter, J., Dirnhofer, S., Rovo, A., Passweg, J., Tzankov, A., 2013. GVHD after allogeneic haematopoietic SCT for AML: angiogenesis, vascular endothelial growth factor and VEGF receptor expression in the BM. Bone Marrow Transplant. 48, 715–721.

Melchers, F., 2015. Checkpoints that control B cell development. J. Clin. Invest. 125, 2203–2210.

Merkley, S.D., Chock, C.J., Yang, X.O., Harris, J., Castillo, E.F., 2018. Modulating T Cell

Responses via Autophagy: The Intrinsic Influence Controlling the Function of Both Antigen-Presenting Cells and T Cells. Front. Immunol. 9, 2914.

Merle, N.S., Noe, R., Halbwachs-Mecarelli, L., Fremeaux-Bacchi, V., Roumenina, L.T., 2015. Complement system part II: Role in immunity. Front. Immunol.2015.00257.

Mesin, L., Ersching, J., Victora, G.D., 2016. GERMINAL CENTER B CELL DYNAMICS. Immunity 45, 471.

Messmann, J.J., Reisser, T., Leithäuser, F., Lutz, M.B., Debatin, K.M., Strauss, G., 2015. In vitro-generated MDSCs prevent murine GVHD by inducing type 2 T cells without disabling antitumor cytotoxicity. Blood 126, 1138–1148.

Mittelbrunn, M., Molina, A., Escribese, M.M., Yáñez-Mó, M., Escudero, E., Ursa, Á., Tejedor, R., Mampaso, F., Sánchez-Madrid, F., 2004. VLA-4 integrin concentrates at the peripheral supramolecular activation complex of the immune synapse and drives T helper 1 responses. Proc. Natl. Acad. Sci. U. S. A. 101, 11058–11063.

Miyagawa, F., Tagaya, Y., Kim, B.S., Patel, H.J., Ishida, K., Ohteki, T., Waldmann, T.A., Katz, S.I., 2008. IL-15 serves as a costimulator in determining the activity of autoreactive CD8 T cells in an experimental mouse model of graft-versus-host-like disease. J. Immunol. 181, 1109–1119.

Mongini, P.K.A., Tolani, S., Fattah, R.J., Inman, J.K., 2002. Antigen receptor triggered upregulation of CD86 and CD80 in human B cells: Augmenting role of the CD21/CD19 co-stimulatory complex and IL-4. Cell. Immunol. 216, 50–64.

Moulin, V., Andris, F., Thielemans, K., Maliszewski, C., Urbain, J., Moser, M., 2000. B lymphocytes regulate dendritic cell (DC) function in vivo: Increased interleukin 12 production by DCs from B cell-deficient mice results in T helper cell type 1 deviation. J. Exp. Med. 192, 475–482.

Müskens, K.F., Lindemans, C.A., Belderbos, M.E., 2021. Hematopoietic Dysfunction during Graft-Versus-Host Disease: A Self-Destructive Process? Cells 10.2051.

Nakasone, H., Fukuda, T., Kanda, J., Mori, T., Yano, S., Kobayashi, T., Miyamura, K., Eto, T., Kanamori, H., Iwato, K., Uchida, N., Mori, S., Nagamura-Inoue, T., Ichinohe, T., Atsuta, Y., Teshima, T., Murata, M., 2015. Impact of conditioning intensity and TBI on acute GVHD after hematopoietic cell transplantation. Bone Marrow Transplant. 50, 559–565.

Narsinh, K.H., Sun, N., Sanchez-freire, V., Lee, A.S., Almeida, P., Hu, S., Jan, T., Wilson, K.D., Leong, D., Rosenberg, J., Yao, M., Robbins, R.C., Wu, J.C., 2011. Single cell transcriptional profiling reveals heterogeneity of human induced pluripotent stem cells. J. Clin. Invest. 121, 1217–1221.

Negrin, R.S., 2015. Graft-versus-host disease versus graft-versus-leukemia. Hematology 2015, 225–230.

Nemazee, D., 2017. Mechanisms of central tolerance for B cells. Nat. Rev. Immunol. 2017 175 17, 281–294.

Nicolet, B.P., Guislain, A., van Alphen, F.P.J., Gomez-Eerland, R., Schumacher, T.N.M., van den Biggelaar, M., Wolkers, M.C., 2020. CD29 identifies IFN-γ-producing human CD8+ T cells with an increased cytotoxic potential. Proc. Natl. Acad. Sci. U. S. A. 117, 6686–6696.

Nielsen, M.C., Andersen, M.N., Møller, H.J., 2020. Monocyte isolation techniques significantly impact the phenotype of both isolated monocytes and derived macrophages in vitro. Immunology 159, 63–74.

Noviski, M., Mueller, J.L., Satterthwaite, A., Garrett-Sinha, L.A., Brombacher, F., Zikherman, J., 2018. IgM and igD b cell receptors differentially respond to endogenous antigens and control B cell fate. Elife 7. e35074

Nowak, J., 2008. Role of HLA in hematopoietic SCT. Bone Marrow Transplant.42, S71-S76.

Nunes, E., Heslop, H., Fernandez-Vina, M., Taves, C., Wagenknecht, D.R., Eisenbrey, A.B., Fischer, G., Poulton, K., Wacker, K., Hurley, C.K., Noreen, H., Sacchi, N., 2011. Definitions of histocompatibility typing terms. Blood 118, e180–e183.

Nunes, N.S., Kanakry, C.G., 2019. Mechanisms of Graft-versus-Host Disease Prevention by Post-transplantation Cyclophosphamide: An Evolving Understanding. Front. Immunol. 10, 2668.

O'Reilly, M.K., Tian, H., Paulson, J.C., 2011. CD22 is a recycling receptor that can shuttle cargo between the cell surface and endosomal compartments of B cells. J. Immunol. 186, 1554.

Olson, J.A., Leveson-Gower, D.B., Gill, S., Baker, J., Beilhack, A., Negrin, R.S., 2010. NK cells mediate reduction of GVHD by inhibiting activated, alloreactive T cells while retaining GVT effects. Blood 115, 4293.

Oravecz-Wilson, K., Rossi, C., Zajac, C., Sun, Y., Li, L., Decoville, T., Fujiwara, H., Kim, S., Peltier, D., Reddy, P., 2021. ATG5-Dependent Autophagy Uncouples T-cell Proliferative and Effector Functions and Separates Graft-versus-Host Disease from Graft-versus-Leukemia. Cancer Res. 81, 1063–1075.

Orekhov, A.N., Orekhova, V.A., Nikiforov, N.G., Myasoedova, V.A., Grechko, A. V., Romanenko, E.B., Zhang, D., Chistiakov, D.A., 2019. Monocyte differentiation and macrophage polarization. Vessel Plus 3, 10.

Özgör, L., Brandl, C., Shock, A., Nitschke, L., 2016. Epratuzumab modulates B-cell signaling without affecting B-cell numbers or B-cell functions in a mouse model with humanized CD22. Eur. J. Immunol. 46, 2260–2272.

Panch, S.R., Szymanski, J., Savani, B.N., Stroncek, D.F., 2017. Sources of Hematopoietic Stem and Progenitor Cells and Methods to Optimize Yields for Clinical Cell Therapy. Biol. Blood Marrow Transplant.23, 1241-1249.

Park, M.J., Baek, J.A., Kim, S.Y., Jung, K.A., Choi, J.W., Park, S.H., Kwok, S. -K, Cho, M. La, 2020. Myeloid-derived suppressor cells therapy enhance immunoregulatory properties in acute graft versus host disease with combination of regulatory T cells. J. Transl. Med. 18, 1–14.

Passweg, J., Baldomero, H., Bader, P., Bonini, C., Cesaro, S., Dreger, P., Duarte, R., Dufour, C., Kuball, J., 2016. Hematopoietic stem cell transplantation in Europe 2014: more than 40 000 transplants annually. Bone Marrow Transplant. 51, 786–792.

Pelanda, R., Torres, R.M., 2012. Central B-Cell Tolerance: Where Selection Begins. Cold Spring Harb. Perspect. Biol. 4. a007146

Penack, O., Holler, E., van den Brink, M.R.M., 2010. Graft-versus-host disease: regulation by microbe-associated molecules and innate immune receptors. Blood 115, 1865–1872.

Perera, J., Meng, L., Meng, F., Huang, H., 2013. Autoreactive thymic B cells are efficient antigen-presenting cells of cognate self-antigens for T cell negative selection. Proc. Natl. Acad. Sci. 110, 17011–17016.

Pilon, C.B., Petillon, S., Naserian, S., Martin, G.H., Badoual, C., Lang, P., Azoulay, D., Piaggio, E., Grimbert, P., Cohen, J.L., 2014. Administration of Low Doses of IL-2 Combined to Rapamycin Promotes Allogeneic Skin Graft Survival in Mice. Am. J. Transplant. 14, 2874–2882.

Poe, J.C., Hasegawa, M., Tedder, T.F., 2001. CD19, CD21, and CD22: Multifaceted response regulators of B lymphocyte signal transduction. Int. Rev. Immunol.

Powell, J.D., 2006. The induction and maintenance of T cell anergy. Clin. Immunol. 120, 239–246.

Praditpornsilpa, K., Wang, W., Chan, L., 2003. Upregulation of IL-2 but not IL-15 by allorecognition in human mixed lymphocyte culture. Transplant. Proc. 35, 1599–1602.

Rangaraju, S., Choi, J., Giver, C.R., Waller, E.K., 2013. Pharmacological Inhibition Of

Semi-Direct Alloantigen Presentation and The Generation Of Cross-Dressed Antigen Presenting Cells: A Novel approach To Limit Graft Versus Host Disease Following Allogeneic Hematopoetic Stem Cell Transplantation. Blood 122, 294.

Ratajczak, M.Z., Bujko, K., Cymer, M., Thapa, A., Adamiak, M., Ratajczak, J., Abdel-Latif, A.K., Kucia, M., 2020. The Nlrp3 inflammasome as a "rising star" in studies of normal and malignant hematopoiesis. Leukemia 34, 1512–1523.

Rey-Giraud, F., Hafner, M., Ries, C.H., 2012. In Vitro Generation of Monocyte-Derived Macrophages under Serum-Free Conditions Improves Their Tumor Promoting Functions. PLoS One 7, e42656.

Riesner, K., Shi, Y., Jacobi, A., Kräter, M., Kalupa, M., McGearey, A., Mertlitz, S., Cordes, S., Schrezenmeier, J.-F., Mengwasser, J., Westphal, S., Perez-Hernandez, D., Schmitt, C., Dittmar, G., Guck, J., Penack, O., 2017. Initiation of acute graft-versus-host disease by angiogenesis. Blood 129, 2021–2032.

Roberts, A.D., Ely, K.H., Woodland, D.L., 2005. Differential contributions of central and effector memory T cells to recall responses. J. Exp. Med. 202, 123.

Roche, P.A., Furuta, K., 2015. The ins and outs of MHC class II-mediated antigen processing and presentation. Nat. Rev. Immunol. 2015 154 15, 203–216.

Rodríguez-Pinto, D., 2005. B cells as antigen presenting cells. Cell. Immunol. 238, 67–75.

Rossi, E.A., Goldenberg, D.M., Michel, R., Rossi, D.L., Wallace, D.J., Chang, C.-H., 2013. Trogocytosis of multiple B-cell surface markers by CD22 targeting with epratuzumab. Blood 122, 3020–3029.

Roth, D.B., 2014. V(D)J Recombination: Mechanism, Errors, and Fidelity. Microbiol. Spectr. 2.:10.1128

Roychowdhury, S., Blaser, B.W., Freud, A.G., Katz, K., Bhatt, D., Ferketich, A.K., Bergdall, V., Kusewitt, D., Baiocchi, R.A., Caligiuri, M.A., 2005. IL-15 but not IL-2 rapidly induces lethal xenogeneic graft-versus-host disease. Blood 106, 2433–2435.

Saadoun, D., Terrier, B., Bannock, J., Vazquez, T., Massad, C., Kang, I., Joly, F., Rosenzwajg, M., Sene, D., Benech, P., Musset, L., Klatzmann, D., Meffre, E., Cacoub, P., 2013. Expansion of autoreactive unresponsive CD21-/low B cells in Sjögren's syndrome associated lymphoproliferation. Arthritis Rheum. 65, 1085.

Saas, P., Daguindau, E., Perruche, S., 2016. Concise Review: Apoptotic Cell-Based Therapies-Rationale, Preclinical Results and Future Clinical Developments. Stem Cells 34, 1464–1473.

Sachs, D.H., Kawai, T., Sykes, M., 2014. Induction of Tolerance through Mixed Chimerism. Cold Spring Harb. Perspect. Med. 4: a015529.

Saikh, K.U., Khan, A.S., Kissner, T., Ulrich, R.G., 2001. IL-15-induced conversion of monocytes to mature dendritic cells. Clin. Exp. Immunol. 126, 447.

Sairafi, D., Stikvoort, A., Gertow, J., Mattsson, J., Uhlin, M., 2016. Donor Cell Composition and Reactivity Predict Risk of Acute Graft-versus-Host Disease after Allogeneic Hematopoietic Stem Cell Transplantation. J. Immunol. Res. 2016:5601204.

Sakata, N., Yasui, M., Okamura, T., Inoue, M., Yumura-Yagi, K., Kawa, K., 2001. Kinetics of plasma cytokines after hematopoietic stem cell transplantation from unrelated donors: the ratio of plasma IL-10/sTNFR level as a potential prognostic marker in severe acute graft-versus-host disease. Bone Marrow Transplant. 27, 1153–1161.

Santos e Sousa, P., Bennett, C.L., Chakraverty, R., 2018. Unraveling the mechanisms of cutaneous graft-versus-host disease. Front. Immunol.2018.00963.

Saraiva, M., O'Garra, A., 2010. The regulation of IL-10 production by immune cells. Nat. Rev. Immunol. 10(3):170-81

Sarantopoulos, S., Blazar, B.R., Cutler, C., Ritz, J., 2015. B Cells in Chronic Graft-versus-Host Disease. Biol. Blood Marrow Transplant. 21, 16–23.

Sauter, C.T., Bailey, C.P., Panis, M.M., Biswas, C.S., Budak-Alpdogan, T., Durham, A.,

Flomenberg, N., Alpdogan, O., 2013. Interleukin-15 administration increases graft-versus-tumor activity in recipients of haploidentical hematopoietic SCT. Bone Marrow Transplant. 48, 1237–1242.

Schatz, D.G., Ji, Y., 2011. Recombination centres and the orchestration of V(D)J recombination. Nat. Rev. Immunol. 2011 114 11, 251–263.

Scheurer, J., Kitt, K., Huber, H.J., Fundel-Clemens, K., Pflanz, S., Debatin, K.M., Strauss, G., 2021. Graft-Versus-Host Disease Prevention by In Vitro-Generated Myeloid-Derived Suppressor Cells Is Exclusively Mediated by the CD11b+CD11c+ MDSC Subpopulation. Front. Immunol. 12, 4193.

Schmitt, E. G., & Williams, C. B. (2013). Generation and function of induced regulatory T cells. Frontiers in immunology, 4, 152.

Schrum, A. G., Turka, L. A., & Palmer, E. (2003). Surface T-cell antigen receptor expression and availability for long-term antigenic signaling. Immunological reviews, 196, 7–24.

Segura, E., Villadangos, J.A., 2011. A modular and combinatorial view of the antigen cross-presentation pathway in dendritic cells. Traffic 12, 1677–1685.

Shah, S., Qiao, L., 2008. Resting B cells expand a CD4+CD25+Foxp3+ Treg population via TGF-beta3. Eur. J. Immunol. 38, 2488–2498.

Shiina, T., Hosomichi, K., Inoko, H., Kulski, J.K., 2009. The HLA genomic loci map: expression, interaction, diversity and disease. J. Hum. Genet. 2009 541 54, 15–39.

Shono, Y., Ueha, S., Wang, Y., Abe, J., Kurachi, M., Matsuno, Y., Sugiyama, T., Nagasawa, T., Imamura, M., Matsushima, K., 2010. Bone marrow graft-versus-host disease: early destruction of hematopoietic niche after MHC-mismatched hematopoietic stem cell transplantation. Blood 115, 5401–5411.

Sieger, N., Fleischer, S.J., Mei, H.E., Reiter, K., Shock, A., Burmester, G.R., Daridon, C., Dörner, T., 2013. CD22 ligation inhibits downstream B cell receptor signaling and Ca 2+ flux upon activation. Arthritis Rheum. 65, 770–779.

Simonetta, F., Alvarez, M., Negrin, R.S., 2017. Natural Killer Cells in Graft-versus-Host-Disease after Allogeneic Hematopoietic Cell Transplantation. Front. Immunol. 8, 25.

Siu, J.H.Y., Surendrakumar, V., Richards, J.A., Pettigrew, G.J., 2018. T cell allorecognition pathways in solid organ transplantation. Front. Immunol.2018.02548.

Slukvin, I.I., 2013. Hematopoietic specification from human pluripotent stem cells: current advances and challenges toward de novo generation of hematopoietic stem cells. Blood 122, 4035–4046.

Smith, N.A., Coleman, C.B., Gewurz, B.E., Rochford, R., 2020. CD21 (Complement Receptor 2) Is the Receptor for Epstein-Barr Virus Entry into T Cells. J. Virol. 94: e00428-20.

Spellman, S., Setterholm, M., Maiers, M., Noreen, H., Oudshoorn, M., Fernandez-Viña, M., Petersdorf, E., Bray, R., Hartzman, R.J., Ng, J., Hurley, C.K., 2008. Advances in the Selection of HLA-Compatible Donors: Refinements in HLA Typing and Matching over the First 20 Years of the National Marrow Donor Program Registry. Biol. Blood Marrow Transplant. 14, 37–44.

Srinivasan, L., Sasaki, Y., Calado, D.P., Zhang, B., Paik, J.H., DePinho, R.A., Kutok, J.L., Kearney, J.F., Otipoby, K.L., Rajewsky, K., 2009. PI3 kinase signals BCR-dependent mature B cell survival. Cell 139, 573–86.

Stadinski, B.D., Huseby, E.S., 2020. How to Prevent yourself from Seeing Double. Cytometry. A 97, 1102.

Staffas, A., Burgos da Silva, M., van den Brink, M.R.M., 2017. The intestinal microbiota in allogeneic hematopoietic cell transplant and graft-versus-host disease. Blood 129, 927–933.

Stonier, S.W., Schluns, K.S., 2010. Trans-presentation: a novel mechanism regulating IL-

15 delivery and responses. Immunol. Lett. 127, 85–92.

Strong Rodrigues, K., Oliveira-Ribeiro, C., de Abreu Fiuza Gomes, S., Knobler, R., 2018. Cutaneous Graft-Versus-Host Disease: Diagnosis and Treatment. Am. J. Clin. Dermatol. 19, 33.

Suan, D., Sundling, C., Brink, R., 2017. Plasma cell and memory B cell differentiation from the germinal center. Curr. Opin. Immunol. 45, 97–102.

Sugita, J., 2019. HLA-haploidentical stem cell transplantation using posttransplant cyclophosphamide. Int. J. Hematol. 110, 30–38.

Summers, C., Sheth, V.S., Bleakley, M., 2020. Minor Histocompatibility Antigen-Specific T Cells. Front. Pediatr. 8, 284.

Sun, Y., Tawara, I., Toubai, T., Reddy, P., 2007. Pathophysiology of acute graft-versus-host disease: recent advances. Transl. Res.12: 715424.

Sweeney, C., Vyas, P., 2019. The Graft-Versus-Leukemia Effect in AML. Front. Oncol. 9, 1217.

Symons, H.J., Fuchs, E.J., 2008. Hematopoietic SCT from partially HLA-mismatched (HLA-haploidentical) related donors. Bone Marrow Transplant. 42, 365–377.

Tahvildari, M., Dana, R., 2019. Low-Dose IL-2 Therapy in Transplantation, Autoimmunity, and Inflammatory Diseases. J. Immunol. 203, 2749–2755.

Takahashi, K., Tanabe, K., Ohnuki, M., Narita, M., Ichisaka, T., Tomoda, K., Yamanaka, S., Jaenisch, R., Thomson, J.A., Jaenisch, R., Al., E., 2006. Induction of Pluripotent Stem Cells from Adult Human Fibroblasts by Defined Factors. Cell 131, 861–872.

Tamada, K., Tamura, H., Flies, D., Fu, Y. X., Celis, E., Pease, L. R., Blazar, B. R., & Chen, L. (2002). Blockade of LIGHT/LTbeta and CD40 signaling induces allospecific T cell anergy, preventing graft-versus-host disease. The Journal of clinical investigation, 109(4), 549–557.

Tamang, D.L., Redelman, D., Alves, B.N., Vollger, L., Bethley, C., Hudig, D., 2006. Induction of granzyme B and T cell cytotoxic capacity by IL-2 or IL-15 without antigens: Multiclonal responses that are extremely lytic if triggered and short-lived after cytokine withdrawal. Cytokine 36, 148.

Teague, R.M., Sather, B.D., Sacks, J.A., Huang, M.Z., Dossett, M.L., Morimoto, J., Tan, X., Sutton, S.E., Cooke, M.P., Öhlén, C., Greenberg, P.D., 2006. Interleukin-15 rescues tolerant CD8+ T cells for use in adoptive immunotherapy of established tumors. Nat. Med. 12, 335–341.

Tecchio, C., Cassatella, M.A., 2020. Uncovering the multifaceted roles played by neutrophils in allogeneic hematopoietic stem cell transplantation. Cell. Mol. Immunol. 2020 184 18, 905–918.

Teetson, W., Cartwright, C., Dreiling, B.J., Steinberg, M.H., 1983. The leukocyte composition of peripheral blood buffy coat. Am. J. Clin. Pathol. 79, 500–501.

ten Broeke, T., Wubbolts, R., Stoorvogel, W., 2013. MHC Class II Antigen Presentation by Dendritic Cells Regulated through Endosomal Sorting. Cold Spring Harb. Perspect. Biol. 5: a016873

Teshima, T., Reddy, P., Zeiser, R., 2016. Reprint of: Acute Graft-versus-Host Disease: Novel Biological Insights. Biol. Blood Marrow Transplant. 22, S3–S8.

Thangavelu, G., & Blazar, B. R. (2019). Achievement of Tolerance Induction to Prevent Acute Graft-vs.-Host Disease. Frontiers in immunology, 10, 309.

Thiant, S., Labalette, M., Trauet, J., Coiteux, V., de Berranger, E., Dessaint, J.-P., Yakoub-Agha, I., 2011. Plasma levels of IL-7 and IL-15 after reduced intensity conditioned allo-SCT and relationship to acute GVHD. Bone Marrow Transplant. 46, 1374–1381.

Thiant, S., Yakoub-Agha, I., Magro, L., Trauet, J., Coiteux, V., Jouet, J.-P., Dessaint, J.-P., Labalette, M., 2010. Plasma levels of IL-7 and IL-15 in the first month after myeloablative BMT are predictive biomarkers of both acute GVHD and relapse. Bone

Marrow Transplant. 45, 1546–1552.

Toapanta, F.R., Ross, T.M., 2006. Complement-mediated activation of the adaptive immune responses: Role of C3d in linking the innate and adaptive immunity. Immunol. Res.36. 197-210.

Todorova, D., Kim, J., Hamzeinejad, S., He, J., Xu, Y., 2016. Brief Report: Immune Microenvironment Determines the Immunogenicity of Induced Pluripotent Stem Cell Derivatives. Stem Cells 34, 510–515.

Tonegawa, S., 1983. Somatic generation of antibody diversity. Nat. 1983 3025909 302, 575–581.

Trouw, L.A., Pickering, M.C., Blom, A.M., 2017. The complement system as a potential therapeutic target in rheumatic disease. Nat. Rev. Rheumatol. 13, 538-547.

Tsai, D.Y., Hung, K.H., Chang, C.W., Lin, K.I., 2019. Regulatory mechanisms of B cell responses and the implication in B cell-related diseases. J. Biomed. Sci. 2019 261 26, 1–13.

Tu, S., Zhong, D., Xie, W., Huang, W., Jiang, Y., Li, Y., 2016. Role of toll-like receptor signaling in the pathogenesis of graft-versus-host diseases. Int. J. Mol. Sci.17, 1288.

Van Acker, H.H., Anguille, S., De Reu, H., Berneman, Z.N., Smits, E.L., Van Tendeloo, V.F., 2018. Interleukin-15-cultured dendritic cells enhance anti-tumor gamma delta T cell functions through IL-15 secretion. Front. Immunol. 9, 658.

Vanegas, D., Niño-Quiroga, L., Chaparro, M., Camacho-Rodríguez, B., Estupiñán, M., Perdomo-Arciniegas, A.-M., 2021. Clinical Outcomes of Unrelated Umbilical Cord Blood Graft vs. Haploidentical Donor Transplantation: Critical Issues for an Adequate Comparison. Front. Med. 0, 1930.

Veerapathran, A., Pidala, J., Beato, F., Betts, B., Kim, J., Turner, J.G., Hellerstein, M.K., Yu, X.-Z., Janssen, W., Anasetti, C., 2013. Human regulatory T cells against minor histocompatibility antigens: ex vivo expansion for prevention of graft-versus-host disease. Blood 122, 2251–2261.

Victora, G.D., Mesin, L., 2014. Clonal and cellular dynamics in germinal centers. Curr. Opin. Immunol. 0, 90.

Vijay, K., 2018. Toll-like receptors in immunity and inflammatory diseases: Past, present, and future. Int. Immunopharmacol. 59, 391–412.

Visentainer, J.E.L., Lieber, S.R., Persoli, L.B.L., De, S.C.B., Lima, S., Vigorito, A.C., Aranha, F.J.P., Eid, K.A.B., Oliveira, G.B., Miranda, E.C.M., De Souza, C.A., 2002. Mixed lymphocyte culture and chronic GVHD Brazilian. J. Med. Biol. Res. 35, 567–572.

Walker, J.A., Smith, K.G.C., 2008. CD22: An inhibitory enigma. Immunology.123, 314-25.

Wang, Y., Liu, J., Burrows, P.D., Wang, J.Y., 2020. B Cell Development and Maturation. Adv. Exp. Med. Biol. 1254, 1–22.

Warren, E.H., Fujii, N., Akatsuka, Y., Chaney, C.N., Mito, J.K., Loeb, K.R., Gooley, T.A., Brown, M.L., Koo, K.K.W., Rosinski, K. V, Ogawa, S., Matsubara, A., Appelbaum, F.R., Riddell, S.R., 2010. Therapy of relapsed leukemia after allogeneic hematopoietic cell transplantation with T cells specific for minor histocompatibility antigens. Blood 115, 3869–3878.

Warren, E.H., Zhang, X.C., Li, S., Fan, W., Storer, B.E., Chien, J.W., Boeckh, M.J., Zhao, L.P., Martin, P.J., Hansen, J.A., 2012. Effect of MHC and non-MHC donor/recipient genetic disparity on the outcome of allogeneic HCT. Blood. 8, 27645-27660.

Weber, D., Frauenschläger, K., Ghimire, S., Peter, K., Panzer, I., Hiergeist, A., Weber, M., Kutny, D., Wolff, D., Grube, M., Huber, E., Oefner, P., Gessner, A., Hehlgans, T., Herr, W., Holler, E., 2017. The association between acute graft-versus-host disease and antimicrobial peptide expression in the gastrointestinal tract after allogeneic stem cell transplantation. PLoS One 12, e0185265.

Weng, J., Moriarty, K.E., Baio, F.E., Chu, F., Kim, S.D., He, J., Jie, Z., Xie, X., Ma, W., Qian, J., Zhang, L., Yang, J., Yi, Q., Neelapu, S.S., Kwak, L.W., 2016. IL-15 enhances the antitumor effect of human antigen-specific CD8 + T cells by cellular senescence delay. Oncoimmunology 5. e1237327.

Wherry, E.J., 2011. T cell exhaustion. Nat. Immunol. 12, 492–499.

Wherry, E.J., Kurachi, M., 2015. Molecular and cellular insights into T cell exhaustion. Nat. Rev. Immunol. 15, 486.

Winkler, T.H., Martensson, I.L., 2018. The role of the pre-b cell receptor in b cell development, repertoire selection, and tolerance. Front. Immunol. 9, 2423.

Wortel, C., Heidt, S., 2017. Regulatory B cells: Phenotype, function and role in transplantation. Transpl. Immunol. 41, 1–9.

Wortel, C.M., Heidt, S., 2017. Regulatory B cells: Phenotype, function and role in transplantation. Transpl. Immunol.41, 1-9.

Wu, C., Dunbar, C.E., 2011. Stem cell gene therapy: the risks of insertional mutagenesis and approaches to minimize genotoxicity. Front. Med. 5, 356–71.

Wu, S.M., Hochedlinger, K., 2011. Harnessing the potential of induced pluripotent stem cells for regenerative medicine. Nat. Cell Biol. 13, 497–505.

Yamano, T., Nedjic, J., Hinterberger, M., Steinert, M., Koser, S., Pinto, S., Gerdes, N., Lutgens, E., Ishimaru, N., Busslinger, M., Brors, B., Kyewski, B., Klein, L., 2015. Thymic B Cells Are Licensed to Present Self Antigens for Central T Cell Tolerance Induction. Immunity 42, 1048–1061.

Yang, J., Reth, M., 2010a. The dissociation activation model of B cell antigen receptor triggering. FEBS Lett. 584, 4872–4877.

Yang, J., Reth, M., 2010b. Oligomeric organization of the B-cell antigen receptor on resting cells. Nature 467, 465–470.

Yao, Y., Song, X., Cheng, H., Tang, G., Hu, X., Zhou, H., Wang, J., 2014. Dysfunction of Bone Marrow Vascular Niche in Acute Graft-Versus-Host Disease after MHC-Haploidentical Bone Marrow Transplantation. PLoS One 9, e104607.

Yarkoni, Y., Getahun, A., Cambier, J.C., 2010. Molecular underpinning of B-cell anergy. Immunol. Rev. 237, 249.

Yeh, C.H., Nojima, T., Kuraoka, M., Kelsoe, G., 2018. Germinal center entry not selection of B cells is controlled by peptide-MHCII complex density. Nat. Commun. 2018 91 9, 1–11.

Yi, J.S., Cox, M.A., Zajac, A.J., 2010. T-cell exhaustion: characteristics, causes and conversion. Immunology 129, 474.

Yi, T., Chen, Y., Wang, L., Du, G., Huang, D., Zhao, D., Johnston, H., Young, J., Todorov, I., Umetsu, D.T., Chen, L., Iwakura, Y., Kandeel, F., Forman, S., Zeng, D., 2009. Reciprocal differentiation and tissue-specific pathogenesis of Th1, Th2, and Th17 cells in graft-versus-host disease. Blood 114, 3101–3112.

Zarif, J.C., Hernandez, J.R., Verdone, J.E., Campbell, S.P., Drake, C.G., Pienta, K.J., 2016. A phased strategy to differentiate human CD14+ monocytes into classically and alternatively activated macrophages and dendritic cells. Biotechniques 61, 33–41.

Zeiser, R., Blazar, B.R., 2017. Acute Graft-versus-Host Disease — Biologic Process, Prevention, and Therapy. N. Engl. J. Med. 377, 2167–2179.

Zhang, Y., Garcia-Ibanez, L., Toellner, K.M., 2016. Regulation of germinal center B-cell differentiation. Immunol. Rev. 270, 8–19.

Zhang, Y., Louboutin, J.-P., Zhu, J., Rivera, A.J., Emerson, S.G., 2002a. Preterminal host dendritic cells in irradiated mice prime CD8+ T cell-mediated acute graft-versus-host disease. J. Clin. Invest. 109, 1335–1344.

Zhang, Y., Shlomchik, W.D., Joe, G., Louboutin, J.-P., Zhu, J., Rivera, A., Giannola, D., Emerson, S.G., 2002b. APCs in the liver and spleen recruit activated allogeneic CD8+

T cells to elicit hepatic graft-versus-host disease. J. Immunol. 169, 7111–7118.

Zhao, T., Zhang, Z.-N., Rong, Z., Xu, Y., 2011. Immunogenicity of induced pluripotent stem cells. Nature 474, 212–215.

Zheng, P., Wu, Q., Li, B., Chen, P., Nie, D., Zhang, R., Fang, J., Xia, L., Hong, M., 2017. Simvastatin ameliorates graft-vs-host disease by regulating angiopoietin-1 and angiopoietin-2 in a murine model. Leuk. Res. 55, 49–54.

Zhou, J., He, W., Luo, G., & Wu, J. (2014). Mixed lymphocyte reaction induced by multiple alloantigens and the role for IL-10 in proliferation inhibition. Burns & trauma, 2(1), 24–28.

Zhu, L., Xie, X., Zhang, L., Wang, H., Jie, Z., Zhou, X., Shi, J., Zhao, S., Zhang, B., Cheng, X., Sun, S.C., 2018. TBK-binding protein 1 regulates IL-15-induced autophagy and NKT cell survival. Nat. Commun. 9. 2812.

Zitzer, N.C., Snyder, K., Meng, X., Taylor, P.A., Efebera, Y.A., Devine, S.M., Blazar, B.R., Garzon, R., Ranganathan, P., 2018. MicroRNA-155 Modulates Acute Graft-versus-Host Disease by Impacting T Cell Expansion, Migration, and Effector Function. J. Immunol. 200, 4170–4179.

Zsef Prechl, J., Baiu, D.C., Horvá Th, A., Erdei, A., 2002. Modeling the presentation of C3d-coated antigen by B lymphocytes: enhancement by CR1/2-BCR co-ligation is selective for the co-ligating antigen, International Immunology.14, 241-7.

Zuber, J., Sykes, M., 2017. Mechanisms of Mixed Chimerism-Based Transplant Tolerance. Trends Immunol. 38, 829.

Chapter 7

Supplementary data

Compensation setup:

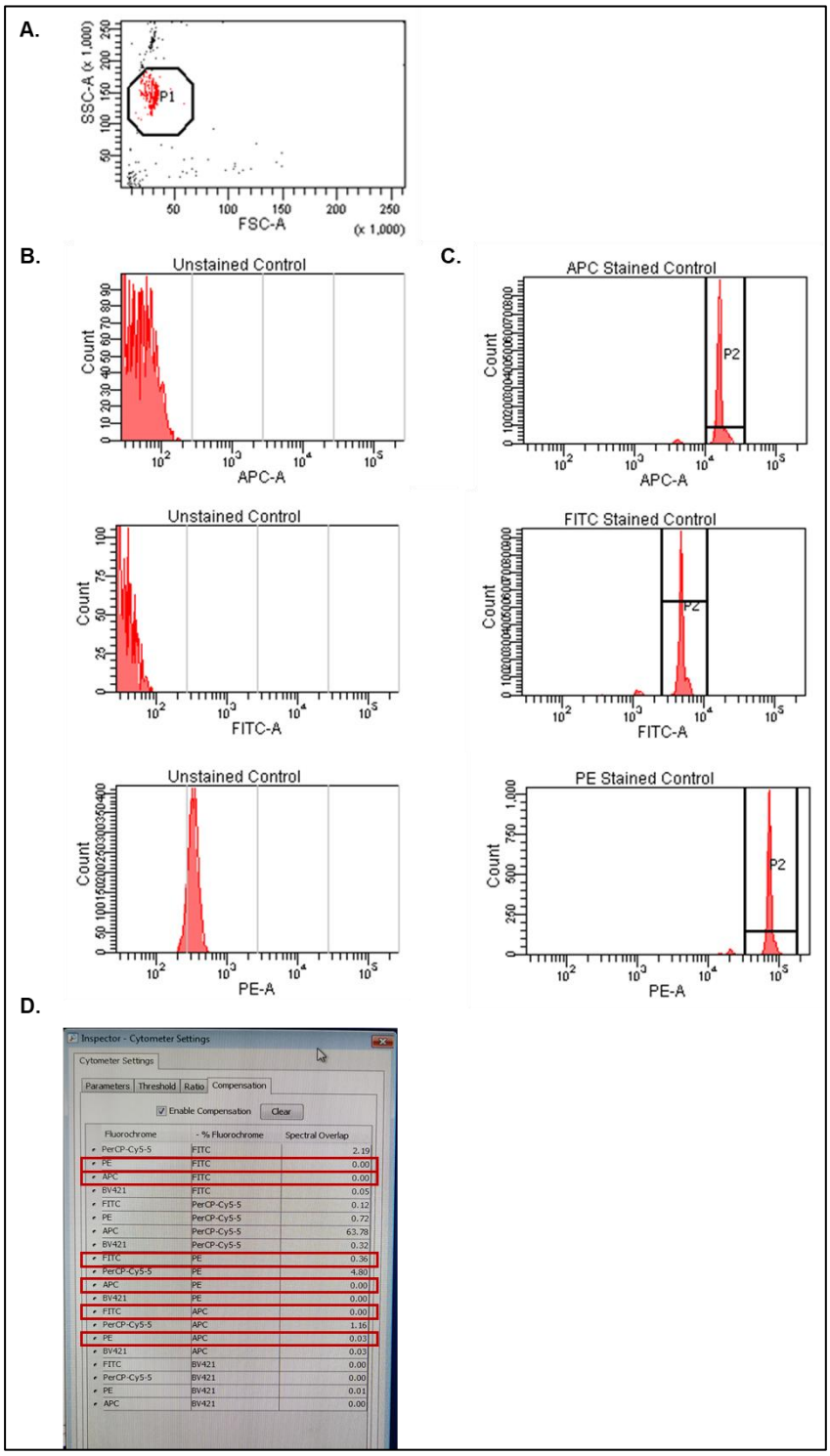

Supplementary figure 1. Compensation setup A) The beads are identified on the P1 gate. **B)** Unstained and **C)** single-stained beads were used to generate **D)** the compensation matrix.

OneComp eBeads™ (ThermoFisher Scientific, Waltham, Massachusetts, United States) were used to setup the compensation. Panel design was established so that minimal compensation was needed by choosing the highest energy emitters of each laser (APC/red laser; 660/20 filter – FITC (CFSE)/green laser; 530/30 filter - PE/yellow-green laser; 585/42 filter). No spectral overlap was recorded between APC↔FITC (both directions), PE→FITC (unidirectional) or APC→PE (unidirectional), otherwise near-zero spectral overlaps were recorded for FITC→PE (unidirectional; 0.36%), PE→APC (unidirectional; 0.03%). Despite having minimal spill over, the compensation matrix was applied.

Chapter 8

Appendix

Statement on the Impact of Covid-19 restrictions on PhD project work

The Covid-19 restrictions came at the critical phase for my PhD project work. Namely, my project was in the final year when the key experiments were planned. Prior to Covid-19 restrictions, the experimental model was fully optimised, theoretical concepts were clearly defined and detail experimental plans were developed. Furthermore, the University has acquired the new, sophisticated flow cytometry instrument, BD LSR Fortessa X-20. In contrast to CyAn ADP instrument, 2 laser flow cytometer with modest specifications that I have used for the first 2 years of my PhD work, this new instrument has 4 lasers and is able to detect up to 18 parameters simultaneously. However, my plan to fully exploit the potential of the new instrument for multicolor flow cytometry were severely hampered by Covid-19 restrictions. Indeed, due to restrictions in access to the laboratory, limitations in training options and support by supervisory team, I was unable to develop the new flow cytometry protocols that would be tailored to LST Fortessa instrument. Instead, I had to continue relying on previously developed methods that were optimised for CyAn ADP flow cytometer. This has created some issue in flow cytometry experimental design that were difficult to address, particularly as I had to conduct the analysis with limited support due to Covid-19 restrictions.

Furthermore, the ordering procedure and delivery of critical reagents were severely delayed due to Covid-19 restrictions. This has impacted the number of experiments that were feasible resulting in limited repeats of some important observations. Also, the late delivery of the essential reagents has resulted in forced cancelation of the planned experimental work that could have generated additional novel data. Consequently, the quantity of the results and to a lesser extent the quality of the data were curtailed by Covid-19 restrictions.

I acknowledge that due to Covid-19 my research activities could not be performed as planned and that it was not possible to acquire the results that would enhance the thesis. In such difficult circumstances, with restricted access to reagents and limited supervisory support, alternative choices had to be made to adapt the work. Consequently, there are weaknesses in the quantity of the experimental data that could not be overcome.